Renewable 2,3-Butanediol as Platform Monomer for the Synthesis of Biobased Polymers

Zur Erlangung des akademischen Grades eines

DOKTORS DER NATURWISSENSCHAFTEN

(Dr. rer. nat.)

von der KIT-Fakultät für Chemie und Biowissenschaften

des Karlsruher Instituts für Technologie (KIT)

genehmigte

DISSERTATION

von

M. Sc. Anja Kirchberg

aus Offenburg

1. Referent: Prof. Dr. Michael A. R. Meier

2. Referent: Prof. Dr. Patrick Théato

Tag der mündlichen Prüfung: 07.12.2023

FÜR MEINE FAMILIE

UND

FÜR MICH

“Sage der Welt was du vorhast,
aber erst nachdem du es gezeigt hast“
Napoleon Hill

Declaration of Authorship

Die vorliegende Arbeit wurde von Oktober 2020 bis Oktober 2023 unter Anleitung von Prof. Dr. Michael A. R. Meier am Institut für Organische Chemie (IOC) des Karlsruhe Instituts für Technologie (KIT) angefertigt.

Hiermit versichere ich, dass ich die Arbeit selbstständig angefertigt, nur die angegebenen Quellen und Hilfsmittel benutzt und mich keiner unzuverlässigen Hilfe Dritter bedient habe. Insbesondere habe ich wörtlich oder sinngemäß aus anderen Werken übernommene Inhalte als solche kenntlich gemacht. Die Satzung des Karlsruhe Instituts für Technologie (KIT) zur Sicherung wissenschaftlicher Praxis habe ich beachtet. Des Weiteren erkläre ich, dass ich mich derzeit in keinem laufenden Promotionsverfahren befinde und auch keine vorausgegangene Promotionsversuche unternommen habe. Die elektronische Version der Arbeit stimmt mit der schriftlichen Version überein und die Primärdaten sind gemäß Abs. A (6) der Regelung zur Sicherung guter wissenschaftlicher Praxis des KIT beim Institut abgegeben und archiviert.

Karlsruhe, den 24.10.2023 ----------

Anja Kirchberg

I Danksagung

Mit vollem Stolz und unendlicher Dankbarkeit, freue ich mich sehr, dass der Tag gekommen ist an dem Du/Sie, als Leser, meine Doktorarbeit in den Händen halten und all meine Forschungsergebnisse lesen kannst.

Ich konnte drei wundervolle Jahre im Arbeitskreis Meier genießen und möchte mich hiermit zuallererst bei Dir, **Mike**, bedanken! Vielen Dank, dass du mir diesen Weg ermöglicht hast, indem du mich 2020 als Doktorandin in deinen Arbeitskreis aufgenommen hast. Es war mir jeden Tag eine Freude an meinen Projekten zu forschen und durch meine Aufgaben weiterzuwachsen. Danke, für alle Freiheiten, die du mir gegeben hast, dass du mich stets unterstützt hast, deine Tür immer offenstand und ich durch Dich viele Erfahrungen sammeln konnte. Danke für jede interessante Konferenz, die ich besuchen durfte, wodurch ich Kontakte zu wundervollen Menschen knüpfen konnte. Ich habe mich in Deinem Arbeitskreis immer sehr wohl gefühlt und hätte mir keinen besseren Chef vorstellen können.
Danke auch an Dich, **Pinar**, für die immer schnellen Antworten zu organisatorischen Fragen und all Deine Hilfestellungen.

--------- Meine Kooperationen ----------

Weiter sage ich Danke, an meine **Förderer**, das Bundesministerium für Bildung und Forschung zur Ermöglichung meines Projektes und allen Finanzierungen. Vielen Dank an all meine **Kooperationspartner**: Röchling Industrial GmbH, Frauenhofer Institut, alle beteiligten Mitarbeiter des Arbeitskreises Horn am KIT, des Arbeitskreis Kerzenmacher an der Universität Bremen und des Arbeitskreises Gescher an der Technischen Universität Hamburg. Danke für die interessante Zusammenarbeit, die halbjährlichen Meetings und euer kontinuierliches Feedback.
Danke, an all meine Kooperationen mit Arbeitskreisen des KIT, wie beispielsweise dem **Arbeitskreis Wilhelm** für die kontinuierliche Unterstützung bei Materialmessungen. Danke **Masood**, dass Du dir immer Zeit genommen hast und jedes Mal aufs Neue überraschende Ideen hattest. Danke **Marie**, für Deine Unterstützung bei Schäumungsprozessen. Danke an den **Arbeitskreis Théato**, für die Ermöglichung aller TGA-Messungen an eurem Standort und Danke an Dich, **Birgit**, für die immer unkomplizierte Kommunikation. Ein weiterer Dank geht an das **Analytik Zentrum Campus Nord** für Messungen meiner Polymerlösungen.

Nun komme ich zu meinem Arbeitskreis und allen wundervollen Menschen, die mich während meiner Promotion begleitet und unterstützt haben.
Zuallererst geht ein Dank an meine Arbeitskollegen/innen, wobei ich chronologisch vorgehen werde, von meinem Start der Masterarbeit 2019 bis heute, dem Ende meiner Promotion.

---------- Meine Zeit am KIT ----------

Danke **Pia** und **Ben**, dass ihr mir am Tag meines Vorstellungsgespräches 2019 und damit meinem ersten Tag am KIT, alles gezeigt habt und ich mich direkt willkommen fühlen konnte. Danke **Ben**, für den besten Schreibtischspot im Großraumbüro. Thank you **Eren**, for giving me a spot in your lab and showing me around. I still remember how you explained to me the dissolution of cellullose on my first working day. Ein Dank geht an **Julian** und **Luca**, für die lustige Zeit mit euch im Labor 409. Durch euch konnte ich so einiges lernen, unter anderem auch, mich für Ordnung und Sauberkeit durchzusetzen. Den Ruf des „Punsherlabors 409“ habe ich bis heute nicht losbekommen und ich muss sagen, mittlerweile bin ich auch irgendwie stolz auf den Rufnamen.
Schon an Tag zwei durfte ich die offene und trinkfreudige Seite von Dir, **Michi**, kennenlernen, vielen Dank für jedes Feierabendbier und die absolut fantastische Einführung des Rauschsessels, in welchem man äußerst bequem die ein oder anderen Stunden bei intensiven Gesprächen verbringen kann. Danke an Dich, **Dani**, für Deine immer gutgelaunte Art, Dein tägliches breites Grinsen, nette Gespräche und die passende Schlagermusik zum Wochenendauftakt am Freitag. **Bohni**, Dir möchte ich Danken für alle Tipps und Tricks, die Du mir sowohl im Labor als auch am Laptop beigebracht hast. Deine vielen Erfahrungen, durch die ich schon im Vorhinein das ein oder andere Fauxpas vermeiden konnte. Vielen Dank für die Einführung der aktiven Tischtennispause, die immer Spaß gemacht hat und für die zahlreichen Fotos, die mir für immer als Erinnerung bleiben werden.
Ich kann mich noch genau an deine erste Arbeitswoche erinnern, **Jow**, Dein Lachen wird mir hoffentlich noch lang in den Ohren bleiben. Danke für jeden Spruch, den Du rausgehauen hast und Deine immer feinen Kochkünste, die zur Einführung unserer „FoodPorn“ Gruppe beigetragen haben. Hierbei komme ich auch direkt zu Dir, **Maxi**. Danke für alle unterhaltsamen Kochabende und unser wöchentliches Treffen im Schwimmbad. Vielen Dank, **Katha**, dass auch Du immer bei unserem Klatsch und Tratsch dabei warst. Danke euch Zwei, für Eure vielen Erzählungen, immer offenen Ohren und sonnigen Stunden. Apropos offenes Ohr, Danke **Roman**, für jede Hilfestellung bei den noch so komplizierten NMR-Spektren und Deine immer entspannte Art, die jedes Mal aufs Neue beruhigende Wirkung hatte.

Clara, Dir möchte ich danken, dass du immer für Ordnung und Seelenfrieden gesorgt hast, Deine Meinung stets von Bedeutung war und für die schöne Zeit bei der Bordeaux Konferenz. **Timo** und **Luis**, Danke für den witzigen Abend mit dem bisher teuersten Gin Tonic auf der Konferenz in Dortmund. Danke auch an Dich, **Hatice**, für Deine vielen Bekanntschaften und Menschen die Du mir auf Konferenzen vorgestellt hast.
Federico, thanks for always helping with the GPC. Thank you, **Caitlyn**, for always being in a good mood and coming into the office telling me: “Good morning beautiful girl”. **Francesca**, it was my absolute pleasure to share 409 with you, being always friendly, telling the truth and wanting to have fun. I want to say thanks to you, **Celeste**, for sitting together each lunch break. For having someone that also always wants to go outside for some fresh air. It was my pleasure and thank you for the funny days and nights in Paris at the conference. **Sandra**, pass gut auf 409 auf, ich weiß, dass das Labor bei Dir in guten Händen sein wird.
Pete, **Qianyu**, **Henni**, **Andreas** und **Leon** es war mir immer eine Freude mit euch zusammenzuarbeiten, die ein oder andere Kaffeepause zu verbringen und beim abendlichen Grillen nette Gespräche zu führen.

Danke an meine **Studenten/innen**: Anna, Vinh-Hao und Dir, Sandra für deine Ergebnisse der **Vertieferarbeit**. Danke an alle **HIWIs**: Elin, Philipp, Natalia, Mike und Elena, dass Ihr mir Arbeit abgenommen habt.
Vielen Dank an meine **Korrekturleser**: Sandra, Jonas, Melanie, Janek, Clara, Francesca, Timo, Katharina, Qianyu, Celeste, Pete, Philipp, Leon, Nichollas.

---------- Aus sportlicher Sicht ----------

Ich bedanke mich zudem bei meinen Trainern, **Nico** und **Sandy**, **meinem Verein** und meiner Betreuerin, **Mama**. Danke, dass ihr mich neben meinem Studium und meiner Promotion immer im Sport weiter motiviert habt, mir gezeigt habt was es heißt für ein Ziel zu kämpfen und wie es sich anfühlt nach Niederlagen aufzustehen und noch erfolgreicher zu werden.– *Alles oder Nichts* – Der Sport ist meine Art von Meditation geworden und wird es auch immer bleiben.

---------- Das Beste kommt zum Schluss – Meine Familie ----------

Vielen Dank **Mama** und **Papa**, dass ihr immer an mich geglaubt und mich stets unterstützt habt, ohne euch hätte ich den Weg bis hier hin nicht geschafft. Danke **Liza**, dass Du mir als große Schwester immer ein Vorbild gewesen bist und zusätzlich eine beste Freundin, die immer da war, wenn ich sie gebraucht habe. Danke **Oma**, für alle Telefonate in denen ich

einfach mal Dampf ablassen konnte und Deine immer positiven Worte. Danke **Opa**, dass Du, obwohl Du nicht da sein konntest, immer bei mir gewesen bist. Danke **Oma Elli** für jeden Pfälzer Geburtstags-Stift, der für gute Stimmung gesorgt hat. Danke **Laura**, für alle lustigen Abende, die mir den Kopf komplett frei gemacht haben. Danke, dass Du seit ich denken kann an meiner Seite bist und Dir immer Zeit für mich genommen hast. Vielen Dank **Janik**, dass Du so bist wie Du bist, mich immer unterstützt hast und sich durch Dich jedes Wochenende wie Urlaub angefühlt hat. Danke für jedes Tennismatch, den Miracle Morning, Deine ansteckende gute Laune und jedes Abenteuer. Danke **Stefano**, für die kontinuierliche Erinnerung, dass ich mich außerhalb des Labors mit Finanzthemen beschäftigen sollte und demnach Danke für alle Bänker-Tipps.

DANKE AN EUCH ALLE, FÜR DIE UNVERGESSLICHEN JAHRE!!

Und nun, ganz viel Spaß beim Lesen meiner Doktorarbeit.

Eure Anja

II Abstract

Most of the polymers used in our daily lives are petroleum-based which cannot be considered as sustainable. Due to the depletion of fossil resources, scientists are searching for ways to implement renewable resources in the production of polymers. Lignocellulosic biomass constitutes an important carbon resource, with which well-known fermentation technologies can be used to produce commodity chemicals, such as 2,3-butanediol. This diol is not yet widely researched in polymer chemistry. Thus, demonstrates an interesting biobased starting material to investigate. Therefore, the focus of this thesis was on implementing 2,3-butanediol for sustainable polymer syntheses, more precisely for the synthesis of polyurethanes and polyesters. The 12 Principles of Green Chemistry were used within all projects, as guideline to investigate more sustainable routes to polyurethanes and polyesters. Besides using renewable starting materials, also catalyst screenings were performed, to find environmentally benign and cheap alternatives to commonly used procedures.

In a first project, a three-step synthesis was developed to obtain polyurethanes. First, the renewable 2,3-butanediol was successfully converted into its cyclic carbonate using an organocatalyst and dimethyl carbonate. This carbonate was ring-opened by using a biobased amino acid methyl ester. The formed carbamate was then successfully polymerized to a non-isocyanate polyurethane. Its thermal and mechanical properties were compared to polyurethanes based on commonly used diols. Rheology measurements led to the idea to successfully foam the biobased polymer.

In the second project of this thesis, the focus was on polyesters based on 2,3-butanediol and other renewable dicarboxylic acids, such as the sugar-based 2,5-furandicarboxylic acid. Within this procedure, an established catalyst screening method, the so-called deconvolution method, was applied, revealing iron(III)chloride as an environmentally friendly and cheap catalyst to be used in polycondensation reactions. The thermal properties of all polyesters and copolyesters were analyzed accordingly. However, no mechanical properties were measured due to the brittleness of the obtained polymers.

Finally, collaboration partners of the Technical University Hamburg were optimizing the fermentation process towards 2,3-butanediol. Herein, a purification after fermentation is successfully reported yielding a stereoisomeric mixture of 2,3-butanediol. This mixture was further analyzed, and stereoisomers of the diol were tested individually in a polycondensation reaction to form a desired polyester. Thermal properties of all biobased polymers were reported.

This thesis therefore gives an overview about fundamental research based on 2,3-butanediol to form biobased polymers, which showed promising properties.

III Zusammenfassung

Alltäglich verwendete Polymermaterialien werden noch immer größtenteils aus erdölbasierenden Chemikalien hergestellt. Aufgrund der zuneige gehenden fossilen Rohstoffen, ist es überfällig neue Strategien, mit Fokus auf der Verwendung von nachhaltigen und erneuerbaren Ressourcen, zu entwickeln. Hierzu bietet sich insbesondere Lignocellulose, ein essenzieller Baustein aller Pflanzen, an. Lignocellulose kann über bereits entwickelte Fermentationsverfahren in Basischemikalien, wie 2,3-Butandiol, umgewandelt werden. Dieser zweiwertige Alkohol ist für die Herstellung von Polymeren noch nicht weitgehend untersucht und daher von großem Interesse. Das Hauptaugenmerk dieser Arbeit lag somit auf der Implementierung von 2,3-Butandiol in der Polymersynthese zu biobasierten Materialien. Hierbei wurden die 12 Prinzipien der Grünen Chemie als Leitfaden verwendet, um neben des biobasierten Ausgangstoffes, auch weitere Aspekte der Nachhaltigkeit zu beachten, wie beispielsweise durch Screenings zu reaktiven Katalysatoren.

In einem ersten Projekt dieser Arbeit wurde eine Drei-Schritt-Synthese entwickelt, um biobasierte Polyurethane herzustellen. Hierbei handelte es sich um isocyanat-freie Polyurethane, genauer Polyesterurethane. Zunächst wurde aus 2,3-Butandiol und Dimethylcarbonat erfolgreich ein cyclisches Carbonat synthetisiert. Dieses Carbonat wurde mit dem Methylester einer biobasierten Aminosäure in ein Carbamat umgewandelt, welches anschließend erfolgreich zur Herstellung eines isocyanat-freien Polyurethans verwendet wurde. Die thermischen und mechanischen Eigenschaften dieses Polymers konnten erfolgreich analysiert und mit Polyurethanen, basierend auf handelsüblichen zweiwertigen Alkoholen, verglichen werden. Zudem wurde das biobasierte Polymer erfolgreich aufgeschäumt.

In einem zweiten Projekt dieser Arbeit wurde 2,3-Butandiol für die Herstellung von Polyestern untersucht. Hierzu wurde primär die zuckerbasierte 2,5-Furandicarbonsäure sowie weitere biobasierte Dicarbonsäuren verwendet. In einem Katalysatorscreening, der sogenannten Dekonvolutionsmethode, wurde innerhalb einer Polykondensation das Eisen(III)chlorid als kostengünstiger, reaktiver und nicht toxischer Katalysator identifiziert. Die thermischen Eigenschaften der synthetisierten Polyester und Copolyester wurden erfolgreich analysiert, mechanische Eigenschaften konnten jedoch aufgrund ihrer Brüchigkeit nicht untersucht werden.

In einem letzten Projekt dieser Arbeit wurde über eine Kooperation mit der Technischen Universität Hamburg die Optimierung der fermentativen Synthese von 2,3-Butandiol verfolgt. Die Aufreinigung des zweiwertigen Alkohols wurde im Zuge dieser Arbeit erfolgreich

durchgeführt und dessen Struktur nähergehend untersucht. Daraufhin konnte erfolgreich ein Polyester synthetisiert und die Struktureigenschaften analysiert werden.
Zusammenfassend stellt diese Arbeit somit verschiedene Möglichkeiten da, wie durch nachhaltigere Synthesen, basierend auf 2,3-Butandiol, biobasierte Polyester und Polyurethane hergestellt werden können.

Table of Contents

1. Introduction

In the last decade, not only academia and industry, but also consumers discuss more often about the sustainability of products, life, and the challenges of next generations. Important in this context is, how we can define the term sustainability in science and more importantly, how can each individual contribute to change the world into a greener and therefore healthier planet?

Looking back in time, an important industrial chapter began with the use of oil and gas to produce chemicals, followed by a revolutionary development of numerous human-made polymers, which get still further invented by scientists all over the world researching every day for new strategies.[1]

Polymer science belongs to the oldest fields of science, as human beings have always been using polymers, even without knowing the molecular structure of these materials. In 1910, a synthetic polymeric material was prepared by Leo Baekeland, called Bakelite, later succeeding in preparing a hard plastic that is still manufactured in industrial applications of rods and tubes. It was a breakthrough, when the German chemist Hermann Staudinger first formulated the science of polymers, in 1920.[2][3] In the period of 1945 to 1960, new monomers from petrochemical industry accelerated the development of polymers.[4]

Today, 99% of plastics are made from chemicals sourced from fossil fuels used in all kinds of areas, from cosmetics to packaging, automotives, and the pharmaceutical industry. In Europe, ~53 metric tonnes of plastic waste were produced in 2019, of which Germany accounts for ~3 million tons yearly.[5] In Germany, ~42% (2020) of waste was recycled through chemical recycling or downcycling to reuse and ~57% (2020) were used as energy recovery. Besides Germany, the Netherlands, Norway, and Spain are the world leading countries with recycling rates >40%. However, in other countries, only little amounts of plastic materials get recycled (e.g., 25%, 2020 in France) and most of the plastic wastes accumulate in landfills or the natural environment, like the ocean.[6] This global plastic pollution is related to the emission of greenhouse gases. Especially microplastics, accumulating in natural ecosystems and the ocean, destroy the habitats of living beings.[7]

Furthermore, 80% of the worlds global energy mix is fossil-based while burning fossil fuel leads to the release of carbon dioxide that is responsible for global warming.[8] Less than one percent of more than 390 million tons of plastic production annually is based on renewable resources.[6] At least, the global bioplastic production capacities are set to increase from 2.2 million tons in 2022 to around 6.3 million tons in 2027, which was analyzed according to the latest market data compiled by European Bioplastics.[9] The problems of increasing plastic productions are

paired with the growing population, especially in China with 1.4 billion people in 2021 and an overall increasing standard of living.[10]

To reduce the human impact on nature, all humans must learn to use less materials, while producing less waste. Furthermore, scientists need to investigate ways to do more from less, with, e.g., recycling technologies, to reduce the need of resources, especially petroleum-based.[11]

In 1980s, the World Commission on Environment and Development stated for the first time that a sustainable development *"should meet the needs of the present without compromising the ability of future generations to meet their own needs".*[12]

Therefore, the implementation of Green Chemistry, the design of chemical products and processes, that reduce or eliminate the use or generation of hazardous substances, is essential. With Green Chemistry including the collaboration of industry, academia, and governments, a sustainable future society can be achieved by adopting greener technologies.[13] With the 12 Principles of Green Chemistry, a guideline for scientists, as a framework for sustainable designs in polymer syntheses, is given. Waste prevention, safer solvents, environmentally friendlier reagents and catalysts are all important principles that must be implemented in the synthesis of everyday used materials.[14] Furthermore, the shrinking fossil fuels, which are predicted to be exhausted around 2050, lead scientists to research for renewable alternatives to rapidly move to a plant-based economy.[15]

With this thesis, the author wishes to contribute on finding more sustainable alternatives to produce biobased polymers using renewable feedstock.

2. Theoretical Background

2.1 Green and Sustainable Chemistry

The human society of the 21st century must deal with inherit challenges, like global warming, depleting fossil resources and environmental plastic pollution. Therefore, it is important to exchange knowledge and start acting sustainable in all kind of areas.[11] Sustainability is known with its three-pillar conception, including society, economics, and the environment (see *Figure 1*). These three pillars should be an attempt to find a balance between sociological, economical, and ecological aspects to generate a sustainable future. An important basis is represented by the interdisciplinary network of scientific research, education, consumer awareness, and sustainable entrepreneurship.[13][16] However, the concept remains open with space for interpretation, depending on the area to be used in and is not internationally spread.[17]

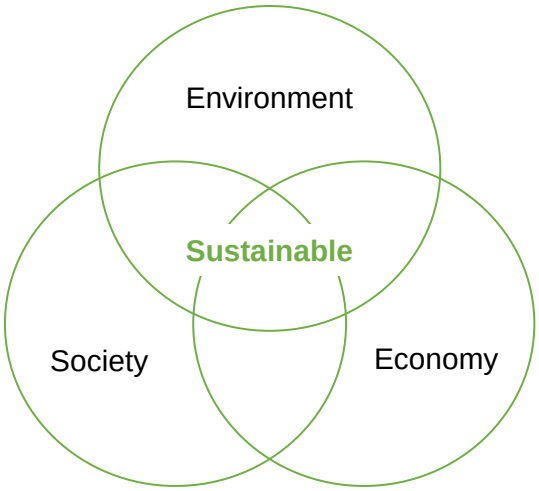

Figure 1. The three pillars of sustainability.[17]

A definition of sustainability in chemistry was recently proposed, in which resources, including energy, should be used *"at a rate at which they can be replaced naturally, and the generation of wastes cannot be faster than the rate of their remediation".*[12]

Nearly every bulk chemical used in industry is derived from fossil-based resources and is used in chemical processes, e.g., to produce commercially available polymeric materials. Thus, the research for effective sustainable strategies is in competition with well-optimized, cost-effective synthesis routes to chemicals that are already on the market.[18] In 1991, the Office of Pollution Prevention and Toxics of the U.S. Environmental Protection Agency published the first research of a Green Chemistry.[19]

Since then, Green Chemistry has been grown internationally into a significant focus area in science (see *Table 1*). The breath of this research area is wide and incorporated in different areas like plastic production, packaging, pharmaceutical, and the cosmetic industry. Over the past 10 years, an active area of Green Chemistry was the design of environmentally benign solvents and solventless systems.[20] Ionic liquids demonstrate a relatively new area of solvent investigations.[21] It has been widely recognized in recent years that the manufacture of polymers poses many hazards, which can be changed by applying the principles of Green Chemistry.[22] Therefore, research on renewable feedstocks is a promising alternative.[23] Catalysis often permits the use of toxic substances and reduces energy requirements. Furthermore, catalytic reactions can increase the selectivity and can minimize the quantity of reagents needed.[24] Green Chemistry also includes the incorporation of analytical methods into real time processes for continuous process monitoring to eliminate the generation of waste before it is formed and to reduce accident potential.[20]

The 12 Principles of Green Chemistry offer a framework to encourage scientists to tune their protocols by planning chemical syntheses on a molecular design to achieve the goal of sustainability.[14] This systematic concept was introduced by P. Anastas and J. Warner in 1998.[25] Safety, environmental impact, toxicity, and biodegradability are all factors that should be taken into account while investigating new strategies.[26]

In 2009, Anastas *et al.* additionally summarized the framework of Green Chemistry in three main points:

“1. Green Chemistry designs across all stages of the chemical life-cycle.

2. Green Chemistry seeks to design the inherent nature of the chemical products and processes to reduce their intrinsic hazard.

3. Green Chemistry works as a cohesive system of principles or design criteria.”[14]

Table 1. The 12 Principles of Green Chemistry developed and published by P. Anastas and J. Warner in 1998.[25]

1.	**Prevention.** It is better to prevent waste than to treat or clean up waste after it is formed.
2.	**Atom Economy.** Synthetic methods should be designed to maximize the incorporation of all atoms used in the process into the final product.
3.	**Less Hazardous Chemical Synthesis.** Whenever practicable, synthetic methodologies should be designed to use and generate substances that pose little or no toxicity to human health and the environment.
4.	**Designing Safer Chemicals.** Chemical products should be designed to preserve efficacy of the function while reducing toxicity.
5.	**Safer Solvents and Auxiliaries.** The use of auxiliary substances (e.g., solvents, separation agents, etc.) should be made unnecessary whenever possible and, when used, innocuous.
6.	**Design for Energy Efficiency.** Energy requirements of chemical processes should be recognized for their environmental and economic impacts and should be minimized. If possible, synthetic methods should be conducted at ambient temperature and pressure.
7.	**Use of Renewable Feedstocks.** A raw material or feedstock should be renewable rather than depleting whenever technically and economically practicable
8.	**Reduce Derivatives.** Unnecessary derivatization (use of blocking groups, protection/deprotection, temporary modification of physical/chemical processes) should be minimized or avoided, if possible, because such steps require additional reagents and can generate waste.
9.	**Catalysis.** Catalytic reagents (as selective as possible) are superior to stoichiometric reagents.
10.	**Design for Degradation.** Chemical products should be designed so that at the end of their function they break down into innocuous degradation products and do not persist in the environment.
11.	**Real-Time Analysis for Pollution Prevention.** Analytical methodologies need to be further developed to allow for real-time, in-process monitoring and control prior to the formation of hazardous substances.
12.	**Inherently Safer Chemistry for Accident Prevention.** Substances and the form of a substance used in a chemical process should be chosen to minimize the potential for chemical accidents, including releases, explosions, and fires.

A modern and more convenient way to summarize the 12 Principles of Green Chemistry was published as “PRODUCIVELY” by Tang *et al.* in 2005, later improved by the wording “IMPROVEMENT”, in 2008 (see *Table 2*).[27][28]

Table 2. The 12 Principles of Green Chemistry summarized by Tang et al.[28] with “PRODUCTIVELY” and optimized with the wording “IMPROVEMENTS” by Tang et al.[27] in 2008.

P	Prevent waste	**I**	Inherently non-hazardous and safe
R	Renewable materials	**M**	Minimize material diversity
O	Omit derivatization steps	**P**	Prevention instead of treatment
D	Degradable chemical products	**R**	Renewable material and energy inputs
U	Use safe synthetic methods	**O**	Output-led design
C	Catalytic reagents	**V**	Very simple
T	Temperature, pressure ambient	**E**	Efficient use of mass, energy, space & time
I	In-Process monitoring	**M**	Meet the hand
V	Very few auxiliary substances	**E**	Easy to separate by design
E	E-factor, maximise feed in product	**N**	Networks for exchange of local mass & energy
L	Low toxicity of chemical products	**T**	Test the life cycle of the design
Y	Yes, it is safe	**S**	Sustainability throughout product life cycle

2.1.1 Metrics and Assessment of Sustainable Chemistry

The focus of industry remains on the economic development, i.e., to implement chemical reactions with high output, increasing efficiency and scale. Due to diminishing supply of fossil-based resources and the need to find sustainable alternatives, methods and concepts were developed as an evaluation tool to quantify the sustainability of a respective synthesis.[29] In 1991, the first concept was introduced by B. Trost, called the concept of Atom Economy (AE).[30] The concept refers to maximize the use of raw materials converted into a maximum number of atoms in the product. AE is calculated using the following *Equation 1*, measuring the ratio of the molecular weight of the desired product over the molecular weight of all used reactants. This value rapidly provides an idea on how efficient a certain reaction is in theory. An ideal reaction would incorporate all atoms of used reactants, meaning AE would be 100%. A reaction, in which only a few atoms of reagents are appearing in the product (AE <100%), produces side products, thus, waste.[31]

$$AE\ (\%) = \frac{Mn\ of\ desired\ product}{\sum Mn\ \ of\ all\ reagents} * 100\%$$

Equation 1. Calculation of the Atom Economy defined by B. Trost.[30]

However, with AE first, only the reaction equation is considered without looking at solvents or auxiliaries. Therefore, the Environmental factor (E-factor) was introduced by R. Sheldon in 1992.[32] The E-factor is defined as the actual amount of waste produced in a reaction, including everything but the desired product. It is calculated following *Equation 2*, including all solvents and solvents losses, auxiliaries, reagents, and the yield.[33]

$$E - factor = \frac{\sum m\ of\ starting\ materials - m\ of\ product}{m\ of\ product}$$

Equation 2. Calculation of the Environmental factor introduced by R. Sheldon in 1992.[32]

The ideal E-factor is 0, meaning a higher E-factor consequently relates to more waste and a negative impact on the environment. This calculation has been widely adopted by the bulk chemical, pharmaceutical, and fine chemical industry. Water that is used in the process is not included in the calculation, but the water that is formed in the syntheses. *Table 3* gives an overview of E-factors in the chemical industry. The larger E-factor in the fine and pharmaceutical industry is caused due to multi-step syntheses necessary to produce complex products (see *Table 3*).[33]

Table 3. E-factors in the bulk and fine chemical, pharmaceutical, and oil refining industry.[33]

Industry segment	**Product tonnage**	**E-factor (kg waste / kg product)**
Oil refining	10^6 - 10^8	<0.1
Bulk chemicals	10^4 - 10^6	<1 - 5
Fine chemicals	10^2 - 10^4	5 - 50
Pharmaceuticals	10 - 10^3	25 - 100

Often, solvent losses during procedures are not reported in research, what makes the comparison of the environmental impact of processes difficult. Therefore, Roschangar *et al.* suggested that the true E-factor falls between a simple E-Factor (sEF) and a complete E-factor (cEF).[34] The difference between both is, the cEF includes all materials, solvents, and even water used in the syntheses and does not consider recycling, whereas the sEF excludes water

and solvents in its calculation (see *Equation 3*). Therefore, sEF is more likely used in early development phase assessments. The major drawback of the E-factor is, that it does not consider the toxicity of the used materials.[35]

$$sEF = \frac{\sum m(raw\ materials) + \sum m(reagents) - m(product)}{m(product)}$$

$$cEF = \frac{\sum m(raw\ materials) + \sum m(reagents) + \sum m(solvents) + \sum m(water) - m(product)}{m(product)}$$

Equation 3. Calculation of the simple E-factor and complete E-factor, introduced by Roschangar et al.[34]

Further metrics were published over time, as alternatives to the AE and E-factor. The actual atom economy (AAE) was introduced to consider the yield of reactions.[36] The mass intensity (MI) is defined as the total mass used in a process divided by the mass of product and considers the reagents and solvents introducing the stoichiometry of a reaction.[37] The reaction mass efficiency (RME) parameter developed by GlaxoSmithKline, takes the AE, yield, and stoichiometry into account. It is calculated by the mass of the product divided by the total mass of reactants in the stoichiometric equation. However, AAE and RME can only be used when experimental work was already performed.[38]

For a complete assessment of the sustainability of a chemical procedure, a full life cycle assessment (LCA) is necessary. LCA is a powerful tool to understand and characterize the range and scope of the environmental impact in each stage within a process.[39] The whole material and energy supply chain is considered with its emission, transportation, production, use, and waste disposal. LCA can have two main objectives, with 1) to quantify and evaluate the environmental performance of a process ("*cradle to grave*") and 2) to help identify options for improvement in the environmental performance of a system.[40][41] However, often the main problem are multiple, conflicting options identified to improve a system. Multiobjective optimization (MO) is proposed to filter for optimum strategy and the best alternatives within a project. Azapagic *et al.* presents a powerful tool for balancing the environmental and economic performance, by combining MO and LCA, meaning to get the choice of best practicable environmental option (BPEO).[42] A variety of different metrics for process assessment have been developed, with broad applicability. Even in the International Organization for Standardization (ISO), a procedure for conducting LCA is provided as general principle and framework of the concept.[43][44]

Companies have developed their own LCAs as an important tool for decision-making, like the fast life cycle assessment of synthetic chemistry (FLASC) by GlaxoSmithKline or the BASFs

eco-efficiency tool.[45][46] All concepts have the same goal by taking the basic idea of Green Chemistry with "*benign by design*" to prevent the production of waste and reduce the impact of the overall process.[39][47] The next step is "*cradle to cradle*", not only including the life cycle of the raw material to the desired product, but considering the full recycling after disposal.[48] However, AE and the E-factor remain the most widely used metrics in the literature when talking about sustainability of chemical syntheses, as they are easy to implement and offer important decision making tools in an early stage development.[49]

2.2 Renewable Resources for Biobased Polymer Syntheses

Within the next century, the era of a chemical industry mainly based on fossil resources will come to an end. Forecasts of 1995 estimated that in the year 2040, the world must feed 9 to 10 billion people with enough energy, and materials, to further generate a life with a versatile amount of consumer products and thus, a high standard of living. The stocks of fossil resources are depleting and will be exhausted around 2050, if the world continues to live without changing to renewable feedstocks.[15] Furthermore, the world faces a new situation with the increase of the oil price, meaning that the market price of crude is higher than the price of biomass-derived pure molecules.[2][50]

In 2019, only 13% of renewable resources were used in German industry (see *Figure 2*). 87% of all resources were fossil-based and to 100% imported, showing the strong dependency of Germany on this feedstock.[51][52]

The 13% of used renewable resources are divided into 46% from fats and oils from plant or animal origin. 16% come from dissolving pulp, mostly obtained *via* a sulfite process to remove hemicellulose, yielding >90% cellulose content. The remaining percentages are divided into carbohydrates, starch, and proteins followed by further renewables like waxes, resins, or glycerol.[51]

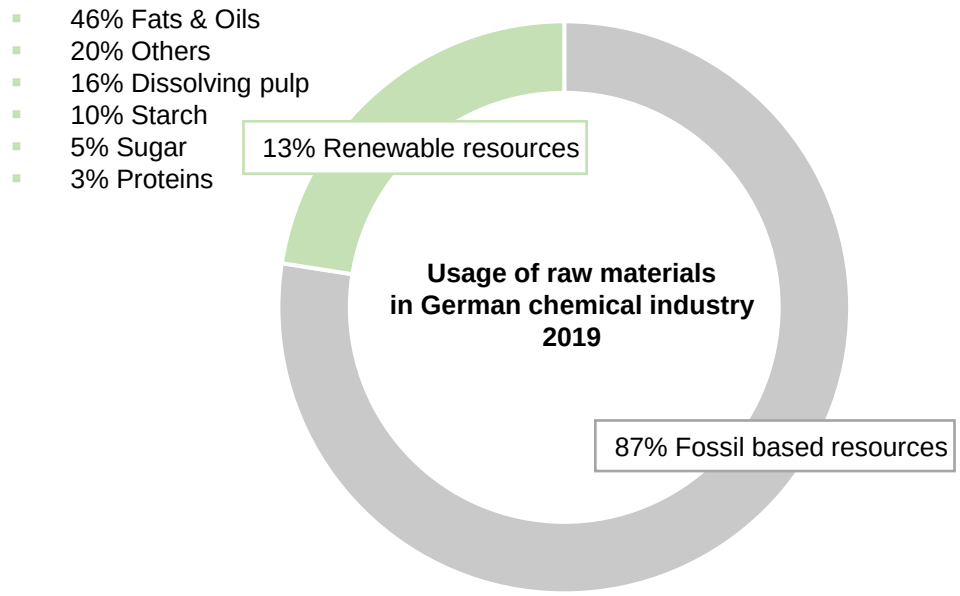

Figure 2. Usage of raw materials in the German chemical industry, in 2019.[51]

The use of renewable feedstock, summarized as biomass to produce energy, chemicals, and materials, is the key issue to thrive the world into the direction of a plant-based economy.[53][54][55] Agriculture, industrial, and domestic wastes can be processed, new crops can be grown on marginal land, and fast-growing vegetative biomass can be used to produce biobased polymers.[55][56] Thus, bio-energy and biobased polymers are the future of our society. The term “biobased polymer” applies to naturally occurring of polymeric materials and to natural substances that have been polymerized.[57]

Polyhydroxyalkanoates, vegetable oil based polyesters, epoxy, and polyurethanes have received much attention as potential sustainable alternatives to existing materials and naturally occurring polymers.[58][59][60] Middle- to long-chain linear diacids derived from natural fats and oils are promising renewable monomers to synthesize polyesters, polyamides, and polyurethanes.[61] Poly(lactide acid) (PLA) represents a compostable polymer playing a central role in replacing fossil-based polymers.[62]

Not all biobased polymers are biodegradable. Native biodegradable polymers include proteins, polysaccharide, or nucleic acids whereas synthetic polymers can be of different types containing hydrolysable backbone, e.g., for polyesters, or non-degradable but renewable materials like bio-PE.[57]

Since the 1970s scientists are researching for biodegradable plastics derived from renewable feedstock.[63] Biodegradable is defined as the complete conversion of the polymer into energy, biomass, water, and carbon dioxide by the action of microorganisms within a certain time period. This property of biodegradability depends on the chemical composition, molecular

weight, and architecture of the polymer and not on the source of the raw material used in its manufacture. Biodegradable polymers would drastically reduce the impacts of plastic waste on the environment.[64]

An example for a biobased and biodegradable polymer synthesized by genetically engineering plants to produce usable polymers within their cellular tissue is poly(hydroxybutyrate) (PHB) with similar properties to polypropylene (PP).[58][65] Nylon-6,6, other selected polyamides, lignin, and chitosan plastics, or cellulose polymers are further biobased polymers obtained from renewable monomers.[52][66] Polyethylene (PE) represents a widely used polymer, synthesized from ethylene, which is generally obtained from petroleum, but nowadays also synthesized in small volumes from bio-ethanol obtained from glucose.[67]

Glucose can be obtained from different biological feedstock such as sugar cane, sugar beet, starch crops, or lignocellulosic materials.[52]

Lignocellulose is one of the most abundant carbon sources on the earth. It demonstrates the most promising renewable feedstock, typically without competing with the food industry.[68][69] Lignocellulosic biomass is composed of 40 – 60% cellulose, 20 – 40% hemicellulose, and 10 – 25% lignin depending on its source.[70] Its feedstock can be based on energy crops, agricultural residues, forestry residues, or industrial and municipal wastes.[71] *Figure 3* gives an overview of various short chain diols and acids, as examples of commodity chemicals that can nowadays be obtained from lignocellulose derived sugars.[72] Diols obtained from these renewables are e.g., used in the manufacture of pharmaceuticals, coatings, packaging materials, and fine chemicals.[73]

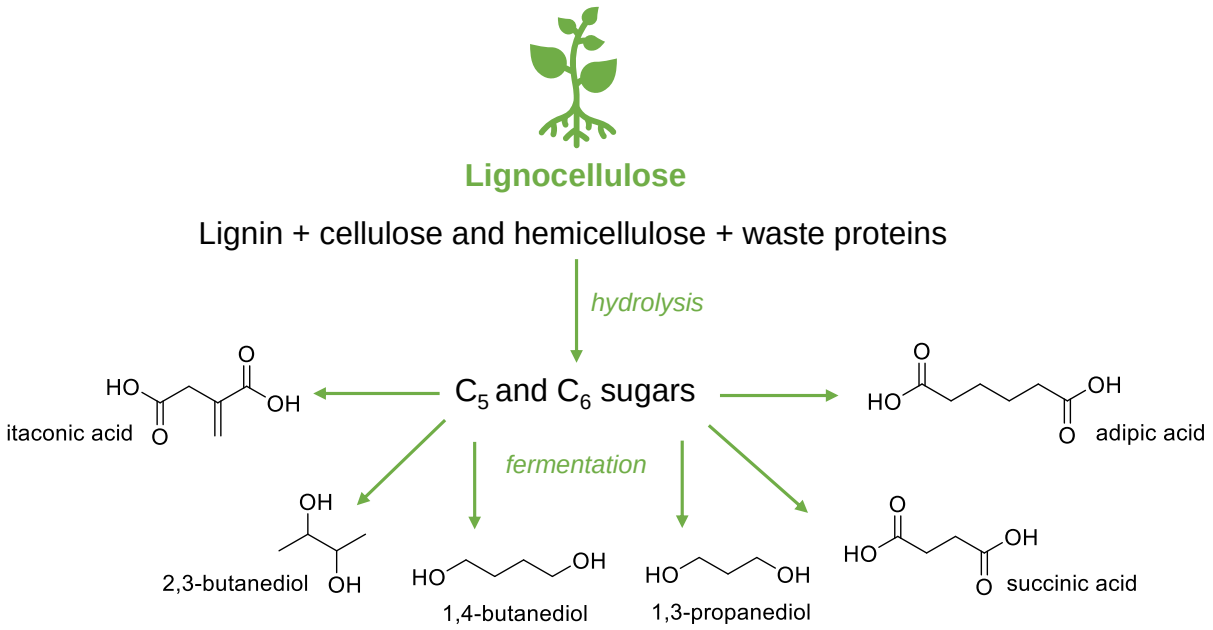

Figure 3. Overview of commodity chemicals that can already be produced in a sustainable manner by fermentation of sugars derived from lignocellulose, e.g., agriculture waste.[72]

Lignocellulosic compounds are naturally converted from carbon dioxide in a photochemical reaction using solar energy. However, carbon dioxide is considered as a waste responsible for global warming. Scientists took inspiration from nature to convert carbon dioxide into useful materials, as this feedstock is not only abundant and inexpensive, but also safe and non-flammable.[74] In the past few years, various processes have been developed to successfully convert carbon dioxide into commodity chemicals such as methanol, carboxylic acids, and dimethyl carbonate (DMC), or building blocks to be polymerized.[75][76] Theoretically the at the beginning added carbon dioxide to produce materials is released in a thermal treatment at the end of the lifetime of the product, which means that this closed loop results in a reduced carbon footprint, thus, reduced greenhouse gas emissions.[77][78]

A biorefinery concept was developed to use such renewable resources to produce commodity chemicals by adapting a concept which is analogous to the well-known petroleum refineries. The aim of biorefineries is to limit the impact of carbon dioxide, thus also global warming and to provide the world with bio-energy, bio-molecules, bio-materials, and bio-food ingredients.[2] To increase the independency of Germany to other countries, a benefit would be the use of locally sourced renewable feedstocks such as trees, grasses, or food and agriculture, industrial, and domestic waste. Before the in the plants containing components like lignocellulose and sugars such as glucose can be further transformed into commodity chemicals, different steps must be performed. Depending on which biomass is used as

renewable feedstock, sometimes grinding is necessary, meaning that for instance the bark gets removed from the trunk.[79][80] Then, cracking or fractionation by biological or physicochemical technologies follow. Different processes were developed over time to successfully fractionate biomass depending on which feedstock it is coming from. The traditional way of fractionation is based on kraft pulping and soda process, an alkali-based fractionation. Furthermore, a sulfur-free route is based on an organosolv fractionation using organic solvents. An alcohol-based fractionation known as ethanol pulping is the most widely studied approach, adding acidic catalysts.[81][82] As last step, enzymes are the key technology to convert thus, to valorize the natural polymers.[79][83]

A further main category of a biorefinery is energy to generate biofuels like bio-ethanol and bio-diesel. Reports of 1945 proposed the use of a low temperature acid hydrolysis of lignocellulose to maximize the overall process yield to ethanol.[84][85] Compared to an acid hydrolysis, an enzymatic hydrolysis using cellulase requires less energy and is less toxic. Further microorganisms are used to digest sugars such as pentose and hexose into ethanol.[86]

The biofuel market was valued with 120 billion U.S. dollar in 2020 and is estimated to increase to 201 billion U.S. dollar in 2030. The global demand of biofuels is set to grow by 28% which are approximately 41 billion liters over 2021 to 2026.[87] Thus, biofuels represent the most important category in volume of biorefineries.[84]

In summary, the use of renewable resources in the production of polymeric materials is beneficial in the following three ways: 1) feedstocks employed can be replaced through natural occurring or human intention, 2) biodegradation of the end product prevents further pollution of the environment, 3) an outcome is the increased balance of social, environment, and economics thus, the aim of sustainability is provided.[58]

The largest field for biobased polymers is the packaging industry with 48% of the overall production of biobased plastics in 2022. The textile industry, consumer goods, automotives, and coatings follow (see *Figure 4*). Biobased PLA, PE and starch, as natural occurring polymer, are the three most produced and used biopolymers of industry in 2022.[9][52]

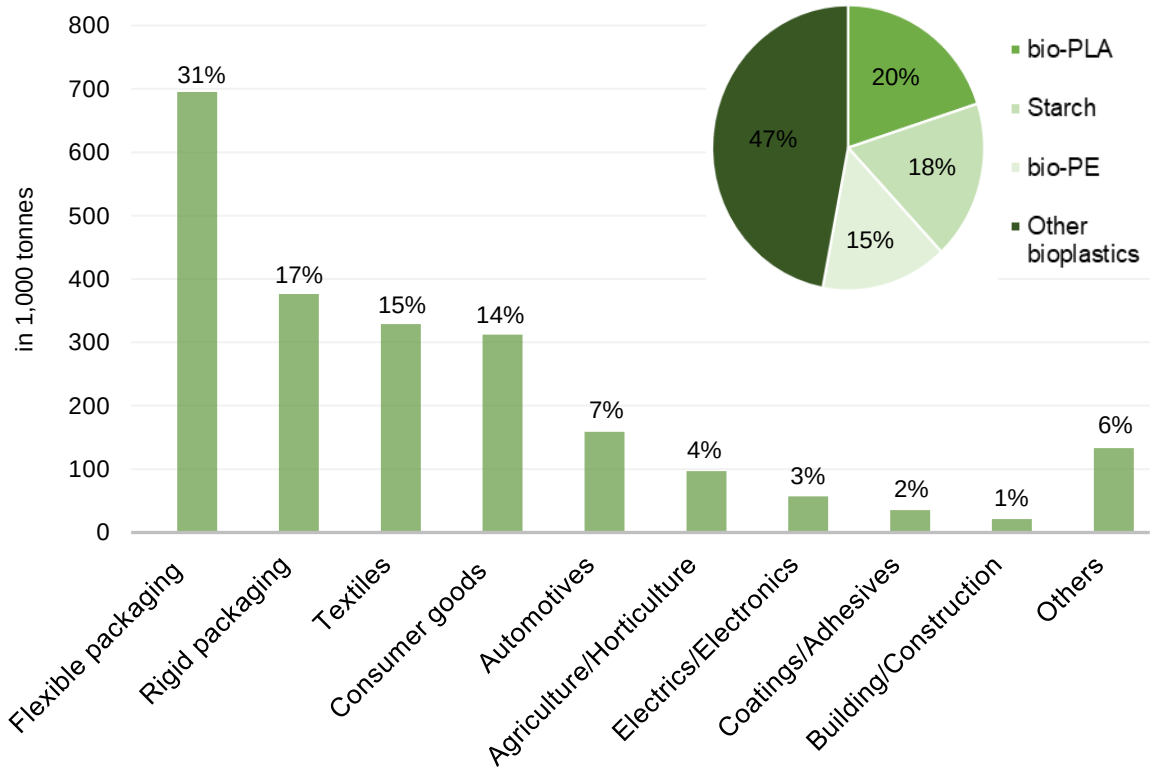

Figure 4. Chart of the areas of biobased polymer usage in the industry of 2022. With the packaging industry as most widely sector for biobased plastics. The three most used and industrial produced biopolymers in 2022.[9]

The production capacities of biobased plastics are set to continuously grow within the next years. Until now, the main drawback is the high cost to process renewable feedstock to generate versatile chemicals. Furthermore, biobased polymers must compete with existing polymeric materials and their optimized properties. However, scientists are further focusing on finding opportunities to successfully implement renewable resources in our daily life used materials to make them an unavoidable part of our future society.[9][88]

2.2.1 2,3-Butanediol as Renewable Monomer

Commodity chemicals commercially produced in the petrochemical industry can nowadays be replaced by utilizing renewable bio-resources. A prominent example is ethylene glycol (EG), used to produce poly(ethylene terephthalate) (PET), the most widely used polyester. EG can be sustainably synthesized using glycerol, a waste product from the bio-diesel industry.[89] Also, propylene glycol (PG), used in various applications of the detergents and cosmetic industry, can be synthesized by using glycerol with the aid of heterogenous catalysis.[90]

Another interesting diol is 2,3-butanediol (BDO), which is applied in the manufacture of perfumes, moistening, and softening agents, explosives, plasticizers, foods, and

pharmaceuticals, but is not yet widely researched for polymer synthesis.[91][92] A dehydration of BDO to methyl ethyl ketone is used as liquid fuel additive.[92] Conversion of 1,3-butandiene leads to possible application in the rubber industry, whereas dehydrogenation of BDO to diacetyl serves a valued flavouring agents in food products. Furthermore, the diol is used in structural analogy to glycerol or glycol as antifreeze agent due to its low freezing point.[93]

BDO can be either synthesized by a direct microbial conversion of carbon dioxide or in the process of carbohydrate biomass fermentation.[94][95][96] The microbial production shows a history of more than 100 years and was first reported by Harden and Walpole in 1906.[97] Industrial-scale production of BDO is believed to have been proposed by Fulmer *et al.* in 1933.[98] Different bacteria have been employed in these early studies, with *Klebsiella pneumoniae* (*K. pneumoniae*) and later cultures of *Peanibacillus polymyxa* (*P. polymyxa*), both demonstrating to be potentially applicable in today's industry.[95][99] *K. pneumoniae* shows advantages with a higher production amount of BDO compared to *P. polymyxa* and an easy cultivation with fast growth in minimal media by using, e.g., wood and agricultural wastes. However, *K. pneumoniae* shows a disadvantage for large-scale production because of pathogenicity of opportunistic infection.[100]

Apart from BDO and depending on the used microorganism and the cultivation conditions, other products are formed in the process, such as ethanol, acetate, lactate, formate, and succinate. Most of the products are synthesized from pyruvate as common precursor in the central metabolic pathway. Acetoin is the precursor of BDO and is enzymatically formed in bacteria. During fermentation, different isomers of BDO are produced, depending on which bacteria and genes are used in the process. Using families of *Enterobacteriaceae* mainly forms meso-BDO and a small amount of S-isomer, while using members of the family of *Paenibacillaceae* mainly R-isomer and small amounts of meso-BDO are produced.[93][101][102] Besides glucose (see *Scheme 1*), also glycerol was found as a cheap and abundant carbon source for the bio-process to produce value-added chemicals such as BDO.[103] Also, *Cupriavidus necator* H16 is studied for the production of acetoin as precursor for BDO. *Cupriavidus necator* is used in the production to PHB and known as the best-studied knallgas bacterium using carbon dioxide as carbon source.[104][105]

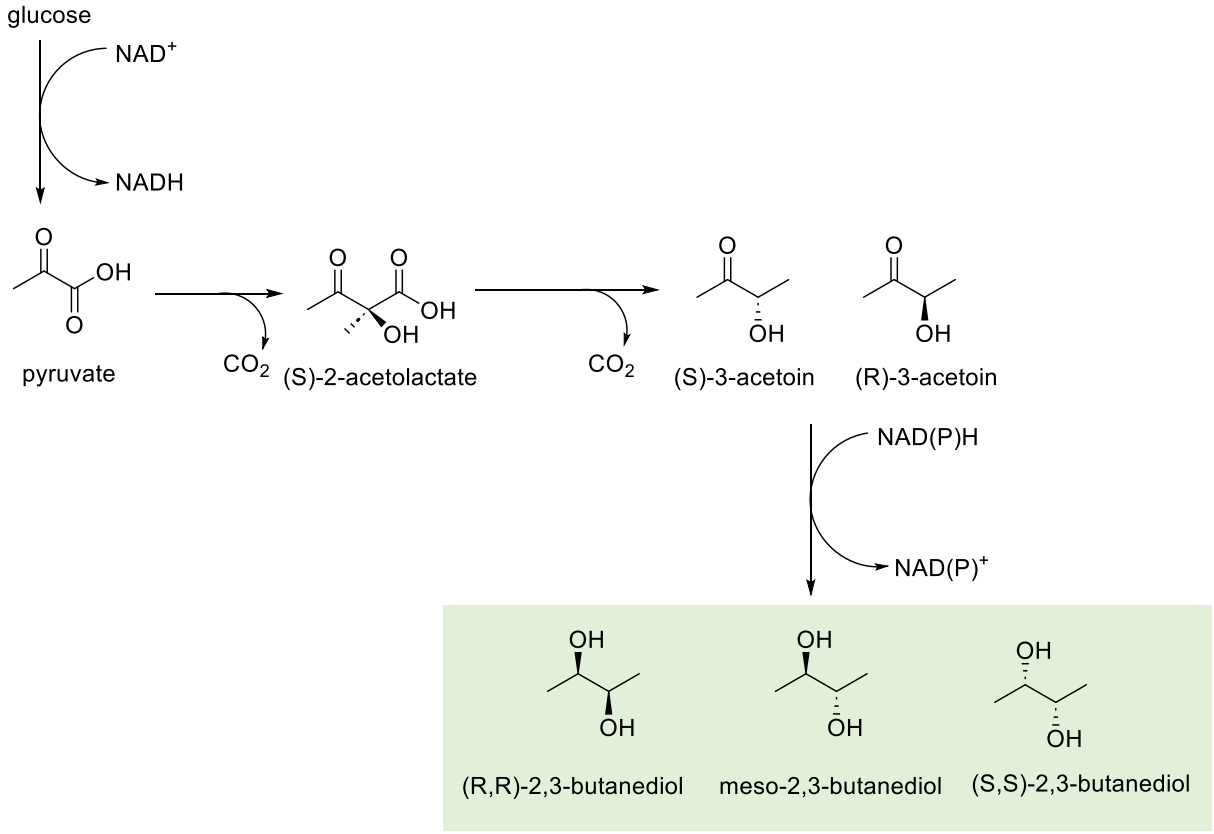

Scheme 1. Simplified scheme of the central metabolic pathway to the isomeric mixture of 2,3-butanediol.[101]

Fermentation products, like BDO, can be distilled from the broth. However, in addition to large bioreactors, high costs are involved in generating the steam required to distil fermentation products. Therefore, scientists studied the organic extraction to remove the product during fermentation and minimize the downstream recovery. An *in-situ* liquid-liquid extraction of BDO fermentation illustrated to be a technique that enhances the product recovery. A main challenge remains through the toxicity of the commonly used organic solvents.[106][107] For instance, oleyl alcohol or isopropanol can be used as extractant. Product concentrations in each liquid phase can be measured *via* gas chromatography (GC). In a study of Anvari and Khayati, oleyl alcohol extraction was successfully tested, leading to a product mixture of BDO, leftovers of glucose and the precursor acetoin.[106][108]

A combination of solvent extraction followed by distillation, called hybrid extraction-distillation, fully ensures the separation and purification of BDO and recovery of solvents.[109] Song *et al.* presented an extraction with isopropanol followed by distillation of BDO, which led to a recovery yield of 76% and a BDO purity of 96%.[108]

Forecasts show that the market size of BDO will reach 300 million U.S. dollar in 2030. Also, the precursor acetoin, which can be successfully separated after fermentation, shows applications as taste and aroma enhancer in butter, milk, and other food manufactures.[110]
One of the main applications of BDO is as anti-freeze agent. Dehydration of BDO leads to methyl ethyl ketone showing higher heat combustion compared to ethanol, considered to be an effective liquid fuel additive. BDO can be converted into 1,3-butadiene, which is used in the production of synthetic rubber. Esterification of BDO forms precursors for the synthesis of polyurethanes.[92] Because of the methyl groups in the BDO structure, the renewable monomer has been successfully applied to restrain the crystallization of polyesters.[111][112] Gubbels *et al.* synthesized various polyester resins based on BDO and 2,5-furandicarboxylic acid (FDCA) to successfully replace petrochemical diols. The fully amorphous polyesters showed improved thermal stability and an increasing glass transition temperature (T_g) with increasing BDO content.[112][113]
Thus, the cheap and abundant renewable monomer BDO is indeed attractive for the development of novel amorphous biopolymers.[112]

2.3 The Class of Polyurethanes

Materials based on polyurethanes (PUs) are used in everyday life in form of foams for thermal insulations, as elastomers for shoe soles and steering wheels as well as in various fields such as automobiles, medical applications, furniture, and electronics.[114][115] The annual worldwide consumption of PUs was about 25 million metric tons in 2022. Forecasts predicted that the global PU market will grow to 31 million tons in 2030.[116] The manufacture of PUs per year accounts to 7 wt% of the total global plastic production.[7][117]
The name PU is derived from the urethane repeating unit in its backbone, which is formed by a polyaddition reaction.(*)[118][119] This polyaddition reaction was discovered by O. Bayer in the laboratories of I. G. Farben in Germany, in 1937.[120] Later, interesting properties of PUs were realized using aliphatic diisocyanates and glycol. In 1952, polyisocyanates became commercially available, followed by different developments to polyester-polyisocyanate systems.[121]

(*) A polyaddition reaction forms polymers *via* independent addition reactions between the functional groups of e.g., diisocyanates and molecules showing at least two hydroxyl groups in its structure.[118][119]

Mostly, polyols are used as reaction partners of isocyanates, with methylene diphenyl diisocyanate (MDI) and toluene diisocyanate (TDI) as the most applied monomers for the manufacture of flexible and rigid PUs.(*)[122] The main advantage of isocyanate chemistry is the good reactivity paired with high yields. The carbon dioxide generated in the urea forming reaction with water and isocyanate can be effectively used to expand PU foams at low pressure.[114][118]

Over time, industry developed a wide choice of additives and polyols available to manufacture versatile and tunable properties of PUs, offering manifold application possibilities. PUs can show a superior hardness, mechanical strength, biocompatibility, and suitable elongation properties to be used in many sectors.[123]

However, the major drawback is the toxicity of isocyanates and their synthesis, which is highly problematic in terms of sustainability and Green Chemistry.[114][118]

In this chapter, the conventional routes to PUs are presented, compared to renewable alternatives such as the synthesis of renewable isocyanates, renewable polyols, and fully biobased PUs. Furthermore, recycling possibilities of PUs are described.

2.3.1 Conventional Synthetic Routes to Polyurethanes

The typical route to PUs is a chemical reaction between di- or polyisocyanates and a diol or polyol forming repeating urethane units. Generally, a chain extender is added with a catalyst, or further additives. Besides urea groups, also ester, ether, and aromatic rings are often present along the PU backbone.[121][124] *Scheme 2* shows the general reaction scheme to PUs.

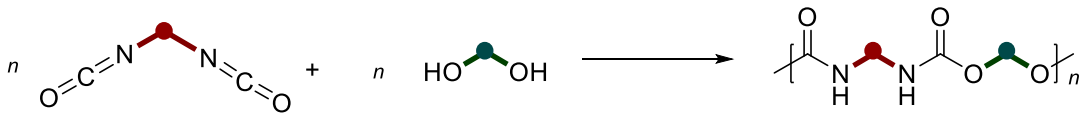

Scheme 2. General route to polyurethanes using diisocyanates and polyols in a polyaddition reaction. Colors marked as possibilities to modification of monomers and the desired polymer.

Isocyanates are formally related to the unstable isocyanic acid and known as versatile compounds in organic and polymer chemistry, showing a high reactivity and toxicity.[125] For instance, hexamethylene diisocyanate shows a toxicity of <960 mg kg^{-1} (LD_{50}, oral, rat).[126][127] The industrial synthesis of isocyanates is based on the treatment of primary amines with toxic phosgene under the release of hydrogen chloride.[125][128][129]

(*) Rigid PU foams show a closed-cell pore structure with crosslinks and high density, whereas flexible PU foams show interconnected pores, allowing compression and resilience.
For more information, see Ates *et al.* [122]

Figure 5 gives an overview about the industrially mostly used isocyanates.

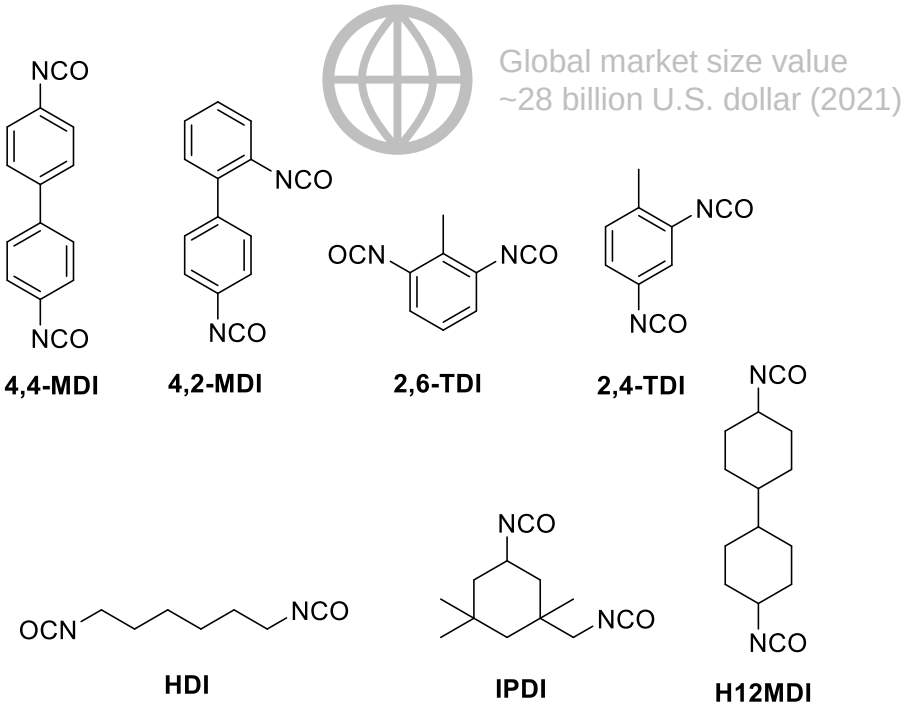

Figure 5. Industrially used aromatic and aliphatic isocyanates. Methylene diphenyl diisocyanate (MDI), toluol diisocyanate (TDI), hexamethylene diisocyanate (HDI), isophorone diisocyanate (IPDI), hydrogenated (H12) MDI.[130]

The overall market size value of isocyanates was about ~28 billion U.S. dollar in 2021. With MDI being the worlds most produced isocyanate, followed by TDI with a market size of ~7403.3 million U.S. dollar (2022) used in the foam manufacture. IPDI shows a market size of ~751.1 million U.S. dollar (2022) and is mostly used for coatings in the automobile industry, as well as for flooring and roofing.[130][131]

Polyester polyols are prepared by a condensation reaction between glycols such as EG, 1,4-butanediol, 1,6-hexanediol, and aliphatic or aromatic dicarboxylic acids. Highly branched polyester polyols, lead to highly rigid PUs, whereas less branched polyester polyols result in flexible PUs. Rigid PUs typically show a good heat and chemical resistance, compared to flexible PUs.[118][119][121] An example for a natural occurring polyester polyol is castor oil. Furthermore, vegetable oils can by chemically transformed into polyester polyols, which all show a sensitivity to hydrolysis because of the presence of ester groups in their structures. Thus, polyether polyols were developed, showing a high moisture stability and low T_g.[121] Mainly, ring-open polymerizations (ROP) of epoxides, such as ethylene oxide or propylene oxide, are performed to generate the desired aliphatic polyether polyols.[132] The

physical properties of such polyols are depending on the M_n and chemical building blocks. A functionality of two to six and M_n up to 18 kDa of polyol is used to synthesize flexible PUs, whereas a functionality of two to three and M_n of 2 kDa for a polyol is used for rigid PU foams.[133][134] *Figure 6* shows the chemical structure of the industrially mostly used polyols.

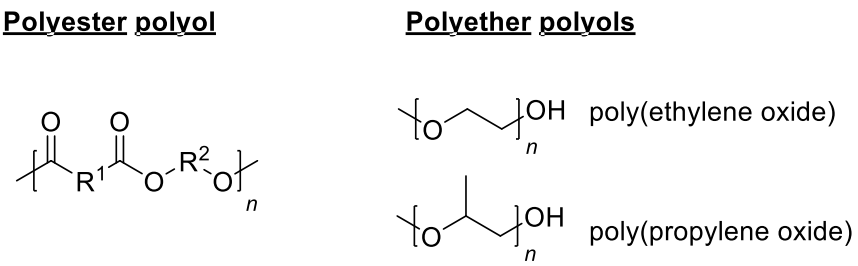

Figure 6. Structure of industrially used polyol types for the manufacture of polyurethanes.

Beside polyols and isocyanates, often additives are required during the PU synthesis. Mostly, additives are used to control the reaction conditions and modify the properties of the final product. Some examples are catalysts, chain extenders, crosslinkers, and colorants. As catalysts, several aliphatic and aromatic amines, organometallic compounds, or alkali metal salts of carboxylic acids are used to reduce the reaction temperatures while enhancing the reaction rates. Difunctional low molecular diols such as EG, 1,4-butanediol, or 1,6-hexanediol as well as diamines are used as chain extenders in the PU manufacture.[121][125]

2.3.2 Polyurethane Foams

The largest application field of PUs is in form of foams, with 67% of the global PU consumption. Furthermore, besides polystyrene or poly(vinyl chloride) foams, PU foams correspond to half of the worldwide polymeric foam market.[135] The two main classes of PU foams being rigid or flexible are adjusted by the choice of polyol, isocyanate, catalyst, surfactant, blowing agent, and additives used for their synthesis. The reactants are mixed followed by the polymerization with simultaneous expansion. Either low boiling point solvents such as pentane or acetone, defined as physical blowing agents, or chemical blowing agents such as water are added to vaporize or expand the PU by forming carbon dioxide.[136][137] Different technologies can be used to manufacture PU foams with the most often used being molding, slabstock, and spraying.[135] In the molding process, all reactants are mixed in a mold cavity, being removed after curing to then cut the molded foams into desired pieces, most often used in the automotive industry.[138] The slabstock process is used to continuously pour the reactant mixture in a moving conveyer, mostly used to produce cushioning and comfort materials, such as mattresses.[139] To produce insulation layers on flat or non-flat surfaces such as roofs, tanks,

and building structures, the spraying technology was developed using high-pressure to directly spray the protected PU onto the desired surface.[140]

Recycling

The PU waste produced commercially and industrially is growing yearly. For example, in 2011 a total amount of 14 million refrigerators were discarded in China, with a PU foam weight of ~6 kg per refrigerator, leading to a PU foam waste of 93 kilotons produced in one year.[141][142] Therefore, producers and industries are putting much effort into recycling possibilities. In principle, several recycling options are possible with I) landfill, II) incineration, III) mechanical recycling, and IV) chemical recycling (see *Figure 7*).[114]

PU foams show a large volume due to their low apparent density. Thus, a great amount of air or blowing agent is trapped in the cells of the foams providing oxygen for fires, leading to reduced success in extinguishing flames. Furthermore, toxic fumes might occur in landfills caused through the PU combustion process. Incineration was studied with automobile seats under grate incineration with exhaust gas recirculation conditions.[143] However, the easiest and most basic way to recycle PU foams is *via* mechanical downcycling, which involves the change of solid waste into flakes, granules, or powder. These materials can be then used to fill e.g., pillows, toys, or they are used as substrates for further processes.[144] The usage of waste PU powder in the manufacture to new PUs is limited due to the change in viscosity to PU foams and the reduced product quality.[145] With mechanical reprocessing, the PU foam waste in form of pellets can be used to re-bond to adhesives which can be then used for the manufacture to car mats or covers of tires.[146] Also, rigid PU foams can be recycled in hot compressing molding to be reused as dashboards or door panels.[147] The chemical recycling of used feedstocks is based on the conversion of PU foams into smaller molecules through e.g., hydrolysis, glycolysis, aminolysis, or gasification. Compared to mechanical recycling, the chemical recycling is much more demanding with higher costs, needed energy for reaction temperatures, and additional substrates.[142][144]

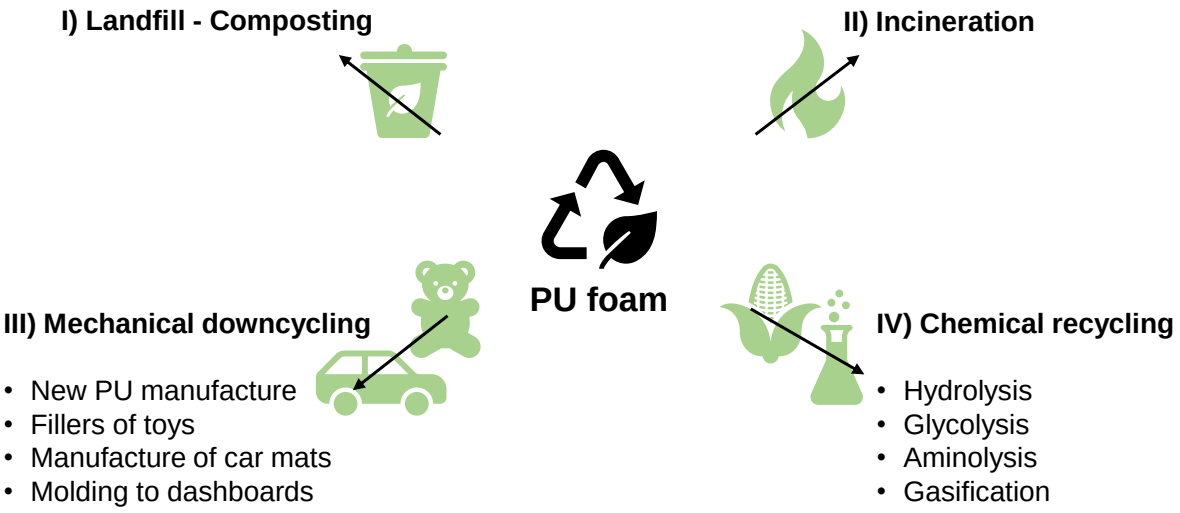

Figure 7. Possible ways to recycle PU foams through I) landfill via compositing, II) controlled incineration, III) mechanical downcycling into flakes, granulates or powder, IV) chemical recycling of used feedstocks.

2.3.3 Renewable Alternatives to Industrially Synthesized Polyurethanes

In terms of Green Chemistry, industry and academy are currently developing sustainable alternatives to conventional PUs, using monomers derived from renewable feedstock. One way to increase the sustainability of PUs is the use of renewable isocyanates and renewable polyols.[114][148] Carbohydrate-containing biomass have led to the successful large-scale production of diols used as monomers for a biobased polyether polyol synthesis.[114]

Industries developed biobased polyols with e.g., renewable polytrimethylene ether glycols (DuPont) or polytetrahydrofuran (BASF) as well as several polyester polyols with renewable content.[149][150] Natural oils from seeds of oilseed plants can be epoxidized *via* a two-step process to biobased polyols. The most attractive oils are palm oil, soybean oil, and rapeseed oil which were implemented in the industrial large scale production.[132][133] The compatibility and hydrophobicity of polyester polyols is industrially improved by using renewable glycerol and fatty acids incorporated into polyesters or polyester-ether polyols. These polyols can then be used in the PU foam production by adding physical blowing agents.[151] Furthermore, biodiesel and crude glycerol can be used for the synthesis of polyols implemented in the rigid PU foam production.[114][152] Aromatic polyester polyols are obtained from PET or the renewable FDCA, reacting in an esterification with renewable aliphatic dicarboxylic acids such as adipic acid (AA) and sebacic acid (SBA). Such a fully biobased aromatic polyester polyol was implemented in the rigid PU foam production using renewable FDCA and diethylene glycol.[153]

Several studies about the sustainable synthesis to isocyanates are reported in literature. As an alternative to the commonly used synthesis to TDI and MDI, a phosgene-free route was reported as reductive carbonylation of aromatic nitro compounds, in 1967.[154][155] However, high temperatures as well as high pressure were needed and toxic-catalyst residues were detected.[125] Another phosgene-free route was reported as two-step carbonylation to *N*-phenyl carbamates in the presence of alcohols followed by thermal decomposition to isocyanates.[155] Different catalytic systems for this route were studied with e.g., platinum complex catalysts.[155][156] Rearrangement reactions were developed by Curtius, Hofmann, and Lossen yielding isocyanates *in situ* without the need of phosgene.[157][158][159]
Recently, Le and Ganem reported an efficient route to isocyanates starting from isonitriles. An eco-friendly procedure in which isocyanides are oxidized to isocyanates using dimethyl sulfoxide and trifluoroacetic anhydride as catalyst.[160] Renewable raw materials for the synthesis to isocyanates are reported with vegetable derivatives such as soybean or castor oil and other renewables such as isosorbide.[161]

However, future PUs must be non-toxic, non-hazardous, with low impact on the environment. Thus, the trend of nowadays research is on non-isocyanate polyurethanes (NIPUs). In the literature, several studies are reported including I) rearrangements, II) polycondensation, III) polyaddition reactions, and IV) ROP to NIPUs (see *Scheme 3*).[162]
Rearrangement reactions are promising routes with *in-situ* production of isocyanates, which then react with alcohols to the desired PUs.[163] Also, a Lossen rearrangement to NIPUs is reported using renewable carbamate monomers with sustainable dithiols in thiol-ene reactions to the desired polymer.[164] For polycondensation reactions, several opportunities to NIPUs are reported such as the reaction of polycarbamates with polyols, or polycarbonates with polyamines.[162] A promising sustainable synthesis was reported as a polycondensation reaction of dimethyl carbamate monomers or ethylene carbonate and diamines with diols.[165]
Polyaddition reactions can be used to react bifunctional cyclic carbonates with diamines to NIPUs, more particular poly(hydroxy urethane)s (PHU).[166][167][168] ROP of aliphatic cyclic urethanes is reported to successfully synthesize NIPUs as well.[169][170] The synthesis to the needed cyclic urethanes was developed in a sustainable way by reactions of alkylene diamines or amino alcohols with e.g., diallyl carbonate.[125][171]

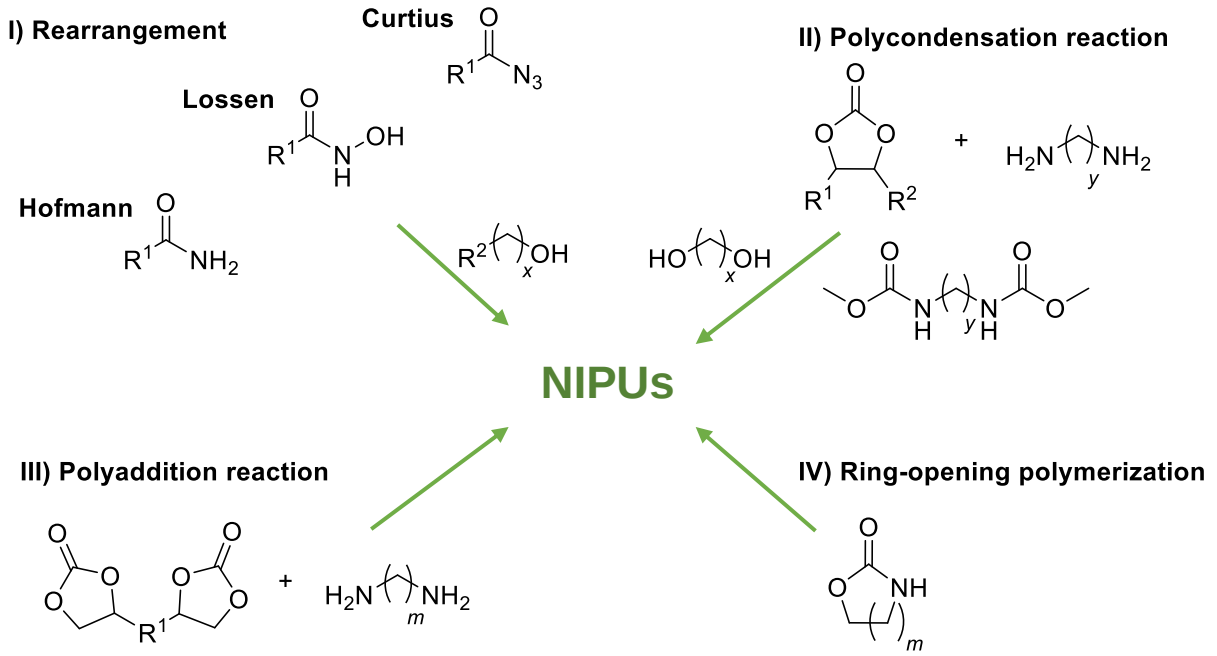

Scheme 3. General reaction schemes of in literature reported strategies to sustainable synthesized non-isocyanate polyurethanes (NIPUs) with I) rearrangement (Lossen[159], Hofmann[158] and Curtius[157]), II) polycondensation reaction (dimethyl carbamate with diols or cyclic carbonates with diols and diamines[165]), III) polyaddition reaction (bifunctional cyclic carbonates with diamines[167]) and IV) ring-opening polymerization (cyclic urethanes[170]).

Besides the already mentioned most common syntheses possibilities to NIPUs, further developments are reported in literature. Another interesting route is based on carbon dioxide, replacing phosgene. Carbon dioxide as abundant and renewable monomer leads to cyclic urethanes and polymers with urethane and amino units by reacting with aziridines.[75][125][172] Furthermore, it is worth to mention the AB-type polyaddition method discussed by Cramail *et al.* to obtain fully biobased NIPUs.[173] Fatty acid derivatives such as ricinoleic acid, methyl oleate and methyl 10-undecanoate were polymerized in bulk to the desired polymer. The major drawback is the rather low M_n of obtained NIPUs.[174][175]

In 1957, the preparation of NIPUs based on ethylene glycol was reported by Dyer and Scott.[176] Since then, this polyaddition reaction became more and more established.[177] Nowadays, a variety of routes is reported to synthesize the reagents of the desired polymerization with the use of renewable feedstock.[117] For instance, the use of renewable cyclic carbonates and amines gained interest. The main advantage in using cyclic carbonates and amines instead of isocyanates and polyols, for the synthesis to PUs, is the reduced toxicity of these compounds.

For instance, ethylene carbonate shows a toxicity of >10 g kg^{-1} (LD_{50}, oral, rat), whereas the industrial used isocyanate hexamethylene diisocyanate shows a toxicity of <960 mg kg^{-1} (LD_{50}, oral, rat).[126][127][178] However, mostly catalysts are needed during the reaction of cyclic carbonates and amines, because of the lower reactivity compared to isocyanates.[179] The primary reagents to NIPUs are differentiating between 5- to 7-membered rings. 5-Membered rings have been reported in literature more often compared to larger rings, since they are produced more easily.[180] *Figure 8* gives an overview about the industrially mostly used cyclic carbonates.

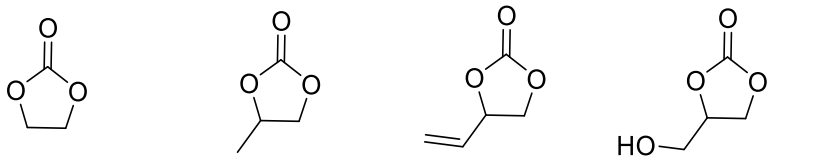

Figure 8. Most common industrially synthesized cyclic carbonates.

The most common and also industrial way to 5-membered cyclic carbonates is the use of carbon dioxide, which gets inserted into epoxides.[181][182] The first catalyzed reaction of carbon dioxide and epoxides was reported in 1969 to synthesize polymers with carbonate containing linkages.[183] Since then, catalytic systems of this reaction were researched and reported in literature as well as the employment of a variety of epoxide substrates. A common example for a biobased epoxide substrate is limonene oxide.[184][185] Often, Lewis Bases are reported to act as nucleophiles in such reactions, with the combination of Lewis Acids showing one or more metal centers.[182]

Recently, the use of DMC in polycondensation reactions was reported, acting simultaneously as reagent and solvent. DMC covers fundamental aspects in terms of Green Chemistry, being non-toxic (LD_{50}, oral, rat >5 g kg^{-1}), biodegradable with little to no environmental impact, thus, widely used as organic solvent.[186][187] Our group recently reported a direct condensation of diols using DMC catalyzed by 1,5,7-triazabicyclo[4.4.0]dec-5-ene (TBD) as superbase (see *Scheme 4*).(*)[188][189] Renewable and biodegradable diols such as EG and PG are reported to be simply transferred into cyclic carbonates during such condensation reactions.[190][191]

(*) A superbase is defined as base, which resulted from mixing two bases leading to new basic species. Superbases are organocatalysts, used to replace organometallic catalysts and enzymes.[188][189]

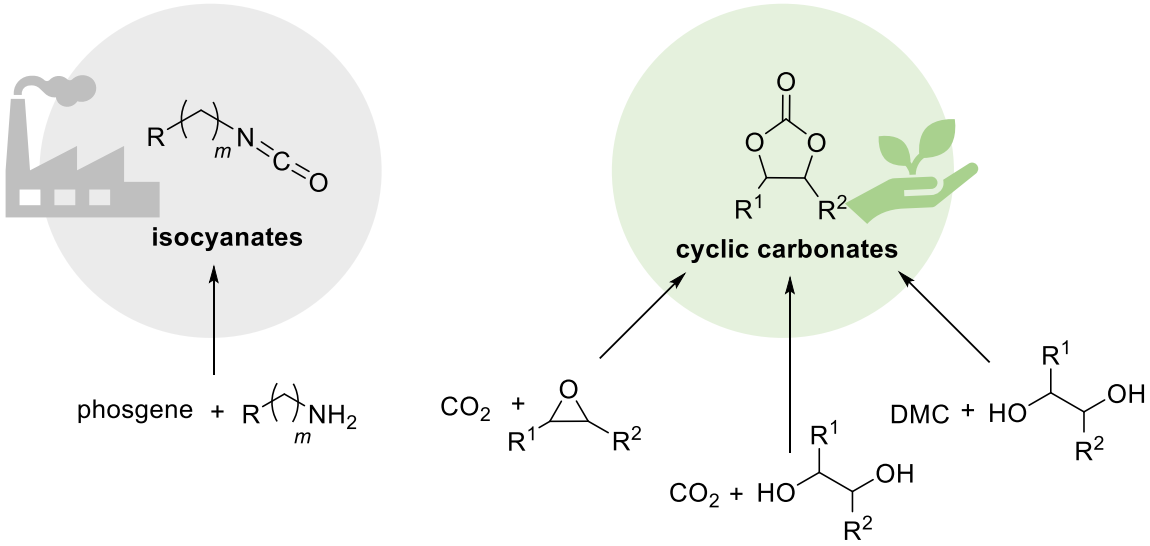

Scheme 4. General chemical reaction scheme to isocyanates versus sustainable syntheses strategies to cyclic carbonates. Three strategies are depicted with carbon dioxide and epoxides[182], carbon dioxide and diols[192], as well as the use of dimethyl carbonate (DMC) and diols[188] to cyclic carbonates. Isocyanates are primary reagents to polyurethanes, and cyclic carbonates lead to non-isocyanate polyurethanes, more precisely, poly(hydroxy urethane)s.

The synthesis to 6-, 7-, or 8-membered cyclic carbonates was demonstrated in a sustainable manner by using carbon dioxide and diols. Here the organic base, 1,8-diazabicyclo[5.4.0]undec-7-ene (DBU) was used in combination of a tosyl chloride/triethylamine as catalytic system.[192] Besides TBD, also DBU is a commonly used organocatalyst (see *Figure 9*).[189][193][194]

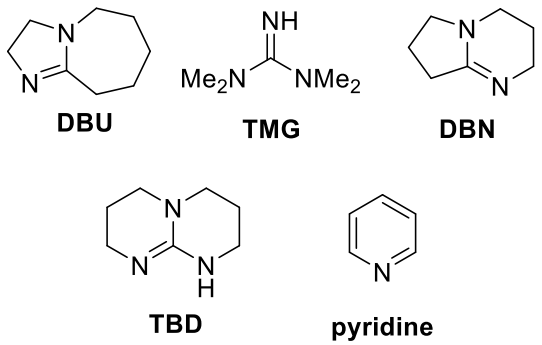

Figure 9. In organic reactions commonly used organocatalysts with 1,8-diazabicyclo[5.4.0]undec-7-ene (DBU), 1,1,3,3-tetramethylguanidine (TMG), 1,5-diazabicyclo[4.3.0]non-5-ene (DBN), 1,5,7-triazabicyclo[4.4.0]dec-5-ene (TBD) and pyridine.

Suitable key intermediates for the direct conversion to NIPUs are carbamates polymerized *via* transurethanization reactions.[125] It is literature reported to synthesize such carbamates by using phosgene or its derivatives in combination with alcohols and amines.[120] However, phosgene and its derivatives are toxic, thus, cyclic carbonates are certainly a promising alternative to sustainably synthesize carbamates.[125] A suitable method is the reaction of amines with cyclic carbonates, which was reported by Garipov *et al.*, in 2003.[195] Despite the use of amines to ring-open cyclic carbonates, also the use of amino acid methyl esters is reported in literature.[179] Methyl 10-undecenoate was investigated as starting material for the polymer synthesis to AA and AB-type-monomers.[174] *Scheme 5* gives an overview about the in literature reported ways to sustainably synthesize carbamates based on cyclic carbonates.

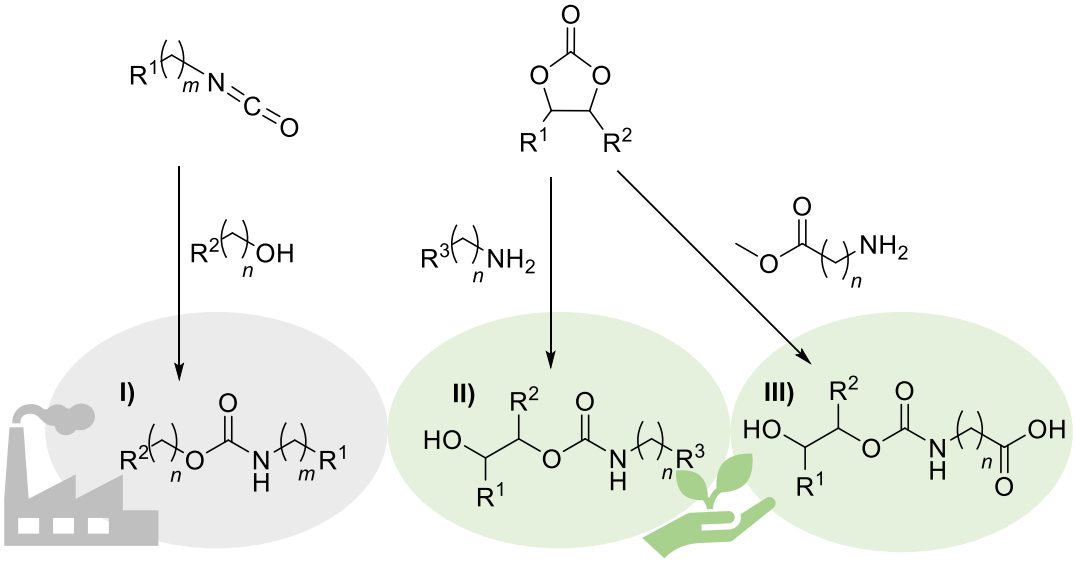

Scheme 5. General reaction schemes to carbamates. I) Traditionally based on isocyanates versus the synthesis to carbamates based on renewable cyclic carbonate by II) reacting with amines[195] or III) using amino acid methyl esters[179].

The final step to NIPUs, more precisely PHUs, is the polymerization of carbamates, which was reported to be performed at increased temperature, as the viscosity during polymerization is increasing. Furthermore, increasing temperature largely increases the reaction rate and decreases hydrogen bonding. However, side-reactions, such as amidification, can occur if temperatures are set >120 °C. Therefore, polymerizations to NIPUs mostly run for several hours or days <120 °C.[115][162][180] Different catalytic systems were investigated with which TBD leads to high M_n PHUs.[196][197] Our group investigated a polycondensation of dimethyl carbamates and diols, in which TBD was identified as the catalyst leading to the highest M_n polymer when adding incrementally. As temperatures were increased >120°C, TBD

would degrade, thus, three portions of catalyst were added stepwise when increasing the reaction temperature.[165]

The NIPU investigations opened a broad window of opportunities to renewable PU materials. All investigated NIPUs show different polymeric properties and some show advantages compared to common industrial synthesized and in daily life implemented PUs. An example is the application of NIPUs in the coating industry, showing long corrosion protection and a good robustness compared to conventional PU coatings.[198] Furthermore, NIPUs are implemented in the foam manufacture to rigid, flexible, and soft biobased foams.[153][199] In the biomedical industry, researchers were focusing on NIPUs to avoid the traditional toxic isocyanate-based thermoplastics and found application of renewable PHUs for example as hydrogels.[200]

Further improvements are in progress to further adjust the properties of NIPUs and PHUs synthesized with biobased building blocks, which fulfill the requirements for a wide range of applications.[180][201]

2.4 The Class of Polyesters

Polyesters are a ubiquitous polymer class, in general including all polymers with ester groups in their backbone. The structural units, the connecting ester groups, vary in a broad range, covering versatile polymeric applications.[202] Historically, the first condensation reaction to linear polyesters was investigated by Carothers and coworkers in the 1930s.[203] For the synthesis, trimethyl glycol and hexadecamethylene dicarboxylic acid were used. Fibres obtained from molten polyester had a poor hydrolytic stability and low melting point. In 1941, Whinfield and Dickson discovered PET, which showed a high melting point of 265 °C and a good hydrolytic stability. PET is used in today's industrial production of synthetic fibres, films, beverage bottles, and plastics, as the most widely used polyester.[204] Many other aromatic polyesters have been studied from that on, with poly(butylene terephthalate) (PBT) being used as insulator in the electrical industry for more than 50 years.[205]

In general, polyesters are thermoplastic, water resistant, and typically biodegradable with exception of polyesters showing extensive aromatic backbones.[206]

Despite aromatic polyesters, also semi-aromatic, and aliphatic polyesters were investigated over the last decades. Semi-aromatic polyesters show properties suited for the use as liquid crystalline polymers.[207] Aliphatic polyesters have received attention as potential renewable alternatives to petroleum-based polyesters because of their numerous biobased sources that can be used for their synthesis.[208][209] Furthermore, aliphatic polyesters show an increased biocompatibility and can be used in versatile applications from specialized biomedical devices to bulk packaging.[210]

This chapter gives an overview of conventional synthetic routes to polyesters, environmental concerns, and sustainable developments towards biobased polymeric materials.

2.4.1 Conventional Synthetic Routes to Polyesters

One typical route of polyester syntheses is a two-step polycondensation. Through a transesterification, using dimethyl esters and diols, or an esterification using diacids and diols, oligomers are formed. A polycondensation in melt follows, to form the desired polyester (see *Scheme 6*). This step-growth polymerization to polyesters involves harsh reaction conditions, with high temperatures (>200 °C) and reduced pressure (<1 mbar) as well as long reaction times (10 to 15 hours).(*)[211]

Due to the step-growth mechanism, high monomer conversion is required to obtain high molecular weight polymers, which will in general show dispersities of approximately 2.[205][212]

Catalyst-free Brønsted Acid Ionic Liquids were investigated as greener reaction medium, enabling to perform the synthesis of polyesters under milder reaction conditions.[213][214] Furthermore, an alternative synthesis routes based on highly selective enzymatic polymerization reactions with lipases as catalyst were investigated.[215] However, the costs to synthesize suitable ionic liquids or enzymes are the key limitations of both approaches.[216]

A common synthesis route towards aliphatic AB-type polyesters is represented by ROP, which follows a step-growth mechanism and typically proceeds under milder temperatures than in the case of step-growth polycondensation (see *Scheme 6*). Furthermore, no condensates are produced during a ROP polymerization reaction, thus, there is no requirement of high vacuum. Such chain-growth polymerizations can offer high molecular weight polyesters with controlled dispersities. Poly(lactone) is a common example of a polyester obtained by ROP. The major drawback of a ROP based synthesis route is the limited range of cyclic monomers that can be polymerized, resulting in a limited range of properties of the final product.[217][218]

An emerging trend in the polyester synthesis is a chain-growth copolymerization route involving epoxides and cyclic anhydrides under mild reaction conditions. For this copolymerization, a diverse array of metal complexes has been used as catalysts.[210] However, further improvements are necessary to increase the catalyst efficiency and the molecular weight of obtained polyesters.[216]

(*) A step-growth polymerization needs difunctional monomers through which a reaction between both functional groups is possible, forming a dimer. The dimer may react further with a monomer to a trimer and so on. This process continues until, over a relatively long period of time, a polymer is formed.
For further information, see J. K. Stille.[211]

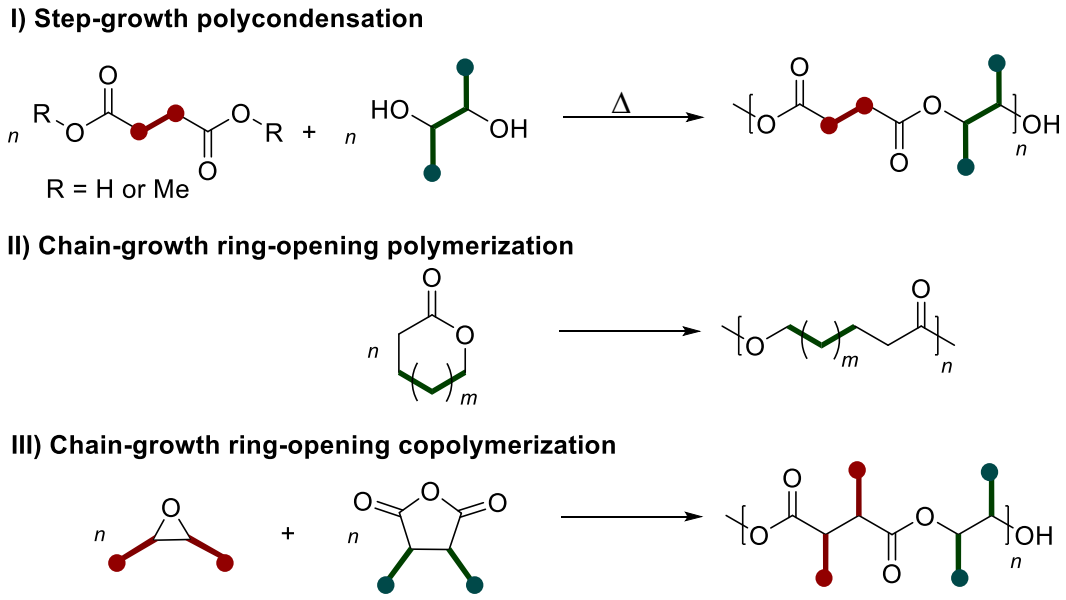

Scheme 6. Schematic representation of conventional syntheses routes to polyesters. I) step-growth polymerization reaction of diols and diacids or diols and dimethyl esters performed at high temperatures and low pressure, II) chain-growth ring-opening polymerization and III) chain-growth ring-opening copolymerization. The colors indicate possible modifications of the polyesters and its monomers.

For the industrial manufacture of the most widely used polyester, PET, a two-step polycondensation reaction is performed using purified terephthalic acid (TPA) and EG (see *Scheme 7*). TPA is industrially synthesized from *p*-xylene, which is catalytically formed from a petroleum based BTX mixture (benzene, toluene, xylene isomers) and air-oxidized in acetic acid. A main impurity in TPA is 4-carboxybenzaldehyde (4-CBA). The aldehyde group would act as chain terminator in PET polymerization. Thus, TPA needs to be purified before further used.[205] This purification is challenging because of the similar structure of TPA and its main byproduct 4-CBA.[219] After recrystallization, the pure TPA is used in esterification with EG, performed at reaction temperatures around 240 - 260 °C, without catalyst. The oligomeric intermediate bis-(2-hydroxylethly) terephthalate (BHET) is formed. Subsequently, the polycondensation is performed in an evacuated low-pressure reactor at 280 °C for 5 to 10 hours. At these high temperatures and low pressure, byproducts such as water and alcohols are removed from the system. Here, a catalyst is needed, with antimony acetate used in industry, to polymerize BHET to PET.[205][220][221][222]

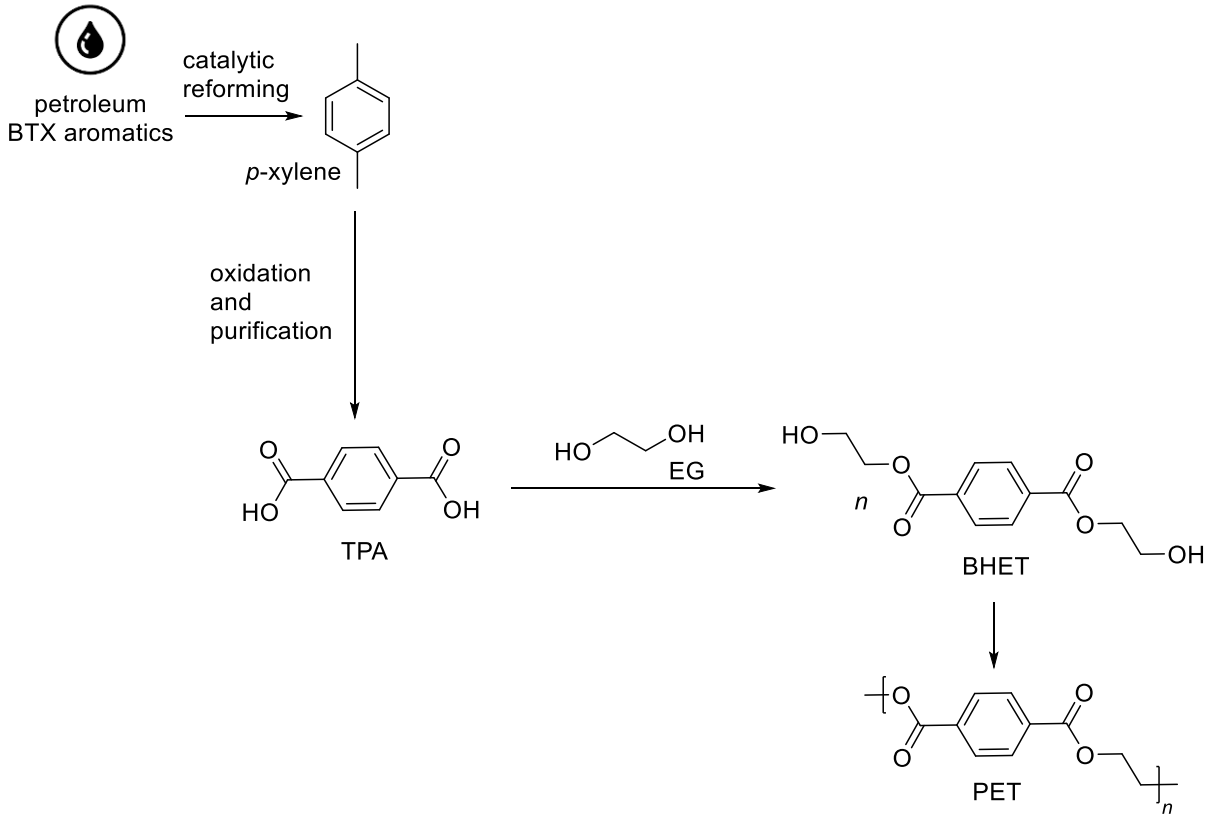

Scheme 7. Industrial manufacture of poly(ethylene terephthalate) (PET), starting from petroleum to synthesize p-xylene which is further oxidized to terephthalic acid (TPA). Purified TPA is then used in an esterification with ethylene glycol (EG) to form the oligomeric bis-(2-hydroxyethyl) terephthalate (BHET) being polymerized in a polycondensation reaction to form PET.

During the time of the PET development, several catalyst screenings were researched to further improve the PET process. Germanium oxide was studied by MacDonald and zinc acetate and manganese acetate were studied by Tomita *et al.*.[223][224] The use of metal catalysts was furthermore studied by Shah *et al.*.[225] However, antimony oxide historically emerged as the catalyst of choice given the balance between catalytic activity and cost.[205] Recently, antimony-containing compounds have been questioned because of their potential hazard to health, thus, there is an ongoing research for new catalytic systems.[205][216] Meanwhile, less toxic Lewis Acid catalysts, such as titanium(IV) butoxide, were identified to successfully replace antimony catalysts for industrial scale PET synthesis.[113]

2.4.2 Renewable Alternatives to Industrially Synthesized Polyesters

Facing the environmental problems associated with plastic production, the carbon footprint needs to be reduced, to decrease the impact of human on the environment. One possibility for an increasing sustainability is the exploitation of renewable monomers for industrial processes

to polyesters. Polyesters, with a broad range of applications such as clothing, food packaging, and biomedical devices, must be reinvestigated to find greener synthesis strategies compared to conventional routes.[113][226][227][228]

Some investigated strategies to produce biobased polyesters already gained industrial interest and are summarized in this chapter.

As PET shows excellent properties for versatile applications, much effort has been taken to find a suitable synthesis routes towards biobased PET.[216] EG and TPA are the key raw materials for the manufacture of PET. Thus, to increase the sustainability, bio-EG and bio-TPA can be used in the PET process. The former can be produced from bio-ethanol, derived from the fermentation of sugars such as glucose and sorbitol or directly from cellulose.[72] Using bio-EG in the established synthesis route generates a ~30% plant-based PET which was introduced by Coca Cola.[229] To obtain 100% plant-based PET, it is necessary to access bio-*p*-xylene as raw material for TPA. Several synthesis routes were investigated, e.g., the isolation of *p*-xylene from a BTX mixture (benzene, toluene, and xylenes). This mixture can be obtained using C_6 sugars that undergo an aqueous phase reforming process and a subsequent dehydrocyclization to successfully form *p*-xylene, as developed by Virent.[72][216] This strategy was used by Pepsi Cola, resulting in a 100% plant-based “green bottle”.[229]

Instead of replacing PET by bio-PET, ongoing research has focused on finding novel polymers based on renewable feedstock to fully replace PET.[230]

Furan(IV) dicarboxylic acid

In 2004, FDCA was identified by the U.S. Department of Energy as one of the twelve sugar-based building blocks with the greatest potential to produce biobased chemicals and materials.[231][232] FDCA is a rigid diacid derived from lignocellulosic fructose by oxidation of 5-hydroxymethylfurfural (HMF) (see *Scheme 8*). First, glucose is produced by acid-catalyzed hydrolysis of cellulose and hemicellulose followed by a series of oxidation steps to HMF and then FDCA, depending on the used catalytic system.[69] For instance, initial oxidation of the aldehyde functional group of HMF leads to 5-hydroxymethylfuran-2-carboxylic acid (HMFCA), whereas initial oxidation of the alcohol group results in 2,5-diformylfuran (DFF).[233][234] Further oxidation of these products lead to the formation of 5-formylfuran-2-carboxylic acid (FFCA) and ultimately the production of FDCA. For this route, several catalytic systems were developed, such as the use of homogeneous metal salts and enzymes.[69][235]

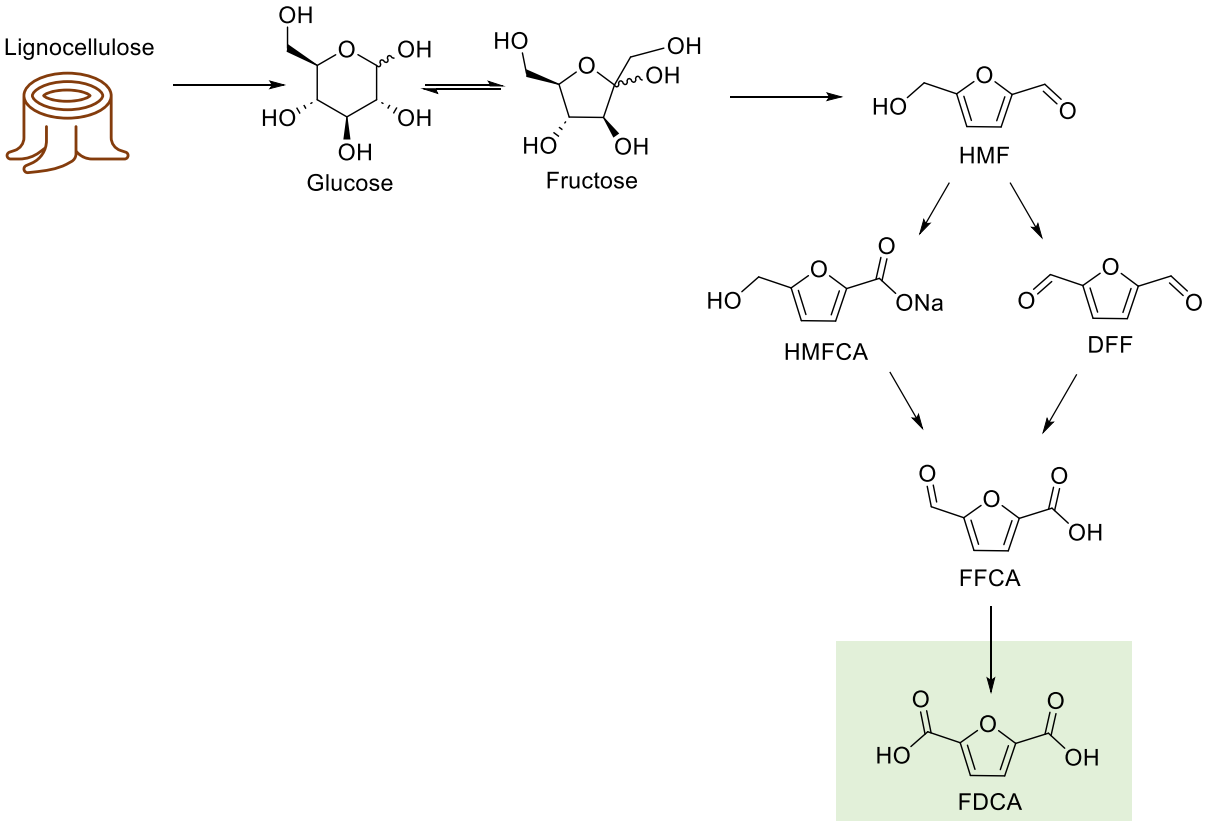

Scheme 8. Simplified scheme of the synthesis route to renewable furan(IV)dicarboxylic acid (FDCA) starting from lignocellulose. 5-Hydroxymethylfurfural (HMF) is produced from the sugars of lignocellulose with further oxidation possibilities to be converted into 5-formylfuran-2-carboxylic acid (FFCA) and further oxidized to FDCA.[69]

As renewable aromatic dicarboxylic acid, FDCA is a potential alternative to fossil-based TPA. Biobased poly(ethylene furanoate) (PEF) was studied for its potential to replace PET. Besides, using the from lignocellulose produced FDCA, also renewable EG produced *via* fermentation, is used in the process.[230][236]

The biobased polyester PEF can be used for the manufacture of bottles with improved barrier properties, if compared to PET bottles, such as gas permeability of oxygen, carbon dioxide, and water. Also, the T_g of 86 °C (PEF) (PET: T_g = 74 °C) is more attractive with its higher ability to withstand heat. Moreover, PEF shows a melting temperature (T_m) of 235 °C compared to the T_m of PET at 265 °C (see *Figure 10*). Thus, the manufacture temperature of PEF can be decreased compared to the process temperature to PET. Furthermore, the greenhouse gas emissions of the PEF production can be a cut down by about 50% compared to that of fossil-based PET.[237][238]

The switch from corn-based PEF to the usage of lignocellulose from agriculture waste would further result in a reduction of greenhouse gas emissions.[72][236]

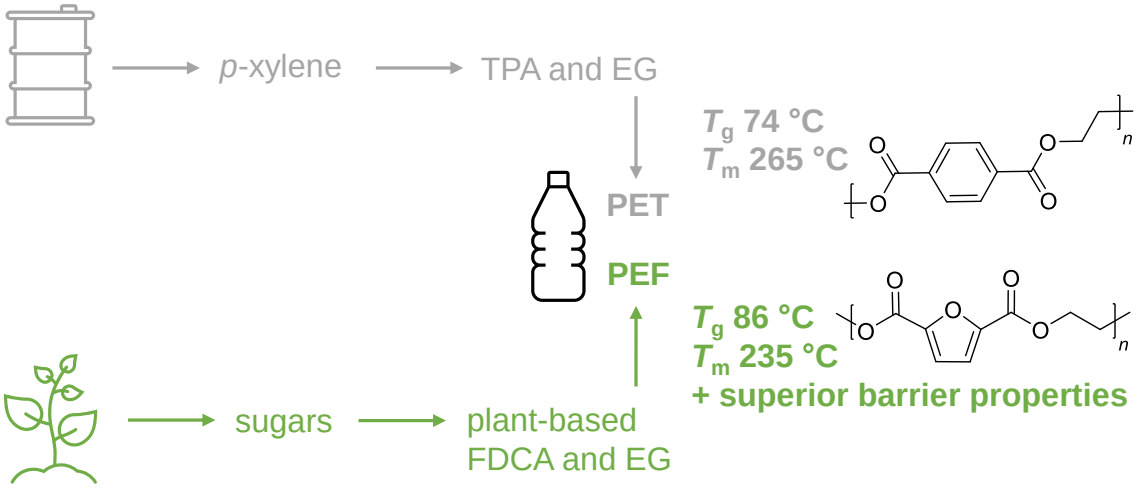

Figure 10. Comparison of industrially produced PET from petroleum to 100% plant-based PEF, as sustainable alternative.[236]

Besides the established PEF, a large number of polyesters synthesized from renewable FDCA were developed, with FDCA therefore known as the "*sleeping giant*".[228] Zhou *et al.* reported the synthesis of furan-based polyesters using a series of C_3 to C_8 diols in a direct polycondensation reaction. Polyesters based on FDCA and 1,3-propanediol, 1,4-butanediol, 1,6-hexanediol, or 1,8-octanediol showed T_g values of 21 °C up to 89 °C and T_m values of 148 °C up to 210 °C. Thus, T_m and T_g were decreasing compared to PEF (T_g 86°C, T_m 235 °C) and PET (T_g 74 °C , T_m 265 °C).[239] Bikiaris *et al.* investigated polyesters based on FDCA and longer diols (C_8 to C_{10} and C_{12}). Here, the more ductile polyesters showed even lower T_g values of <0 °C and inferior mechanical properties. This study revealed that the critical parameters to obtain polyesters with useful properties is not only a high molecular weight, which can be adjusted by reaction temperature and reaction time, but, also the length of alkyl groups in the polymer backbone highly influence the T_g and T_m, paired with mechanical properties.[240] With 1,20-eicosanediol and FDCA an aliphatic polyester was introduced by Sousa *et al.* showing a T_m of 107 °C and T_g around 7 °C, with biodegradable properties.[241]

Furthermore, the constitutional isomers of FDCA are reported in literature. Thiyagarajan *et al.* investigated the influence of 2,5-FDCA compared to 2,4-FDCA and 3,4-FDCA in poly(1,4-butylene furan dicarboxylate) (PBF) and PEF. By measuring the polymer properties, a difference was observable with higher glass transition temperature and degradation temperature for 2,4-PEF, compared to 2,5-PEF and 3,4-PEF. Thus, the lower symmetry of the former indeed showed an influence on the polymer property, expected to be caused due to a different dipole moment in the polymer backbone.[242]

A major drawback in the development of FDCA based polyesters, are the high costs to obtain sufficient amounts of high purity FDCA. However, scientists and industry do think that the prices will decrease with the increasing interest on this renewable monomer, paired with increasing possibilities in implementing FDCA in the polyester industry.[222][243]
Another major problem in FDCA based polyester synthesis was discussed by Gubbels *et al.* and is related to the discoloration of the final product. It was reported that the origin of discoloration can mainly come from 1) sugar-based impurities, 2) side reactions such as decarboxylation, c) the presence of additives, 4) leftovers of catalyst. To overcome this problem, different antisolvents were tested, the previous purification of FDCA was reported as well as the use of FDCA methyl ester, to successfully decrease the discoloration.[244]
However, among all reported renewable FDCA based polyester investigations regarding different properties of obtained polymers, PEF remains the most promising FDCA based polyester with its similar or even improved properties compared to PET.[228]

Succinic acid

Another dicarboxylic acid with potential to become a main future platform chemical derived from renewable resources is succinic acid (SA). SA is an intermediate of the tricarboxylic acid cycle which is used for the biotechnological production of SA. Various species of fungi and gram-positive bacteria have been screened and studied for SA production, including microorganisms that consume carbon dioxide.[245] R. Koch proved that SA shows no risk of accumulation in the human body and therefore can be used in the food industry.[246][247] Altogether, SA is a versatile potential building block for the use in the niche of personal care products, as food additive, and for the manufacture of bio-polyesters, polyamides, and poly(ester amide)s.[248] Similar to FDCA, SA was classified by the U.S. Department of Energy as one of the twelve most promising future chemical biobased building blocks.[232]
Poly(butylene succinate) (PBS) based on fossil raw materials is implemented in industry. The biobased synthesis of PBS gained great attention as novel biobased polymer based on renewable SA and 1,4-butanediol (see *Scheme 9*).[249][250] The polyester production capacity is expected to grow with the profit of the used biobased SA production which is cheaper compared to the petrochemical alternatives. Some producers already gained interest to use the biobased polyester for commercial applications. The crystalline polyester shows a T_m of 100 °C and a T_g of -32 °C paired with high molecular weight (>100 kDa).[248][250][251]
Comparing the properties of PBS with commercial polymers, it is best suited to substitute fossil-based low density polyethylene (LDPE).[250] Mitsubishi Chemical Corporation has developed its own biodegradable plastic based on SA and 1,4-butanediol.[252] Furthermore, the

packaging industry has a considerable interest to use PBS as biobased and biodegradable alternative to non-biodegradable PE.[248]

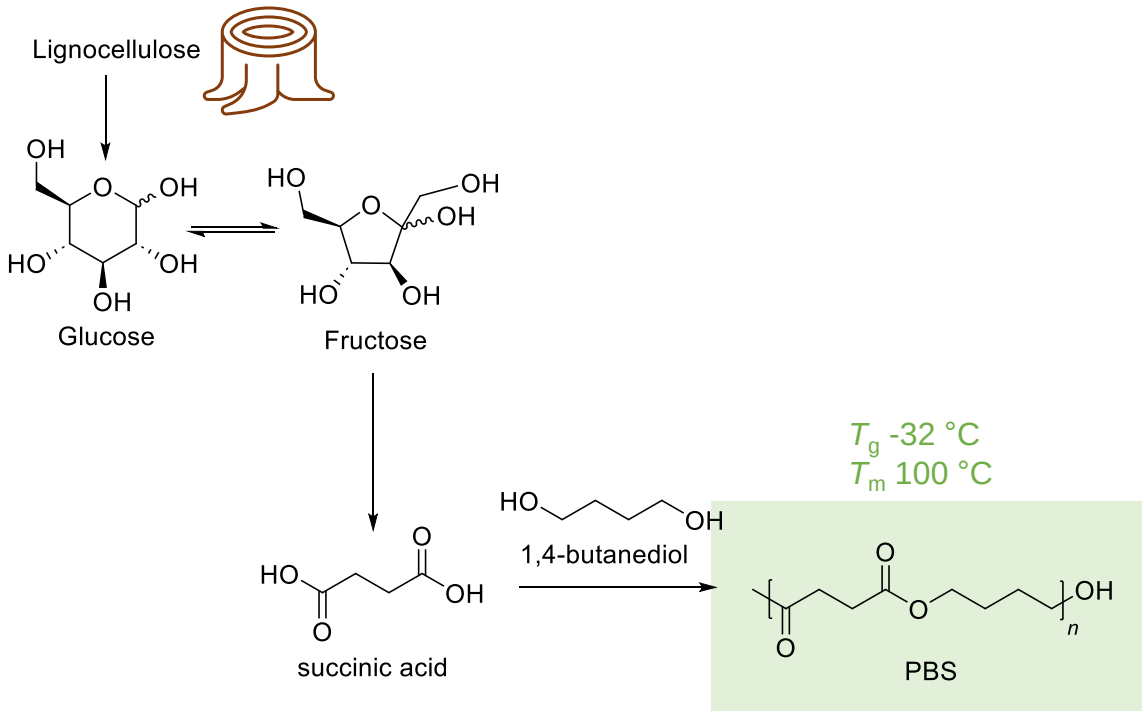

Scheme 9. Simplified scheme of the synthesis route to biobased polybutylene succinate (PBS) using succinic acid (SA) and 1,4-butanediol obtained from lignocellulose fermentation.[248]

The properties of PBS can be tuned by copolymerization with other dicarboxylic acids or diols.[249][250] Copolymerization can result in different polymeric properties, for instance decreased melting points, lower tensile strength, or higher elongation at break. A typical two-step polycondensation was studied by using SA, 2-methylsuccinic acid, and 1,4-butanediol to synthesize a biobased and biodegradable polyester, poly(butylene succinate-co-butylene 2-methylsuccinate).[253] Here, a constant melting point was observed with a copolymer composition of up to 20 mol%.[254] Moreover, copolymerization with AA and with biobased 1,3-propanediol was researched.[250][255] With a AA content of up to 15 mol% in PBS, a higher degree of crystallinity and tensile strength was observed, compared to PBS. The properties of a PBS copolymer with 1,3-propanediol was limited because of a low melting point at 50 °C.[250]

However, industrial processes of SA obtained *via* fermentation are not state of the art yet. The fermentation to SA needs further improvements. Thus, further investigations to promising SA based polymeric materials are ongoing.[247]

Adipic acid

AA is one of the largest volume commodity chemicals, regarded as a pivotal building block for a range of processes in the chemical, pharmaceutical, and food industry. Approximately 75% of the overall production of AA is utilized towards the polymerization to Nylon-6,6 *via* polycondensation with hexamethylenediamine.[256][257] Furthermore, AA can be used as raw material for the synthesis of polyurethanes or polyesters (see *Scheme 10*).[258][259][260]

Multiple sustainable routes to AA have been designed as alternatives to the current fossil-based production. The three most promising production pathways of AA are 1) a chemical catalytic process, in which glucose is catalytically oxidized followed by hydrodeoxygenation using potassium perrhenate and palladium on carbon as catalysts. 2) Indirect fermentation can be performed by producing precursors of AA from glucose.[70] 3) Direct fermentation represents the most interesting way to synthesize AA, using genetically modified yeast species as cheap commercial feedstock (see *Scheme 10*).[261] With this approach, the greenhouse gas emissions of the AA synthesis can be reduced from 78% to 62%, compared to conventional used fossil-based processes. Here, the emissions are calculated with estimation of a biobased production causing ~4.87 kg carbon dioxide per kg AA.[262][256] However, the large-scale biobased production of AA is still hindered by some lacks in the developed synthesis pathways and therefore not yet implemented in industry.[261][256] *Scheme 10* gives an overview on the conversion of lignocellulose *via* fermentation to AA. Furthermore, a cake chart is depicted to schematically show the ratio of the main usage of AA in the Nylon industry, compared to the usage in the polyester and polyurethane manufacture.

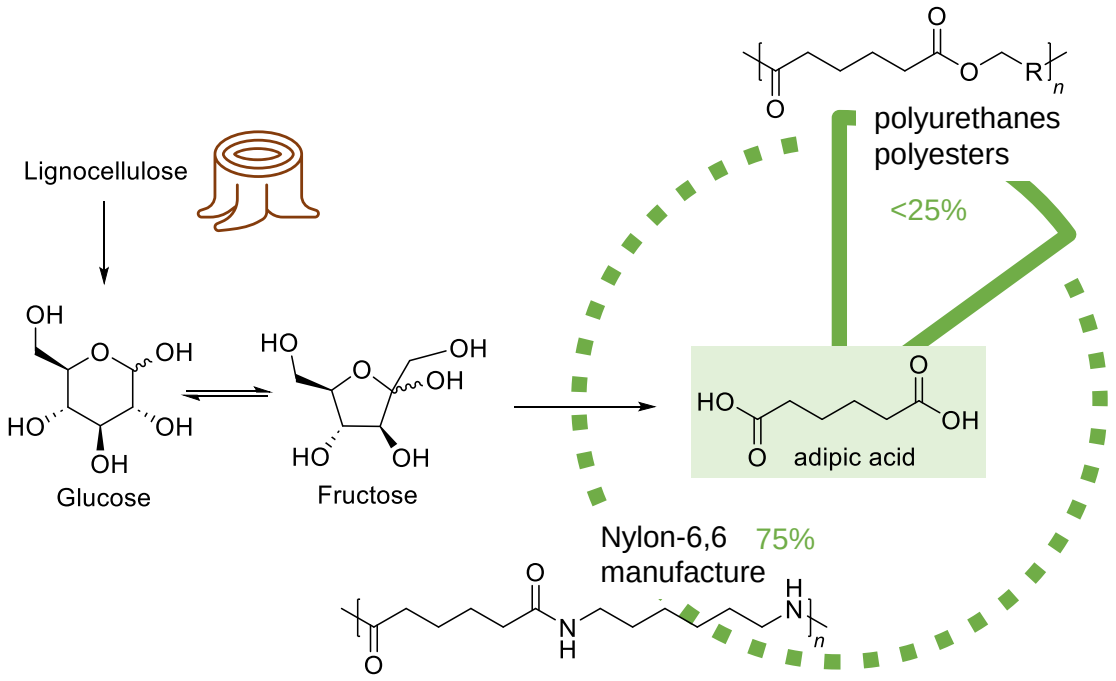

Scheme 10. Simplified scheme of lignocellulosic fermentation to sugars converted to yield adipic acid, mainly used in the manufacture towards Nylon-6,6 and potentially used for the manufacture of biobased polyurethanes and polyesters. With R = Residues.[256]

In the polyester synthesis, AA has been mostly studied in copolymerization reactions with other biobased dicarboxylic acids and diols, like described in the previous chapter about PBS tuning properties.[250][263] Furthermore, AA was investigated as monomer in combination with glycerol to obtain hyperbranched polyesters, which represent an own class of polymers.[264] Still, in the research of biobased polymers, AA remains of high interest as potential biobased alternative. Thus, further investigations are ongoing.[256]

Sebacic acid

The castor oil derived SBA is used in a variety of industrial applications. In the polyamide polymer production, SBA confers important properties such as flexibility, hydrophobicity, durability, and low melting temperatures. In the synthesis to dibasic polyesters, SBA leads to a good flexibility and chemical resistance.[265][266] These versatile polymeric properties can be applied to polyesters when copolymerizing with SBA.[267] Zhou *et al.* performed a copolymerization of FDCA, 1,4-butanediol, and SBA contents of 0 to 20%. Compared to PEF the introduction of SBA led to a decrease of T_m and T_g as well as a lower crystallinity leading to a decrease of tensile strength.[268] Furthermore, SBA is used in the production of lubricants

or the development of biocompatible chitosan- and collagen-based 3D scaffold materials.[265][269]

The traditional route to SBA is by alkaline pyrolysis of ricinoleic acid or castor oil under high temperatures (~280 °C). In this process considerable amounts of sulfuric acid are needed.[270] To increase the sustainability, genetically engineered oxidation of from yeast converted fatty acids was researched to produce SBA. Furthermore, a microbial biotransformation gained interest and is under ongoing investigation.[265]

2.4.3 Catalysis for the Synthesis of Polyesters

One focus in the development of biobased polymers are monomers from renewable feedstock to be used in the polycondensation reactions to polyesters. A common possibility to improve a reaction, with regard to sustainability, is the use of catalysts which decrease the required energy and at the same time often lead to a higher selectivity. Considering Green Chemistry, these catalysts should be non-toxic without environmental impact.[14][27]

Not only the toxicity of some commercially used catalysts, also the use of finite elements as well as high extraction costs, make some catalysts critical from a sustainability viewpoint.[271][272] To define a catalyst as sustainable, no finite elements must be used, organocatalysts must be prepared from renewable feedstock, and the recovery of the catalyst must be considered.[272]

New scientific and technological innovations are needed using efficient catalytic strategies to convert plant-based commodity chemicals into platform monomers, polymers thus, products.[273] In 1894, the term catalysis was defined by F. W. Oswald as followed: "*A catalyst affects the rate of the chemical reactions without being consumed and without influencing the thermodynamic equilibrium of reactant and products*".[274] In many cases, catalytic transformations of reactions are not completely understood, and often the catalytic activity is almost impossible to be predicted in advance. This makes it difficult for scientists to find suitable catalysts for a system.[275]

Lewis Acids are often reported as suitable choice to be used as catalysts in polycondensations of diacids or dimethyl esters and diols. Theses catalysts increase the electrophilicity of the carbon in the carboxylic acid unit and facilitate the nucleophilic attack of an alcohol group (see *Scheme 11*). According to the definition proposed by G. N. Lewis in 1932, Lewis Acids can accept one pair of electrons due to an empty orbital and low electron density.[276]

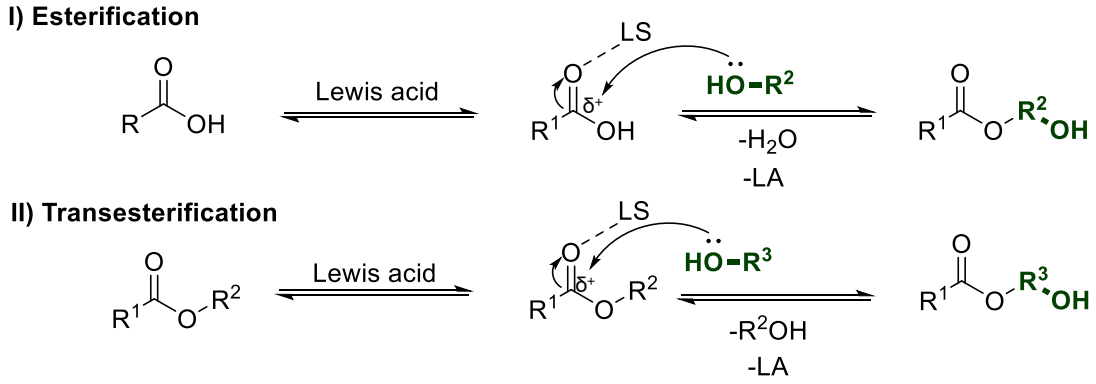

Scheme 11. Interaction of Lewis Acids (LA) catalysts with carboxylic groups of acids I) esterification or methyl esters II) transesterification to facilitate the nucleophilic attack of an alcohol group. R = Residues.

Some metal triflates gained interest in polycondensation reactions because of their strong Lewis acidity. More specifically, bismuth triflate received attention due to its low toxicity and low cost.[277] Gubbels *et al.* identified titanium(IV) butoxide, tin(II)-ethylhexanoate, and zirconium(IV) butoxide as suitable catalysts in the reaction of FDCA and BDO, or dimethyl-FDCA and BDO.[113] Other than that, Khrouf *et al.* identified antimony(II)oxide and Terzopoulou *et al.* screened titanium(IV) isopropoxide (TTIP) as well as dibutyltin(IV) oxide as suitable catalysts for polycondensation of dicarboxylic acids and diols.[278][279] Furthermore, often catalysts are reported containing zinc, copper, magnesium, aluminum, or other ions and chloride as counterion.[277] G. Zhou, J Tang, and M. Jiang *et al.* reported the successful use of a zinc(II)-catalyst to obtain high molecular weight PEF.[280]

All catalyst screenings and future screenings for new catalytic systems often require extensive experimentation. Thus, a high number of time-consuming experiments must be performed leading to a high amount of needed chemicals. Therefore, high-throughput instrumentation has been developed to screen different reaction parameters simultaneously.[275] As an alternative to laboratory scale experiments, Moran *et al.,* investigated the deconvolution method as tool to effectively screen for suitable catalysts in a defined system, by performing a small number of reactions.[281]

First, a mixture of predefined catalysts is added to a system, which is then screened for different reaction parameters such as time, temperature, and solvents. If the catalyst mixture shows activity in successfully producing the desired polymer, the reaction parameters can be set. Then a complex mixture of catalysts is used in one batch at previously defined reaction parameters. This batch is partly separated into smaller batches, to perform several independent reactions until the catalyst leading to the highest product yield or molecular weight

polymer is identified. Therefore, the deconvolution method drastically reduces the number of needed screening reactions.[281] For a better understanding of the principle of this method, an explanation is schematically depicted in *Figure 11*. It must be considered that interactions between the catalysts might influence the overall process, either by increasing their activity or by inhibiting their individual action.[282]

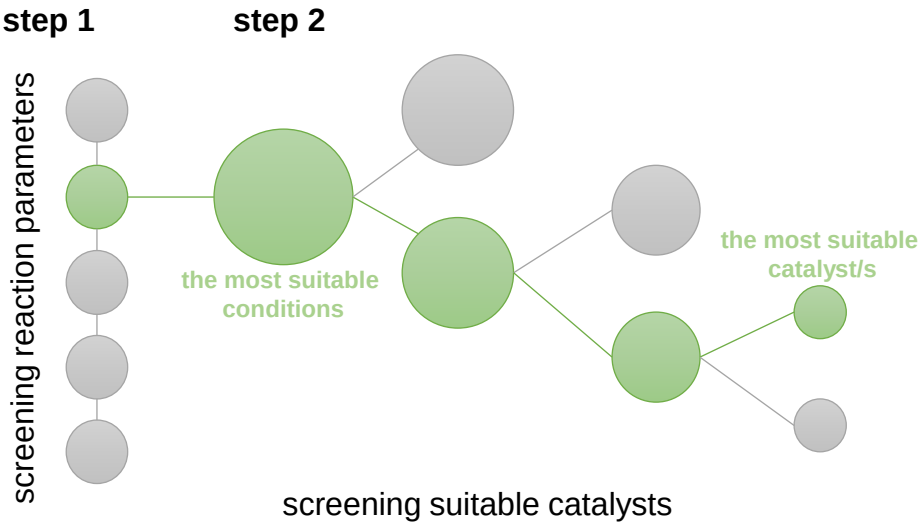

Figure 11. Schematic explanation of the deconvolution method, developed by Moran et al., with step 1: searching of reaction parameters, and step 2: screening of catalysts.[281]

3. Aim of this Work

With the depletion of fossil-based resources, the overall aim of this thesis is to implement renewable resources for the synthesis to biobased polymers. Thus, the focus is on using 2,3-butanediol as renewable platform monomer in the synthesis of novel polymers. Besides using renewable feedstock, several more factors need to be considered to increase the sustainability of processes. In particular the 12 Principles of Green Chemistry give a guideline to design safe and sustainable procedures. However, the fulfillment of all these principles remains challenging, thus, the aim is to cover as many of the 12 Principles as possible within the context of this work. Herein, the focus is on two main polymer classes, with the synthesis of polyurethanes and polyesters.

More specifically, polyurethanes are industrially synthesized with isocyanates coming from toxic phosgene. Thus, the aim of the first project is to investigate a sustainable isocyanate-free route to polyurethanes based on 2,3-butanediol. Considering the Principles of Green Chemistry, organocatalysts are the choice of catalyst to be screened for a full conversion of each reaction step while screening for suitable reaction conditions. Furthermore, the Environmental factor plays an important role, to define the actual amount of waste produced in a reaction, including everything but the desired product. Thus, within all investigated synthesis steps this factor should be as low as possible. Therefore, suitable purification strategies of the obtained products are screened towards this purpose.

Regarding the class of polyesters, biobased materials are industrially manufactured by using renewable ethylene glycol and the sugar-based 2,5-furandicarboxylic acid. Thus, in the second part of this thesis, the focus is on implementing renewable 2,3-butanediol instead of using ethylene glycol in the synthesis of polyesters with the use of the sugar-based dicarboxylic acid. Herein, a simple and fast synthetic procedure is of interest, with an easy precipitation step to isolate the product. Furthermore, a catalyst screening is performed to find the most active catalyst for such polycondensation reactions. By copolymerization reactions with further renewable dicarboxylic acids and 2,3-butanediol, the aim is to find a processable polymer with high molecular weight and high glass transition temperature.

Besides, a fermentation of biobased 2,3-butanediol was achieved by the collaboration partners of the Technical University Hamburg, with which a purification of the diol is aimed to directly utilize this monomer in the synthesis of a desired polyester. Furthermore, the chemical properties of this biobased polymer are of interest.

Overall, this work focusses on the development of environmentally benign routes to biobased polymers, based on 2,3-butanediol, with the aim to replace fossil-based materials. To do so, the 12 Principles of Green Chemistry are implemented in all synthesis strategies.

4. Results and Discussion

Biobased non-isocyanate polyurethanes are discussed in detail in **chapter 4.1. Sustainable Synthesis Strategy to Poly(ester urethane)s based on 2,3-Butanediol**. Furthermore, structural properties of the obtained poly(ester urethane)s are reported and discussed, further resulting in foaming experiments.

Chapter 4.2 Polymerization of 2,3-Butanediol and Renewable Dicarboxylic Acids using Iron(III)chloride as Catalyst provides a detailed overview about the obtained results related to biobased polyesters including a discussion about the deconvolution method, used for a catalyst screening. Polymer properties are disclosed and discussed accordingly. **Chapter 4.3 Polycondensation Reaction of Fermentation-generated 2,3-Butanediol towards a Renewable Polyester** summarizes a purification method of 2,3-butanediol obtained from fermentation. Furthermore, the screening of investigated polycondensation reaction to polyesters with 2,3-butanediol enantiomers is discussed.

4.1. Sustainable Synthesis Strategy to Poly(ester urethane)s based on 2,3-Butanediol

This chapter is based on previously published results by the author of this thesis:

A. Kirchberg, M. K. Esfahani, M. Röpert, M. Wilhelm, M. A. R. Meier, *Macromol. Chem. Phys.* **2022**, 220010.[111]

Text, figures, and data are reproduced from this article and were adopted and modified with permission of the Macromolecular Chemistry and Physics Journal. The author of this thesis developed the synthetic procedures, planned, and evaluated the experiments.

M. K. Esfahani gave input on rheology measurements and wrote the chapter about small-amplitude oscillatory shear and uniaxial elongational measurements.

M. Röpert gave input on the proof-principle and wrote the chapter about foaming experiments.

The bachelor thesis of La, Vinh Hao, co-supervised by the author of this thesis, was about the preparation of cyclic carbonate, carbamate, and polyurethane based on 1,2-octanediol. Further experiments including the separation of constitutional isomers and analyses of polymeric properties were then performed by the author of this thesis. The here given discussion about all experiments, was written by the author of this thesis.

For all experiments of this project, 2,3-butanediol (BDO) was purchased from industry (SIGMA ALDRICH) as mixture of racemic and meso forms.

Abstract

Four different cyclic carbonates were obtained from renewable diols and transformed into carbamates by reacting them with renewable 11-amino undecanoic acid methyl ester to synthesize non-isocyanate polyurethanes (NIPUs) in a sustainable manner. A procedure using 2,3-buanediol (BDO) as renewable starting material to synthesize a cyclic carbonate with dimethyl carbonate (DMC) is introduced, catalyzed by 1,5,7-triazabicyclo[4.4.0]dec-5-en (TBD). Three purification strategies, i.e., column chromatography, extraction, and distillation, were compared regarding their Environmental factors. Propylene glycol (PG), ethylene glycol (EG), and 1,2-octanediol (Oct) were used as alternative starting materials to broaden the substrate scope and compare material properties. Their cyclic carbonates likewise reacted to carbamates with 11-amino undecanoic acid methyl ester. All carbamates were then polymerized in a bulk polycondensation reaction, yielding poly (ester urethane)s. Complete characterization is reported using differential scanning calorimetric (DSC), size exclusion chromatographic measurements (SEC), thermogravimetric analysis (TGA), ^{1}H-NMR as well as IR spectroscopy. The rheological properties of the poly(ester urethane)s were investigated in the framework of small amplitude oscillatory shear (SAOS) and uniaxial elongation. As proof-of-principle a foaming process was tested successfully.

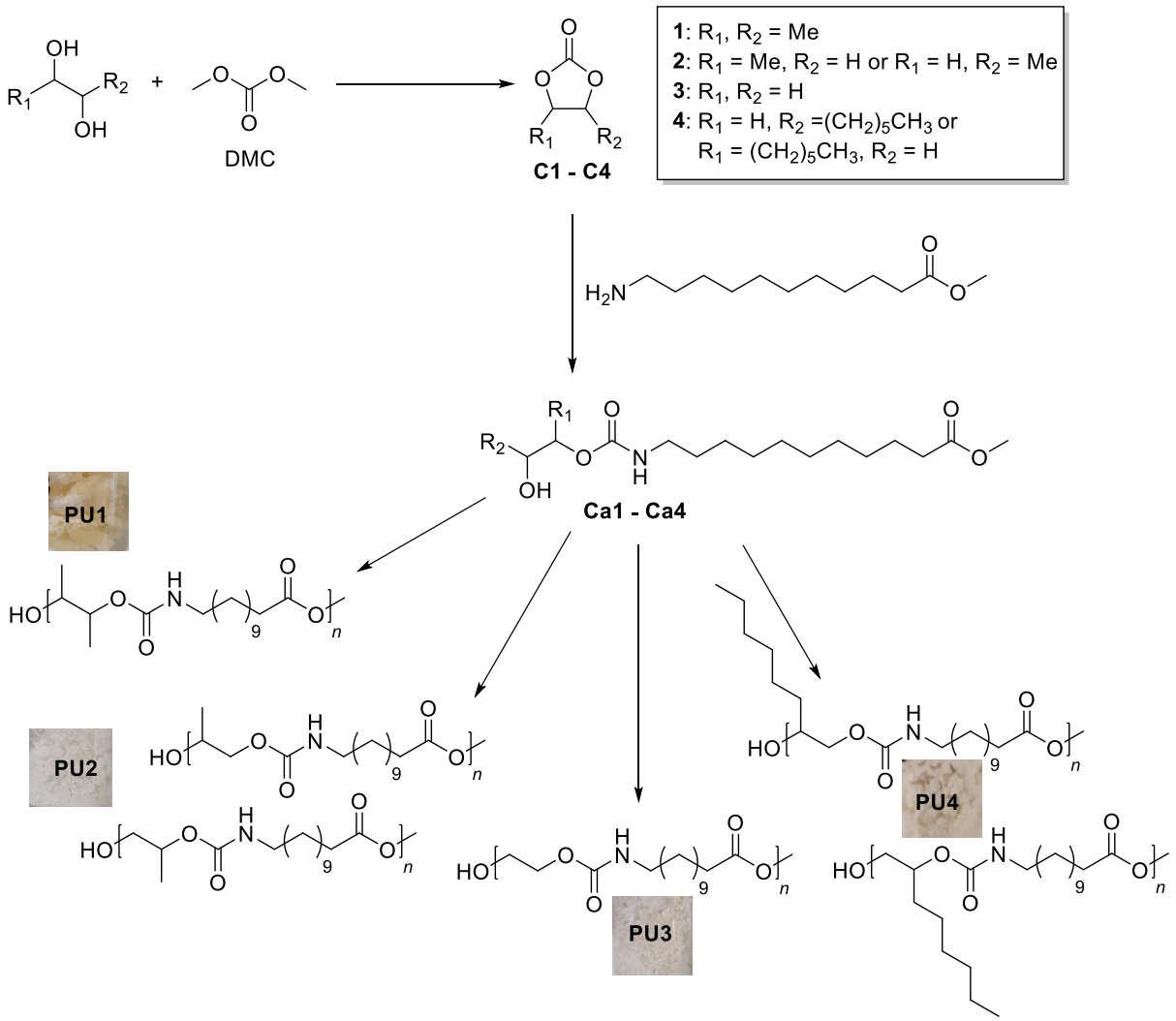

4.1.1 Monomer Synthesis

Polyurethanes (PUs), which demonstrate one of the most important polymer classes in the world, can be tuned in their properties on a molecular and macroscopy level.[115][123][165] Nowadays, many different synthetic routes are already well-known, in which cyclic carbonates and amines represent one of them.[117] Cyclic carbonates are interesting starting materials as they can be converted from renewable diols and show a lower toxicity compared to isocyanates.[126] With a wide range of amines, it is possible to ring-open cyclic carbonates to highly diversified carbamates.[179][195] Suitable key intermediates to NIPUs are carbamates which can be polymerized *via* a transurethanization reaction.[125]

The synthesis of symmetric and unsymmetric organic carbonates was already investigated by our group, using DMC with the organocatalyst TBD.[188]

As part of this thesis, a direct condensation of renewable BDO was first investigated at atmospheric pressure and 80 °C using DMC. DMC can act simultaneously as solvent and reactant. The direct condensation was studied using TBD in different concentrations

(0.10 mol% to 10 mol%, *Table 4*) using gas chromatography (GC-FID) to follow the reaction progress. In further approaches, 1,8-diazabicyclo[5.4.0]undec-7-ene (DBU), 1,5-diazabicyclo[5.4.0]non-5-en (DBN), and 1,1,3,3-tetramethylguanidin (TMG) were tested as alternative organocatalysts, at otherwise identical reaction conditions (see *Table 4*). The condensation reaction to cyclic carbonate **C1** is depicted in *Scheme 12*, accordingly, with marked focusses of this thesis.

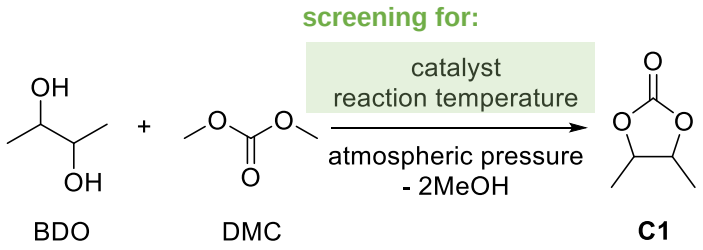

*Scheme 12. Condensation reaction of 2,3-butanediol (BDO) and dimethyl carbonate (DMC) to cyclic carbonate **C1** with focus on screening for a suitable catalyst and reaction temperature to obtain the highest conversion of this reaction.*

Table 4. GC-FID screening of the direct condensation of BDO using DMC to the respective cyclic carbonate. The reaction was catalyzed using different organocatalysts, in otherwise identical reaction conditions, screening the conversion to the desired cyclic carbonate. Different amounts of organocatalyst were screened additionally. (n.a.: not applicable, as no further experiments were performed)

Base / mol%	**Conversion / %**				
	TBD	**DBU**	**DBN**	**Pyridine**	**TMG**
0.1	<1	n.a.	n.a.	n.a.	<1
1.0	26	15	4	<1	2
3.0	47	42	28	<1	16
5.0	61	53	37	12	23
10.0	78	67	n.a.	n.a.	n.a.

Conditions: 1.00 equiv. BDO and 1.20 equiv. DMC. The reaction was running for 3 h at 80 °C in a round-bottom flask with reflux condenser. Biphenyl was used as internal standard.

Having a closer look onto the results listed in *Table 4*, the GC-FID screening was successfully used for the screening of the conversion to the cyclic carbonate based on BDO. The conversion was calculated by adding biphenyl as internal standard in each screening.

Using 5 mol% of the five tested organocatalysts revealed that by using DBN, pyridine, and TMG the lowest conversions were obtained, with 12% (for pyridine), 23% (for TMG), and 37% (for DBN). Instead, using 5 mol% TBD led to a conversion of 61% and 5 mol% DBU to 53%. Thus, no further measurements were performed with DBN, pyridine or TMG. Instead, the focus was shifted to the use of TBD and DBU. The results showed that 10 mol% TBD led to the highest conversion of 78%, whereas 10 mol% DBU led to a conversion of 67%.
All in all, the screening proved that a higher conversion is paired with the use of increased catalyst loadings. However, as DBU led to a brownish solution while the condensation with TBD remained colourless with increased yield, the latter was used for further optimizations with closer look onto the reaction time.
Again, TBD was used in different concentrations and now furthermore measured at different reaction times *via* GC-FID, to screen the conversion of the condensation reaction of BDO and DMC (see *Figure 12*).

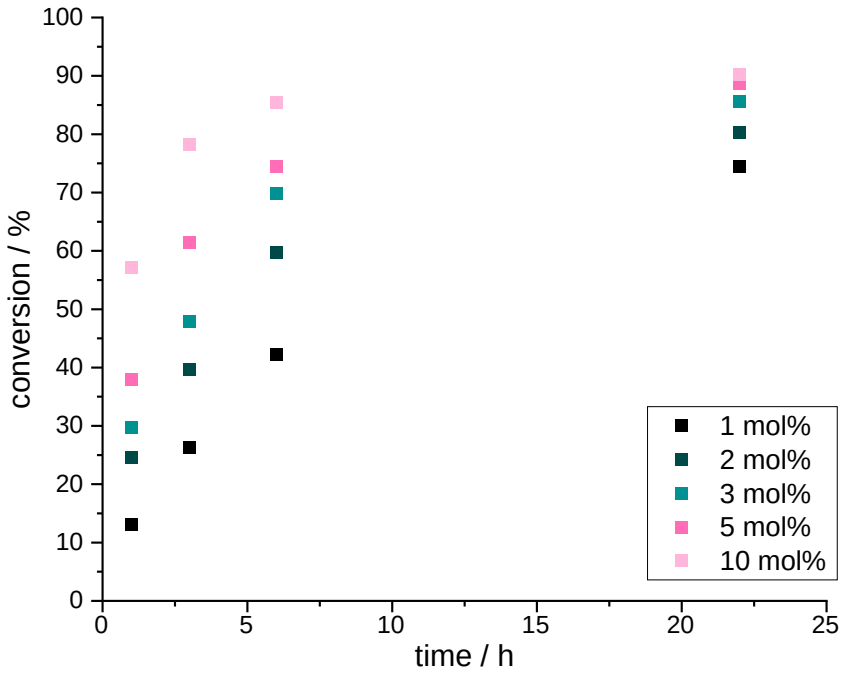

*Figure 12. Conversion of condensation reaction of BDO and DMC to cyclic carbonate **C1**, using TBD as organocatalyst in different concentrations and analysis via GC-FID at varying reaction times from 3 h up to 22 h.*

As depicted in *Figure 12* the reaction screening shows that the conversion of the condensation reaction is increasing with its reaction time. The highest conversion of ~90% was achieved after 22 h using 10 mol% TBD. Nevertheless, with a rising TBD concentration, by-products were detected *via* GC-FID.

In terms of Green Chemistry low catalyst loadings are of interest. Thus, 1 mol% TBD was chosen as optimum, leading to ~75% conversion within 22 h, without generating a side-product formation. Increasing the reaction time further (up to 66 h) did not enhance the conversion of the reaction.

Using a reaction temperature of 90 °C and 1 mol% TBD increased the conversion to 85%. Performing the reaction at 100 °C increased the conversion even further with 98% yield (GC-FID). Thus, a full conversion in the condensation reaction of BDO and DMC to its cyclic carbonate **C1** was obtained when using 1 mol% TBD at 100 °C for 22 h.

Three purification strategies were evaluated for the purification of the cyclic carbonate **C1**, namely vacuum distillation, column chromatography, and extraction. The different methods were compared regarding their efficiency and E-Factor with the aim to reduce the amount of waste production and use as less solvents and energy as possible (see *Table 5*).(*)[35]

Here, the E-Factor of each purification strategy was calculated as simple E-Factor (sEF, meaning the exclusion of solvents in the calculation) and the complete E-Factor (cEF, including solvents used during the purification).[35]

The reaction mixture of the condensation reaction, including unreacted BDO, DMC, TBD, and the product **C1**, was always prepurified using a rotary evaporator to remove remaining solvents under reduced pressure.

The first purification strategy was then tested using vacuum distillation. Temperatures of 130 °C were needed, combined with vacuum of at least 24 mbar to distil **C1**, yielding 38% as yellowish liquid. TBD remained in the flask, as analyzed by ^{1}H-NMR spectroscopy. The E-Factor for the distillation was 3.44 (sEF as well as cEF).

As second purification strategy, column chromatography was tested. Ethyl acetate and cyclohexane in a 1:1 (v/v) ratio proved to be a suitable solvent mixture, leading to an R_F-value 0.47 (for **C1**) on TLC. For the column, 2.70 L of solvent mixture was needed, yielding the cyclic carbonate in 45% as colorless liquid. Thus, this purification led to an E-Factor of 2.82 (sEF) and 520 (cEF), respectively.

(*) The E-Factor is generally accepted as a useful measure to compare the environmental acceptability of chemical processes. The calculation includes the actual amount of waste produced in the process and therefore considers solvent losses, chemical yield, and includes all reagents in principle. Thus, the ideal E-Factor is zero.
For more information, see R. A. Sheldon.[35]

Extraction of the reaction mixture was tested as third purification strategy. First, the reaction mixture was dissolved in 20 mL of ethyl acetate, followed by washing three times with ~30 mL of water. The organic phase was dried over sodium sulphate and ethyl acetate was removed under reduced pressure, yielding 43% **C1** as a colorless liquid. The E-Factor of the extraction was 2.99 (sEF). When including the used solvents, the E-Factor increased to 223 (cEF).

*Table 5. Purification strategies for **C1**, listed with the related E-Factors; sEF (excluding solvents) and cEF (including solvents) and resulting yields of purified product. (n.a.: not applicable, as no additional solvents had to be used)*

Purification strategies	**sEF**	**cEF**	**Yield / %**
Vacuum Distillation	3.44	n.a.	38
Column Chromatography	2.82	520	45
Extraction	2.99	223	43

Regarding the calculated sEF of the purification strategies, column chromatography showed the lowest with 2.82, followed by an sEF of 2.99 for extraction. However, concerning the cEF with 520, the chromatographic purification strategy showed the highest E-Factor, followed by extraction with 223 (cEF). No recovery of the solvents was tested but should be feasible.
Concerning time issues, extraction was the fastest purification strategy of the three listed. For vacuum distillation, energy was necessarily caused by heating and vacuum. Regarding the resulting yields, all purification strategies were quite similar. However, column chromatography showed the highest yield with 45% followed by a yield of 43% through extraction.
The obtained cyclic carbonate **C1** was further analyzed *via* ^{1}H NMR spectroscopy to confirm its purity (see *Figure 13*).

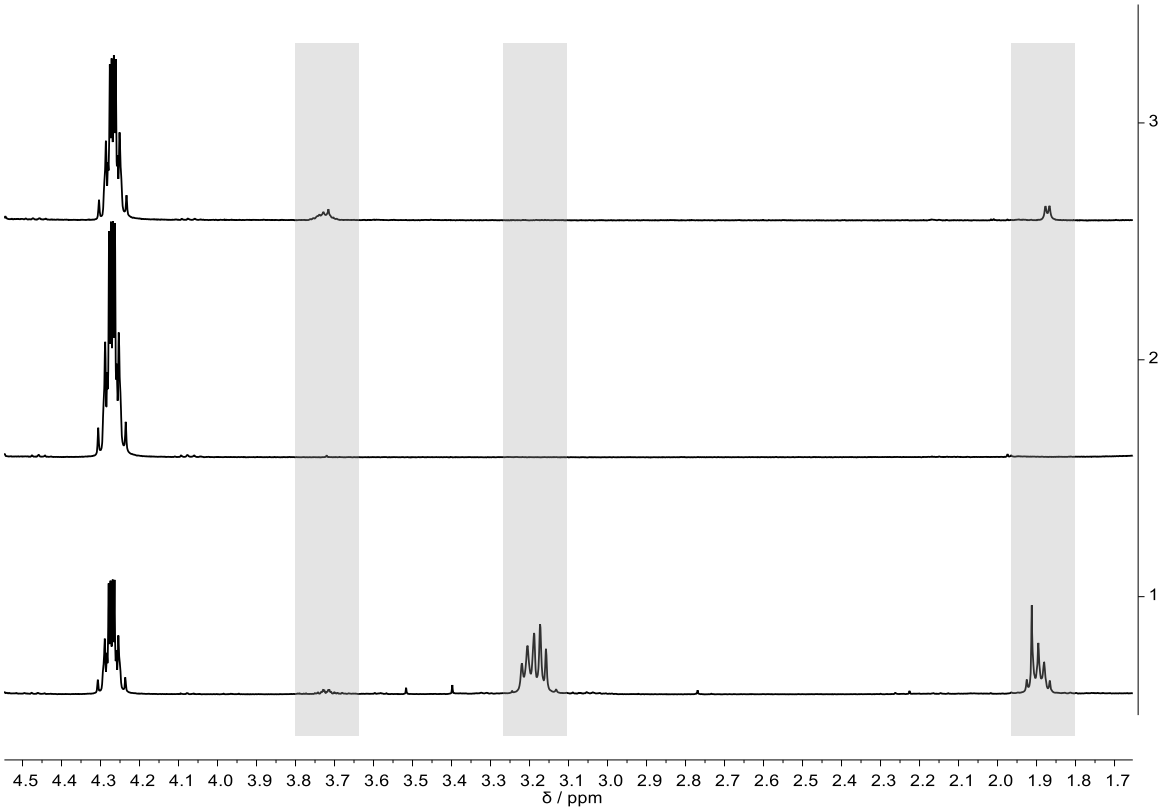

*Figure 13. Zoomed-in ^{1}H NMR spectra of **C1** after purification via vacuum distillation (1), via column chromatography (2), via extraction (3).*

After purification *via* column chromatography and extraction, **C1** appeared to be pure according to ^{1}H NMR analysis. The ^{1}H NMR spectrum of **C1** obtained after vacuum distillation still showed impurities (see Figure 13).

Comparing all discussed advantages and disadvantages of the purification strategies paired with calculated E-Factors, purification *via* extraction revealed to be the greenest, fastest, and cheapest strategy to **C1**.

To broaden the substrate scope, PG, EG, and Oct were tested in the condensation reaction to form the respective cyclic carbonates under the same reaction conditions as for **C1** formation. Here, the conversion and the effect of 1 mol% TBD as catalyst was screened *via* GC-FID for each condensation reaction using the renewable diols.

For the reaction of PG with DMC a conversion of ~82% (GC-FID) was screened after 24 h at 80 °C. Increasing the reaction time to 30 h led to a nearly full conversion (~92%, GC-FID) of the respective cyclic carbonate **C2** (see *Scheme 13*). A GC-FID screening for the formation of cyclic carbonate **C3**, obtained by using EG as monomer, was not possible as the signals were overlapping with the solvent signals. However, for both diols (EG and PG) the reaction time

was increased to 30 h to obtain a full conversion. As a reminder, longer reaction times did not increase the yield in case of **C1**.

Using Oct as renewable starting material in the condensation reaction with DMC, cyclic carbonate **C4** was obtained (see *Scheme 13*). Here, a full conversion (~93%, GC-FID) to **C4** was observed after 5 h reaction time at 100 °C.

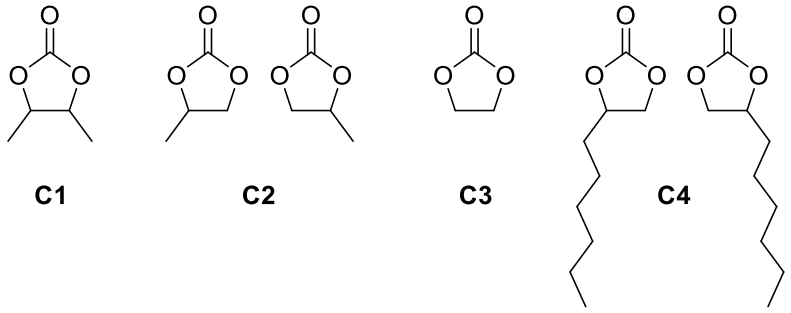

*Scheme 13. Synthesized cyclic carbonates **C1** – **C4**, obtained in optimized reaction conditions of a direct condensation of the respective diols and DMC, catalyzed by 1.00 mol% TBD.*

To purify **C2** – **C4** an extraction, as most sufficient purification method to **C1**, was unsuitable. Instead, column chromatography of the cyclic carbonates **C2** – **C4** was performed. The obtained E-Factors are listed in *Table 6* accordingly.

*Table 6. E-Factors related to column chromatography used to purify **C2** – **C4**. sEF (excluding solvents) and cEF (including solvents) and resulting yields of purified product. (n.a.: not applicable, as no calculations were performed)*

Purification of	sEF	cEF	Yield / %
C2	1.10	387	86
C3	4.71	1671	65
C4	n.a.	n.a.	89

The experiments revealed that through the improved reaction conditions of the previously described condensation reaction of diols, a full conversion of all cyclic carbonates **C1** – **C4** was observed, paired with high yields after purification. To overcome the problem of high E-factors caused by purification *via* column chromatography, it was successfully tested if the cyclic carbonate can be further used without purification. As a full conversion to the cyclic carbonates was observed, the unpurified reaction mixtures only showed the used amount of TBD in the ^{1}H NMR spectra.

Thus, the ring-opening of cyclic carbonates discussed in the following, was carried out successfully by using the unpurified cyclic carbonate mixtures **C1** – **C4**.

One approach to ring-open cyclic carbonates using unprotected amino acids was already investigated by Olsén *et al.*[179] As part of this thesis, biobased 11-amino undecanoic acid, industrially derived monomer of Nylon-11, was first transformed into its methyl ester **A1**.[283] Subsequently, **A1** was used to ring-open the above described cyclic carbonates, as depicted in *Scheme 14*.

In the report of Olsén *et al.* TEA catalyst yielded a full conversion in a ring-opening reaction to carbamates.[179] In this thesis, the solvent DMSO was used to dissolve **C1** – **C4**, reacting with **A1**, being catalyzed by the organocatalyst DBU. After 6 h reaction time at 40 °C a full conversion to the desired carbamates was detected *via* GC-FID. All carbamates were successfully isolated by column chromatography, yielding 81% of **Ca1**, 88% of **Ca2**, and 91% of **Ca3**. Ring-opening of **C4** led to a full conversion of **Ca4**. Its constitutional isomers were separated *via* column chromatography, yielding 86% **Ca4-A** and 6% **Ca4-B** (see *Scheme 14*). **Ca4-A** was isolated as white solid, whereas **Ca4-B** was obtained as colourless liquid.

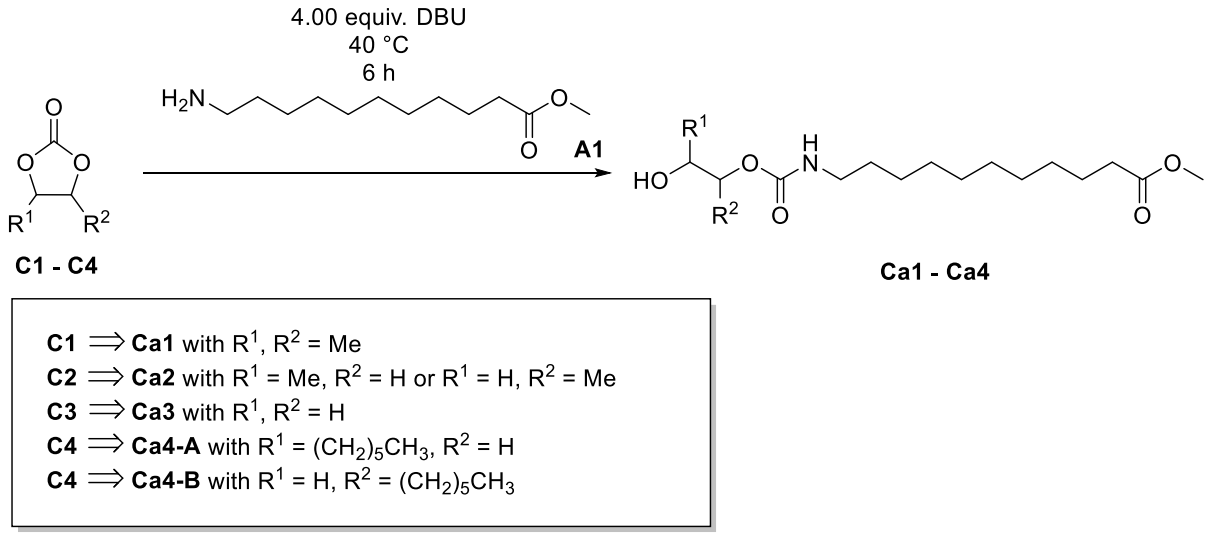

*Scheme 14. Ring-opening reaction of cyclic carbonates **C1** – **C4** using 11-amino undecanoic acid methyl ester **A1**, catalyzed by DBU, to obtain the desired carbamates **Ca1** – **Ca4**.*

4.1.2 Step-growth Polymerization to Poly(ester urethane)s

A TBD catalyzed polycondensation reaction of fatty acid derived dimethyl biscarbamates and diols was previously investigated by our group. In the reported study, the polymerizations were performed under neat conditions in open reaction tubes, using 0.10 equiv. of catalyst. Since TBD is considered to degrade at elevated temperatures, the catalyst was added in three portions at increasing temperatures under continuous vacuum.[165]

This optimized approach was used to polymerize the carbamate monomers **Ca1** – **Ca4** as part of this thesis. The organocatalyst TBD was used with a loading of 0.20 equiv., added in three portions at an increasing temperature from 120 °C to 160 °C under reduced pressure (<1 mbar). For poly(ester urethane)s **PU1**, **PU2**, and **PU4** the polycondensation was performed for 20 h at 160 °C, leading to an increasing viscosity of the reaction mixture over time. For **PU3** the reaction time was decreased to 8 h at 160 °C, as longer reaction times resulted in an insoluble viscous mixture. The catalyst loading remained the same in all polymerizations. All obtained poly(ester urethane)s were precipitating in ice-cold methanol (**PU2** – **PU4**) or ethanol (**PU1**), resulting in a polymer solid after drying under vacuum (<1 mbar) (see *Figure 14*). For **PU2**, a mixture of its constitutional isomers **Ca2** was polymerized. For **PU4**, the constitutional isomers **Ca4-A** and **Ca4-B** were separated *via* column chromatography and polymerized individually to **PU4-A** and **PU4-B**.

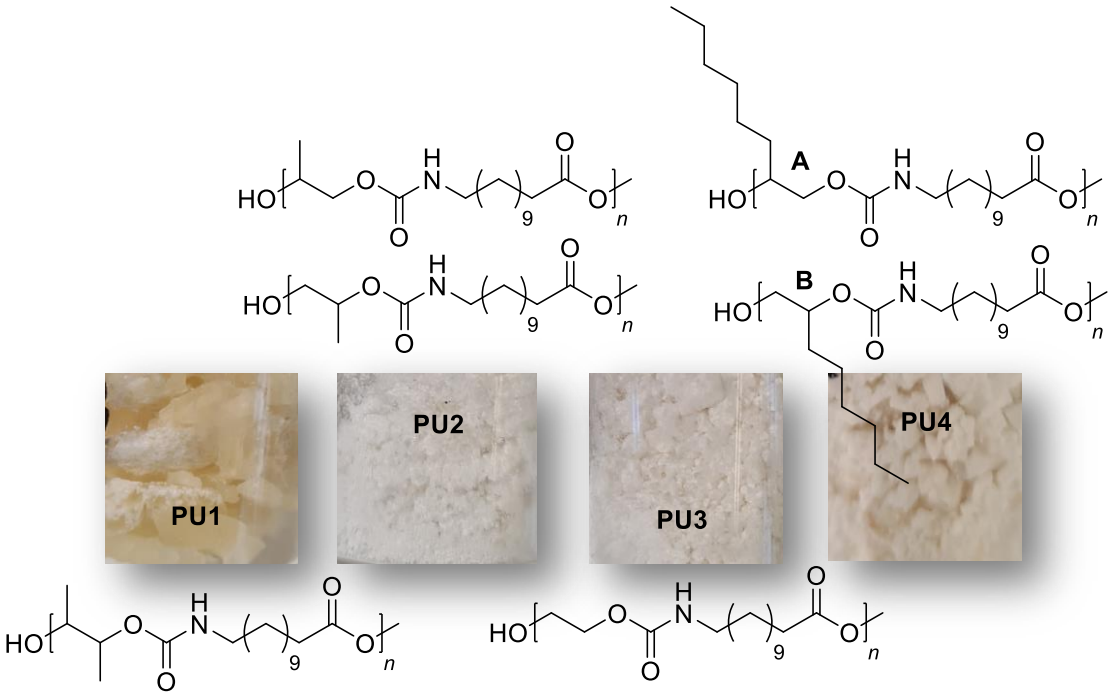

*Figure 14. Poly(ester urethane)s **PU1** – **PU4** obtained by polycondensation reaction in melt of the respective carbamate monomers, catalyzed by TBD. The reaction was stepwise heated from 120 °C to 160 °C. 0.20 equiv. TBD was added in three portions. The reaction mixture was dissolved in HFIP and precipitated in either ice-cold ethanol or methanol to obtain the depicted polymer solids, dried under vacuum (<1 mbar).*

Because of solubility issues, NMR spectroscopy of all poly(ester urethane)s was performed using a solvent mixture of hexafluoroisopropanol (HFIP) and $CDCl_3$. Despite the significant HFIP solvent peak, overlapping with some polymer signals, the structure of **PU1** – **PU4** was confirmed in ^{1}H NMR spectroscopy. Furthermore, IR spectroscopy confirmed typical signals of

the desired polymer (find attached the respective spactra). To gain information about the molecular weight distribution (M_n) and dispersity ($Đ$) of the polymers, SEC measurements were performed using HFIP as solvent (see *Table 7*). No other solvent was suitable to dissolve these polymers (typical observation for a range of polyurethanes and polyamides). Due to instrument problems, a different SEC instrument was used for **PU4** as for **PU1** – **PU3**, however the results remained comparable.

*Table 7. Molecular weight distribution (M_n) and dispersity ($Đ$) of the in SEC measured poly(ester urethane)s **PU1** – **PU4**.*

Poly(ester urethane)	M_n in kDa	$Đ$	Instrument
PU1	11	2.17	SEC-HFIP-2
PU2	10	1.94	SEC-HFIP-2
PU3	5	2.13	SEC-HFIP-2
PU4-A	3	1.37	SEC-HFIP
PU4-B	19	2.20	SEC-HFIP

Conditions: 1.30 mmol carbamate, 0.20 equiv. TBD, 120 – 160 °C, full vacuum (<1 mbar), precipitation in antisolvent.

In case of **PU3**, the necessary decrease of the reaction time from 20 h to 8 h resulted in a lower molecular weight polymer (~5 kDa), corresponding to oligomers. Higher molecular weights were no longer soluble in HFIP. For **PU1** and **PU2**, which were synthesized within 20 h, higher molecular weights of M_n 10 kDa (**PU2**) and M_n 11 kDa (**PU1**) were reached. In case of **PU4-A** the lowest molecular weight of M_n 3 kDa was measured, whereas polymerizing **PU4-B** led to M_n 19 kDa. Having a closer look on the SEC-HFIP traces of the **PU4** constitutional isomers, it seems likely that a ring-closing reaction has occurred for **PU4-A**, resulting in a lower molecular weight and the sharp signal at a retention time of 9.45 minutes. Here, the unstable baseline of in *Figure 15* depicted HFIP traces occurred because of instrument problems coming from the pump and not influenced the results of the measurements. The presumed ring-closing in **PU4-A** was not proven *via* ^{1}H NMR spectroscopy because of solubility issues. Furthermore, **PU4-A** was precipitated as white and brittle solid, whereas **PU4-B** was a colourless and flexible solid (see *Figure 16*).

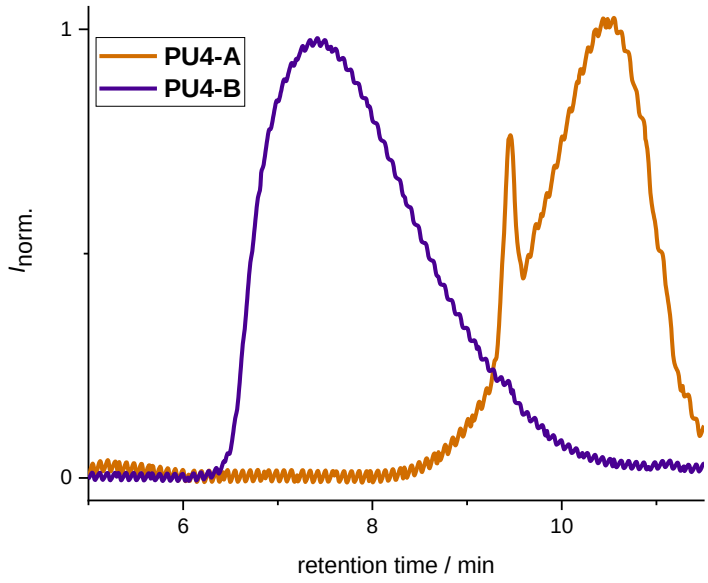

*Figure 15. SEC-HFIP traces of **PU4-A** (M_n 3 kDa, Đ 1.37) and **PU4-B** (M_n 19 kDa, Đ 2.20).*

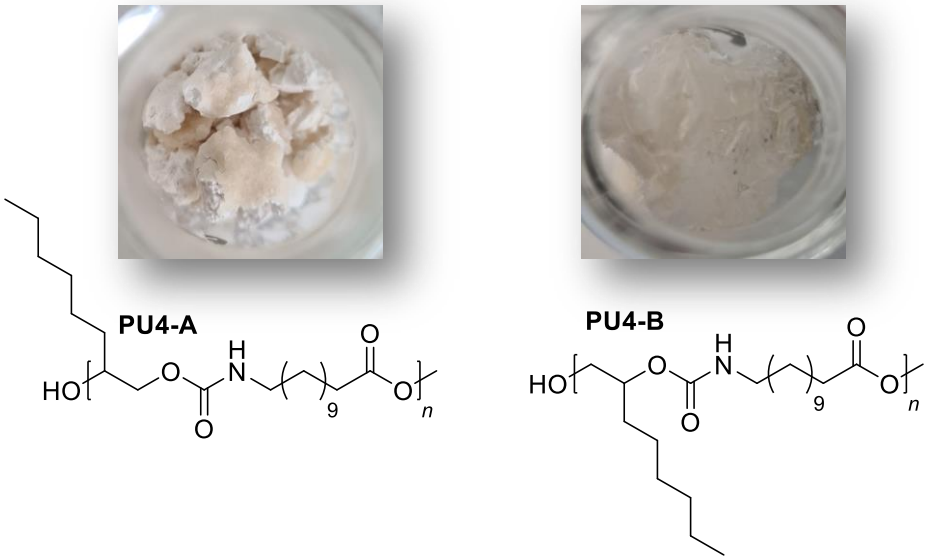

*Figure 16. Comparison of **PU4-A** and **PU4-B** obtained as solid, with **PU4-A** being white and brittle and **PU4-B** being colourless and flexible.*

For the poly(ester urethane)s **PU4-A** and **PU4-B**, the DSC measurements are depicted in *Figure 17* and *Figure 18*, given the respective melting, crystallization, and glass transition temperature. Herein, differences were observable when comparing the two polymers.

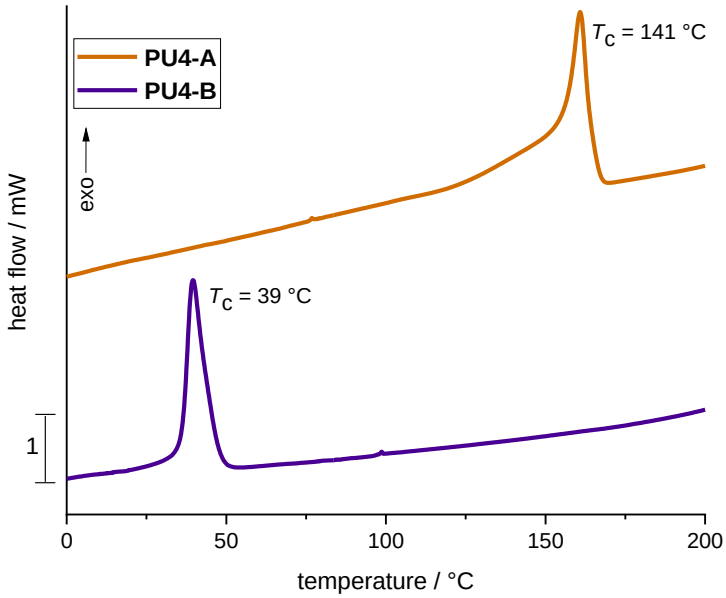

*Figure 17. Cooling trace of poly(ester urethane) **PU4-A** and **PU4-B** measured with DSC from 150 – -10 °C in the second scan, sowing crystallization temperature (T_c).*

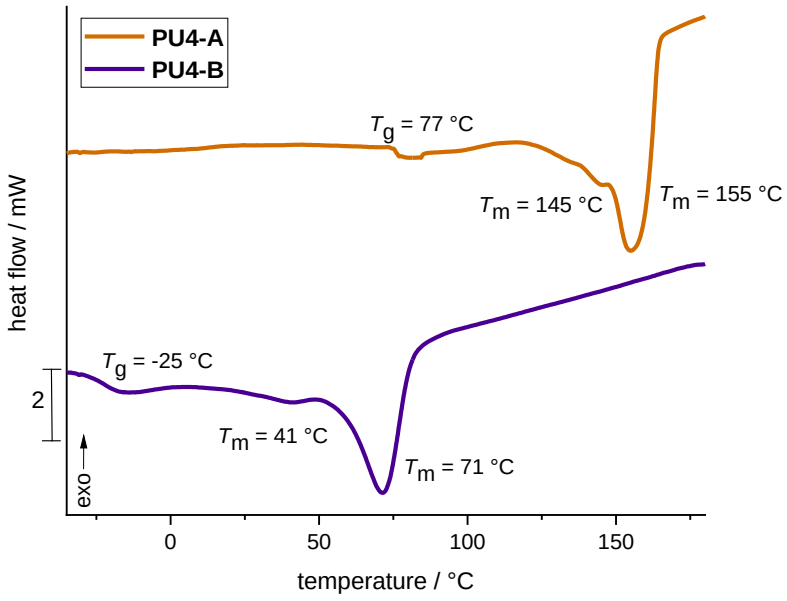

*Figure 18. Heating trace of poly(ester urethane)s **PU4-A** and **PU4-B** measured with DSC from -10 – 150 °C in the second scan, showing the glass transition (T_g) and melting temperature (T_m).*

For **PU4** both constitutional isomers showed two melting points or at a least a shoulder. **PU4-B** showed a much lower melting with 71 °C compared to **PU4-A** with 155 °C. According to literature it is known that semicrystalline polymers start to soften above the glass transition temperature but do not show a fluid behavior until the melting temperature is reached ("rubbery region").[284]

Also, a large temperature difference between the glass transition temperatures was measured with **PU4-B** showing a T_g at -25 °C, whereas **PU4-A** showed a T_g at 77 °C. Here, a higher T_g was expected for **PU4-B** compared to **PU4-A**, if both polymers show a linear backbone, as the T_g is known to increase with increasing molecular weight.[285] However, the high T_g of **PU4-A** confirms a possible ring-closure in the polymer backbone, which decreases the rotation of the polymer backbone thus, increases the T_g.[286]

Furthermore, the crystallization temperature was different (**PU4-A** with 141 °C and **PU4-B** with 39 °C), indicating the structural difference of both polymers and their change in crystallization behavior. However, due to the low M_n obtained for **PU4-A** and the low amount of obtained polymer solid for **PU4-B** (**Ca4-B** yield of 6%), no further mechanical testing was performed with these polymers.

For **PU1 – PU3** further experiments were performed and are discussed in the following.

TGA was measured for **PU1** – **PU3**, revealing a two-step degradation of all poly(ester urethane)s. It is literature known that urethane units are not very thermally stable and might break easily depending on the used alcohol and isocyanate type.[287][288] Therefore, it was expected that first a degradation step in TGA is visible, due to the breaking of the urethane units (~120 – 160 °C), followed by a second degradation step caused by the breaking of ester bonds in the polymer backbone (~260 – 320 °C) and a third degradation step due to complete degradation of the polymer (~435 – 440 °C). Only for **PU1**, a fourth degradation step at ~97 °C was visible in the TGA measurement, what was presumed to be caused due to solvent leftovers (see *Figure 19*).

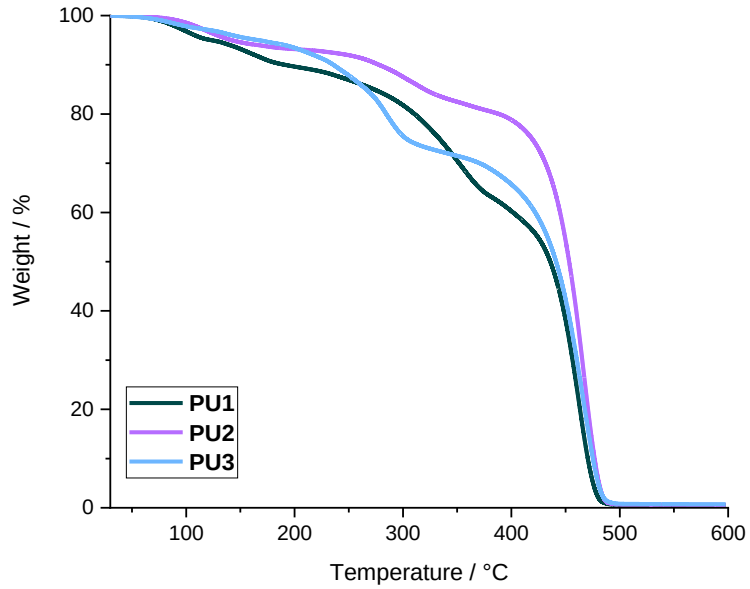

*Figure 19. TGA measurements of **PU1** – **PU3**, showing a three-step degradation.*

The measurements of DSC using ~12 mg of **PU1** – **PU3** are depicted in *Figure 20* and *Figure 21*, showing a melting, glass transition, and crystallization for all poly(ester urethane)s.

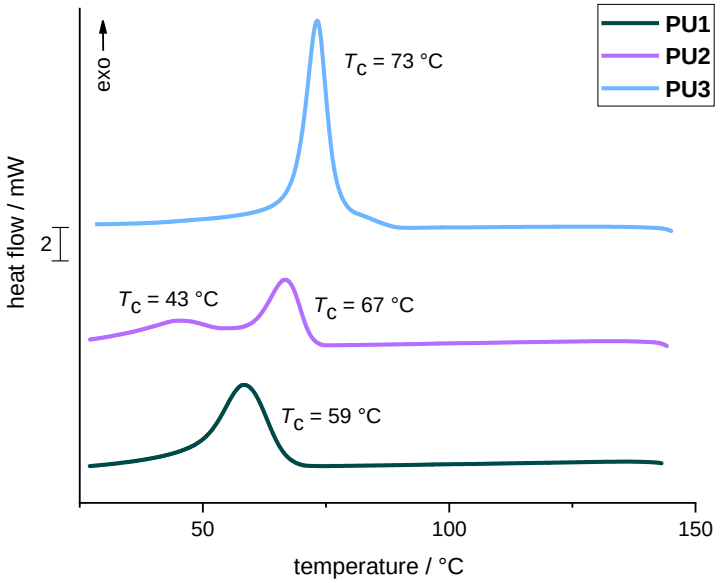

*Figure 20. Cooling trace of poly(ester urethane)s **PU1** – **PU3** measured with DSC-2 from 150 – -90 °C in the second scan, sowing crystallization temperature (T_c).*

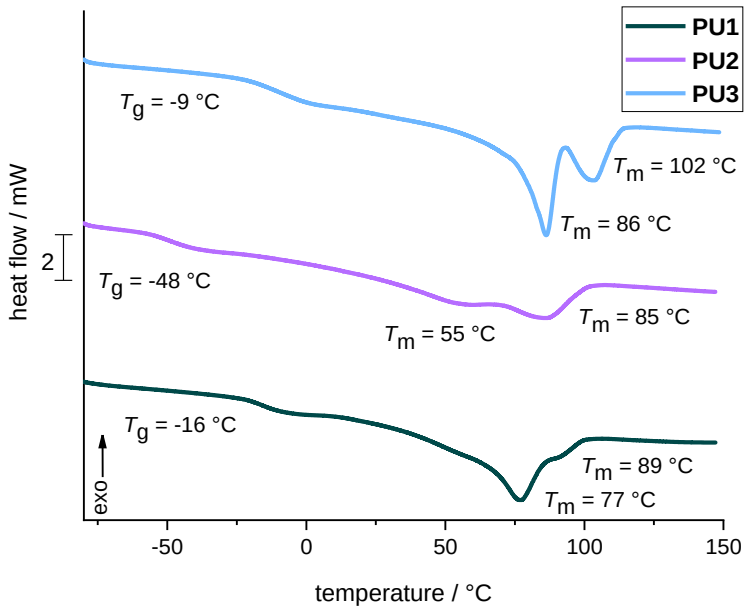

*Figure 21. Heating trace of poly(ester urethane)s **PU1** – **PU3** measured with DSC-2 from -90 – 150 °C in the second scan, sowing the glass transition (T_g) and melting temperature (T_m).*

The crystallization temperature increased with decreasing methyl group content from 59 °C (**PU1**) to 73 °C (**PU3**). **PU2** showed a second crystallization peak at 43 °C (see *Figure 20*). The T_g of the poly(ester urethane)s **PU1** – **PU3** ranged between -48 °C to -9 °C. Furthermore, each polymer showed two melting peaks or at least a shoulder, indicating a semicrystalline structure. Both minima of **PU1** and **PU3** differ about ~15 °C, while the difference of **PU2** is ~27 °C (see *Figure 21*). The melting enthalpy increased with decreased methyl group content from 29 J g^{-1} to 45 J g^{-1}, providing information on the crystalline fraction of the polymer. This also relates to a loss in transparency, as can be seen in *Figure 22*, after pressing the polymers accordingly. Only **PU1** was obtained in bone form as the two other polymers **PU2** and **PU3** were too brittle to be removed from the shape form.

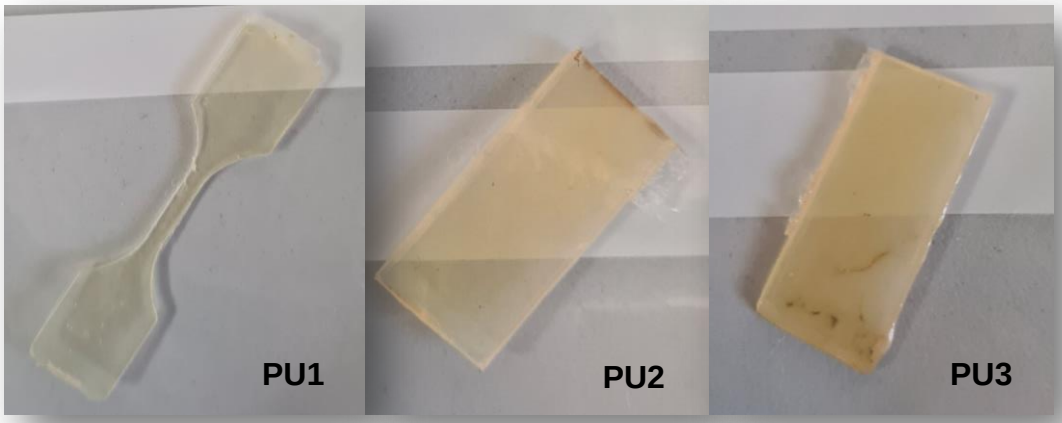

*Figure 22. Bone shape form (1.45 mm thickness, 3.30 mm width, 45.0 mm length) of **PU1** pressed at 130 °C under vacuum and square forms (1.33 mm thickness, 7.75 mm width, 34.0 mm length) of **PU2** pressed at 150 °C and of **PU3** pressed at 130 °C.*

These, in *Figure 22*, depicted pressed specimens were used for mechanical and rheological characterization. **PU1** appeared more transparent than **PU2**, most likely a result of the additional methyl branching, as **PU2** also seemed more transparent than **PU3**. Tensile tests of the pressed polymers were measured using different grips. Manual vise grips, wedge grips, and pneumatic grips were tested, resulting in the break of square and bone forms in the grip. Thus, tensile elongation of all three polymers was unsuccessful to measure as the polymers were simply too brittle for the used grips. However, **PU3** seemed to be the most brittle polymer, followed by **PU2**. **PU1** showed the lowest brittleness of the three poly(ester urethane)s, which is an indication of an influence of the methyl groups based on renewable BDO.

Furthermore, poly(ester urethane) **PU2** and **PU3** were too brittle to produce specimens which can be used for small-amplitude oscillatory shear (SAOS) and uniaxial elongational measurements. Here, a thickness between 0.5 – 1 mm was necessary. **PU2** and **PU3** directly broke already during sample preparation. Thus, rheological measurements were only performed using **PU1**.

First, the storage and loss modulus of **PU1** was analyzed, which is related to the materials ability to store energy.(*)[289]

Figure 23 and *Figure 24* show the storage (G') and loss modulus (G'') as well as the magnitude of the complex viscosity ($|\eta^*|$) of **PU1** analyzed at 130 °C and 150 °C.

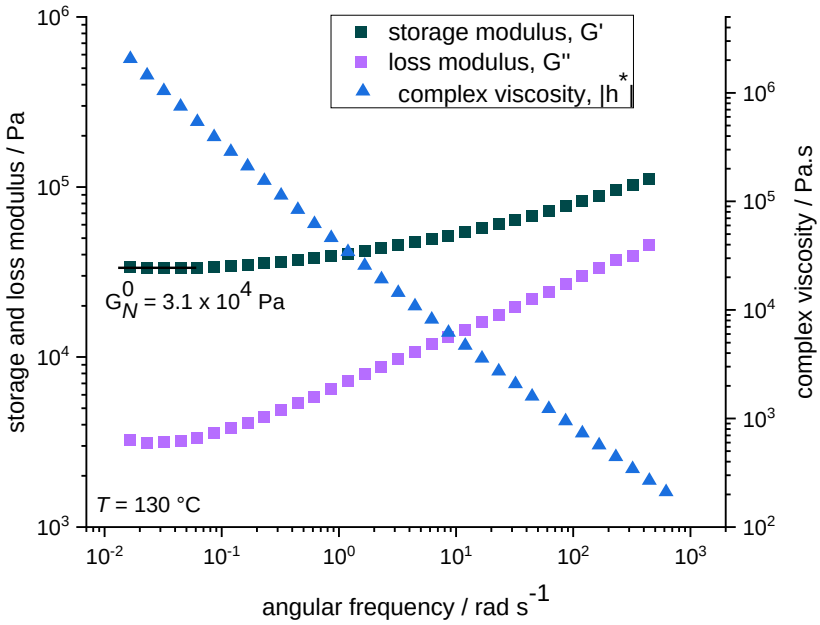

Figure 23. Small-amplitude oscillatory shear (SAOS) measurements of poly(ester urethane) ***PU1*** *at 130 °C (new pressed specimen with a thickness between 0.5 – 1 mm).*

(*) The loss modulus is the ratio of the viscous component to the stress, thus, related to the materials ability to dissipate stress through heat.
For more information, see www.tainstruments.com.[289]

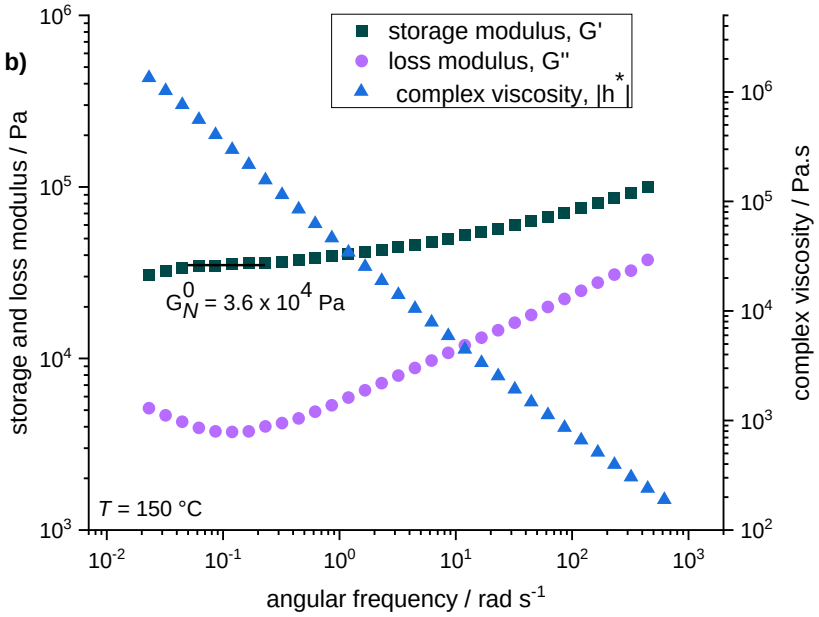

Figure 24. Small-amplitude oscillatory shear (SAOS) measurements of poly(ester urethane) ***PU1*** *at 150 °C (new pressed specimen with a thickness between 0.5 – 1 mm).*

Both measurements depicted in *Figure 23* and *Figure 24* showed neither flow behavior nor crossover, even at the lowest measured angular frequency of ω = 0.01 rad s^{-1}. According to DSC measurement of **PU1** (see *Figure 21*, T_m 89 °C and 77 °C), the polymer was expected to be melted at 130 °C and 150 °C. Thus, a flow behavior in SAOS measurement was expected. Not seeing this expected melt behavior indicates that the polymers chemistry of **PU1** was changing, for instance, with branching or crosslinks formed at high temperatures (>130 °C), caused during polymer pressing and/or SAOS measurements. To analyze the change of the **PU1** sample at higher temperatures over time, a time sweep at 130 °C was performed.(*)[290] The applied temperature corresponds to the temperature used for press-molding. The time sweep of **PU1** was performed at a frequency of ω = 1 Hz and 130 °C, confirming that poly(ester urethane) was likely changing over time at a temperature of 130 °C, as expected through the above discussed results of SAOS measurements (see *Figure 25*).

(*) An oscillatory time sweep monitors certain viscoelastic parameters of the sample, over a certain time-period. Temperature and frequency are held constantly throughout such a rheology test.
For more information, see www.tainstruments.com.[290]

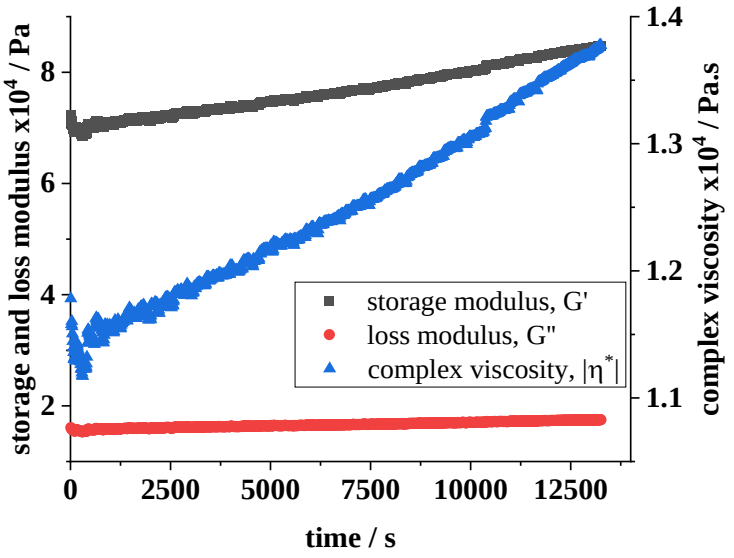

Figure 25. Time sweep of poly(ester urethane) ***PU1*** *at 130 °C at a frequency of ω = 1 Hz. Measurement performed and provided by M. K. Esfahani, copied with permission of the Journal of Macromolecular Chemistry and Physics.*[111]

A further indication of a permanent change of **PU1** was, that the sample was not soluble in HFIP after the pressing anymore. This was further analyzed by using an optical microscope (see *Figure 26*).

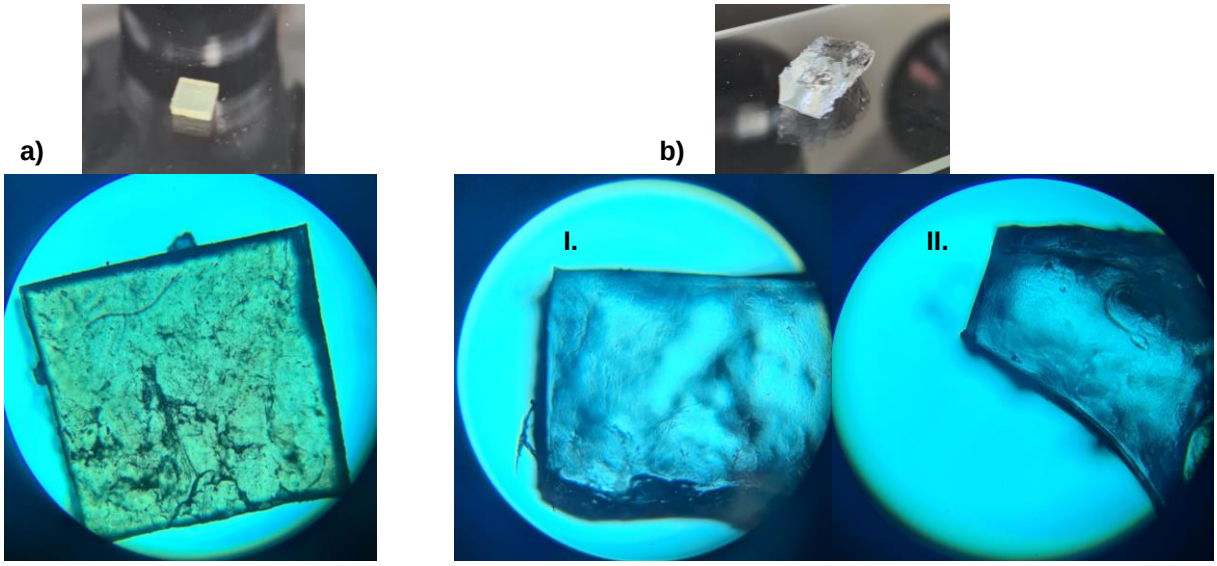

Figure 26. Using an optical microscope to compare ***a)*** *the pressed* ***PU1*** *sample at 40x magnitude with* ***b)*** *after being in HFIP solution for 24 h, showing an insolubility, depicted with 40x magnitude* ***I.*** *from top and* ***II.*** *from sideways.*

After pressing **PU1**, the sample was immersed in HFIP, and the solvent was removed afterwards. Then the sample was dreid under vacuum (<1 mbar) to remove HFIP, followed by weighing the sample. It was tested, if the sample gets soluble over time, when repeating this cycle more often. Furthermore, it was tested if the weight of the polymer is changing over time. The HFIP solvent was analyzed in IR spectroscopy and SEC measuremtents after the sample was immersed in the solvent. The cycle was performed for 5 times. ^{1}H NMR and IR spectroscopy of the pressed polymer confirmed that **PU1** was not changing during each cycle. Also, a weight loss of the pressed sample was not measured, i.e., only HFIP was removed through drying under vacuum.

To further test the stress and strain of the polymeric material **PU1**, uniaxial elongation rheology was performed.(*)[291][292] Herein, different Hencky strain rates were used, ranging from $\dot{\varepsilon}$ = 1 – 0.01 s^{-1}. *Figure 27* and *Figure 28* shows the elongational viscosity of **PU1** at 130 °C and 150 °C. The strain hardening was analyzed, described as the rise of viscosity above the predicted values from the linear viscoelastic behavior (LVE). The strain hardening factor (SHF) is the ratio of the maximum measured tensile stress growth coefficient η_E^+ over the predicted value of the LVE $\eta_{E,LVE}^+$.

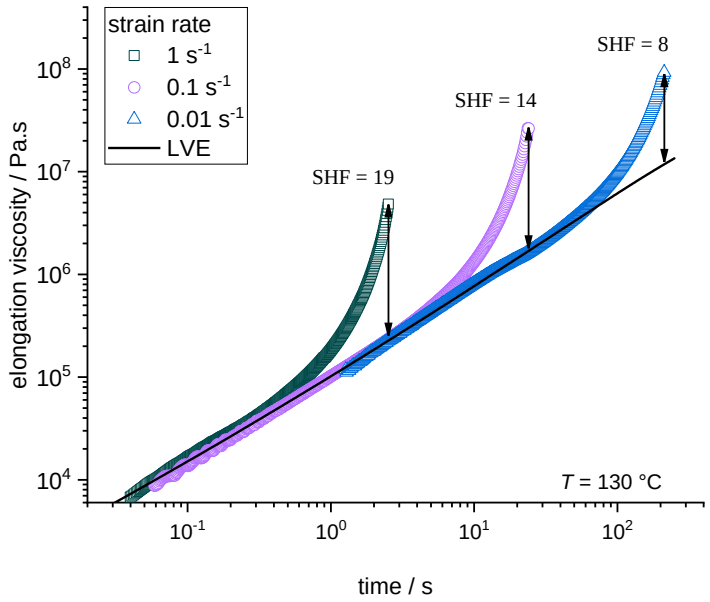

Figure 27. Elongational viscosity versus time for poly(ester urethane) ***PU1*** *at Hencky strain rates ranging from 1 s^{-1} to 0.01 s^{-1} at 130 °C, measured with Extensional Viscosity Fixture (EVF).*

(*) The elongation at break evaluates the polymeric property to plastically deform before fracturing. Incorporating long-chain branched or crosslinks into a polymer chain improves the stretchability of a material.
For more information, see M. Wilhelm *et al.* or J. M. Dealy and R. G. Larson.[291][292]

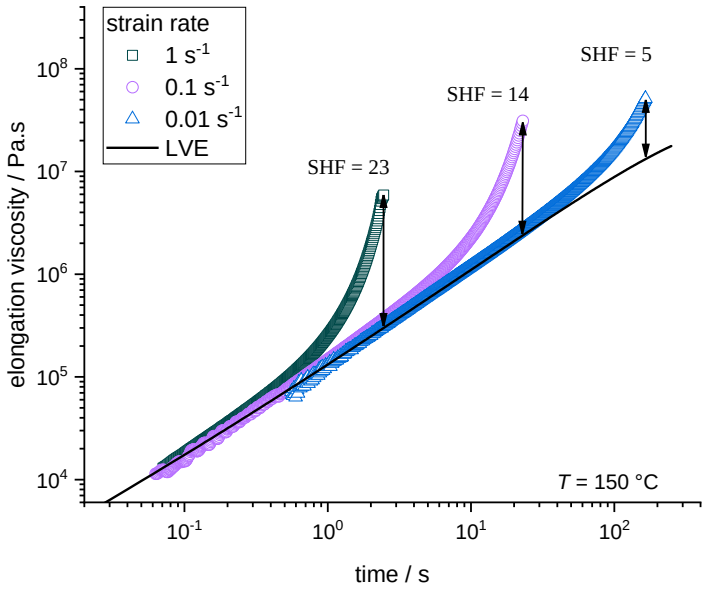

Figure 28. Elongational viscosity versus time for poly(ester urethane) ***PU1*** *at Hencky strain rates ranging from 1 s^{-1} to 0.01 s^{-1} at 150 °C, measured with Extensional Viscosity Fixture (EVF).*

PU1 showed strain hardening behaviour for all investigated strain rates at both temperatures. The SHF decreased with decreasing Hencky strain rate, which led to SHF = 19 – 8 (for 130 °C) and SHF = 23 – 5 (for 150 °C), respectively. The higher temperature had only a minor impact on the SHF, and in both cases, the steady state value was not reached. Since strain hardening is hardly seen in linear polymers, this behaviour indicated that the molecular structure of poly(ester urethane) **PU1** contains some amount of long chain branching or crosslinks.[291] In **PU1** such crosslinked behaviour was expected to come from hydrogen bonding between the polymer chains. Therefore, poly(ester urethane) **PU1** was expected to be a good candidate for some polymer processing operations in which strain hardening behaviour in uniaxial deformation is necessary, e.g., in foaming processes.[293][294]

As part of this thesis, a proof-of-principle was carried out for **PU1**, investigated to confirm an expected foaming. One method to foam polymers is the one-step physical foaming process.[295]

Within this process, polymeric materials are pressed into a certain form, then used to be saturated with a foaming agent. Typically, supercritical carbon dioxide ($scCO_2$) is used. The saturation occurs at a specific temperature and pressure until the sample is completely saturated. Then, the nucleation of the cells is triggered by a sudden pressure drop. This pressure drop leads to the expansion of the cells. The cells can expand until the pressure within the cells is no longer sufficient to deform the surrounding polymer.[296] The cell stability during expansion can be enhanced by using a polymer that shows strain hardening, since the polymer melt becomes more stretchable. Thus, strain hardening prevents the cells from rupture and coalescence, compared to a polymer without any strain hardening behavior.[297]

As part of this project, the expected strain hardening of **PU1** was confirmed with the ability to foam this material. A physical foaming behaviour of **PU1** with $scCO_2$ was observed.(*)[136][298] The sample was allowed to saturate for 8 h at 120 °C at 500 bar and was foamed during a depressurization rate of approximately 200 bar s^{-1}. The resulting foam structure was analyzed using scanning electron microscopy (SEM), depicted in *Figure 29*.

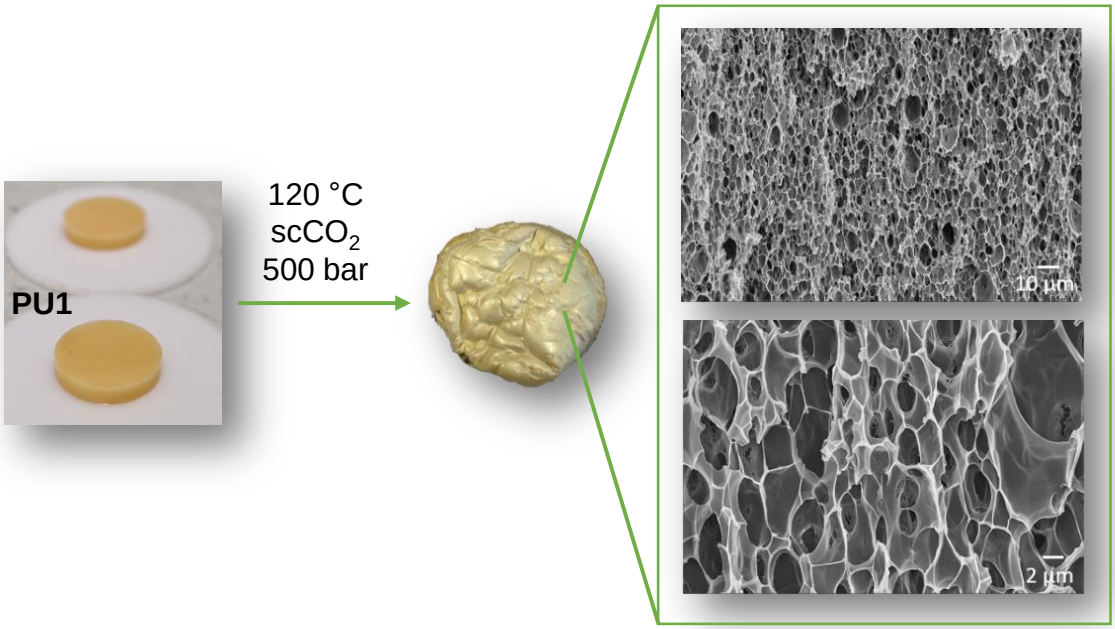

*Figure 29. SEM images at different magnifications (10 µm and 2 µm) of **PU1** foamed with $scCO_2$ at 120 °C and 500 bar with a depressurization rate of ~200 bar s^{-1}.*

(*) PU foams are typically produced by chemical foaming.
For more information, see R. L. Heck or A. S. Dutta.[136][298]

The **PU1** foam showed a predominantly closed-cell structure. However, in the magnification, it was noticeable that some cells are ruptured. The foam had a density of 0.16 g cm^{-3} and a volume expansion ratio of 7.2. The cell sizes were rather inhomogeneous, showing some isolated cells with a mean diameter of around 6 µm, whereas most cells ranged from 1.25 µm to 3.53 µm. The mean cell density was about 1.77×10^{12} cells cm^{-3}. For semi-crystalline polymers, not only the SHF is a relevant parameter, but also the crystallization behaviour. Therefore, further to this proof-of-concept, the foaming behaviour of this material must be analyzed more in detail to find correlations between the structure-property relationship. However, as part of this thesis no more measurements were performed.

Conclusion

A sustainable synthesis of poly(ester urethane)s was investigated using renewable diols as starting materials. BDO, PG, EG, and Oct were transformed into respective cyclic carbonates using DMC, subsequently ring-opened using the methyl ester of 11-amino undecanoic acid. The obtained carbamate monomers were then polymerized to poly(ester urethane)s with M_n up to 19 kDa, characterized by ^{1}H NMR and IR spectroscopy, SEC, DSC and TGA analysis. SAOS and elongational viscosity were measured with the poly(ester urethane) derived from BDO. Especially this poly(ester urethane) showed interesting properties, offering a reasonably high melting point of 89 °C in combination with transparency. SAOS, time sweep, and uniaxial elongation measurements indicated that the sample starts branching and forms crosslinks. Poly(ester urethane) based on BDO showed no flow behavior in shear, an increasing viscosity over time, and strain hardening in elongation with an SHF of up to 23 at 150 °C, at a Hencky strain rate of 1 s^{-1}. A foamed sample showed a density of 0.16 g cm^{-3} and a mean cell size ranging from 1.25 µm to 3.53 µm.

4.2 Polymerization of 2,3-Butanediol and Renewable Dicarboxylic Acids using Iron(III)chloride as Catalyst

The author of this thesis developed the synthetic procedure, planned, evaluated the experiments, and wrote the manuscript.

S. Wegelin, co-supervised by the author of this thesis, was performing the deconvolution method and first tests on finding suitable polycondensation reaction conditions.

For all experiments of this project, 2,3-butanediol (BDO) was purchased from industry (SIGMA ALDRICH) as mixture of racemic and meso forms.

Abstract

The renewable diol, 2,3-butanediol (BDO), which can be obtained by fermentation of biomass, was used in polycondensation reactions with renewable 2,5-furandicarboxylic acid (FDCA), to obtain a fully renewable polyester. With regards to Green Chemistry, a catalyst screening based on a deconvolution method was performed. 16 randomly chosen Lewis Acids were screened with the aim to identify the most active catalyst. With iron(III)chloride, as most active catalyst, further investigations of a polycondensation reaction in melt are presented. Further dicarboxylic acids were used within this project, (co)polymerized with BDO and FDCA, to polyesters and copolyesters. The renewable dicarboxylic acids, succinic acid (SA), sebacic acid (SBA), and adipic acid (AA) were implemented. A full characterization of all polymers, including ^{1}H NMR and IR spectroscopy as well as, differential scanning calorimetry (DSC), size exclusion chromatographic measurements (SEC), and thermogravimetric analysis (TGA) is provided, with comparison of their polymeric properties.

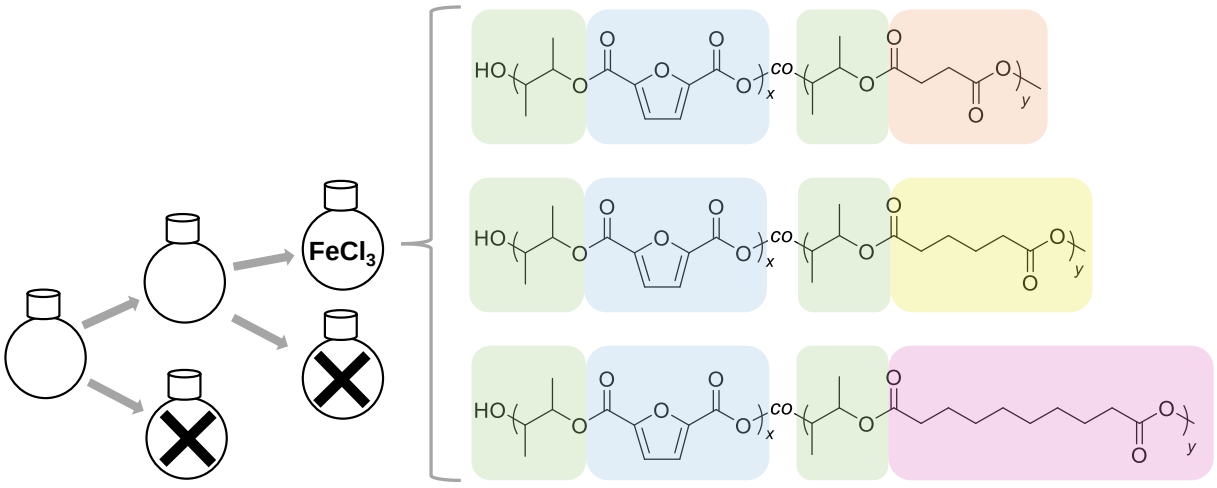

4.2.1 Catalyst Screening *via* a Deconvolution Method

With regards to sustainability in polymer syntheses, catalysts are an important part to, e.g., decrease the required energy of a synthesis route, or increase the selectivity, while decreasing the production of waste. Lewis Acids are typically used in polycondensation reactions to polyesters, as they facilitate the nucleophilic attack of alcohol groups.[276] For polycondensation reactions, titanium(IV) butoxide (TBO) and titanium(IV)isopropoxide (TTIP) were previously identified as catalysts leading to high M_n polyesters.[113]

To overcome the problem of catalysts screenings, such as the requirement of extensive experimentation paired with a high number of time-consuming experiments, the so-called deconvolution method was introduced by Moran *et al.*[281] This method describes an efficient and fast way to screen for suitable catalysts in a defined system.

In this project, a two-step polycondensation reaction of BDO and FDCA was screened with 16 randomly chosen Lewis Acids (see *Scheme 15*). The layout of the performed experiments is depicted in *Figure 30*.

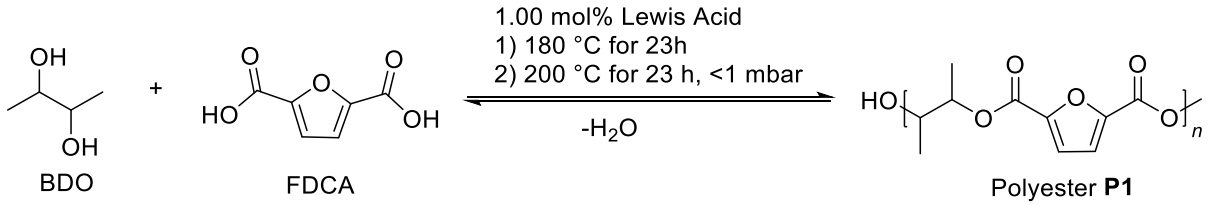

*Scheme 15. Two-step polycondensation reaction of 2,3-butanediol (BDO) and 2,5-furandicarboxylic acid (FDCA) to polyester **P1**. 1) Formation of oligomers at 180 °C for 23 h, subsequently followed by 2) polycondensation in melt at 200 °C for 23 h at reduced pressure.*

In initial experiments of the here presented deconvolution method, the Lewis Acids were directly divided into batch 1 (**B1**) to batch 4 (**B4**), as the reaction mixtures with all 16, as well as the two batches of 8 different Lewis Acids each, were neither stirring nor soluble, thus, no polyesters were precipitating. Therefore, the 16 Lewis Acids were directly split randomly into **B1** to **B4** (see *Figure 30*).

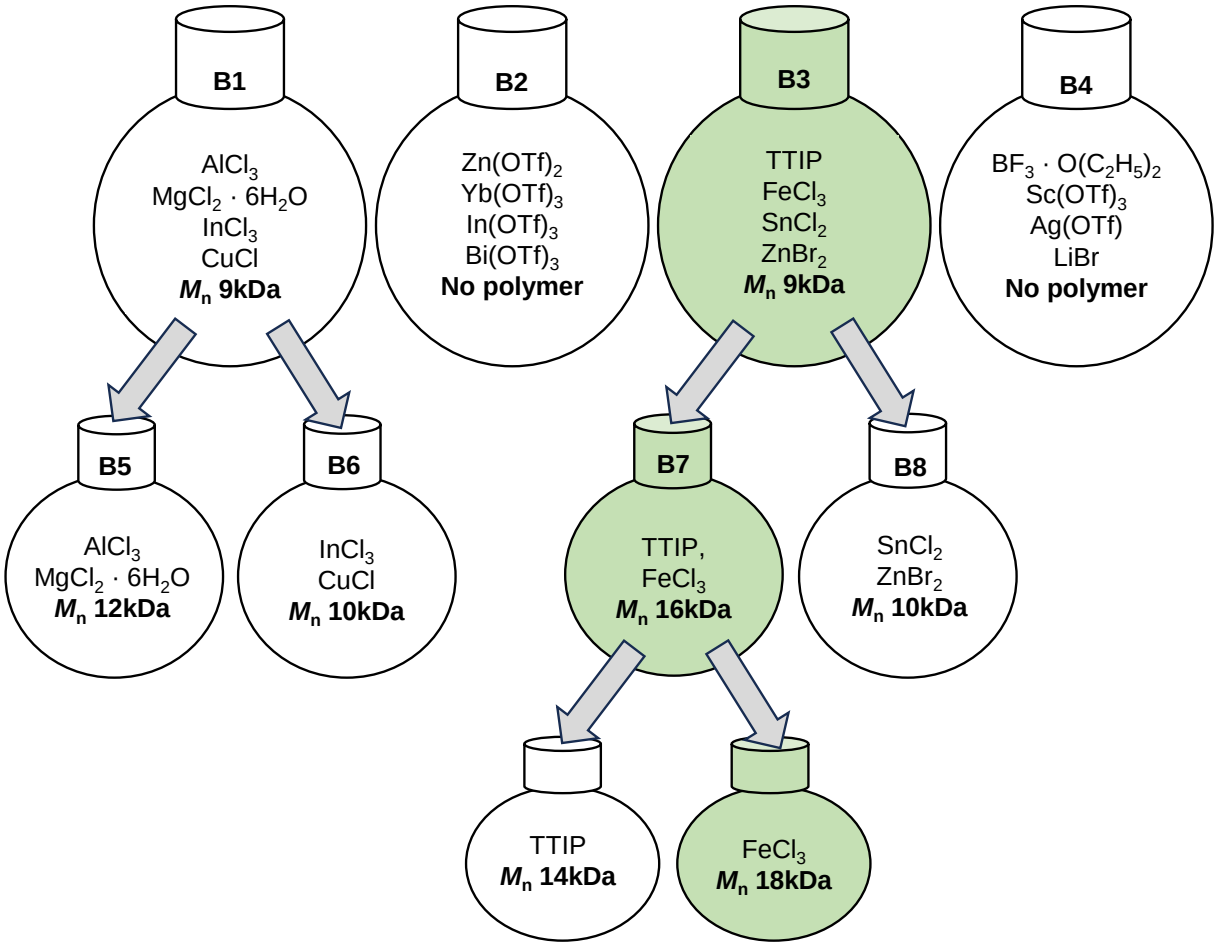

*Figure 30. Used Lewis Acids in the deconvolution method, introduced by Moran et al.[281], to screen for the most efficient catalyst in a polycondensation reaction of BDO and FDCA, using 1.00 mol% catalyst loading. Splitting of batches into **B1** to **B4** was performed randomly and is depicted accordingly with obtained M_n of the desired polymers, measured in SEC-HFIP.*

The reaction conditions were set, with the reaction of BDO and FDCA to oligomers at 180 °C, followed by a polycondensation in melt at 200 °C and low pressure (>1 mbar) (see *Scheme 15*). In each batch, 1.00 mol% of each catalyst was used. Size exclusion chromatography (SEC) was performed for all precipitated polyesters to screen for the highest M_n polymer, i.e., for the best performing catalyst, or catalyst mixture.

The precipitated polyesters obtained from **B1** and **B3** showed M_n values of ~9 kDa, whereas products obtained from **B2** and **B4** were insoluble black solids, which were not suitable for any workup or characterization. As the results of **B2** and **B4** indicated side reactions, only **B1** and **B3** were further deconvoluted into smaller batches, **B5** to **B8**, containing two catalysts each (see *Figure 30*).

In **B5**, the catalysts $AlCl_3$ and $MgCl_2 \cdot 6H_2O$ led to the formation of a polyester with M_n of 12 kDa. For **B6**, containing $InCl_3$ and CuCl, as well as for **B8**, using $SnCl_2$ and $ZnBr_2$, a polyester with M_n of 10 kDa was observed.

The highest M_n polymer, with 16 kDa, was obtained when performing the polycondensation reaction in **B7**, using the combination of TTIP and $FeCl_3$.

However, it must be considered that the catalysts might interact during the deconvolution method, which might lead to increased or decreased catalytic activity.[281]

Therefore, the catalysts used in **B5** to **B8** were furthermore screened individually in the polycondensation reaction of BDO and FDCA (see *Table 8*).

Table 8. Polycondensation reaction of BDO and FDCA using the listed catalysts individually, yielding the listed M_n and Đ of the desired polyesters.

Catalyst	M_n / kDa	*Đ*
$AlCl_3$	15	1.65
$MgCl_2 \cdot 6H_2O$	11	1.19
$InCl_3$	9	1.86
CuCl	-	-
TTIP	14	1.95
$FeCl_3$	18	1.55
$SnCl_2$	11	1.23
$ZnBr_2$	10	2.26

In **B6** (polyester with M_n of 10 kDa), a possible interaction of catalysts was noticed. Using only $InCl_3$ in the polycondensation reaction, a polyester with M_n of 9 kDa was obtained, whereas by using CuCl, no workup was successful, as the reaction resulted in an insoluble black solid. Thus, is seemed likely for **B6**, that only $InCl_3$ showed a catalytic activity, whereas CuCl is not suitable for a polycondensation reaction of BDO and FDCA.

For **B5**, resulting in a polyester with M_n of 12 kDa, an even higher M_n polyester with 15 kDa was obtained, when using $AlCl_3$ individually. This was also the case for **B7**, leading to a polyester with M_n of 16 kDa, whereas by using $FeCl_3$ individually, a polyester with M_n of 18 kDa was formed. In these cases, the catalysts seemed to have negatively influenced each other in the reaction mixture.

Thus, the deconvolution method was used successfully, revealing $FeCl_3$ as the most suitable and active catalyst for the tested polycondensation reaction of BDO and FDCA. This was further confirmed by the reactions of individual catalysts shown in *Table 8*. $FeCl_3$ is known to catalyze reactions as a typical Lewis Acid, for instance, oxidations, reductions, or cyclisation, with the advantage of a high efficiency, stability, and low cost.[299]

Herein, this non-toxic catalyst was compared to industrially commonly used TTIP and TBO catalysts in polycondensation reactions to poly(2,3-butylene-2,5-furan dicarboxylate) (PBF).

Both, TTIP and TBO yielded a polyester with slightly lower M_n (~15 kDa), compared to the use of $FeCl_3$ (18 kDa). Furthermore, in the study of Thiyagarajan *et al.*, FDCA was polymerized with BDO using TTIP as catalyst, resulting in a polyester with M_n of 8 kDa.[242]

Thus, $FeCl_3$ not only presents an environmentally friendly and cheaper catalyst to TTIP and TBO, but this catalyst also shows a higher reactivity in a polycondensation reaction.

However, for TTIP as well as for polyesters obtained by using $FeCl_3$, the yielded polyesters showed a slightly brown discoloration. This discoloration is reported in the literature for polyesters based on FDCA. A reason for the brown color might be related to side reactions, such as decarboxylation, leftovers of catalyst, or sugar-based impurities, coming from FDCA.[113]

Therefore, it was tested, if the discoloration is decreased when changing the reaction temperature and time of the esterification reaction between FDCA and BDO from 180 °C for 23 h, to 160 °C for 17 h. The reaction time of the subsequent polycondensation reaction in melt was shortened from 23 h at 200 °C (<1 mbar), to 7 h at 215 °C (<1 mbar). Furthermore, the catalyst loading was increased from 1.00 mol% to 1.25 mol% $FeCl_3$. The reduced reaction time paired with increased catalyst loading did not influence the M_n of the desired polyester (see *Table 9*). Thus, it was tested, if the discoloration is changing when using prepurified FDCA (**F1**) as monomer to yield the polyester **P1-F1** based on BDO, catalyzed by $FeCl_3$. Furthermore, it was tested if differences are noticeable when using FDCA dimethyl ester (**F2**), to yield the polyester **P1-F2** based on BDO, catalyzed by $FeCl_3$. SEC-HFIP measured a similar M_n of the obtained polymers (see *Table 9*).

*Table 9. SEC-HFIP measurements of polyesters obtained by using BDO and FDCA to yield **P1**, or the use of prepurified FDCA (**F1**) to yield **P1-F1**, or FDCA dimethyl ester (**F2**) to yield **P1-F2**. All reactions performed under the same reaction conditions.*

Polyester	**10 mmol of**	**M_n in kDa**	**$Đ$**
P1	FDCA	18[a]	1.55
P1-F1	**F1**	19[a]	1.85
P1-F2	**F2**	17[a]	1.53
P1	FDCA	17[b]	1.95

Condition a: 30.0 mmol of BDO, 1.25 mol% $FeCl_3$, 160 °C for 17 h, followed by 215 °C and low pressure (<1 mbar) for 7 h. Precipitation in 1:1 (v/v) ethanol to water.
Condition b: 30.0 mmol of BDO, 1.00 mol% $FeCl_3$, 180 °C for 23 h, followed by 215 °C and low pressure (<1 mbar) for 23 h. Precipitation in methanol.

In all cases, similar discoloration was observed. Thus, different anti-solvents were tested for the precipitation of the desired polyester. For PBF based on a reaction catalyzed by TTIP, ice-cold methanol seemed to be a suitable anti-solvent, as reported in literature.[242] For **P1**, obtained in a polycondensation reaction of BDO and FDCA, catalyzed by $FeCl_3$, a mixture of ice-cold water and ethanol (1:1, v/v) yielded a less brownish polyester solid, compared to using methanol (see *Figure 31*). Furthermore, a threefold redissolution and precipitation decreased the discoloration of **P1** even further. The multiple precipitation steps did not change the M_n of **P1**. To check if the catalyst $FeCl_3$ is washed out through precipitation in water and ethanol, the antisolvent mixture was analyzed by *Prussian Blue* staining after each precipitation step, depicted in *Figure 31*.(*)[300]

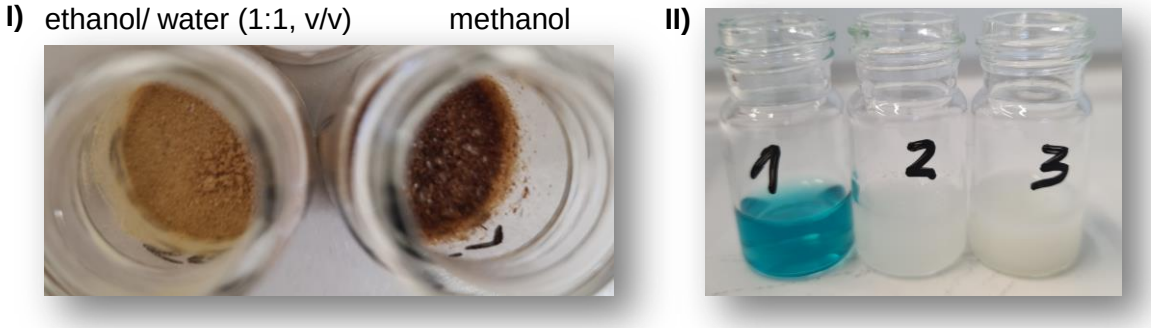

*Figure 31. **I)** Polyester **P1** precipitated in an antisolvent mixture of ethanol and water (1:1, v/v) compared to using the antisolvent methanol. **II)** Prussian Blue staining of antisolvent mixture of ethanol and water after each precipitation step, of a total of three times.*

Prussian Blue staining showed that $FeCl_3$ was largely washed out in the first precipitation step, using ethanol and water as antisolvent mixture. To analyze the amount of washed out $FeCl_3$, and to get an idea if the discoloration occurred because of catalyst leftovers in the polyester solid, inductively coupled plasma-optical emission spectroscopy (ICP-OES) was used.
For the polycondensation reaction 1.25 mol% $FeCl_3$ were used. The ICP-OES measurements showed, that in the first precipitation step, 6 to 10 wt% of the used amount of $FeCl_3$ was washed out. Followed by the second precipitation step, washing out <0.20 wt% and the third precipitation step with less than 0.05 wt% (see *Figure 32*).

(*) *Prussian Blue* is a method to identify ferric iron in solution. The ferric iron reacts with a dilute acidic potassium ferrocyanate solution to produce an insoluble blue compound, known as *Prussian Blue* or *Berlin Blue*.[300]

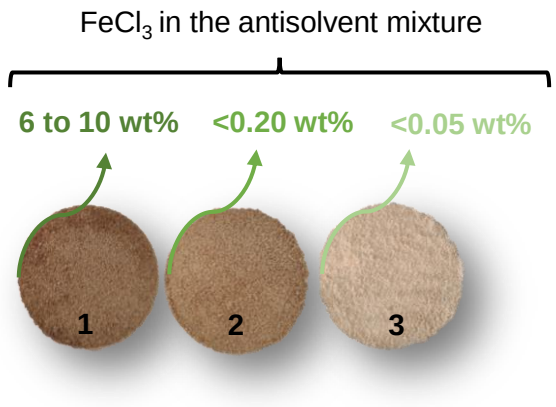

*Figure 32. Threefold precipitation of **P1**. Inductively coupled plasma optical emissions spectroscopy (ICP-OES) of antisolvent mixture (ethanol to water, 1:1, v/v) was used after each precipitation step (**1** to **3**), to measure the iron content.*

ICP-OES measurements revealed that most of the used catalyst remained in the polyester solid, yet its color improved significantly, leading to the conclusion that the discoloration was likely caused by other impurities, maybe due to side-reaction of sugar-residues of FDCA, which were removed by precipitation.

4.2.2 Polyester Synthesis

The improved reaction conditions of a polycondensation reaction, as previously described in the deconvolution method, were further used in all following reactions. Always, 30.0 mmol of BDO were mixed with 10.0 mmol of a dicarboxylic acid, using 1.25 mol% $FeCl_3$, heated to 160 °C for 17 h, subsequently followed by 215 °C at <1 mbar for 7 h.

The polyester **P1**, obtained from polymerizing FDCA and BDO, showed no melting temperature (T_m) or crystallization temperature (T_c) in differential scanning calorimetry (DSC), which is according to literature.[242] Gubbels *et al.* reported fully amorphous polyesters, when using BDO in increasing contents.[113]

A glass transition temperature (T_g) of 106 °C was measured in DSC and a degradation temperature ($T_{d,5\%}$) of 303 °C was measured by thermogravimetric analysis (TGA), for **P1**. Compared to literature, in the report of Thiyagarajan *et al.*, PBF, based on FDCA and BDO, was isolated with a lower T_g of 90 °C and lower $T_{d,5\%}$ of 279 °C, compared to the here presented study. Thiyagarajan *et al.* used a reaction temperature of 260 °C for 4 hours during polymerization in melt, while using TTIP as catalyst.[242] The literature described lower molecular weights might be the reason for the differences observed in thermal properties, further pointing to the benefits of $FeCl_3$ as catalyst.

P1 was soluble in aprotic solvents, such as acetone, dichloromethane, HFIP, THF, cyclohexane, and ethyl acetate whereas being insoluble in water, methanol, and ethanol.

In addition to FDCA, also SA, SBA, and AA are interesting renewable dicarboxylic acids for the research on novel biobased polymers. SA gained great attention when introducing the dicarboxylic acid in polymerization with 1,4-butanediol, yielding PBS, which is already implemented in industry.[248] While copolymerizing PBS with AA, the obtained polymer showed an increased tensile strength.[250] SBA is known for its good flexibility when polymerizing to polyesters.[265] However, it is literature known that the T_g is decreasing with increasing SBA content.[268]

To investigate if the identified catalyst, $FeCl_3$, is also suitable for other polycondensation reactions, further polyesters were synthesized. Each of the dicarboxylic acids was used in polycondensation reactions with BDO, following the same reaction procedure as for **P1**, catalyzed by 1.25 mol% $FeCl_3$ (see *Scheme 16*). All obtained copolyesters were precipitated in an ice-cold antisolvent mixture of water and ethanol (1:1, v/v) and dried under vacuum (<1 mbar) before analysis in SEC-HFIP and TGA (see *Table 10*).

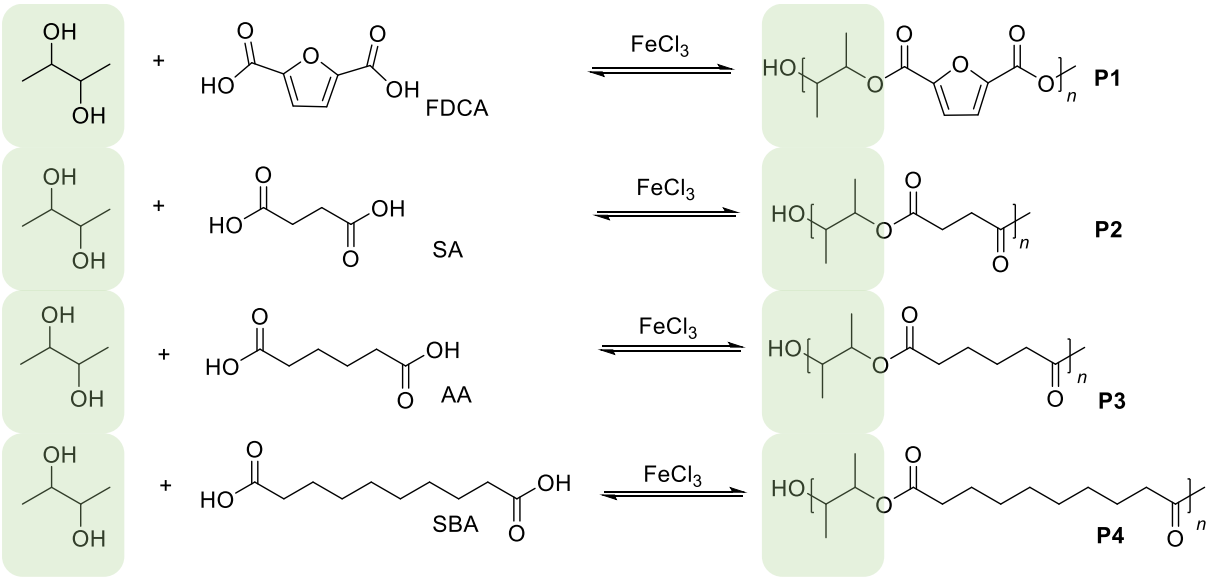

*Scheme 16. Polyesters **P1** to **P4**, using 2,3-butanediol (BDO) with 2,5-furandicarboxylic acid (FDCA) to **P1**, succinic acid (SA) to **P2**, adipic acid (AA) to **P3**, or sebacic acid (SBA) to **P4**.*

*Table 10. Polyesters based on a polycondensation reaction with BDO and FDCA (**P1**), or BDO with SA (**P2**), AA (**P3**), or SBA (**P4**), listed with respective M_n and Đ, measured in SEC-HFIP. T_d was measured in TGA.*

Polymer	M_n / kDa	Đ	$T_{d,5\%}$ / °C	Appearance
P1	18	1.55	303	brittle solid
P2	5	1.47	280	viscous liquid
P3	8	1.44	326	viscous liquid
P4	10	1.47	358	viscous liquid

P1 showed the highest M_n with 18 kDa, whereas **P2** showed the lowest M_n with 5 kDa, compared to **P3** (8 kDa) and **P4** (10 kDa). The degradation temperature was increasing from **P1** with 303 °C ($T_{d,5\%}$) to 358 °C ($T_{d,5\%}$) for **P4**. Thus, an increasing carbon chain length in the polymer backbone led to an increasing $T_{d,5\%}$, therefore a higher thermal stability.

The main difference between the obtained polyesters, was that **P1** was precipitated in form of a polyester solid, whereas **P2** to **P4** were isolated as highly viscous liquids. However, regarding the processability of a polyester used for, e.g., foil or fibre production, it is of interest to isolate the polymer in form of a solid, later transferred into, e.g., pellets or granulates.(*)[301] Thus, the focus was on isolating a solid polyester which is processable. **P1** was too brittle to be used for mechanical testing.

4.2.3 Copolymerization of BDO and Renewable Dicarboxylic Acids

To tune the properties of the polyester, copolymerization reactions were performed.

As **P1** was isolated as solid, but was brittle, the focus of this part of the project, was on using FDCA and BDO as monomers for copolymerization reactions with a third monomer. Thus, the renewable dicarboxylic acids, SA, AA, and SBA were used as third monomers. 30 mmol of BDO were polymerized with 10 mmol of a dicarboxylic acid mixture, containing FDCA, and SA, AA, or SBA in varying contents, resulting in the following copolyesters (see *Figure 33*).

Here, the abbreviations of the copolyesters demonstrate the used amount of the third monomer in the desired polycondensation reaction. For instance, **SA6** contained 6% SA, thus 94% FDCA.

(*) For instance, the industrial PET process consists of different plant sections, with first a polycondensation in melt, followed by a route of typical stages, to produce PET bottles: crystallization or pelletization, annealing, solid state polymerization, and cooling.[301]

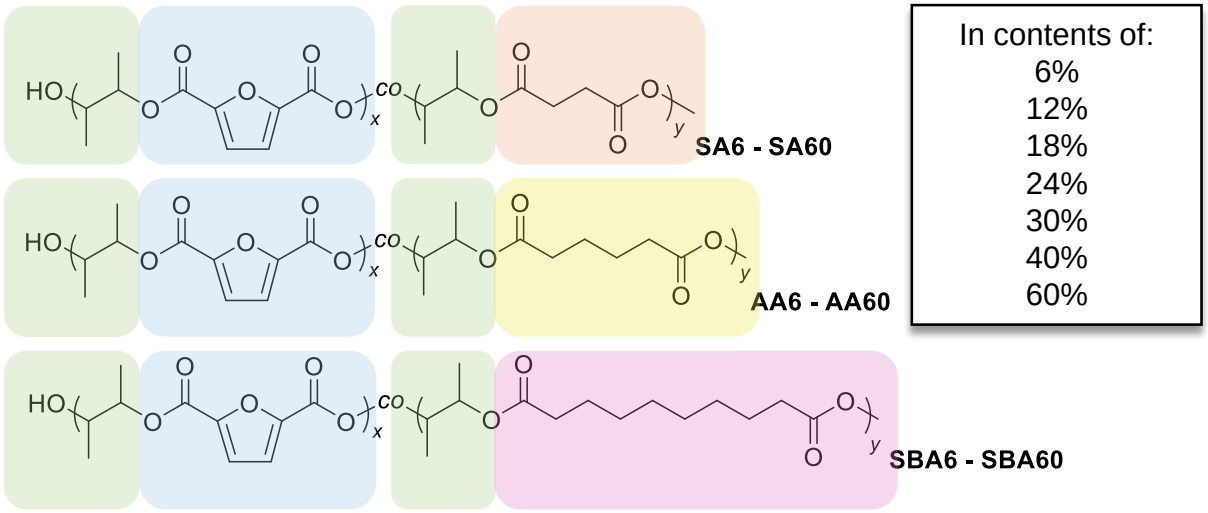

Figure 33. Chemical structures of obtained copolyesters when copolymerizing BDO, FDCA, and a third monomer, the renewable dicarboxylic acids, SA, AA, or SBA in varying contents. co = unspecified.

For copolyesters based on using SA as third monomer, here **SA6** – **SA60**, all polyesters were precipitated as slightly brown solids. In contrast, by copolymerization with AA, only the copolyesters **AA6** – **AA30** were isolated as slightly brownish solids. If further increasing the AA content to 40% and 60%, the copolyesters **AA40** and **AA60** were obtained as highly viscous liquids.

Using the renewable dicarboxylic acid with the longest carbon backbone of the here investigated monomers, SBA, the copolyesters **SBA6** – **SBA30** were precipitated as slightly brownish solids. Copolyesters **SBA40** and **SBA60**, with the two highest SBA contents, were obtained as viscous liquids.

All copolyesters were characterized using DSC, TGA, and SEC. The M_n and $Đ$ measured in HFIP-SEC are listed for each copolyester in *Table 11*.

Table 11 gives the degradation temperature at a weight loss of 5% as well as 15%. Due to copolyesters which were not drying properly, even after several hours under full vacuum (<1 mbar) and slightly increased temperatures (~30 °C). Thus, it was presumed that the copolyesters were sensitive to humidity, showing absorption of water. However, to compare the degradation temperature of all copolyesters accordingly, the temperature is listed in *Table 11* at two different weight losses.

Table 11. List of synthesized copolyesters with BDO, varying contents of FDCA, and a third monomer as dicarboxylic acid (SA, AA, or SBA). The content of FDCA is given in %, whereas the copolyesters abbreviation gives the information about the used amount of SA, AA, or SBA (in %). Measured SEC-HFIP and TGA results are listed for each copolyester.

Copolyester	**FDCA content / %**	M_n **/ kDa**	$Đ$	$T_{d,5\%}$ **/ °C**	$T_{d,15\%}$ **/ °C**
SA6	94	13	1.71	300	329
SA12	88	12	1.64	318	343
SA18	82	10	1.46	145	328
SA24	76	14	1.70	137	329
SA30	70	10	1.58	141	316
SA40	60	8	1.50	209	328
SA60	40	7	1.56	269	336
Copolyester	**FDCA content / %**	M_n **/ kDa**	$Đ$	$T_{d,5\%}$ **/ °C**	$T_{d,15\%}$ **/ °C**
AA6	94	15	1.62	310	340
AA12	88	21	1.80	324	343
AA18	82	16	1.84	149	337
AA24	76	14	1.68	145	338
AA30	70	10	1.73	245	338
AA40	60	12	1.67	243	337
AA60	40	6	1.48	274	343
Copolyester	**FDCA content / %**	M_n **/ kDa**	$Đ$	$T_{d,5\%}$ **/ °C**	$T_{d,15\%}$ **/ °C**
SBA6	94	11	1.59	313	340
SBA12	88	15	1.35	328	346
SBA18	82	14	1.67	165	338
SBA24	76	23	2.17	214	339
SBA30	70	17	1.82	299	348
SBA40	60	8	1.48	333	354
SBA60	40	5	1.30	322	357

Conditions: 30.0 mmol of BDO, 10.0 mmol of a mixture of FCDA and the desired third monomer, 1.25 mol% $FeCl_3$, 160 °C for 17 h, followed by 215 °C and low pressure (<1 mbar) for 7 h. Precipitation in 1:1 (v/v) ethanol to water.

The differences in the water content of the obtained copolyesters, was measured in TGA and visible when regarding the polymer solids. It was expected that with increasing content of the third monomer, the possibility is increasing to isolate the polymer as viscous liquid instead of a solid. This assumption comes from the fact that the polyesters **P2** to **P4**, showing no FDCA in their backbone, were isolated as viscous liquids. However, there was no trend observable within the series of copolymerization reactions. *Figure 34* gives an example when comparing **SA6**, obtained as dry solid, to **SA30** a wet solid, even after drying under vacuum (<1 mbar) for 24 h. Increasing the SA content in the copolymerization reaction further, to **SA60**, the copolyester was obtained as dried solid, showing no water content, even after being stored for 24 h in an open vessel.

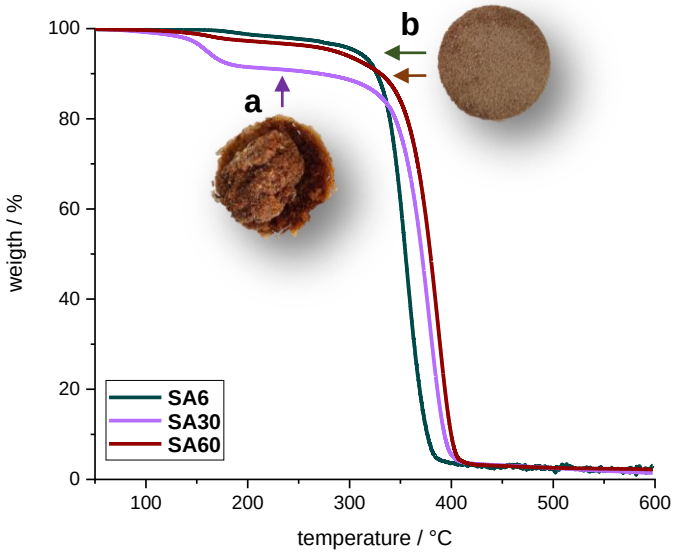

*Figure 34. TGA traces when measuring **SA6**, **SA30**, and **SA60**. Comparison of the obtained copolyesters solids with **a)** as wet solid due to sensitivity to humidity and **b)** dry solid, no sensitivity to humidity.*

For copolyesters based on SA, **SA24** showed the highest M_n of 14 kDa, within this series. For the series of copolyesters based on AA, **AA12** showed the highest M_n of 21 kDa. Comparing all copolyesters, the highest M_n polyester was obtained when copolymerizing with SBA, for **SBA24** with 24 kDa (see *Table 11*).

DSC measurements were performed for all copolyesters, which were obtained as solids. All DSC traces showed no T_m or T_c, what was expected according to literature, showing that an increasing content of BDO lead to a decreasing crystallinity of the polymer.[242] Thus, all discussed copolyesters were fully amorphous. A clear trend was observed for T_g (*Figure 35)*.

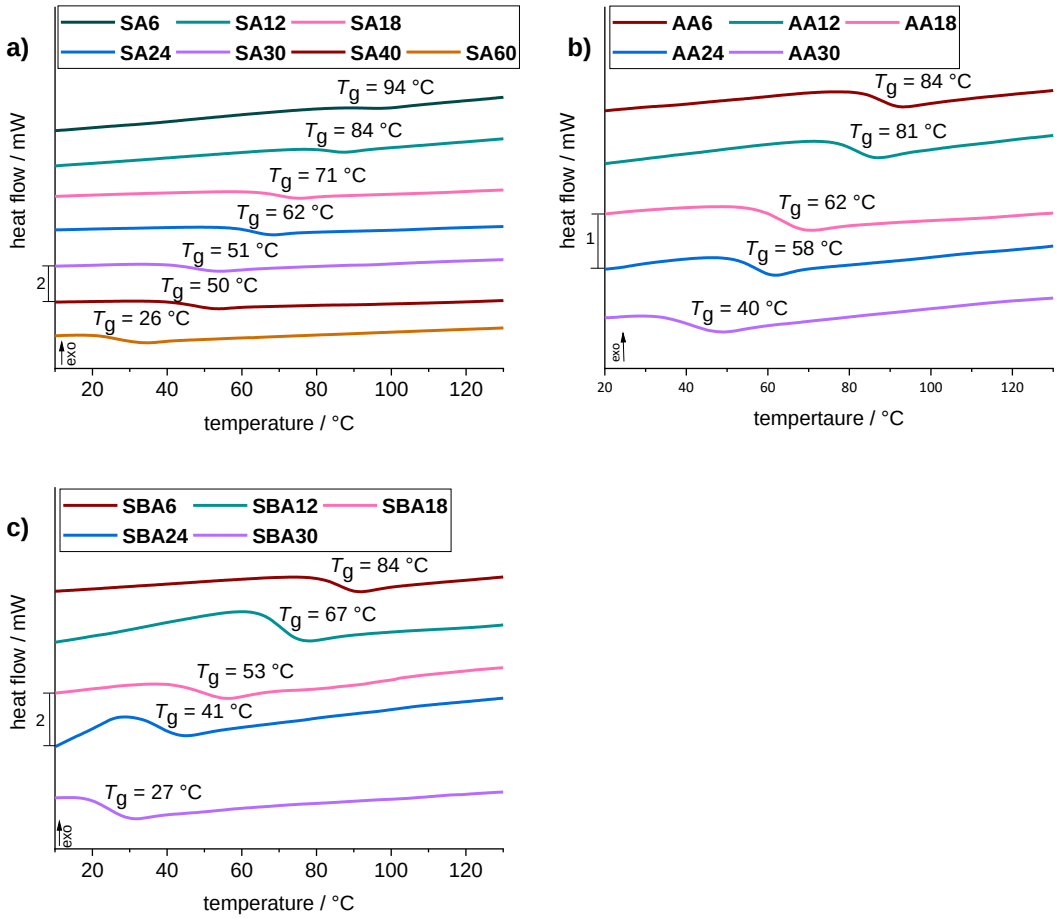

*Figure 35. Heating curves of all copolyesters, obtained as solid, measured in DSC from -10 – 150 °C in the second scan, showing the glass transition temperature (T_g) of polymers **a)** based on BDO, FDCA, and varying contents of SA **b)** based on BDO, FDCA, and varying contents of AA **c)** based on BDO, FDCA, and varying contents of SBA.*

For copolyesters **SA6** – **SA60**, the T_g varied between 26 °C and 94 °C. Copolyesters **AA6** – **AA30** showed T_g values between 40 °C and 84 °C. For copolyesters **SBA6** – **SBA30** the T_g values were between 27 °C to 84 °C. For SA, AA, and SBA copolyesters, the T_g decreased continuously with increasing content of the dicarboxylic acid, what was expected according to literature.[268] **SA6** showed the highest T_g of 94 °C, compared to the lowest T_g of 27 °C for **SBA30** (see *Figure 35*) which is caused due to the increased flexibility of the polymer chain when incorporating SBA in high contents, compared to SA as third monomer.

All copolyesters were prepared to investigate the influence of the three dicarboxylic acids on the thermal properties of **P1**. After copolymerization with the dicarboxylic acid as third monomer, the obtained copolyesters were, compared to **P1**, not soluble in cyclohexane anymore. In all cases, the introduction of one of the dicarboxylic acids reduced the T_g and T_d. This effect was most pronounced when increasing the content of AA, SA, or SBA.

The copolyester with the highest M_n of 24 kDa, was obtained when copolymerizing BDO with 76% FDCA and 24% SBA (**SBA24**). Compared to polyester **P1**, with 18 kDa, the M_n increased. However, **SBA24** showed a drastically decreased T_g with 41 °C, compared to polyester **P1** with 106 °C. **SBA24** was tested in the processability to form fibres, as the introduction of this dicarboxylic acid into polymers was expected to increase the flexibility. To do so, the polymer was molten and squirted through a 3 mm hole, then wound (see *Figure 36*).

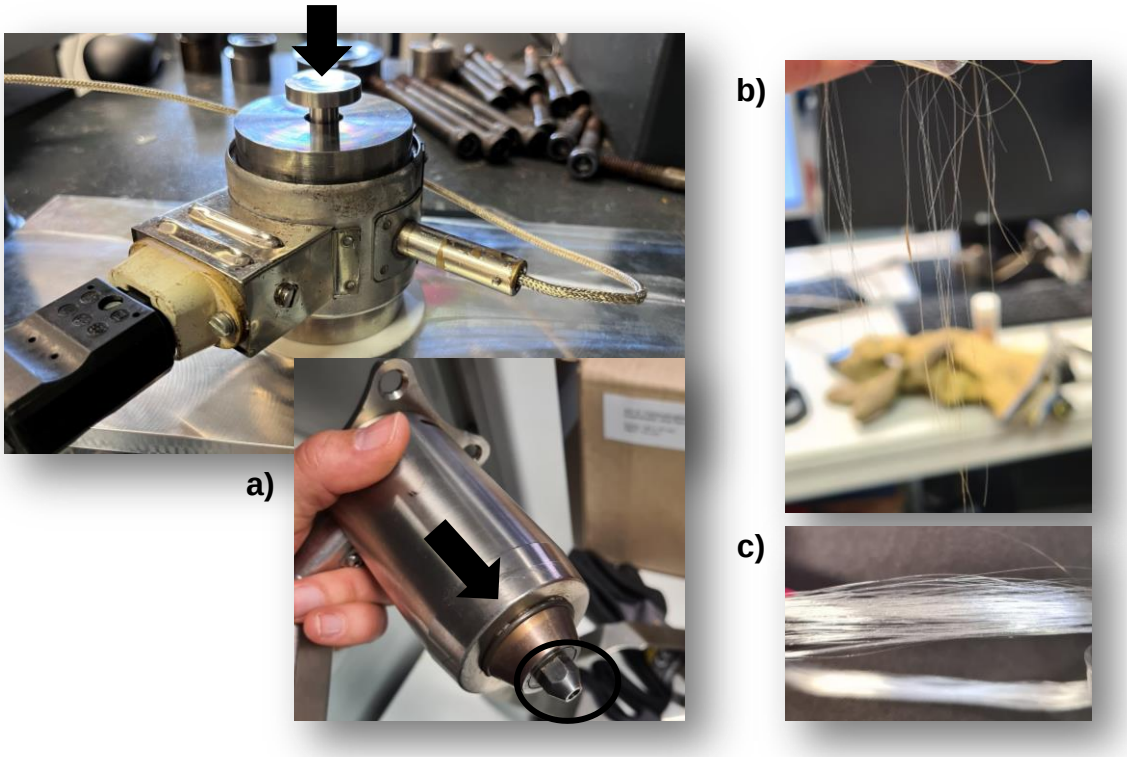

*Figure 36. Built-up experiment for fibre production out of the melt using copolyester **SBA24**. Copolyester solid heated to 100 °C **a)** molt squirt through hole **b)** fibres cooled to room temperature, **c)** fibre obtained when melting industrially purchased PET pellets.*

The here presented setup was working successfully in case of using industrial purchased PET pellets to form the desired fibre (see *Figure 36*, **c**). However, even by using the highest M_n copolyester within this project, showing SBA in its backbone, the obtained fibres were brittle (see *Figure 36*, **b**). Thus, attempts to analyze mechanical properties of the copolyester **SBA24** fibres unfortunately failed due to their remaining brittleness.

Conclusion

The deconvolution method was successfully used for the two-step polycondensation reaction of FDCA and BDO, revealing $FeCl_3$ as an environmentally friendly, more active, and cheaper catalyst compared to commonly used TTIP. After polymerization, a solid polyester was obtained with M_n of 18 kDa and a high T_g of 106 °C. Copolymerization reactions were performed to tune the properties of this polyester. The introduction of SA, AA, or SBA always led to a decrease in T_g, with SBA leading to the lowest T_g copolyesters. All obtained polymers remained brittle even after copolymerization. Thus, no mechanical properties were analyzed.

4.3 Polycondensation Reaction of Fermentation-generated 2,3-Butanediol towards a Renewable Polyester

The author of this thesis developed the synthetic procedure, planned, evaluated the experiments, and wrote the manuscript.

Samples of 2,3-butanediol from fermentation were provided by the working group of Prof. Dr. J. Gescher from Technical University Hamburg.

Abstract

While collaborating with bioengineers, who optimized the fermentation process of biomass to 2,3-butanediol (BDO-F), in the here presented work, the use of BDO-F in polycondensation reactions was studied. The purification of BDO-F via vacuum distillation is presented. The reactivity of the stereoisomers of the diol are compared in polycondensation reaction to polyesters based on 2,5-furanedicarboxylic acid (FDCA). A full characterization of all polymers is provided, with ^{1}H NMR and IR spectroscopy, differential scanning calorimetry (DSC), size exclusion chromatography (SEC), and thermogravimetric analysis (TGA).

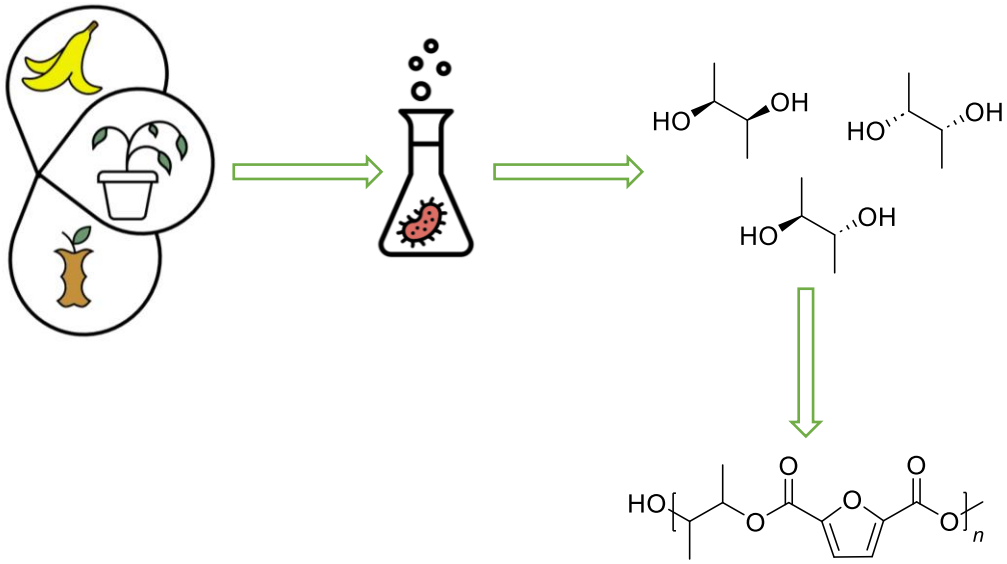

4.3.1 Purification of 2,3-Butanediol

Nowadays, several commodity chemicals, that are commercially produced in the petrochemical industry, can be synthesized *via* fermentation of renewable feedstock. Biomass is one of the most promising feedstocks for such processes, as it is available in high quantities.[68] As part of this thesis, the focus was on using BDO as renewable monomer in polymer syntheses. BDO can be synthesized *via* fermentation of biomass (here, named **BDO-F**). Some publications described the fermentation towards **BDO-F**, using glucose and included studies about the production of different isomeric mixtures, depending on the used bacteria and genes.(*)[101]

Our collaboration partners in Hamburg focused on the improvement of such fermentation processes based on fructose. For cultivation, they decided on using *Cupriavidus necator* H16 and furthermore studied the influence of different genes and enzymes, to increase the yield of BDO in the fermentation broth.(**)[104] This study is not published yet and currently still under investigation (date: October 2023).

After performing the fermentation, it is literature reported to extract the diol *via* liquid-liquid extraction using organic solvents.[106] This *in-situ* liquid-liquid extraction was performed successfully, by our collaboration partners, using isopropanol. To remove cells or other ingredients based on the fermentation broth, the sample mixture was furthermore centrifuged after extraction. To test the reactivity of **BDO-F** in polymerization reactions, the sample mixture was sent to our department. The received mixture was mainly based on isopropanol, **BDO-F** in an unknown stereoisomeric mixture and amount, unknown impurities, as well as unknown amounts of BDO precursors, such as acetoin. As a possibility to isolate **BDO-F**, it is literature reported that vacuum distillation is suitable.[108]

Isopropanol was removed under reduced pressure, followed by a vacuum distillation at 130 °C and <20 mbar to distill **BDO-F** (see *Figure 37*).

(*) For instance, *Enterobacteriaceae* mainly produces meso-BDO, whereas *Paenibacillaceae* mainly produces R-BDO.[101]

(**) *Cupriavidus necator* H16 is known as the best-studied knallgas bacterium using carbon dioxide as carbon source.[104]

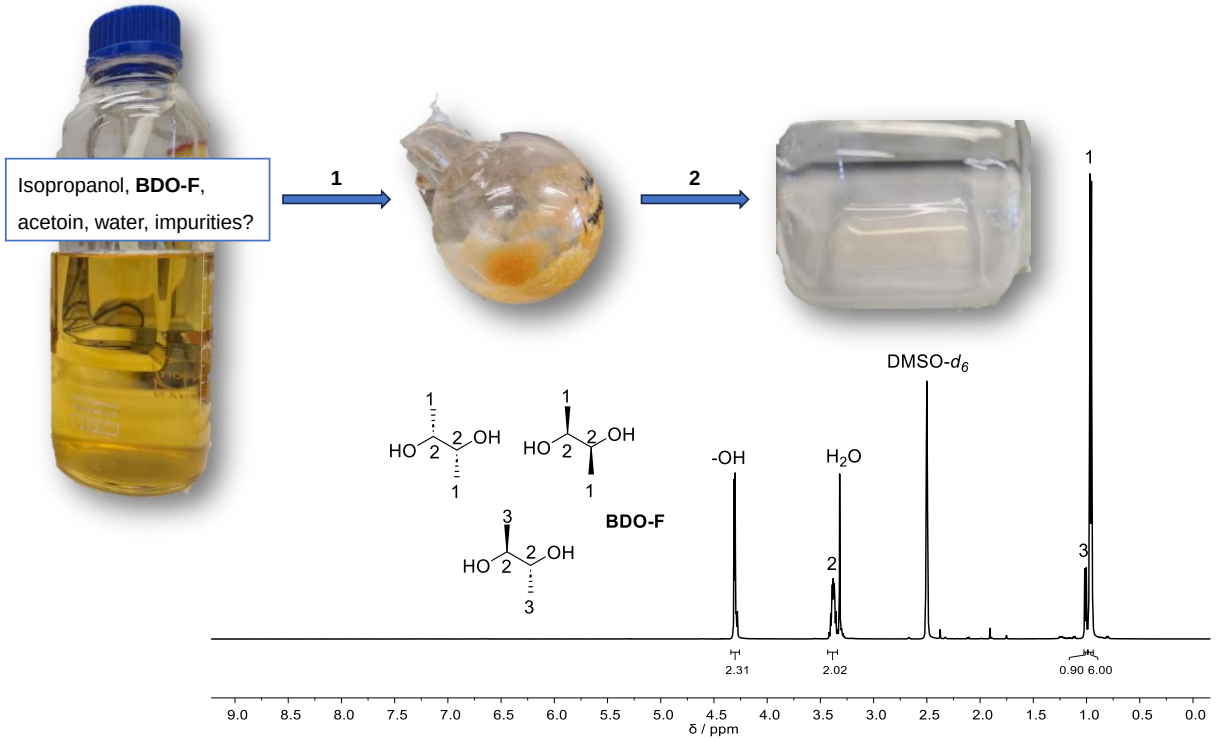

*Figure 37. [1]H NMR spectrum of **BDO-F** after 1: Removing isopropanol at reduced pressure and 2: Performing a vacuum distillation at 130 °C and <20 mbar.*

Small impurities of **BDO-F**, after distillation, were still visible at ~1.35 to 1.99 ppm (see *Figure 37*). However, no second distillation was performed.

Meso-BDO purchased from industry was obtained as solid, whereas RR/SS-BDO purchased from industry were liquids. **BDO-F** was isolated as liquid, suggesting that mainly RR/SS-BDO and only small amounts or no meso-BDO should be contained in the mixture. Furthermore, the ^{1}H NMR spectrum in *Figure 37* showed two signals for the methyl groups of BDO, at 1.03 – 0.99 ppm (integral = 0.90) and 0.98 – 0.94 ppm (integral = 6.00) in an integral ratio of 15% to 85%. To further prove which signal comes from which stereoisomer, *Figure 38* gives a comparison of the ^{1}H NMR spectra of **BDO-F**, RR/SS-BDO, and meso-BDO, with assignment of the signals.

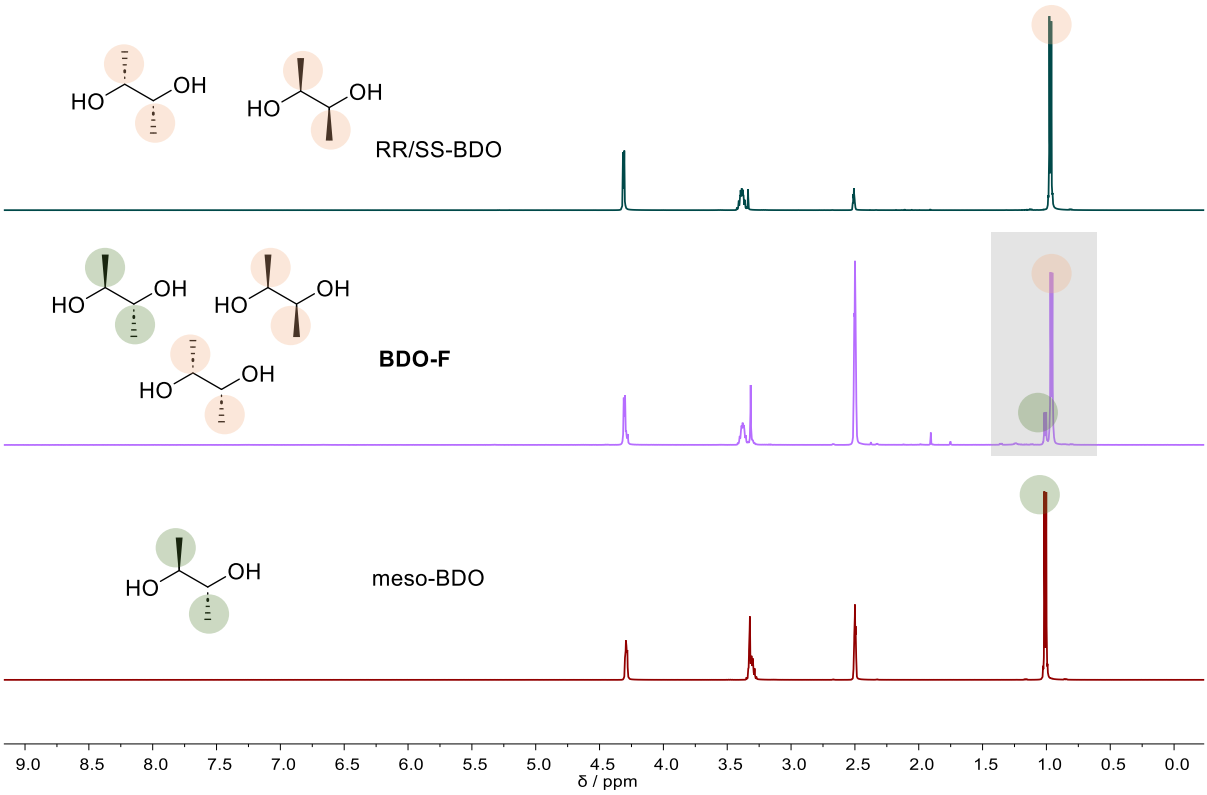

*Figure 38. ^{1}H NMR spectra comparison of meso-BDO, **BDO-F**, and RR/SS-BDO, measured in DMSO-d_6.*

RR/SS-BDO showed characteristic signals of the CH_3 protons at 3.37 ppm, whereas meso-BDO showed the characteristic CH_3 proton signal at 3.28 ppm (see *Figure 38*). Thus, the ratio of RR/SS-BDO to meso-BDO can be assigned in the **BDO-F** sample, with the ^{1}H NMR spectrum in *Figure 37*, ~15% meso-BDO to ~85% RR/SS-BDO. However, the proton signals where slightly overlapping, therefore gas chromatographic measurements were used for a more precise result of the obtained stereoisomeric mixture.

Furthermore, in GC, the enantiomers were separated accordingly, leading to the obtained signal ratio at certain retention times, listed in *Table 12*. Thus, **BDO-F** was obtained in a mixture of ~75% RR/SS-BDO to ~25% meso-BDO.

*Table 12. Signal ratios of in GC-2 measured samples of **BDO-F** and purchased BDO stereoisomers.*

Sample	Signal ratio at certain retention time / min	
	2.27	**2.32**
(2S, 3S)-butane-2,3-diol (SS-BDO) purchased from BLD PHARM	1.00	0.00
(2R, 3R)-(-)-2,3-butanediol (RR-BDO) purchased from SIGMA-ALDRICH	1.00	0.00
meso-2,3-butanediol (meso-BDO) purchased from SIGMA-ALDRICH	0.02	0.98
BDO-F	0.75	0.25

4.3.2 Polymerization of 2,3-Butanediol Stereoisomers

The influence of using FDCA in polymerization reaction with 1,4-butanediol or ethylene glycol, compared to using 2,4-FDCA or 3,4-FDCA, was researched by Thiyagarajan *et al.*[242] Main differences were observable when measuring DSC or TGA, with which 3,4-PEF showed the lowest T_g of 35 °C and the lowest degradation temperature with $T_{d,5\%}$ of 321 °C, compared to the other two isomers.

As part of this thesis, the influence on using different stereoisomers of BDO in the polycondensation reaction with FDCA, to a polyester (here, polyester **P1**), was researched. SS-BDO, RR-BDO, meso-BDO, purchased from industry, were compared to **BDO-F**. For RR-BDO and SS-BDO no differences in its reactivities were presumed, here mainly the reproducibility of the reaction was tested.

In each reaction, 30.0 mmol of the desired BDO were mixed with 10 mmol of FDCA, catalyzed by 1.25 mol% of $FeCl_3$. For more information about the used reaction conditions see **chapter 4.1. Sustainable Synthesis Strategy to Poly(ester urethane)s based on 2,3-Butanediol**. All polymers, **P1-SS**, **P1-RR**, **P1-meso**, and **P1-F** were precipitated as slightly brownish solids (see *Figure 39*). **P1-F** showed the darkest color compared to the other polymers, which might be caused due to small amounts of impurities, which were still present in the **BDO-F** sample even after purification *via* distillation (see ^{1}H NMR spectrum in *Figure 36*).

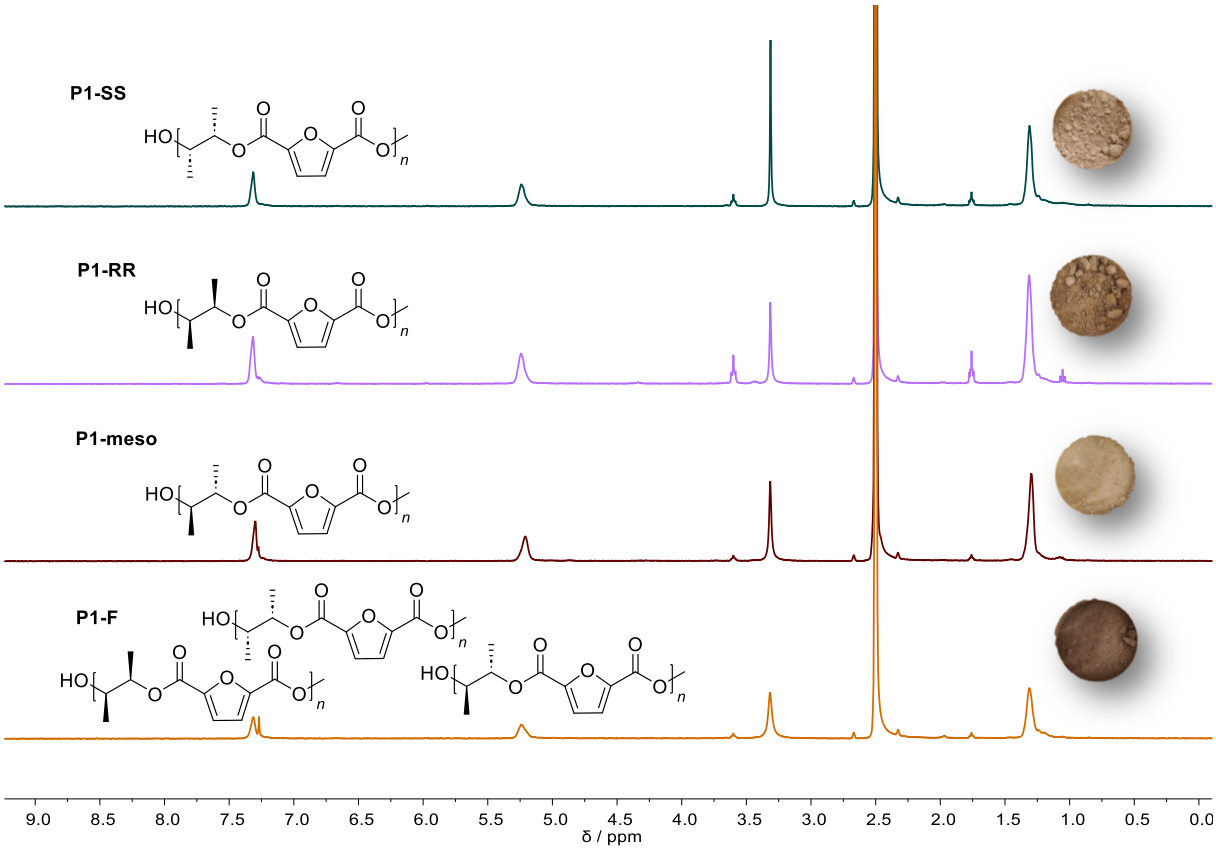

*Figure 39. ^{1}H NMR spectra of polyesters obtained via polycondensation reaction of FDCA and BDO measured in DMSO-d_6. **BDO-F** used to form **P1-F**, meso-BDO used to form **P1-meso**, RR-BDO used to form **P1-RR** and SS-BDO used to form **P1-SS**.*

All NMR spectra looked similar, when comparing the polymers based on different BDO stereoisomers (see *Figure 39*). The obtained polyesters were measured in SEC-THF, DSC, and TGA, listed in *Table 13*.

Table 13. SEC-THF results (M_n and Đ) of the respective polyesters and their thermal properties, i.e., T_g (DSC) and T_d (TGA).

Sample	M_n / kDa	Đ	T_g / °C	$T_{d,5\%}$ / °C
P1-F	3.0	2.35	89	264
P1-RR	2.4	1.85	88	166
P1-SS	3.6	2.18	102	267
P1-meso	5.0	1.68	100	280

It must be mentioned that the molecular weights of all polymers where decreased compared to **P1** of **chapter 4.1. Sustainable Synthesis Strategy to Poly(ester urethane)s based on 2,3-Butanediol** with M_n of 18 kDa. In **chapter 4.1**, HFIP-SEC was used, whereas in this chapter THF-SEC was used. Due to the different solvents the hydrodynamic volume of the polymers was different leading to different results in the molecular weight distribution. Thus, for instance **P1** sowed a M_n of 18 kDa in HFIP-SEC, whereas in THF-SEC a M_n of 6.0 kDa was measured.

In SEC-THF measurements, **P1-F** showed a M_n of 3.0 kDa with Đ of 2.35. **P1-meso** showed the highest M_n of 5.0 kDa (Đ = 1.68). **P1-SS** showed a M_n of 3.6 kDa (Đ = 2.18), whereas **P1-RR** showed a M_n of 2.4 kDa (Đ = 1.85). Comparing **P1-SS** and **P1-RR**, no differences in their molecular weight distributions were expected, therefore the measurements revealed that the polymerization might not be 100% reproducible. To test the reproducibility of the polymerization, e.g., always the same stirrer, heating plate, and flask should be used for each reaction and the reaction should be performed for at least three times under the same reaction conditions. However, no further tests were carried out as part of this project.

The polymers were analyzed *via* DSC showing the respective T_g, depicted in the corresponding traces in *Figure 40*. No T_m and T_c was observable, what was expected due to literature reported polymerization reactions, showing that BDO was used to restrain the crystallization of polymers.[112] Furthermore, Gubbels *et al.* reported fully amorphous polyesters, when using BDO in increasing contents.[113]

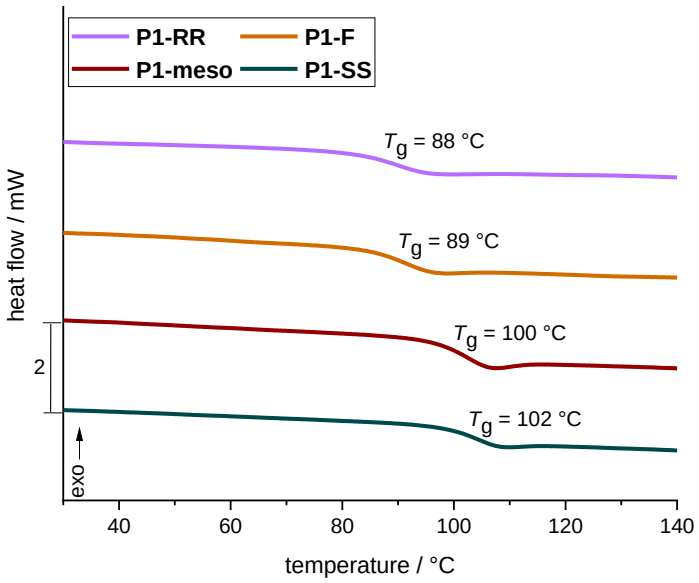

*Figure 40. Heating trace of **P1-RR**, **P1-SS**, **P1-meso**, and **P1-F** measured with DSC from -10 °C - 150 °C in the second scan.*

P1-SS showed the highest T_g with 102 °C, compared to the here discussed polyesters. The T_g of **P1-meso** with 100 °C was similar to **P1-SS**, followed by the T_g of **P1-F** with 89 °C. For the polyester with the lowest M_n, also the lowest T_g was observed, with 88 °C for **P1-RR**. For these low molecular weight oligomers, the T_g seemed to decrease with decreasing M_n of the respective polymer. This might also be the reason for the different T_g of **P1-RR** compared to **P1-SS**.

In TGA measurements, the polyester with the highest M_n (here: **P1-meso** with 5.0 kDa) showed the highest $T_{d,5\%}$ with 280 °C. The lowest $T_{d,5\%}$ was observed for **P1-RR** with 166 °C, being the polyester with the lowest M_n and T_g. Thus, it seemed that the T_d is decreasing with decreasing M_n of the polymer, therefore a higher M_n polymer shows a higher heat resistance. For **P1-F** a $T_{d,5\%}$ of 264 °C was measured, similar to the $T_{d,5\%}$ of **P1-SS** with 267 °C (*Table 13*). No differences in the brittleness of the obtained polyester solids or a change in the solubility of the polymers was noticeable. As the used stereoisomeric diols showed differences in their appearance, with meso-BDO being solid, whereas RR/SS-BDO were liquids, it was expected that such a difference might also be seen when comparing the brittleness of the desired polymer solids. However, it seemed that the BDO stereoisomers do not have an influence on the properties of the desired polyester.

Conclusion

BDO was successfully extracted from fermentation broths after fermenting biomass, carried out by our collaboration partners of the Technical University Hamburg. The literature reported vacuum distillation was suitable to isolate **BDO-F** in a stereoisomeric mixture. With GC and ^{1}H NMR spectroscopy, the stereoisomeric ratio of the **BDO-F** sample was analyzed, followed by successful polymerization of the diol with FDCA, catalyzed by $FeCl_3$. The obtained polyester was compared to polymers which were polymerized at the same reaction conditions, by using industrially purchased BDO enantiomers. The experiments revealed that by using meso-BDO, the highest M_n polymer with 5.0 kDa (SEC-THF) was observed. Furthermore, the polyester showed the highest degradation temperature ($T_{d,5\%}$ = 280 °C) as well as a noticeable high glass transition temperature (T_g = 100 °C). However, it was proven that the obtained experiments were not 100% reproducible to, e.g., always obtain the same M_n polymer. All in all, the stereoisomeric diols and the stereoisomeric mixture of **BDO-F** showed a similar reactivity with FDCA in polycondensation reaction. For our collaboration it was an important step forward, to prove that **BDO-F** can be extracted after performing their investigated fermentation, then purified, followed by successfully polymerizing to the desired polyester.

5. Conclusion and Outlook

This thesis concentrated on the contribution to find sustainable alternatives to produce biobased polymers using renewable feedstock. Having in mind that a sustainable development should meet the present necessities without compromising the needs of future generations, the herein presented research focused on investigating sustainable synthesis strategies in polymer science. The overall aim was to use 2,3-butanediol as renewable feedstock in the synthesis of biobased polyesters and non-isocyanate polyurethanes.

First, a synthesis strategy, following the 12 Principles of Green Chemistry, was investigated for poly(ester urethane)s. Renewable 2,3-butanediol was compared to renewable ethylene glycol, propylene glycol, and 1,2-octanediol, in the conversion to cyclic carbonates, while using dimethyl carbonate as solvent and reagent. A catalyst screening with different organocatalysts, revealed that 1,5,7-triazabicyclo[4.4.0]dec-5-ene was suitable to achieve a full conversion. Furthermore, while focusing on reducing the Environmental factor through different purification strategies, it was found that the ring-opening reaction of the cyclic carbonates, with renewable 11-amino undecanoic methyl ester, can be performed without a previous purification step. The obtained carbamates were successfully polymerized in bulk polycondensation reactions by using 1,5,7-triazabicyclo[4.4.0]dec-5-ene as organocatalyst to obtain the desired poly(ester urethane)s. All polymers were successfully characterized and showed suitable properties, i.e., the poly(ester urethane) based on 2,3-butanediol offered a reasonably high melting point (T_m 89 °C), paired with transparency of the pressed species. With small amplitude oscillatory shear, time sweep, and uniaxial elongation measurements a sample branching was indicated with increasing temperatures, showing no flow behavior as expected through DSC measurement. Thus, this poly(ester urethane), based on renewable 2,3-butanediol, was successfully used to produce foam samples, with a density of 0.16 g cm^{-3} and a cell size ranging from 1.25 µm to 3.53 µm.

Moreover, a two-step polycondensation in melt to polyesters was investigated by using 2,3-butanediol, with the sugar derived 2,5-furandicarboxylic acid. The deconvolution method was successfully used to screen for a suitable catalyst in an easy and fast way. With a screening of 16 randomly chosen Lewis Acids, iron(III)chloride revealed to be the most active catalyst in the system, being cheaper compared to industrially used titanium(IV) isopropoxide. The renewable polyester showed a M_n of 18 kDa and a T_g of 106 °C. To tune the properties of the polyester, copolymerization reactions were performed, introducing further renewable dicarboxylic acids. However, all obtained copolyesters remained brittle with low glass transition temperature, decreasing further when increasing the content of the third monomer.

The influence of the stereoisomers of 2,3-butanediol in polycondensation reactions was tested in a collaboration project with the Technical University Hamburg. After successful fermentation, the diol was isolated and purified *via* vacuum distillation. The 2,3-butanediol obtained from fermentation was then compared to its stereoisomers, in a polycondensation reaction with 2,5-furandicarboxylic acid. No significant differences in the polymer properties were recorded.

Overall, fundamental research was performed with 2,3-butanediol as renewable monomer in different polymer syntheses. Besides, using biobased materials, also catalyst screenings were successfully performed, and waste production as well as the use of toxic substances was prevented within all presented strategies. Novel promising polymeric materials were introduced as alternatives to fossil-based polymers. However, further improvements are necessary to successfully find a way in replacing daily used polymeric materials, by implementing biobased polymers using renewable feedstock.

6. Experimental Section

6.1 Solvents and Reagents

Unless otherwise noted, all listed solvents and reagents were used as received without further purification.

Acetic acid (99.9%, CARL ROTH GmbH), acetic acid anhydride (technical grade, FISHER SCIENTIFIC), adipic acid (99%, ACROS ORGANICS), aluminium(III) chloride (98.5%, ACROS ORGANICS), 11-aminoundecanoic acid (97%, SIGMA-ALDRICH), biphenyl (99%, ALFA AESAR), bismuth(III) trifluoromethanesulfonate (99%, ALFA AESAR), boron trifluoride diethyl etherate (technical grade, SIGMA-ALDRICH), 2,3-butanediol (98%, SIGMA-ALDRICH), 2,3-butanediol (98%, mixture of racemic and meso forms, THERMO FISHER), meso-2,3-butanediol (99%, SIGMA-ALDRICH), (2R, 3R)-(-)-2,3-butanediol (97%, SIGMA-ALDRICH), (2S, 3S)-butane-2,3-diol (97%, BLD PHARM), cerium(IV)sulfate anhydrous (99.0%, CHEMPUR), chloroform (technical grade); $CDCl_3$ (99.8%, stabilized with silver foils, EURISOTOP®), copper(I) chloride (97%, SIGMA-ALDRICH), 1,5-diazabicyclo(4.3.0)non-5-en (98%, ACROS CHEMICALS), 1,3-diazabicyclo(5.4.0)undec-7-ene (>98.0%, TCI CHEMICALS), diethyl ether (technical grade), dimethyl carbonate (99%, ACROS CHEMICALS), dimethyl formamide (99.9%, VWR CHEMICALS), dimethyl sulfoxide (99.9%, THERMO FISHER), DMSO-d_6 (99.80%, EURISOTOP®), ethanol (HPLC grade, VWR CHEMICALS), ethyl acetate (HPLC grade), ethylene glycol (≥99.5%, Riedel-de Haën®), furan-2,5-dicarboxylic acid (98%, BLD PHARMATECH), glycine (99.0%, ALFA AESAR), 1,1,1,3,3,3-hexafluoro-2-propanol (fluorochem), indium(III) chloride (99,99%, SIGMA-ALDRICH), indium(III) trifluoromethanesulfonate (SIGMA-ALDRICH), iron(III) chloride anhydrous (>97.0%, FLUKA), itaconic acid (≥99%, SIGMA-ALDRICH), lithium bromide (98%, FLUKA), magnesium chloride hexahydrate (99%, SIGMA-ALDRICH), methanol (VWR CHEMICALS), 1,2-octanediol (99.91%, BLD PHARMATECH LTD.), phosphomolybdic acid hydrate (SIGMA-ALDRICH), potassium ferrocyanide trihydrate (98.5%, THERMO FISHER), potassium trifluoroacetate (98%, SIGMA-ALDRICH), propylene glycol (>99.0%, TCI CHEMICALS), pyridine (≥99.5%, THERMO FISHER), scandium(III) trifluoromethanesulfonate (99,99%, SIGMA-ALDRICH), sebacic acid (for synthesis, SIGMA-ALDRICH), silica gel (technical grade, pore size 60 Å. 230 – 400 mesh particle size, 40 – 63 µm particle size, SIGMA-ALDRICH), silver trifluoromethanesulfonate (≥99%, SIGMA-ALDRICH), sodium bisulfite (SIGMA-ALDRICH), succinic acid (99%, ACROS CHEMICALS), tetradecane (≥99.0%, SIGMA-ALDRICH), tetrahydrofuran (99.7%, VWR CHEMICALS), THF with 250 ppm butylated hydroxytoluene

(≥99.9%, SIGMA-ALDRICH), 1,1,3,3-tetramethylguanidine (99%, ABCR CHEMICALS), thionyl chloride (99.5%, ACROS CHEMICALS), tin(II) chloride (98%, ACROS ORGANICS), tin(II) 2-ethylhexanoate (95%, ALFA AESAR), titanium(IV) isopropoxide (98%, ACROS CHEMICALS), titanium(IV) n-butoxide (>99%, ALFA AESAR), 1,5,7-triazabicyclo[4.4.0]dec-5-ene (>98.0%, TCI CHEMICALS), triethylamine (99.5%, SIGMA-ALDRICH), ytterbium(III) trifluoromethanesulfonate (99,9%, ACROS ORGANICS), zinc bromide (>98%, SIGMA-ALDRICH), zinc(II) trifluoromethanesulfonate (98%, SIGMA-ALDRICH).

6.2 Instruments and Characterization Methods

Column chromatography was performed with silica gel F254 (SIGMA-ALDRICH) and solvents purchased in HPLC grade.

Differential scanning calorimetry (DSC) of poly(ester urethane)s was performed on a DSC Q200 TA instrument operating under nitrogen atmosphere using ~12 mg of the respective polymer for the analysis. All thermal properties (T_g, T_m and T_c) were analyzed on the second heating or cooling scan by using the following method: First, heating from 40 °C to -150 °C (10 °C min^{-1}), the cooling from 150 °C to -90 °C (-10 °C min^{-1}) and subsequently heating from -90 °C to 150 °C (10 °C min^{-1}) for poly(ester urethane)s. Measurements are labelled as DSC-2. Polyesters were measured with the following method and instrument using ~7 mg of the respective sample: METTLER TOLEDO DSC star$_e$ system. The DSC experiments were carried out under nitrogen atmosphere using 100 µL aluminium pan. First, heating from 25 °C to 150 °C (20 °C min^{-1}), the cooling from 150 °C to -10 °C (-20 °C min^{-1}) and subsequently heating from -10 °C to 150 °C (20 °C min^{-1}) per cycle, using 50 mL min^{-1} N_2. Measurements are labelled as DSC.

Electrospray-ionization mass spectrometry (ESI-MS) mass spectra were recorded on a Q Exactive (Orbitrap) mass spectrometer from THERMO FISHER SCIENTIFIC, equipped with an atmospheric pressure ionization source operating in the nebulizer assisted electrospray mode. The instrument was calibrated in the m/z-range 150 – 2000. The standard contained caffeine, Met-Arg-Phe-Ala acetate (MRFA) and a mixture of fluorinated phosphazenes (Ultramark 1621, all purchased from SIGMA-ALDRICH). A constant spray voltage of 3.5 kV, a dimensionless sheath gas of 6, and a sweep gas flow rate of 2 were applied. The capillary voltage and the S-lens RF level were set to 68.0 V and 320 °C, respectively. For the interpretation of the spectra, molecular peaks $[M]^+$, peaks of pseudo molecules $[M+H]^+$ and characteristic fragment peaks are indicated with their mass to charge ratio (*m/z*).

Fast atom bombardment (FAB) mass spectra were recorded on a FINNIGAN MAT 95 instrument. The protonated molecule ion and the sodium adduct are expressed by the terms: $[M+H]^+$ and $[M+Na]^+$, respectively.

Fermentation was carried out by the Technical University of Hamburg. The production trains were cultivated in LB-Medium (Lennox) with added D-fructose (300mM) at 30 °C in a shaking incubator at 180 rpm. The production strain of *Cupravidus necator* H16 was carrying a production plasmid with the codon optimized acetoin production genes *alsS* and *alsD* of *Bacillus subtilis PY79* and the additionally necessary gene *budC* of *Enterobacter cloacae* to produce 2,3-butanediol. The purification *via* liquid-liquid extraction in isopropanol and ammonium sulfate (1.7:1, v/v) was carried out over 10 h. The phases were allowed to settle before separating. After extraction, the isopropanol containing 2,3-butanediol mixture was centrifuged 10.000xg (10.1007/s10529-008-9874-3) for 20 min to remove residuals of media and bacterial cells.

Gas chromatography (GC) was performed on a BRUKER 430 GC instrument equipped with a capillary FACTORFOUR™ VF-5 ms (30.0 m × 0.25 mm × 0.25 µm) column, using flame ionization detection (FID). The oven temperature program was: Initial temperature 95 °C, hold for 1 min, ramp to 100 °C with 15 °C min^{-1}, hold for 4 min, ramp to 300 °C with 15 °C min^{-1}, hold for 2 min. Measurements were performed in split-split mode using nitrogen as the carrier gas (flow rate 30 mL min^{-1}) and were recorded for 20 min in total. Measurements are labelled as GC.

GC measurements of 2,3-butanediol stereoisomers were performed on an AGILENT 8860 GC instrument with a HP-5 column (30 x 0.32 mm x 0.25 µm) and a flame ionization detector (FID). Initial temperature 77 °C, hold for 3 min, ramp to 90 °C with 5 °C min^{-1}, hold for 3 min, ramp to 160 °C with 15 °C min^{-1}, hold for 2 min, ramp to 200 °C with 15 °C min^{-1}, hold for 2 min, ramp to 333 °C with 15 °C min^{-1}, hold for 5 min. Measurements were performed with a split ratio of 50:1 using nitrogen as make-up gas and helium as carrier gas with a flow rate of 1.0 mL min^{-1}. Measurements are labelled as GC-2.

All samples, for both instruments, were prepared by dissolving 1.5 – 2.0 mg of compound in 1.5 mL ethyl acetate, filtered *via* syringe filter (polytetrafluoroethylene, 13 mm diameter, 0.2 µm pore size, AGILENT) prior to measurement.

Inductively coupled plasma optical emission spectroscopy (ICP-OES) was used for the measurement of the iron content in the antisolvent used for precipitation of polyesters. Fa. Agilent, ICP-OES SVDV 5100 G6010A with CCD-Detector, Autosampler SPS3, G8480 A and cooling system G8481A.

Infrared (IR) spectroscopy was performed using a BRUKER ALPHA-P instrument with ATR technology. All spectra were recorded in a frequency range of $\tilde{\nu}$ = 400 – 4000 cm^{-1} with 24 scans per measurement. IR (type of measurement) $\tilde{\nu}$ / cm^{-1} = wave number (signal intensity, molecular oscillator assignment).

Nuclear magnetic resonance (NMR) spectroscopy was performed on a BRUKER AVANCE 400 NMR instrument at 400 MHz with 16 scans for ^{1}H NMR and at 101 MHz with 1024 scans for ^{13}C NMR. The chemical shifts are reported in parts per million (ppm) and referenced to the solvent signal of partly deuterated DMSO-d_6 at 2.50 ppm (^{1}H NMR) or 39.5 ppm (^{13}C NMR) and of $CDCl_3$ at 7.26 ppm (^{1}H NMR) or 77.2 ppm (^{13}C NMR), respectively. All spectra were measured at ambient temperature and in a standard fashion unless otherwise stated. The spin multiplicity and corresponding signal patterns were abbreviated as followed: s = singlet, d = doublet, t = triplet, m = multiplet. Coupling constants (J) were noted in Hertz (Hz). If isomers of a substance were observed, all species which were assigned were clearly labelled with additional appendices (*). If constitutional isomers of a substance were observed, both species were separately labelled with additional appendices (A and B). Full assignment of structures was aided by 2D NMR analysis (COSY, HSQC, and HMBC).

Pressing of polymers was prepared in a Hotpress using a WEBER-PRESS with a hydraulic handpress PW20. For poly(ester urethane) based on ethylene glycol, 130 °C and for poly(ester urethane) based on propylene glycol 150 °C pressing temperature was needed to achieve a square form (1.33 mm thickness, 7.75 mm width, 34.0 mm length). A bone form (1.45 mm thickness, 3.30 mm width, 45.0 mm length) was achieved for poly(ester urethane)s based on 2,3-butanediol using 130 °C and full vacuum while pressing.

Physical foaming of poly(ester urethane)s based on 2,3-butanediol was conducted using supercritical carbon dioxide as foaming agent. The sample was saturated at 120 °C and 500 bar for 8 h. The depressurization rate was around 200 bar sec^{-1}. The density (ρ) of the foam was measured using a density kit based on Archimedes' principle and the volume expansion ratio (VER) was calculated by *Equation S 1.*

$$VER = \rho_p/\rho_f$$

Equation S 1. Calculation of the volume expansion ratio of foams.

Here, ρ_p and ρ_f are the densities of the neat polymer and the foam, respectively.
The cell structure was analyzed *via* scanning electron microscopy (SEM). Then, the cell density was calculated by *Equation S 2.*

$$N = (n/A)^{3/2}(VER)$$

Equation S 2. Calculation of the cell density of foams.

Here, N is the cell density in cell cm^{-3}, n is the number of cells in an observed area A. The average cell size can be calculated by *Equation S 3.*

$$D = 10^4[(VER-1)/(N\pi/6)]^{1/3}$$

Equation S 3. Calculation of the average cell size of foams.

Here, D is the diameter in µm. Furthermore, the cell size was measured using ImageJ and compared to the calculated value.

Size exclusion chromatography (SEC) of poly(ester urethane)s was performed in 1,1,1,3,3,3-hexafluoro-2-propanol (HFIP) containing 0.10 wt% potassium trifluoroacetate on a Tosoh EcoSEC HLC-8320 SEC system, with a solvent flow of 0.40 mL min^{-1} at 30 °C and a sample concentration of 1 mg mL^{-1} injecting 50 µL. The analysis was performed on a three-column system: PSS PFG Micro precolumn (3.0 × 0.46 cm, 10000 Å), PSS PFG Micro (25.0 × 0.46 cm, 1000 Å) and PSS PFG Micro (25.0 × 0.46 cm, 100 Å). The system was calibrated with linear poly(methyl methacrylate) standards (Polymer Standard Service, Mp: 800 Da - 1600 kDa). Measurements are labelled as SEC-HFIP-2.
For polyesters SEC measurements were performed in 1,1,1,3,3,3-hexafluoro-2-propanol (HFIP) containing 0.10 wt% potassium trifluoroacetate on a Tosoh EcoSEC HLC-8320 SEC system, with a solvent flow of 0.40 mL min^{-1} at 35 °C and a sample concentration of 1 mg mL^{-1} injecting 50 µL. The analysis was performed on a two-column system:
PSS PFG Micro column (8.00 × 55.0 mm, 50000 Å) and PSS PFG Linear S column (8.00 × 300 mm, 50000 Å). The system was calibrated with linear poly(methyl methacrylate) standards (Polymer Standard Service, Mp: 800 Da - 1600 kDa). Measurements are labelled as SEC-HFIP.
If polymers were soluble in tetrahydrofuran and for SEC screenings over time, further measurements were performed on a Shimadzu SEC system equipped with a Shimadzu isocratic pump (LCYCLO20AD), a Shimadzu refractive index detector (24 °C, RID-20A), a

Shimadzu autosampler (SIL-20A) and a Varian column oven (model 510, 50 °C). For separation, a three-column setup was used with one SDV 3 µm, 8 x 50 mm precolumn and two SDV 3 µm, 100 Å, 3 x 300 mm columns supplied by PSS, Germany. Anhydrous tetrahydrofuran stabilized with 250 ppm butylated hydroxytoluene (≥99.9%) supplied by SIGMA-ALDRICH was used at a flow rate of 1.0 mL min^{-1}. For calibration, linear poly(methyl methacrylate) standards (Aglient) ranging from 875 Da to 1677 kDa were used. Dispersity was determined by integration of the peak in LabSolution software. The program calculates M_w/M_n which are obtained *via* the calibration. Measurements are labelled as SEC-THF.

Small-amplitude oscillatory shear (SAOS) experiments with poly(ester urethane) based on 2,3-butanediol were performed using 13 mm parallel plates on an ARES G2 RHEOMETER (TA instruments) under nitrogen atmosphere to minimize polymer oxidation or degradation. Oscillatory strain sweeps (γ_0 = 0.01 – 200%) at a constant angular frequency of ω = 10 rad sec^{-1} were utilized to determine the linear viscoelastic (LVE) regime at 130 °C and 150 °C, followed by oscillatory frequency sweeps. Both frequency sweeps were carried out with a strain amplitude of γ_0 = 5%.

Solubility tests of polyesters were performed by using 5 mL glass tubes with ~2 mg of sample, adding the respective solvent. Mixing by hand was carried out at room temperature. Solubility was checked visually.

Tensile elongation tests were tested for poly(ester urethane)s using different grips. As sample preparation the desired polymer solid was pressed in a HotPress (see ***Pressing of polymers***). Manual vise grips, wedge grips, and pneumatic grips (SCHUNK). 3 bar and 50 N were used during the measurements, all performed on a ZWICK ROELL UNIVERSAL testing machine Z2.5m with a maximum force of 1 kN. Evaluation was performed using TEXTXPERTLL (DIN ISO 527_Zugversuche an Kunststoffen).

Thermogravimetric analysis (TGA) of all samples was performed on a TA INSTRUMENT TGA 5500 under nitrogen atmosphere using platinum TGA sample pans. A heating rate of 10 K min^{-1} in a temperature range from 25 °C to 600 °C was applied.

Thin layer chromatography (TLC) was performed on silica gel coated aluminium plates (silica gel 60 F_{254}, SIGMA-ALDRICH). Compounds were visualized by staining with Seebach-solution (mixture of phosphomolybdic acid hydrate, cerium(IV)-sulfate, sulfuric acid, and water) or potassium permanganate solution (mixture of potassium permanganate, potassium carbonate, 10% sodium hydroxide, and water).

Time sweeps with poly(ester urethane) based on 2,3-butanediol were performed with a strain of 10% at a temperature of 130 °C for 13,000 sec.

Uniaxial elongational measurements of poly(ester urethane) based on 2,3-butanediol were performed with extensional viscosity fixture (EVF) under nitrogen flow at 130 °C and 150 °C. Extensional rates were varied between $\dot{\varepsilon}$ = 1 sec^{-1} – 0.01 sec^{-1}. Samples are pressed under vacuum to the desired geometry *via* compression moulding at 130 °C and 150 °C for 10 min (under 10 bar, if necessary) and then cooled down to room temperature.

6.2 General Reaction Procedures

6.2.1 Experimental Procedures of 4.1. Sustainable Synthesis Strategy to Poly(ester urethane)s based on 2,3-Butanediol

This chapter is based on previously published results by the author of this thesis:

A. Kirchberg, M. K. Esfahani, M. Röpert, M. Wilhelm, M. A. R. Meier, *Macromol. Chem. Phys.* **2022**, 220010.[111]

Text, figures, and data are reproduced from this article and were adopted and modified with permission of the Macromolecular Chemistry and Physics Journal. The author of this thesis developed the synthetic procedure, planned, and evaluated the experiments.

M. K. Esfahani gave input on rheology measurements and wrote the chapter about small-amplitude oscillatory shear and uniaxial elongational measurements.

M. Röpert gave input on the proof-principle and wrote the chapter about foaming experiments.

The bachelor thesis of La Vinh Hao, co-supervised by the author of this thesis, was about the preparation of cyclic carbonate, carbamate, and polyurethane based on 1,2-octanediol. Further experiments including the separation of constitutional isomers and analyses of polymeric properties were then performed by the author of this thesis.

For all experiments of this project, 2,3-butanediol (BDO) was purchased from industry (SIGMA ALDRICH) as mixture of racemic and meso forms.

Synthesis of 11-amino undecanoic methyl ester (A1)

The here used procedure, to synthesize an undecanoic acid methyl ester, was previously published in a manuscript of our group, Meier *et al.*[302]

1.00 equiv. of 11-amino undecanoic acid (10.0 g, 50.0 mmol) was suspended in 37.5 equiv. methanol (75.0 mL, 1.88 mol), followed by cooling the suspension in an ice bath. Then, 3.10 equiv. of thionyl chloride (18.4 g, 0.155 mol) were added dropwise at ~0 °C, during which the solution became clear. The mixture was warmed to room temperature and stirred overnight while the product was precipitating. The mixture was poured into a round-bottom flask containing 350 mL diethyl ether, then stored in a freezer overnight. The product, 11-amino undecanoic acid methyl ester **A1**, was filtered off and dried under vacuum. **A1** was isolated as white powder in a yield of 88% (43.9 mmol, 9.45 g). Reaction control was performed *via* NMR spectroscopy in DMSO-d_6.

A1:

^{1}H NMR (400 MHz, DMSO-d_6) δ / ppm = 7.84 (s, 2H, NH_2), 3.57 (s, 3H, CH_3^6), 2.77 – 2.70 (m, 2H, CH_2^1), 2.28 (t, J = 7.4 Hz, 2H, CH_2^5), 1.59 – 1.43 (m, 4H, CH_2^2 and CH_2^4), 1.24 (s, 12H, CH_2^3).

^{13}C NMR (101 MHz, DMSO) δ / ppm = 173.84, 51.63, 33.73, 29.22, 29.11, 28.97, 28.91, 27.41, 26.29, 24.89.

IR (ATR) $\tilde{\nu}$ / cm^{-1} = 3034, 2985, 2919, 2849, 1724, 1611, 1561, 1510, 1479, 1469, 1444, 1419, 1397, 1376, 1362, 1335, 1306, 1277, 1246, 1212, 1174, 1115, 1098, 1002, 971, 938, 887, 743, 724.

HRMS (FAB) *m/z*: $[M]^+$ calc. for $C_{12}H_{25}O_2N$, 215.1880; found 215.1881; Δ = 0.1 mmu.

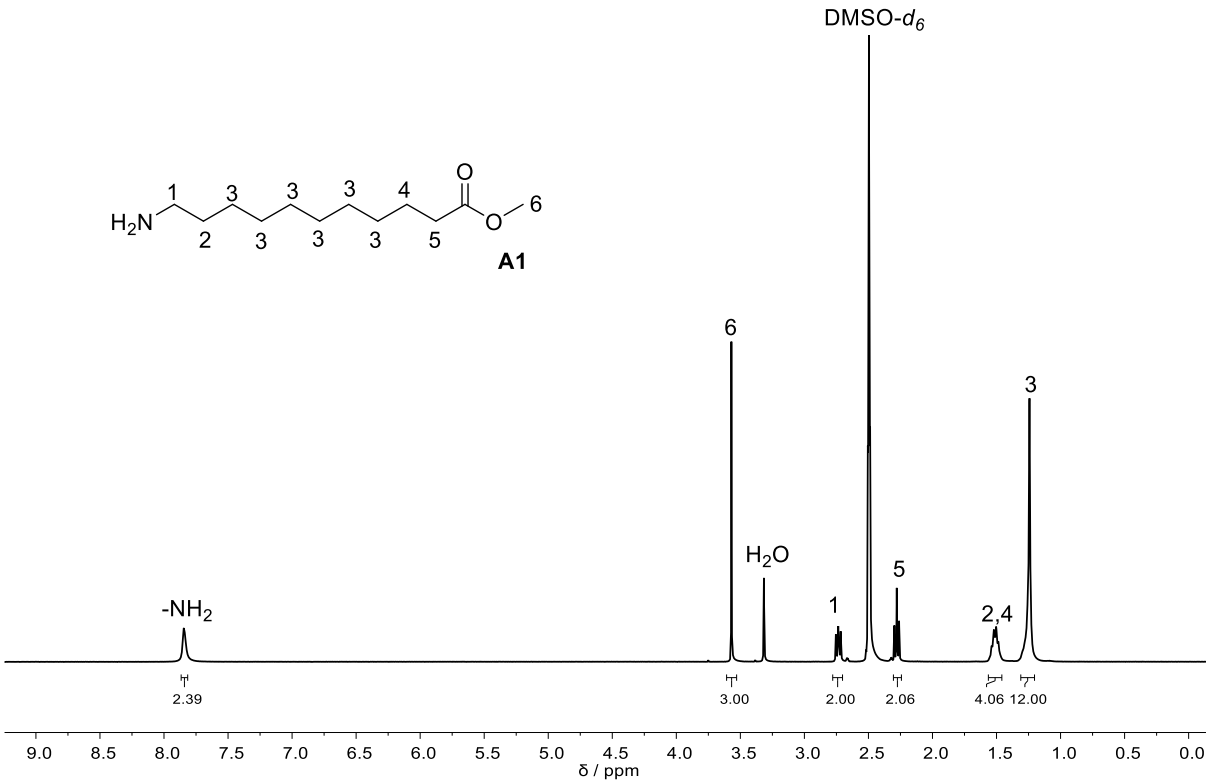

*Figure S 1. ^{1}H NMR spectrum of monomer **A1** in DMSO-d_6.*

General procedure for the preparation of cyclic carbonates based on diols and dimethyl carbonate (C1 – C4)

1.00 Equiv. of the desired diol was mixed with 1.20 equiv. of DMC (5.40 g, 60.0 mmol), then 1 mol% TBD (702 mg, 500 µmol) was added. The mixture was heated to 80 °C and stirred for 22 h under reflux adding a reflux condenser onto the flask. Reaction control was performed *via*

TLC and/or GC as well as NMR spectroscopy. All obtained cyclic carbonates were purified *via* column chromatography using a solvent mixture of 1:1 (v/v) ethyl acetate and cyclohexane.

For the preparation of cyclic carbonate **C1**, BDO (4.50 g, 50 mmol) was used. BDO was purchased from SIGMA-ALDRICH in a racemic mixture. Thus, isomers in the **C1** structure, coming from BDO, are marked accordingly (*) in the obtained ^{1}H NMR spectrum. After column chromatography **C1** was obtained as colorless oily liquid, in a yield of 43% (2.50 g, 21.5 mmol).

C1:

R_F (ethyl acetate / cyclohexane 1:1 v/v) = 0.47.

^{1}H NMR (400 MHz, $CDCl_3$) δ / ppm = 4.89 – 4.76 (m, 1H, (CH^{1}), 4.38 – 4.26 (m, 1H, CH^{1*}), 1.48 – 1.41 (m, 3H, $CH_3{}^{2}$*), 1.39 – 1.29 (m, 3H, $CH_3{}^{2}$).

^{13}C NMR (101 MHz, $CDCl_3$) δ / ppm = 154.69, 79.98, 76.10, 18.38, 14.38.

IR (ATR) $\tilde{\nu}$ / cm^{-1} = 2991, 1783, 1465, 1386, 1368, 1356, 1318, 1197, 1152, 1142, 1065, 1028, 1012, 987, 775, 716, 699, 681, 551, 502.

HRMS (FAB) *m/z*: $[M]^+$ calc. for $C_5H_8O_3$, 116.0468; found 116.0467; Δ = 0.1 mmu.

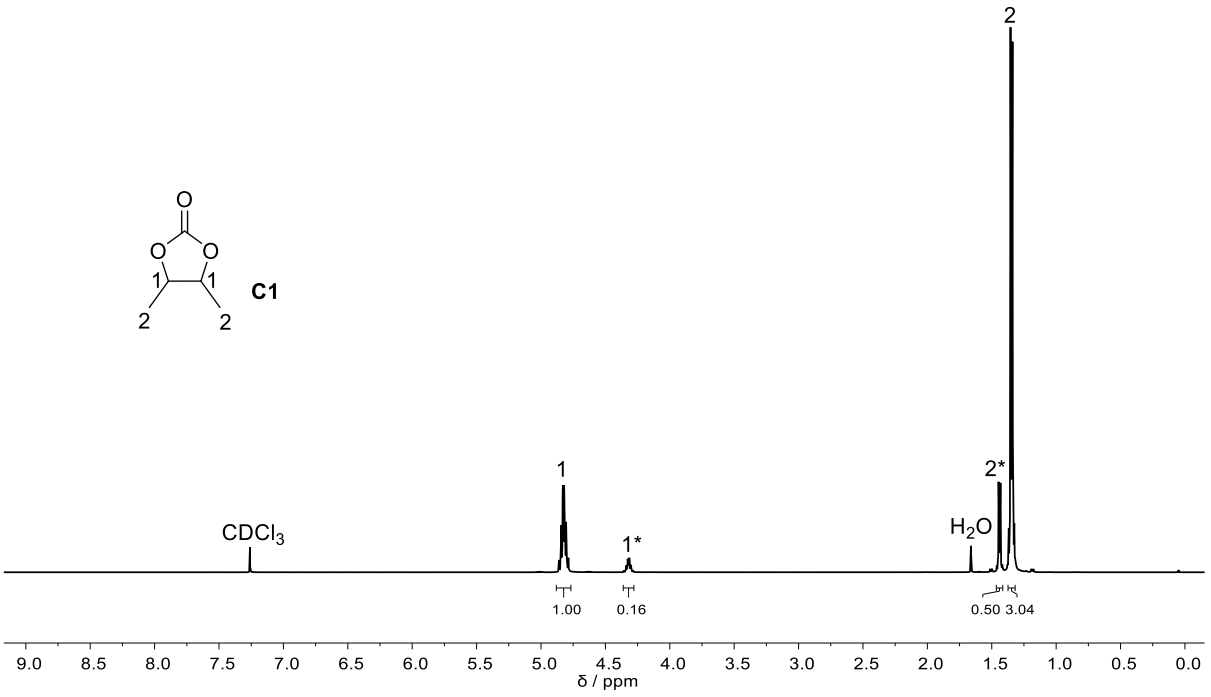

*Figure S 2. ^{1}H NMR spectrum of cyclic carbonate **C1** in $CDCl_3$.*

For the preparation of cyclic carbonate **C2**, PG (3.80 g, 50.0 mmol) was used. After column chromatography **C2** was obtained as colorless liquid, in a yield of 86% (4.41 g, 43.2 mmol).

C2:

R_F (ethyl acetate / cyclohexane 1:1 v/v) = 0.60.

^{1}H NMR (400 MHz, $CDCl_3$) δ / ppm = 4.89 – 4.74 (m, 1H, CH^2), 4.50 (dd, *J* = 8.5, 7.7 Hz, 2H, CH_2^2), 3.97 (dd, *J* = 8.5, 7.2 Hz, 2H, CH_2^{2*}), 1.41 (d, *J* = 6.3 Hz, 3H, CH_3^3).

^{13}C NMR (101 MHz, $CDCl_3$) δ / ppm = 155.00, 73.50, 70.64, 19.46.

IR (ATR) $\tilde{\nu}$ / cm^{-1} = 2989, 2937, 2925, 1781, 1557, 1483, 1450, 1388, 1353, 1273, 1246, 1224, 1172, 1117, 1074, 1043, 954, 946, 919, 847, 775, 710, 541.

HRMS (ESI) *m/z*: $[M+H]^+$ calc. for $C_4H_6O_3$, 103.0390; found 103.0393; Δ = 0.3 mmu.

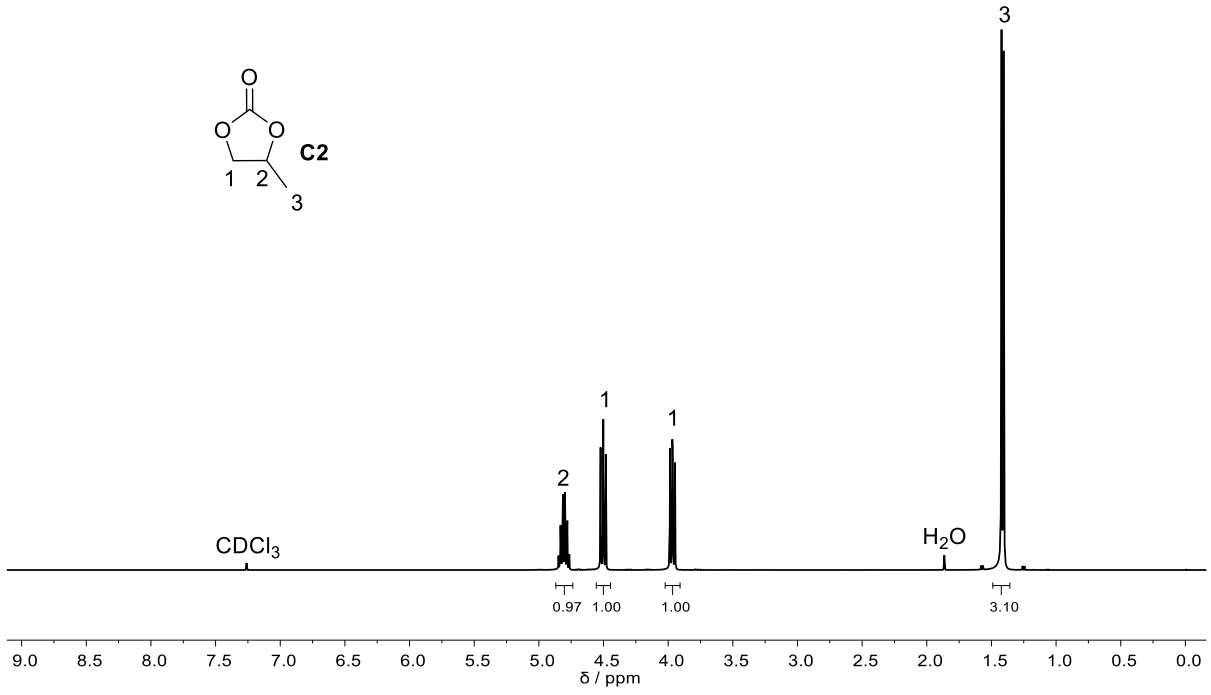

*Figure S 3. ^{1}H NMR spectrum of cyclic carbonate **C2** in $CDCl_3$.*

For the preparation of cyclic carbonate **C3**, EG (3.80 g, 50.0 mmol) was used. After column chromatography **C3** was obtained as colorless liquid, in a yield of 65% (2.88 g, 32.7 mmol).

C3:

R_F (ethyl acetate / cyclohexane 1:1 v/v) = 0.61.

^{1}H NMR (400 MHz, $CDCl_3$) δ / ppm = 4.46 (s, 2H, CH_2[1]).

^{13}C NMR (101 MHz, $CDCl_3$) δ / ppm = 64.55.

IR (ATR) $\tilde{\nu}$ / cm^{-1} = 2995, 1866, 1843, 1790, 1767, 1738, 1683, 1553, 1487, 1471, 1419, 1390, 1230, 1218, 1137, 1057, 1008, 969, 891, 769, 714, 687.

HRMS (ESI) *m/z*: $[M+H]^+$ calc. for $C_3H_4O_3$, 89.0233; found 89.0238; Δ = 0.5 mmu.

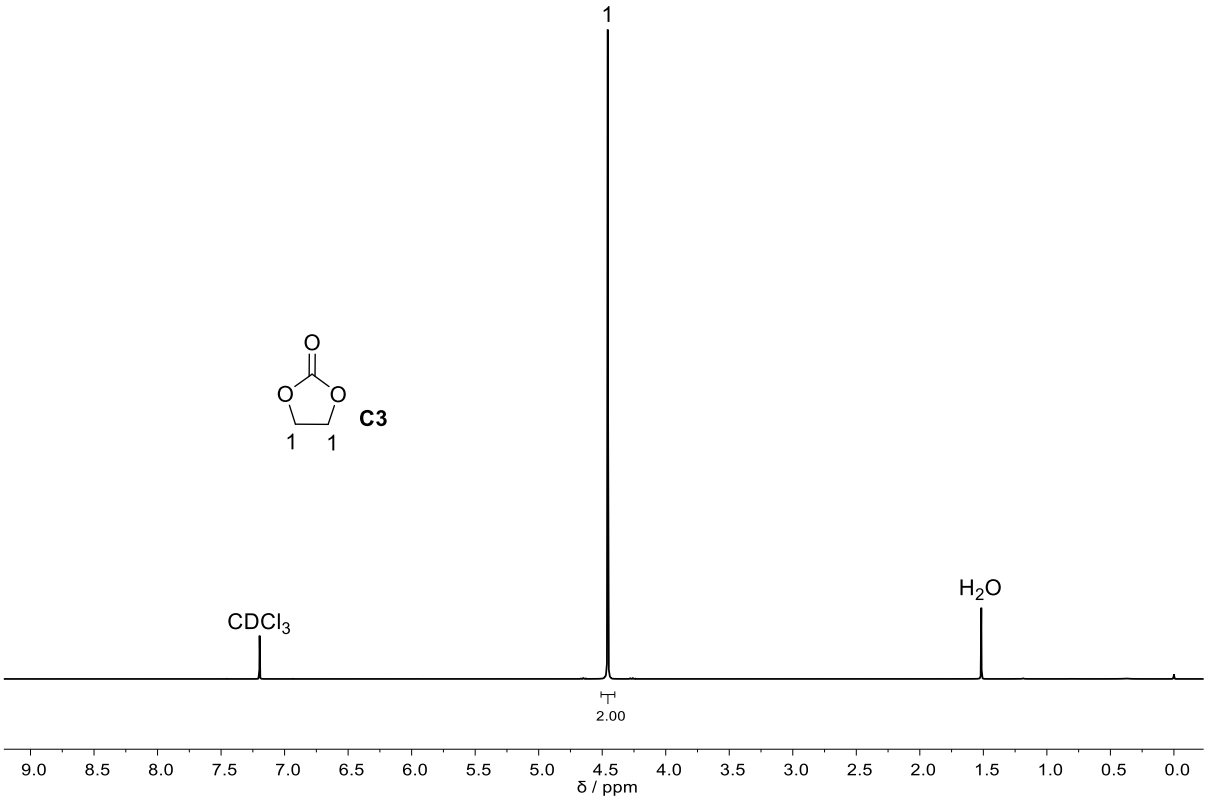

*Figure S 4. ^{1}H NMR spectrum of cyclic carbonate **C3** in $CDCl_3$.*

For the preparation of cyclic carbonate **C4**, Oct (7.31 g, 50.0 mmol) was used. The reaction temperature was set to 100 °C for 5 h instead of 80 °C for 22 h. After column chromatography **C4** was obtained as colorless liquid, in yield of 93% (7.90 g, 45.9 mmol).

C4:

R_F (ethyl acetate / cyclohexane 3:7 v/v) = 0.46.

^{1}H NMR (400 MHz, DMSO-d_6) δ / ppm = 4.84 – 4.70 (m, 1H, CH^4), 4.56 (t, J = 8.1 Hz, 1H, CH_2^5), 4.12 (t, J = 8.3, 7.1 Hz, 1H, CH_2^{5*}), 1.75 – 1.57 (m, 2H, CH_2^3), 1.39 – 1.19 (m, 8H, CH_2^2), 0.96 – 0.78 (m, 3H, CH_3^1).

^{13}C NMR (101 MHz, DMSO-d_6) δ / ppm = 155.36, 77.48, 69.67, 33.31, 31.53, 28.76, 24.35, 22.44, 14.34.

IR (ATR) $\tilde{\nu}$ / cm^{-1} = 2956, 2927, 2859, 1790, 1465, 1384, 1166, 1125, 1059, 773, 718.

HRMS (EI) of $[M]^+$ $[C_9H_{16}O_3]$: calc. 173.1172; found 173.1172; Δ = 0.0 mmu.

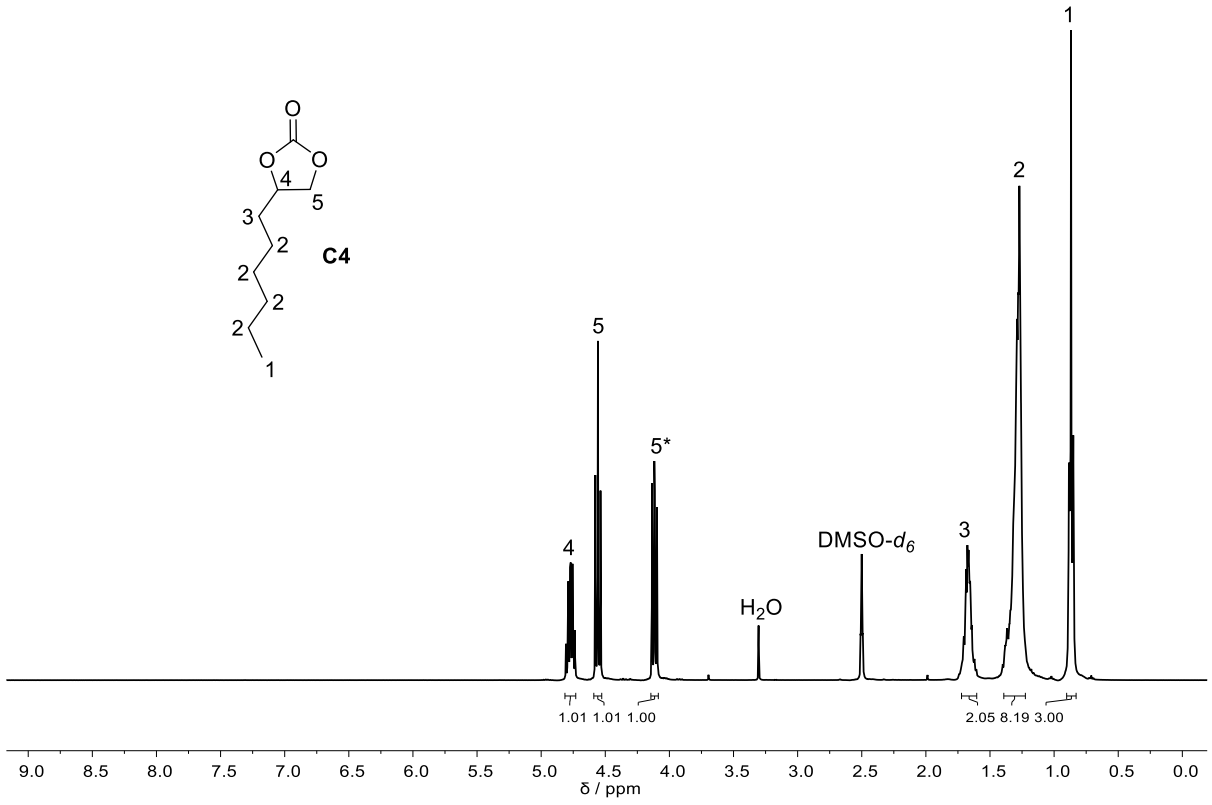

*Figure S 5. ^{1}H NMR spectrum of cyclic carbonate **C4** in DMSO-d_6.*

Calculation of the E-Factor regarding the purification strategies tested to purify cyclic carbonate C1

For the purification of **C1** three strategies were compared according to their calculated E-Factor. The E-Factor was calculated for the purification *via* vacuum distillation, extraction, and column chromatography, following *Equation S 4* and *Equation S 5*. For detailed information see R. A. Sheldon.[35]

$$sEF = \frac{\sum m(starting\ materials) + \sum m(base) - \sum m(product)}{\sum m(product)}$$

Equation S 4. Calculation of the simple E-Factor (sEF), without taking solvents into account. With m = mass.

$$cEF = \frac{\sum m(starting\ materials) + \sum m(base) + \sum m(solvents) - \sum m(product)}{\sum m(product)}$$

Equation S 5. Calculation of the complete E-Factor (cEF), taking all solvents into account. With m = mass.

For the vacuum distillation of **C1**, only the so-called simple E-Factor (sEF, equation 4) was calculated as no further solvents were added. An overview of the used values for each calculation is given in *Table S 1* for vacuum distillation, in *Table S 2* for column chromatography and in *Table S 3* for extraction.

*Table S 1. Values used for the calculation of the simple E-Factor based on the purification of **C1** via vacuum distillation.*

Materials	Masses / g	sEF	cEF
BDO	2.70	3.44	n.a.
DMC	3.24		
TBD	0.049		
C1	1.35 (yield of 38%)		
Further solvents	-		

*Table S 2. Values used for the calculation of the simple E-Factor and complete E-Factor based on the purification of **C1** via column chromatography.*

Materials	Masses / g	sEF	cEF
BDO	9.01	2.82	520
DMC	10.8		
TBD	0.193		
C1	5.22 (yield of 45%)		
Further solvents	2.70 L		

*Table S 3. Values used for the calculation of the simple E-Factor and complete E-Factor based on the purification of **C1** via extraction.*

Materials	Masses / g	sEF	cEF
BDO	9.01	2.99	223
DMC	10.8		
TBD	0.193		
C1	5.00 (yield of 43%)		
Further solvents	1.10 L		

General procedure for the preparation of samples measured in GC-FID screenings

Every synthesis set up for GC-FID-screening of the condensation reaction to cyclic carbonates followed the same previous described general procedure to synthesize **C1 – C4**. As internal standard (IS) for GC-FID-screening reactions, biphenyl was added to the reaction mixture. First, 0.25 equiv. biphenyl was added into a round-bottom flask, followed by adding the desired amount of DMC (1.20 equiv.) to dissolve biphenyl. Then, 1.00 equiv. of the desired diol was added, followed by the addition of 1 mol% of the desired catalyst. After complete dissolution of the compounds, a t_0 sample was taken for GC-FID analysis. Subsequently, the reaction mixture was stirred for the duration of the given reaction time and temperature. After a certain reaction time, t_x samples (1.5 mg mL^{-1} of substance dissolved in ethyl acetate and prefiltered) were taken.

The evaluation of the integral ratios after GC-FID analysis was performed as described by Hong *et al.* using *Equation S 6*.[303]

$$Conversion\ (cyclic\ Carbonate)[\%] = \left(1 - \frac{A(IC, t_x) * A(IS, t_0)}{A(IC, t_0) * A(IS, t_x)}\right) * 100\%$$

$$A(IC, t_x) = Intergal\ of\ cyclic\ carbonate\ peak\ at\ time = x\ min$$

$$A(IC, t_o) = Intergal\ of\ cyclic\ carbonate\ peak\ at\ time = 0\ min$$

$$A(IS, t_x) = Intergal\ of IS\ peak\ at\ time = x\ min$$

$$A(IS, t_0) = Intergal\ of IS\ peak\ at\ time = 0\ min$$

Equation S 6. Calculation in a GC-FID screening performed to calculate the conversion during the synthesis to cyclic carbonates.

General procedure for the preparation of carbamates (Ca1 – Ca4) as monomer to non-isocyanate polyurethanes

2.00 Equiv. of acid methyl ester **A1** (3.46 g, 16.0 mmol) were dissolved in 14 equiv. DMSO (8.60 mL, 8.75 g, 112 mmol). The mixture was stirred at 40 °C for 5 min in an open round-bottom flask. Then, 4.00 equiv. of DBU (4.97 g, 32.0 mmol) were added. After another 10 min of stirring at 40 °C, 1.00 equiv. of the respective cyclic carbonate **C1 – C4** was added. The mixture was stirred for 6 h at 40 °C in an open round-bottom flask. Reaction control was performed *via* ^{1}H NMR spectroscopy and TLC.

After the reaction was performed, DMSO was removed from the reaction mixture under reduced pressure yielding the corresponding carbamate **Ca1 – Ca4**. Further purification was performed *via* column chromatography. All signals in ^{1}H NMR spectra obtained from isomers are labelled accordingly with additionally appendices (*). If constitutional isomers were observed, both species were marked in the ^{1}H NMR spectrum accordingly with additionally appendices (A and B).

For the preparation of carbamate **Ca1**, cyclic carbonate **C1** (929 mg, 8.00 mmol) was used. After purification *via* column chromatography, using a solvent mixture of 1:1 (v/v) ethyl acetate to cyclohexane adding 1.20 wt% acetic acid, the product was isolated as colorless to yellowish, slightly viscous liquid in a yield of 81% (2.15 g, 6.48 mmol).

Ca1:

R_F (ethyl acetate / cyclohexane 1:1 v/v) = 0.36.

^{1}H NMR (400 MHz, DMSO-d_6) δ / ppm = 6.94 (t, J = 5.7 Hz, 1H, N*H*), 4.64 (s, 1H, O*H*), 4.56 – 4.48 (m, 1H, CH^{3*}), 4.45 – 4.38 (m, 1H, CH^3), 3.57 (s, 3H, CH_3^{10}), 3.52 (t, J = 6.1 Hz, 1H, CH^2), 2.93 (q, J = 6.6 Hz, 2H, (CH_2^5), 2.27 (t, J = 7.4 Hz, 2H, CH_2^9), 1.50 (m, 2H, CH_2^8), 1.36 (m, 2H, CH_2^6), 1.23 (s, 12H, CH_2^7), 1.08 (d, J = 6.4 Hz, 3H, CH_3^4), 1.01 (d, J = 6.3 Hz, 3H, CH_3^1).

^{13}C NMR (101 MHz, DMSO) δ / ppm = 173.81, 156.49, 74.03, 73.22, 68.80, 67.84, 51.60, 33.74, 29.89, 29.39, 29.27, 29.16, 29.13, 28.92, 24.90, 19.83, 16.44.

IR (ATR) $\tilde{\nu}$ / cm^{-1} = 3365, 3353, 2976, 2927, 2855, 1736, 1718, 1693, 1528, 1454, 1438, 1417, 1372, 1249, 1199, 1168, 1135, 1100, 1082, 1045, 1006, 924, 882, 775, 722, 631, 617, 607, 594, 586, 529, 522, 516.

HRMS (FAB) *m/z*: $[M]^+$ calc. for $C_{17}H_{33}O_5$, 331.2353; found 331.2355; Δ = 0.2 mm.

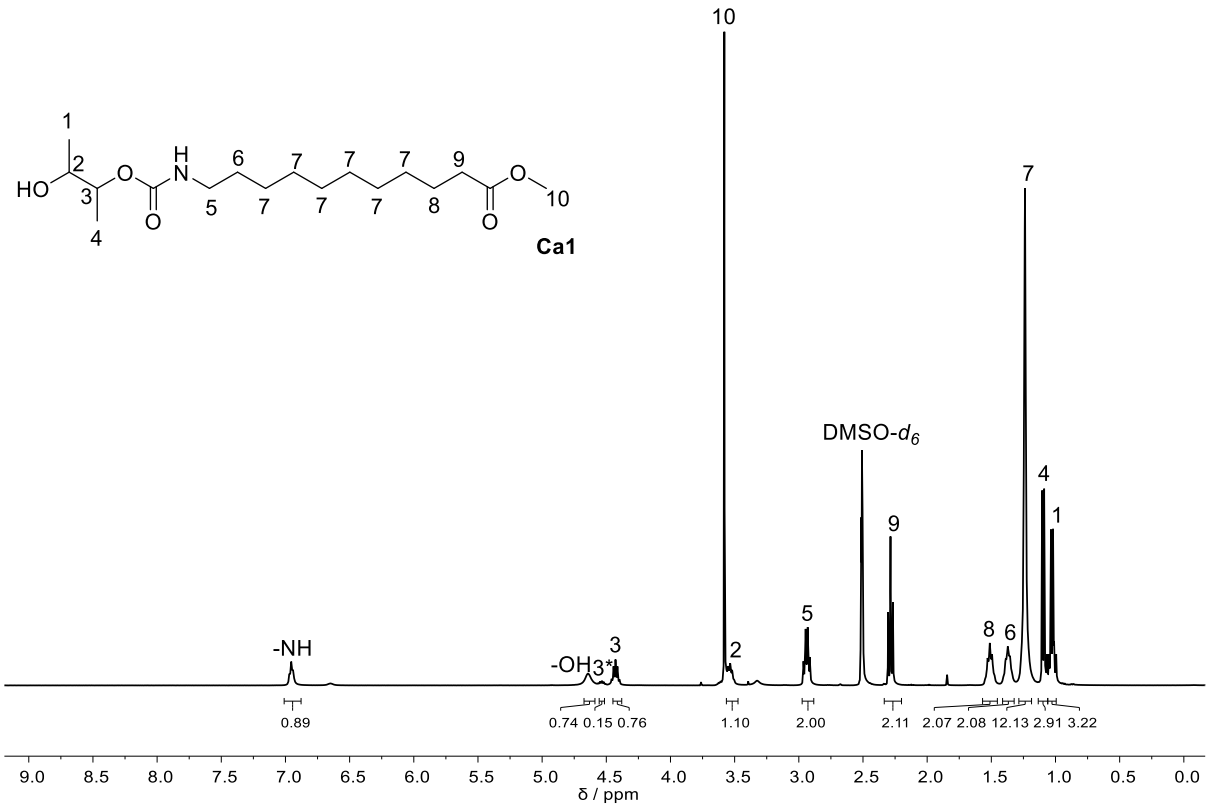

*Figure S 6. ^{1}H NMR spectrum of carbamate **Ca1** in DMSO-d$_6$.*

For the preparation of carbamate **Ca2**, cyclic carbonate **C2** (817 mg, 8.00 mmol) was used. After purification *via* column chromatography, using a solvent mixture of 6:4 (v/v) ethyl acetate to cyclohexane adding 1.2 wt% acetic acid, the product was isolated as colorless solid in a yield of 88% (2.24 g, 7.06 mmol).

Ca2:

R_F (ethyl acetate / cyclohexane 6:4 v/v) = 0.46.

^{1}H NMR (400 MHz, DMSO-d_6) δ / ppm = 7.06 (t, J = 5.8 Hz, 1H, NH^A), 6.97 (t, J = 5.7 Hz, 1H, NH^B), 4.66 – 4.53 (m, 1H, CH^{3B}), 3.83 – 3.68 (m, 2H, CH_2^{2*}), 3.57 (s, 3H, (CH_3^9), 3.42 – 3.37 (m, 1H, CH^2), 2.98 – 2.89 (m, 2H, CH_2^4), 2.28 (t, J = 7.4 Hz, 2H, CH_2^8), 1.56 – 1.43 (m, 2H, CH_2^7), 1.43 – 1.30 (m, 2H, CH_2^5), 1.30 – 1.16 (s, 12H, CH_2^6), 1.09 (d, J = 6.4 Hz, 3H, CH_3^{1*}), 1.03 (d, J = 5.9 Hz, 3H, CH_3^1).

^{13}C NMR (101 MHz, DMSO) δ / ppm = 173.84, 172.46, 156.74, 156.47, 64.87, 64.44, 51.62, 33.74, 29.89, 29.38, 29.27, 29.16, 29.12, 28.92, 26.70, 24.90, 21.54, 20.55.

IR (ATR) $\tilde{\nu}$ / cm^{-1} = 3359, 3347, 3336, 3223, 2927, 2855, 1713, 1697, 1530, 1456, 1438, 1417, 1374, 1323, 1244, 1170, 1148, 1111, 1051, 1008, 850, 778, 722, 605, 522.

HRMS (ESI) m/z: $[M+H]^+$ calc. for $C_{16}H_{31}NO_5$, 318.2275; found 318.2270; Δ = 0.5 mmu.

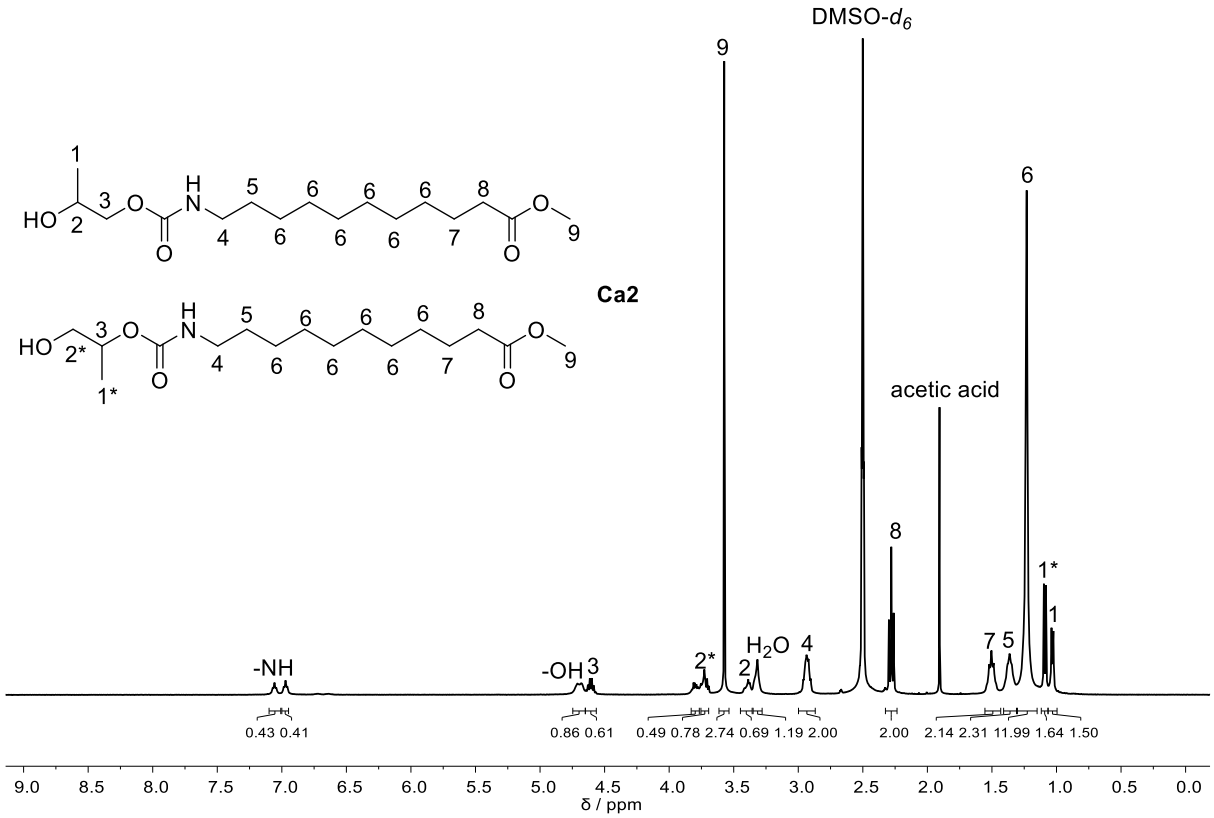

*Figure S 7. ^{1}H NMR spectrum of carbamate **Ca2** in DMSO-d$_6$.*

For the preparation of carbamate **Ca3**, cyclic carbonate **C3** (0.440 g, 5.00 mmol) was used. After purification *via* column chromatography, using a solvent mixture of 7:3 (v/v) ethyl acetate to cyclohexane adding 1.2 wt% acetic acid, the product was isolated as colorless solid in a yield of 91% (2.21 g, 7.28 mmol).

Ca3:

R_F (ethyl acetate / cyclohexane 7:3 v/v) = 0.37.

^{1}H NMR (400 MHz, DMSO-d_6) δ / ppm = 7.07 (t, J = 5.8 Hz, 1H, N*H*), 4.68 (s, 1H, O*H*), 3.93 (t, J = 5.3 Hz, 2H, CH_2^2), 3.57 (s, 3H, CH_3^8), 3.52 (t, J = 5.3 Hz, 2H, CH_2^1), 2.94 (q, J = 6.6 Hz, 2H, CH_2^3), 2.28 (t, J = 7.4 Hz, 2H, CH_2^7), 1.56 – 1.46 (m, 2H, CH_2^6), 1.41 – 1.32 (m, 2H, CH_2^4), 1.23 (s, 12H, CH_2^5).

^{13}C NMR (101 MHz, DMSO) δ / ppm = 173.84, 156.78, 65.84, 59.96, 51.62, 33.74, 29.89, 29.39, 29.28, 29.17, 29.12, 28.92, 26.71, 24.90.

IR (ATR) $\tilde{\nu}$ / cm^{-1} = 3330, 2921, 2851, 1740, 1709, 1687, 1537, 1471, 1462, 1436, 1413, 1380, 1358, 1335, 1302, 1275, 1257, 1234, 1205, 1187, 1164, 1144, 1117, 1100, 1078, 1057, 1045, 1026, 1012, 993, 973, 895, 882, 782, 732, 722, 687, 607, 553.

HRMS (ESI) m/z: $[M+H]^+$ calc. for $C_{15}H_{29}NO_5$, 304.2118; found 304.2114; Δ = 0.4 mmu.

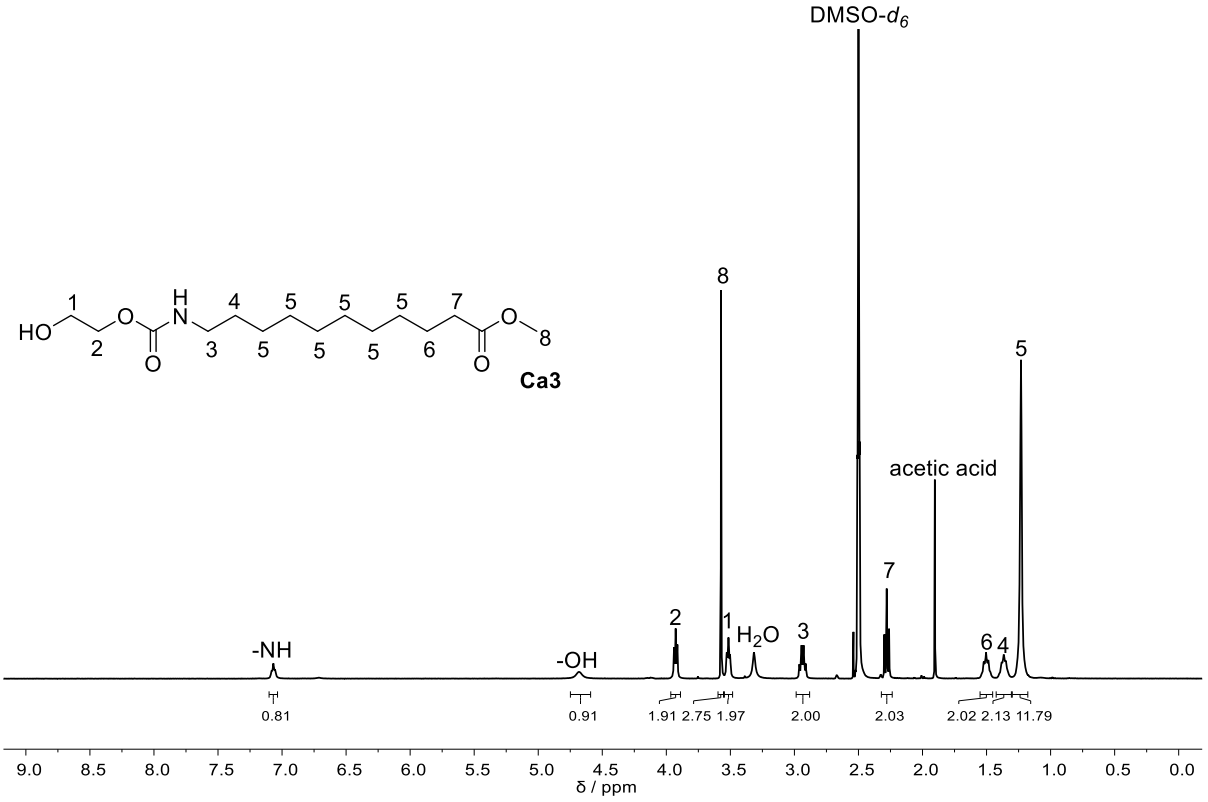

*Figure S 8. ^{1}H NMR spectrum of carbamate **Ca3** in DMSO-d$_6$.*

For the preparation of carbamate **Ca4**, cyclic carbonate **C4** (1.37 g, 8.00 mmol) was used. After column chromatography, the constitutional isomers were separated, thus two fractions were obtained. Isomer A was isolated as white solid with a yield of 86% (2.67 g, 6.88 mmol). Isomer B was isolated as liquid with a yield of 6% (0.19 g, 0.49 mmol). 2D NMR spectroscopy, more specifically COSY and HSQC, was used to identify the constitutional isomers successfully.

Ca4 Isomer A:

R_F (ethyl acetate / cyclohexane 1:1 v/v) = 0.58.

^{1}H NMR (400 MHz, DMSO-d_6) δ / ppm = 7.04 (t, J = 5.7 Hz, 1H, N*H*), 4.61 (d, J = 5.4 Hz, 1H, O*H*), 3.83 – 3.73 (m, 2H, CH_2^5), 3.57 (s, 3H, CH_3^1), 2.93 (q, J = 6.6 Hz, 2H, CH_2^6), 2.28 (t, J = 7.4 Hz, 2H, CH_2^8), 1.57 – 1.44 (m, 2H, CH_2^7), 1.41 – 1.32 (m, 2H, CH_2^3), 1.29 – 1.19 (m, 20H, CH_2^2), 0.90 – 0.81 (m, 3H, CH_3^9).

^{13}C NMR (101 MHz, DMSO-d_6) δ / ppm = 173.84, 156.78, 68.47, 51.62, 34.02, 33.74, 31.75, 29.88, 29.34, 29.16, 28.92, 26.68, 25.35, 24.90, 22.54, 14.42.

IR (ATR) $\tilde{\nu}$ / cm^{-1} = 3532, 3328, 3318, 3303, 2950, 2917, 2849¸ 1732¸ 1668¸ 1541, 1467¸ 1436¸ 1419, 1380¸ 1347, 1333, 1316, 1286, 1286, 1269, 1234, 1205, 1177, 1154, 1111, 1094, 1072, 1035, 1016, 1002¸ 965, 903, 882, 866, 786, 738, 722, 658, 599, 555, 510.

HRMS (EI) m/z: $[M]^+$ calc. for $C_{21}H_{41}NO_5$, 388.3058; found 388.3057; Δ = 0.1 mmu.

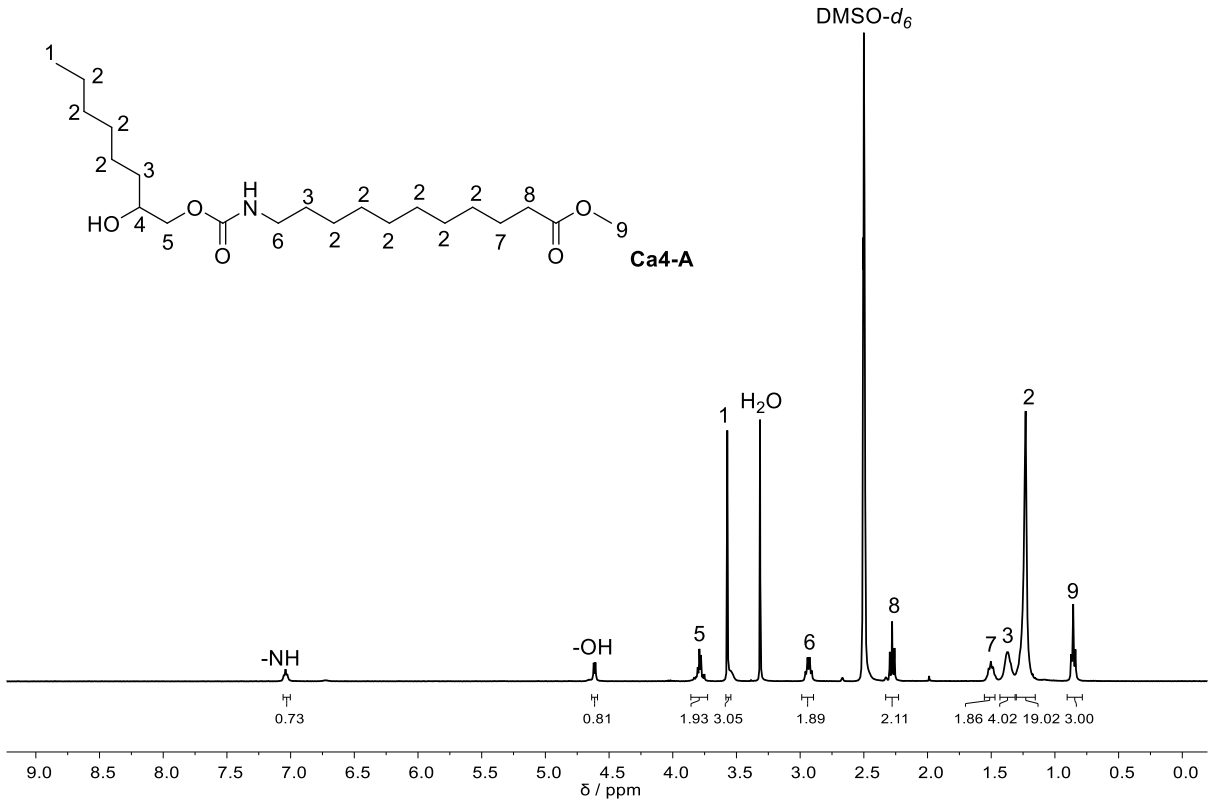

*Figure S 9. ^{1}H NMR spectrum of carbamate **Ca4 Isomer A** in DMSO-d_6.*

Ca4 Isomer B:

R_F (ethyl acetate / cyclohexane 1:1 v/v) = 0.71.

^{1}H NMR (400 MHz, DMSO-d_6) δ / ppm = 6.96 (t, J = 5.8 Hz, 1H, N*H*), 4.66 (t, J = 5.6 Hz, 1H, O*H*), 4.59 – 4.50 (m, 1H, CH^2), 3.57 (s, 3H, CH_3^5), 3.43 – 3.32 (m, 2H, CH_2^1), 3.01 – 2.85 (m, 2H, CH_2^6), 2.27 (t, J = 7.4 Hz, 2H, CH_2^8), 1.58 – 1.46 (m, 2H, CH_2^3), 1.41 – 1.32 (m, 2H, CH_2^7), 1.30 – 1.17 (m, 20H, CH_2^4), 0.89 – 0.80 (m, 3H, CH_3^9).

^{13}C NMR (101 MHz, DMSO-d_6) δ / ppm = 173.80, 156.76, 74.34, 63.20, 51.60, 33.73, 31.71, 31.18, 29.90, 29.58, 28.54, 26.67, 25.21, 24.91, 22.49, 14.38.

IR (ATR) $\tilde{\nu}$ / cm^{-1} = 3371, 3363, 3351, 2925, 2855, 1738, 1720, 1693, 1530, 1460, 1438¸ 1417, 1362, 1249, 1199¸ 1170, 1146¸ 1103, 1055, 775, 724¸ 640, 611¸ 599¸ 559, 516, 504¸ 485, 446.

HRMS (EI) m/z: $[M]^+$ calc. for $C_{21}H_{41}NO_5$,388.3059; found 388.3058; Δ = 0.1 mmu.

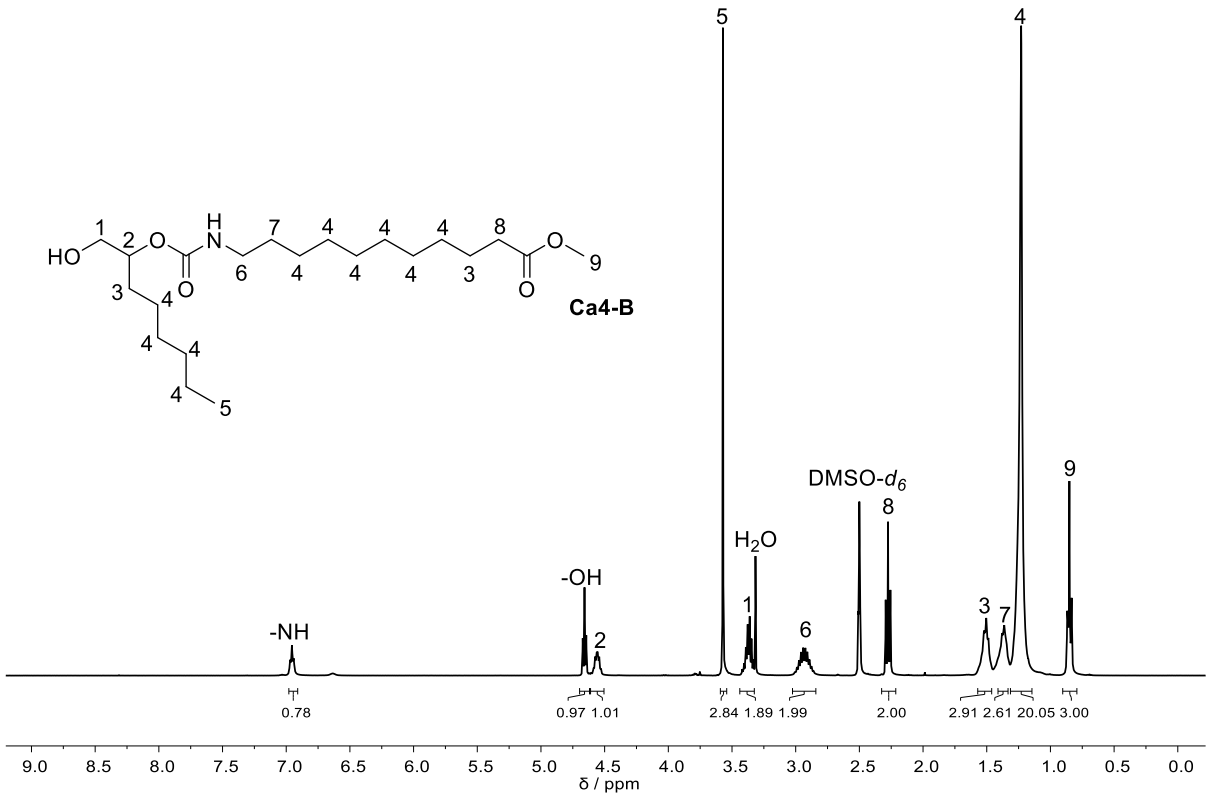

*Figure S 10. [1]H NMR spectrum of carbamate **Ca4 Isomer B** in DMSO-d6.*

General procedure for the preparation of poly(ester urethane)s PU1 – PU4

1.00 Equiv. of the respective carbamate monomer **Ca1 – Ca4** was weight into a round-bottom flask. Subsequently, 0.07 equiv. of TBD (0.036 g, 260 µmol) were added. The mixture was stirred for 2 h at 120 °C under vacuum (<1 mbar). Again, 0.07 equiv. of TBD were added, followed by stirring for another 2 h at 140 °C, still at low pressure (<1 mbar). Then, another 0.07 equiv. of TBD were added, while the mixture was heated to 160 °C stirring for 20 h with applied vacuum (<1 mbar). The colorless to slightly yellow, viscose reaction mixture was cooled to room temperature. Then, the mixture was dissolved in HFIP and precipitated into ice-cold methanol or ethanol. The precipitated polymer was analyzed in NMR spectroscopy and IR spectroscopy.

To overcome solubility problems for NMR analyses, 21.0 mg of each poly(ester urethane) was dissolved in 0.50 mL HFIP, then 0.50 mL $CDCl_3$ were added and the sample mixture used for ^{1}H NMR spectroscopy. Broad HFIP signals at 4.50 – 3.90 ppm overlapped with CH_2 proton signals of the polymers, identified by comparing to monomer spectra measured in a HFIP/$CDCl_3$ mixture. However, a characterization of the poly(ester urethane)s was possible.

In each ^{1}H NMR spectrum, a maximum of three rotamers of poly(ester urethane) were identified using 2D spectra, more specifically COSY and HSQC. However, the coupling of

rotamers signals were be further assigned. A partial ^{1}H NMR spectrum of **PU1** is shown exemplary in *Figure S 11*. A characterization of the polymers was observed by SEC, DSC, and TGA.

For the preparation of poly(ester urethane) **PU1**, **Ca1** (431 mg, 1.30 mmol) was used. **PU1** was precipitated in ice-cold ethanol, obtained as yellowish solid.

PU1:

^{1}H NMR (400 MHz, $CDCl_3$ / HFIP mixture): NH signals of rotamers can be assigned as δ / ppm = 6.00 – 5.91 (m, 1H, N*H*), 5.02 – 4.92 (m, 1H, N*H*), 4.87 – 4.81 (m, 1H, N*H*), 4.79 – 4.71 (m, 1H, N*H*). HFIP solvent signals are overlapping with the proton signals of OHC*H*CH_3 and OHCHC*H*(OC=O). Further proton signals of rotamers can be assigned as the following δ / ppm = 3.27 – 3.18 (m, 2H, C*H*$_2$NH), 3.15 – 3.05 (m, 2H, C*H*$_2$NH), 2.39 – 2.28 (m, 2H, C*H*$_2$C=O), 2.27 – 2.17 (m, 2H, C*H*$_2$C=O). No further rotamers are assigned for the following protons δ / ppm = 1.66 – 1.56 (m, 2H, C*H*$_2$CH$_2$C=O), 1.55 – 1.45 (m, 2H, C*H*$_2$CH$_2$NH), 1.38 – 1.27 (m, 15H, CHC*H*$_3$(OC=O) and NHCH$_2$CH$_2$C*H*$_2$C*H*$_2$C*H*$_2$C*H*$_2$C*H*$_2$C*H*$_2$), 1.28 – 1.15 (m, 3H, CHC*H*$_3$).

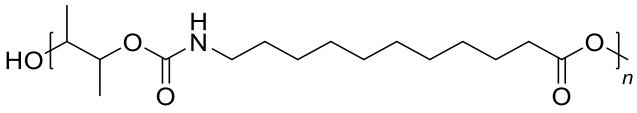

PU1

$T_{d,8\%}$ (Step-1) = 157°C, $T_{d,23\%}$ (Step-2) = 324°C, $T_{d,51\%}$ (Step-3) = 436°C (TGA), M_n = 11 kDa and $Đ$ = 2.17 (SEC-HFIP-2), T_m = 77 °C and 89 °C, T_g = -16 °C and T_c = 59 °C, ΔH = 29 J·g^{-1} (DSC-2).

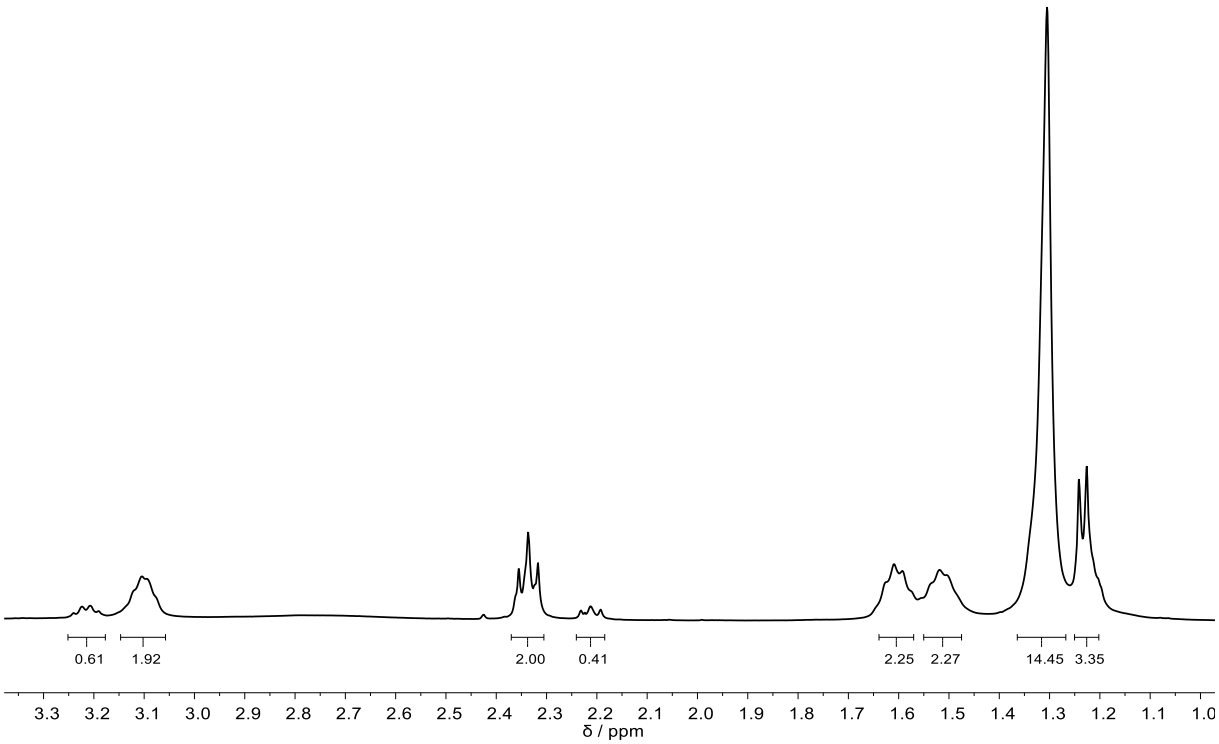

*Figure S 11. Partial given ^{1}H NMR spectrum of **PU1** measured in HFIP/$CDCl_3$, showing rotamers.*

IR (ATR) $\tilde{\nu}$ / cm^{-1} = 2923, 2851, 1730, 1619, 1571, 1467, 1378, 1286, 1261, 1216, 1177, 1135, 1100, 1084, 1043, 1004, 893, 841, 736, 685, 611.

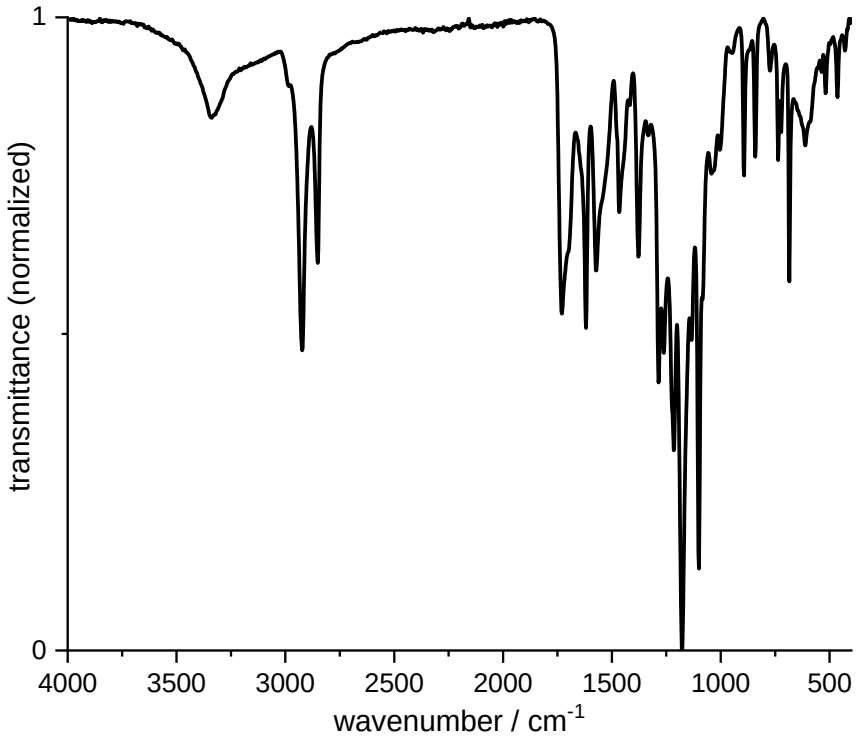

Figure S 12. IR spectrum of poly(ester urethane) ***PU1****.*

For the preparation of poly(ester urethane) **PU2**, **Ca2** (413 mg, 1.30 mmol) was used. **PU2** was precipitated in ice-cold methanol, obtained as white solid.

PU2:

^{1}H NMR (400 MHz, $CDCl_3$ / HFIP mixture): NH signals of rotamers can be assigned as δ / ppm = 5.99 – 5.91 (m, 1H, N*H*), 5.17 – 5.07 (m, 1H, N*H*), 5.06 – 5.00 (m, 1H, N*H*), 4.77 – 4.69 (m, 1H, N*H*). HFIP solvent signals are overlapping with the proton signals of OHC*H*CH_3 and OHCHC*H*$_2$(OC=O). Further proton signals of rotamers can be assigned as the following δ / ppm = 3.36 – 3.28 (m, 2H, C*H*$_2$NH), 3.24 – 3.18 (m, 2H, C*H*$_2$NH), 3.13 – 3.06 (m, 2H, C*H*$_2$NH), 2.39 – 2.30 (m, 2H, C*H*$_2$C=O), 2.24 – 2.18 (m, 2H, C*H*$_2$C=O), 2.08 – 2.01 (m, 2H, C*H*$_2$C=O). No further rotamers are assigned for the following protons δ / ppm = 1.64 – 1.56 (m, 2H, C*H*$_2$CH$_2$C=O), 1.55 – 1.48 (m, 2H, C*H*$_2$CH$_2$NH), 1.34 – 1.28 (m, 12H, NHCH$_2$CH$_2$C*H*$_2$C*H*$_2$C*H*$_2$C*H*$_2$C*H*$_2$C*H*$_2$C*H*$_2$), 1.27 – 1.24 (m, 3H, CHC*H*$_3$).

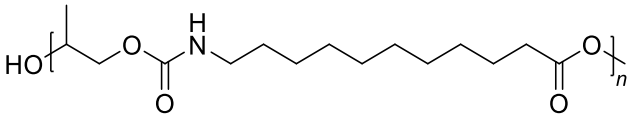

PU2 + constiutional isomer

IR (ATR) $\tilde{\nu}$ / cm^{-1} = 3299, 2919, 2851, 1734, 1693, 1629, 1557, 1543, 1467, 1417, 1376, 1335, 1277, 1261, 1236, 1222, 1216, 1177, 1100, 1080, 736, 722, 685, 611, 601, 584.
$T_{d,3\%}$ (Step-1) = 119°C, $T_{d,13\%}$ (Step-2) = 300°C, $T_{d,35\%}$ (Step-3) = 438°C (TGA), M_n = 10 kDa and $Đ$ = 1.94 (SEC-HFIP-2), T_m = 58 °C and 85 °C, T_g = -48 °C and T_c = 43 °C and 67 °C, ΔH = 33 $J \cdot g^{-1}$ (DSC-2).

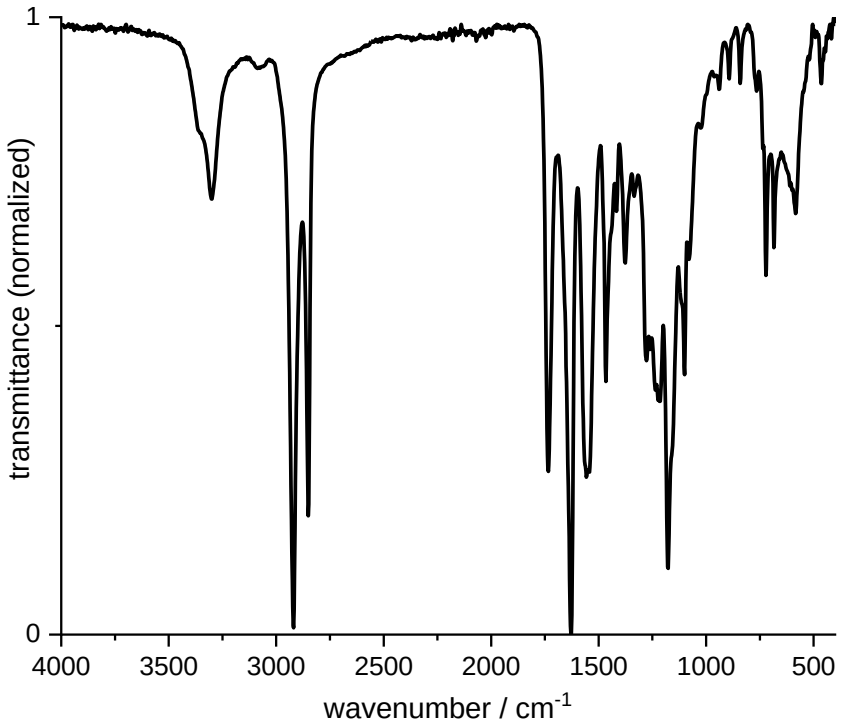

Figure S 13. IR spectrum of poly(ester urethane) ***PU2****.*

For the preparation of poly(ester urethane) **PU3**, **Ca3** (394 mg, 1.30 mmol) was used. **PU3** was precipitated in ice-cold methanol, obtained as white solid.

PU3:

^{1}H NMR (400 MHz, $CDCl_3$ / HFIP mixture): NH signals of rotamers can be assigned as δ / ppm = 5.22 – 5.15 (m, 1H, N*H*), 5.14 – 5.07 (m, 1H, N*H*). HFIP solvent signals are overlapping with the proton signals of OHC*H*$_2$ and OHCH$_2$C*H*$_2$. Further proton signals of rotamers can be assigned as the following δ / ppm = 3.37 – 3.28 (m, 2H, C*H*$_2$NH), 3.27 – 3.18 (m, 2H, C*H*$_2$NH), 3.17 – 3.05 (m, 2H, C*H*$_2$NH), 2.42 – 2.32 (m, 2H, C*H*$_2$C=O), 2.24 – 2.18 (m, 2H, C*H*$_2$C=O). No further rotamers are assigned for the following protons δ / ppm = 1.68 – 1.56 (m, 2H, C*H*$_2$CH$_2$C=O), 1.55 – 1.45 (m, 2H, C*H*$_2$CH$_2$NH), 1.37 – 1.25 (12H, NHCH$_2$CH$_2$C*H*$_2$C*H*$_2$C*H*$_2$C*H*$_2$C*H*$_2$C*H*$_2$).

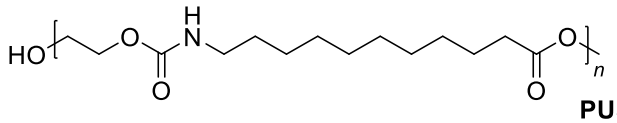

PU3

IR (ATR) $\tilde{\nu}$ / cm^{-1} = 3340, 3328, 2919, 2851, 1728, 1660, 1652, 1619, 1576, 1537, 1467, 1444, 1419, 1382, 1353, 1333, 1273, 1234, 1207, 1172, 1103, 1059, 993, 959, 775, 736, 722, 685, 623, 613, 588.

$T_{d,5\%}$ (Step-1) = 144 °C, $T_{d,15\%}$ (Step-2) = 262 °C, $T_{d,50\%}$ (Step-3) = 440 °C (TGA), M_n = 5 kDa and $Đ$ = 2.13 (SEC-HFIP-2), T_m = 86 °C and 102 °C, T_g = -9 °C and T_c = 73 °C, ΔH = 45 J·g^{-1} (DSC-2).

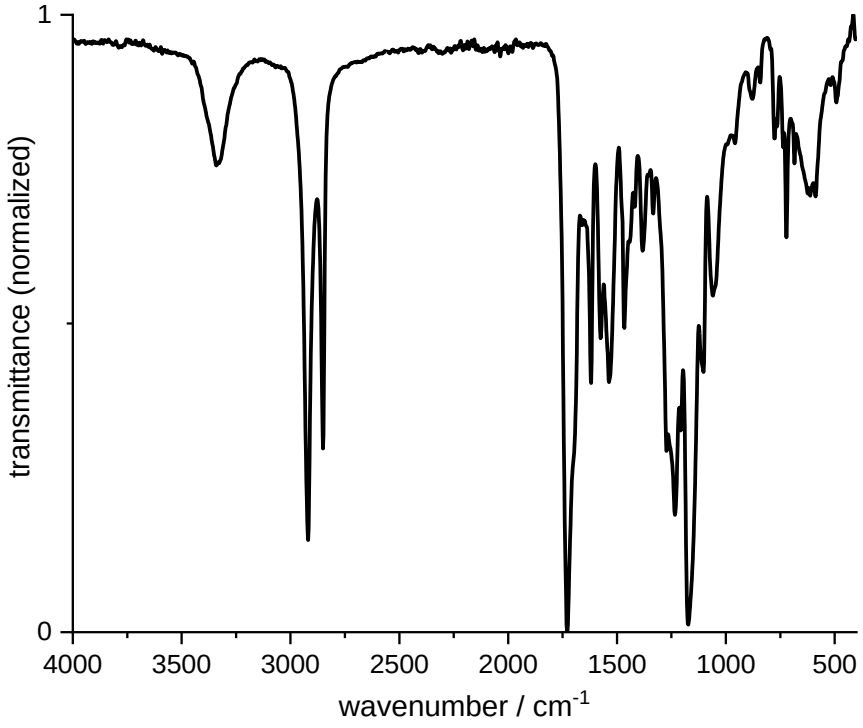

Figure S 14. IR spectrum of poly(ester urethane) ***PU3****.*

Both isolated isomers **Ca4-A** and **Ca4-B** were polymerized. For the preparation of poly(ester urethane) **PU4-A**, **Ca4-A** (504 mg, 1.30 mmol) was used. For the preparation of poly(ester urethane) **PU4-B**, **Ca4-B** (504 mg, 1.30 mmol) was used. No NMR spectroscopy of the desired polymers was measured, because of complete insolubility of the polymers even in a mixture of HFIP/$CDCl_3$. Thus, the obtained polymers were characterized *via* IR spectroscopy, SEC, DSC, and TGA.

After precipitation in ice-cold methanol, **PU4-A** was obtained as white solid, whereas **PU4-B** was obtained as colorless solid.

PU4-A:

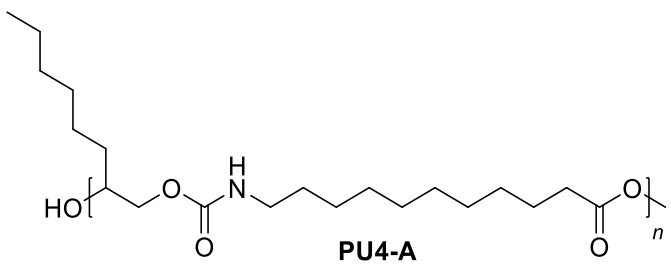

PU4-A

IR (ATR) $\tilde{\nu}$ / cm^{-1} = 3308, 2919, 1736, 1635, 1539, 1469, 1442, 1419, 1376, 1353, 1339, 1327, 1281, 1261, 1240, 1216, 1179, 1100, 1078, 1028, 938, 893, 841, 763, 763, 736, 720, 683, 623, 613, 580, 545.

M_n = 3 kDa and $Đ$ = 1.37 (SEC-HFIP), T_m = 155 °C and T_m = 145 °C, T_g = 77 °C and T_c = 141 °C (DSC).

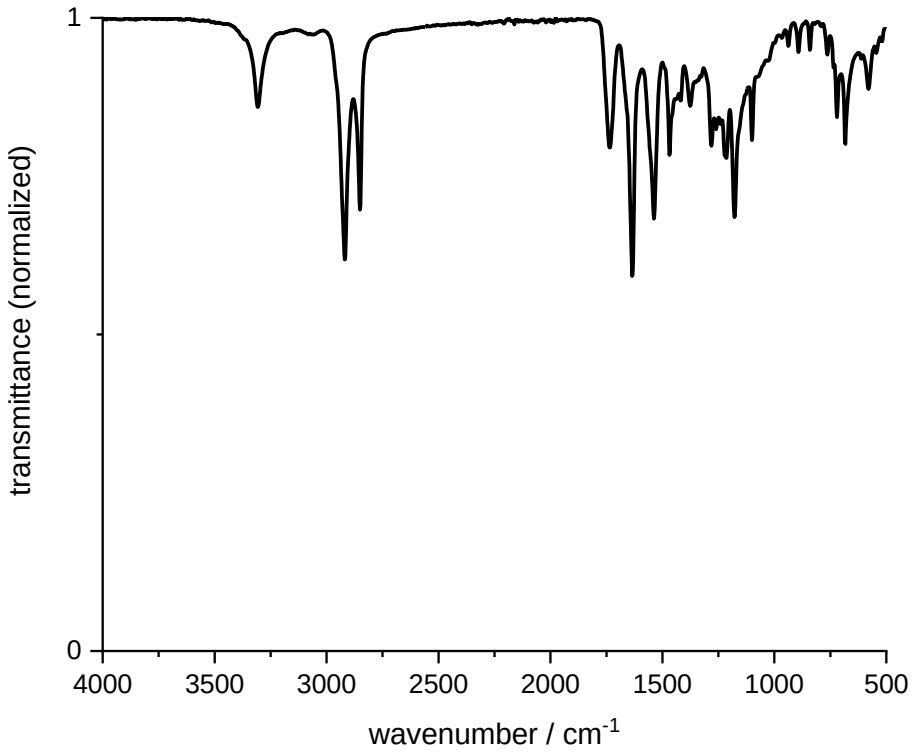

Figure S 15. IR spectrum of poly(ester urethane) ***PU4-A****.*

PU4-B:

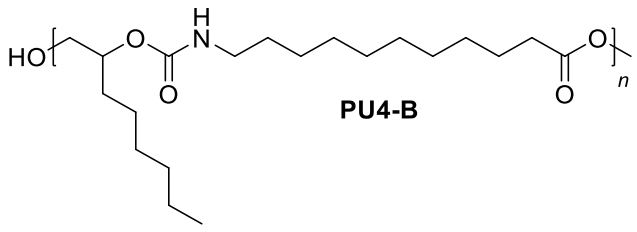

PU4-B

IR (ATR) $\tilde{\nu}$ / cm^{-1} = 3340, 2921, 2853, 1734, 1621, 1571, 1467, 1417, 1376, 1333, 1286, 1261, 1216, 1179, 1100, 967, 893, 841, 773, 734, 722, 685, 668, 611, 590, 518.

M_n = 19 kDa and $Đ$ = 2.20 (SEC-HFIP), T_m = 71 °C and T_m = 41 °C, T_g = -25 °C and T_c = 39 °C (DSC).

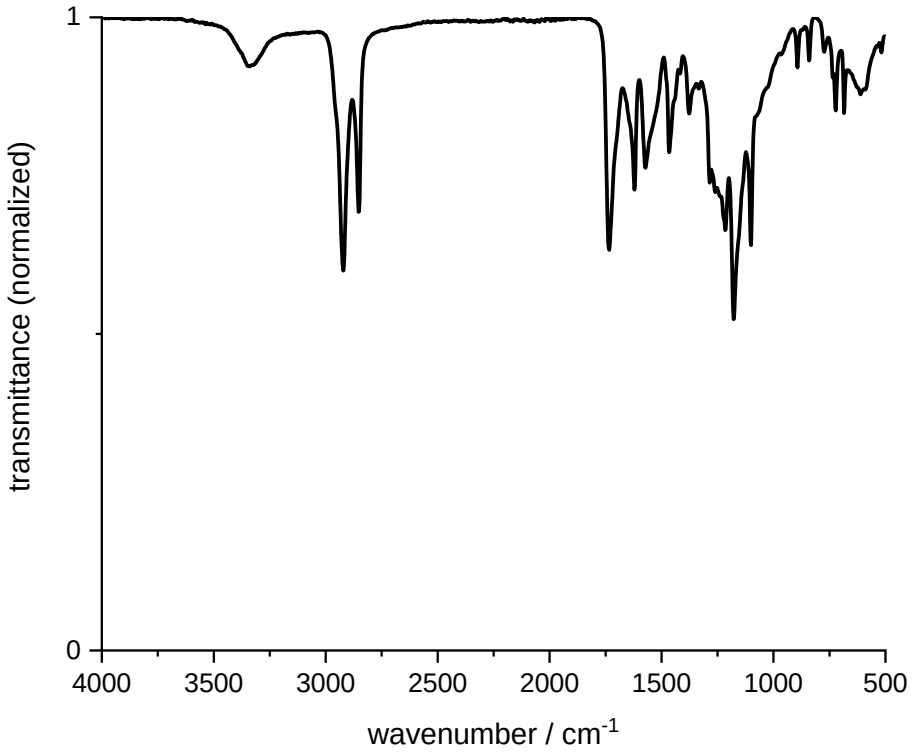

Figure S 16. IR spectrum of poly(ester urethane) ***PU4-B****.*

6.2.2 Experimental Procedures of 4.2 Polymerization of 2,3-Butanediol and Renewable Dicarboxylic Acids using Iron(III)chloride as Catalyst

The author of this thesis developed the synthetic procedure, planned, evaluated the experiments, and wrote the manuscript.

S. Wegelin, co-supervised by the author of this thesis, was performing the deconvolution method and first tests on finding suitable polycondensation reaction conditions.

For all experiments of this project, 2,3-butanediol (BDO) was purchased from industry (SIGMA ALDRICH) as mixture of racemic and meso forms.

Purified FDCA (F1) as monomer for polycondensation reactions to polyesters

The purification of FDCA was performed as described in the US. Patent[304].

To 24.0 g of a water/methanol mixture (3:5, v/v), 1.00 g (6.40 mmol) of unpurified FDCA was added, followed by the addition of 0.30 g (2.88 mmol) sodium hydrogen sulfite. The pressure vial was sealed properly and heated to 90 °C for 30 minutes. Subsequently, an appropriate amount of water was added to dissolve unreacted sodium hydrogen sulfite. The mixture was

cooled in an ice bath to 0 °C, which was maintained for 30 minutes. The precipitated product was filtered and dried under vacuum (<1 mbar). **F1** was obtained as white powder.

F1:

^{1}H NMR (400 MHz, DMSO-d_6) δ / ppm = 7.26 (s, 2H, CH^{1}).

^{13}C NMR (101 MHz, DMSO-d_6) δ / ppm = 159.02, 147.29, 118.13.

IR (ATR) $\tilde{\nu}$ / cm^{-1} = 3151, 3124, 3065, 3055, 3046, 3011, 2999, 2989, 2978, 2970, 2941, 2915, 2884, 2874, 2859, 2797, 2789, 2557, 1680, 1674, 1571, 1522, 1417, 1273, 1228, 1187, 1162, 1041, 961, 845, 763, 525.

HRMS (FAB) *m/z*: $[M]^+$ calc. for $C_8H_8O_5$, 156.0054, found 156.0053; Δ = 0.1 mmu.

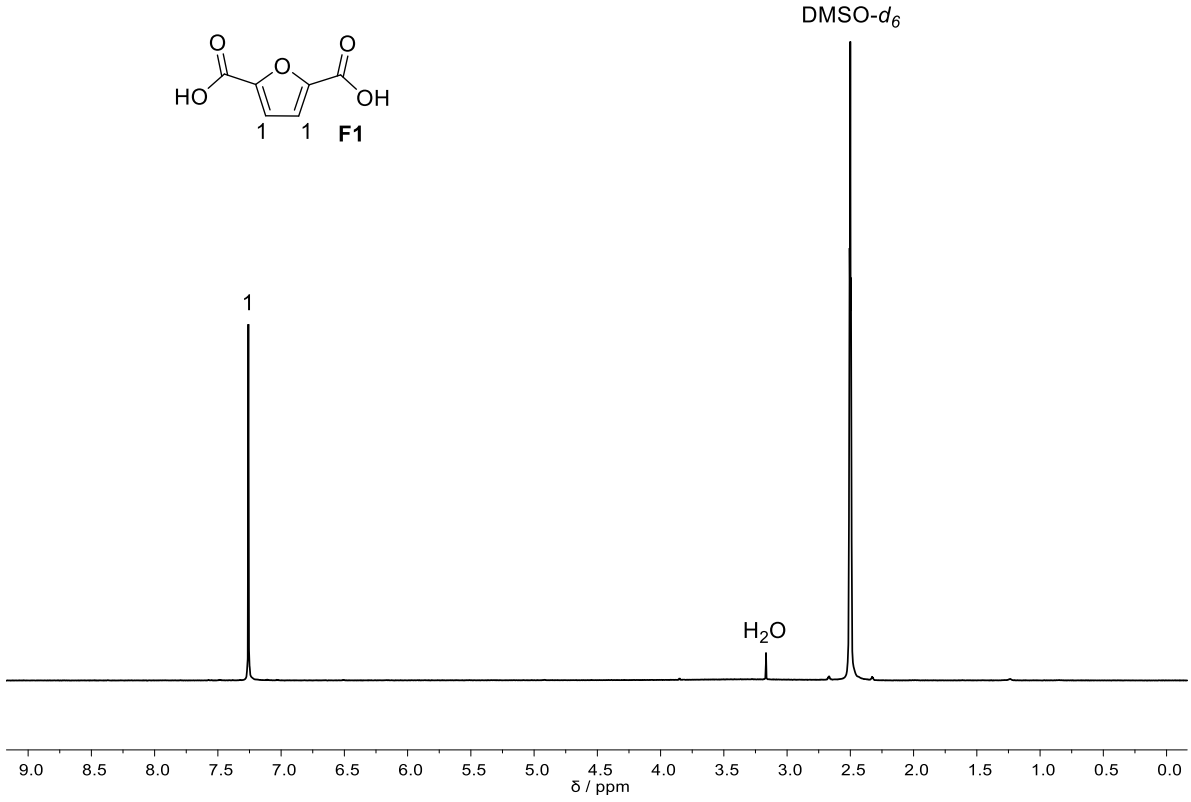

*Figure S 17. ^{1}H NMR spectrum of monomer **F1** in DMSO-d_6.*

2,5-Furandicarboxylic dimethyl ester (F2) as monomer for polycondensation reactions to polyesters

S. Wegelin, co-supervised by the author of this thesis, performed the methylation as followed: 5.00 g FDCA (1.00 equiv., 32.0 mmol) were dissolved in 130 mL methanol (100 equiv., 103 g, 3.20 mol). 85.4 µL sulfuric acid (0.05 equiv., 157 mg, 1.60 mmol) were added, followed by stirring under reflux for 5 days. Full conversion was determined *via* ^{1}H NMR spectroscopy. The reaction mixture was concentrated under vacuum and the precipitated product was washed with water followed by drying under vacuum (<1 mbar). A recrystallization from methanol was performed before drying the product again under vacuum (<1 mbar) to obtain the monomer **F2** as white powder.

F2:

^{1}H NMR (400 MHz, DMSO-d_6) δ / ppm = 7.43 (s, 2H, CH^{2}), 3.86 (s, 6H, $CH_3{}^{1}$).

^{13}C NMR (101 MHz, DMSO-d_6) δ / ppm = 157.83, 146.03, 119.03, 52.39.

IR (ATR): $\tilde{\nu}$ / cm^{-1} = 3116, 1718, 1602, 1584, 1514, 1432, 1378, 1308, 1271, 1236, 1191, 1160, 1131, 1028, 985, 921, 854, 835, 796, 765, 611.

HRMS (FAB) *m/z*: $[M]^+$ calc for $C_8H_8O_5$, 184.0367, found 184.0366; Δ = 0.1 mmu.

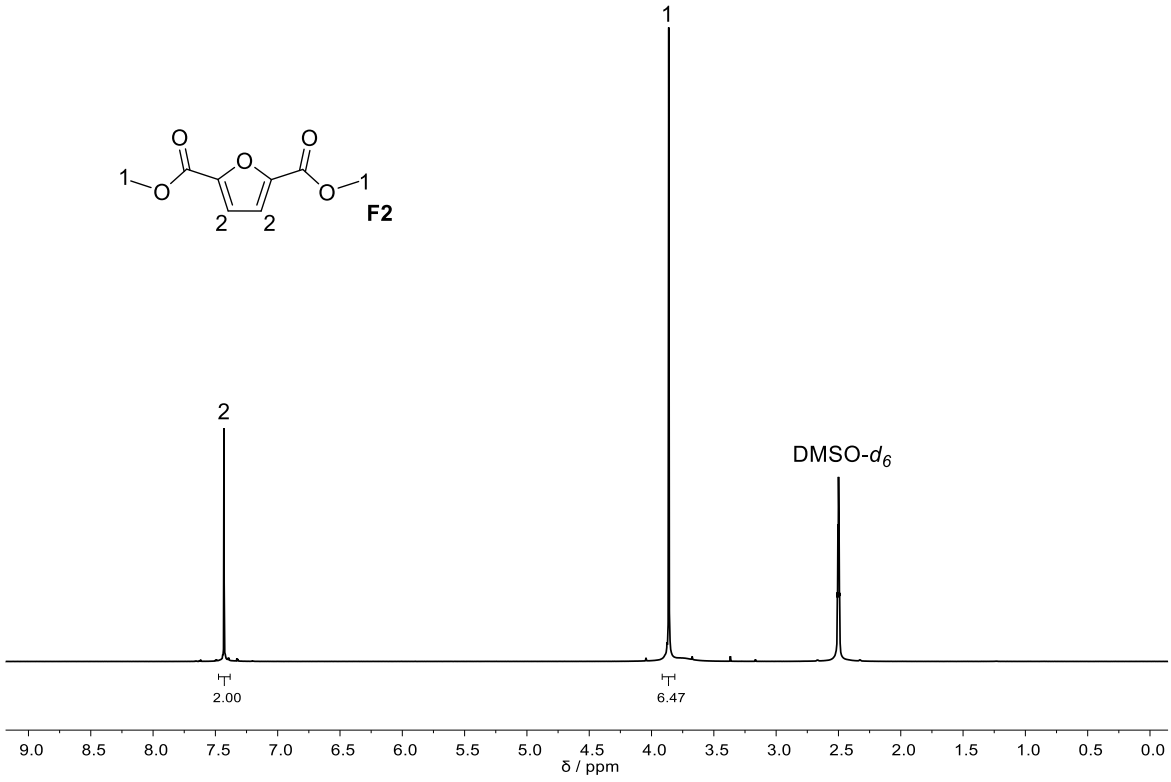

*Figure S 18. ^{1}H NMR spectrum of monomer **F2** in DMSO-d_6.*

Deconvolution method for catalyst screening in polycondensation reactions to polyesters

S. Wegelin, co-supervised by the author of this thesis, performed the screening as followed: 16 different Lewis Acids were tested in a polycondensation reaction of the two monomers BDO (3.00 equiv., 2.70 g, 30.0 mmol) and FDCA (1.00 equiv., 1.56 g, 10.0 mmol).

Table S 4. The 16 different Lewis Acids used for the deconvolution method of a polycondensation reaction using BDO and FDCA as monomers to yield the desired polyester.

1	$AlCl_3$	**5**	TTIP	**9**	$Zn(Otf)_2$	**13**	$In(Otf)_3$
2	$MgCl_2$ $6H_2O$	**6**	$FeCl_3$	**10**	$Yb(Otf)_3$	**14**	$Bi(Otf)_3$
3	$InCl_3$	**7**	$SnCl_2$	**11**	BF_3 $O(C_2H_5)_2$	**15**	Ag(Otf)
4	CuCl	**8**	$ZnBr_2$	**12**	$Sc(Otf)_3$	**16**	LiBr

The catalyst loading per batch during the deconvolution method was 1 mol%. The reaction flask was heated to 140 °C. Then, the temperature was increased to 180 °C within 4 hours. After the reaction was stirred for 19 hours at 180 °C, vacuum (< 1 mbar) was applied to the system to remove excess of BDO and water, and the temperature was further increased to 190 °C for 1 hour. Then, the polycondensation reaction was stirred at to 200 °C under continuous vacuum (<1 mbar) for another 23 hours. The obtained polyesters were dissolved in HFIP, precipitated into methanol, then dried at 80 °C under vacuum (<1 mbar) for 6 hours, before SEC-HFIP was performed to determine M_n and $Đ$.

Table S 5. Polycondensation reaction of BDO and FDCA to polyesters listed with the used catalysts. The M_n and Đ of the respective polyesters was determined by SEC-HFIP.

Batch/Catalyst Number	Catalyst(s)	M_n / kDa	Đ
B1	$AlCl_3$, $MgCl_2 \cdot 6H_2O$, $InCl_3$, CuCl	9	1.47
B2	$Zn(Otf)_2$, $Yb(Otf)_3$, $In(Otf)_3$, $Bi(Otf)_3$	-	-
B3	TTIP, $FeCl_3$, $SnCl_2$, $ZnBr_2$	9	1.93
B4	$BF_3{\cdot}O(C_2H_5)_2$, $Sc(Otf)_3$, Ag(Otf), LiBr	-	-
B5	$AlCl_3$, $MgCl_2 \cdot 6H_2O$	12	1.57
B6	$InCl_3$, CuCl	10	1.47
B7	$FeCl_3$, TTIP	16	2.22
B8	$SnCl_2$, $ZnBr_2$	10	1.82
	$AlCl_3$	15	1.65
	$MgCl_2 \cdot 6 H_2O$	11	1.19
	$InCl_3$	9	1.86
	CuCl	-	-
	TTIP	14	1.95
	$FeCl_3$	18	1.55
	$SnCl_2$	11	1.23
	$ZnBr_2$	10	2.26
	*TTIP	10	2.22
	*$FeCl_3$	17	1.53
	$Ti(OBu)_4$	15	1.96

*monomer **F2** was used instead of FDCA

General procedure of polycondensation reaction based on a dicarboxylic acid and BDO to polyesters

2.70 g of BDO (3.00 equiv., 30.0 mmol, racemic mixture purchased from SIGMA-ALDRICH) were mixed with the respective dicarboxylic acid (1.00 equiv., 10.0 mmol) as second monomer and $FeCl_3$ (1.25 mol%., 20.0 mg, 0.120 mmol) as catalyst. The round-bottom flask including the reaction mixture was put into a preheated oil bath at 160 °C for 17 hours. Then, the temperature was increased to 215 °C for another 7 hours with vacuum (<1 mbar) applied to the system. After the rection time was completed, the reaction mixture was cooled to room temperature and dissolved in THF, then precipitated in a 1:1 (v/v) mixture of ice-cold water and ethanol. The precipitated polymer was dried under vacuum (<1 mbar) at room temperature. However, some polymers still showed water traces in the NMR spectrum, which was also

visible when measuring TGA. Thus, for TGA two degradation temperatures are listed, for a better comparison of all polymers.

For polyester **P1**, FDCA (1.56 g) was used as second monomer with 2.70 g BDO. The product was isolated as brownish solid.

P1:

^{1}H NMR (400 MHz, DMSO-d_6) δ / ppm = 7.43 – 7.19 (m, 2H, CH^3), 5.33 – 5.11 (m, 2H, CH^2), 1.49 – 1.10 (m, 6H, $CH_3{}^1$).

^{13}C NMR (101 MHz, DMSO-d_6) δ / ppm = 157.09, 147.56, 145.40, 119.65, 72.96, 16.17, 14.90.

IR (ATR) $\tilde{\nu}$ / cm^{-1} = 1718, 1578, 1382, 1267, 1224, 1135, 1107, 1080, 1018, 996, 965, 825, 763, 618.

$T_{d,5\%}$ = 303 °C (TGA), M_n = 6 kDa and $Đ$ = 1.80 (SEC-THF), 18 kDa and $Đ$ = 1.55 (SEC-HFIP), T_g = 106 °C (DSC).

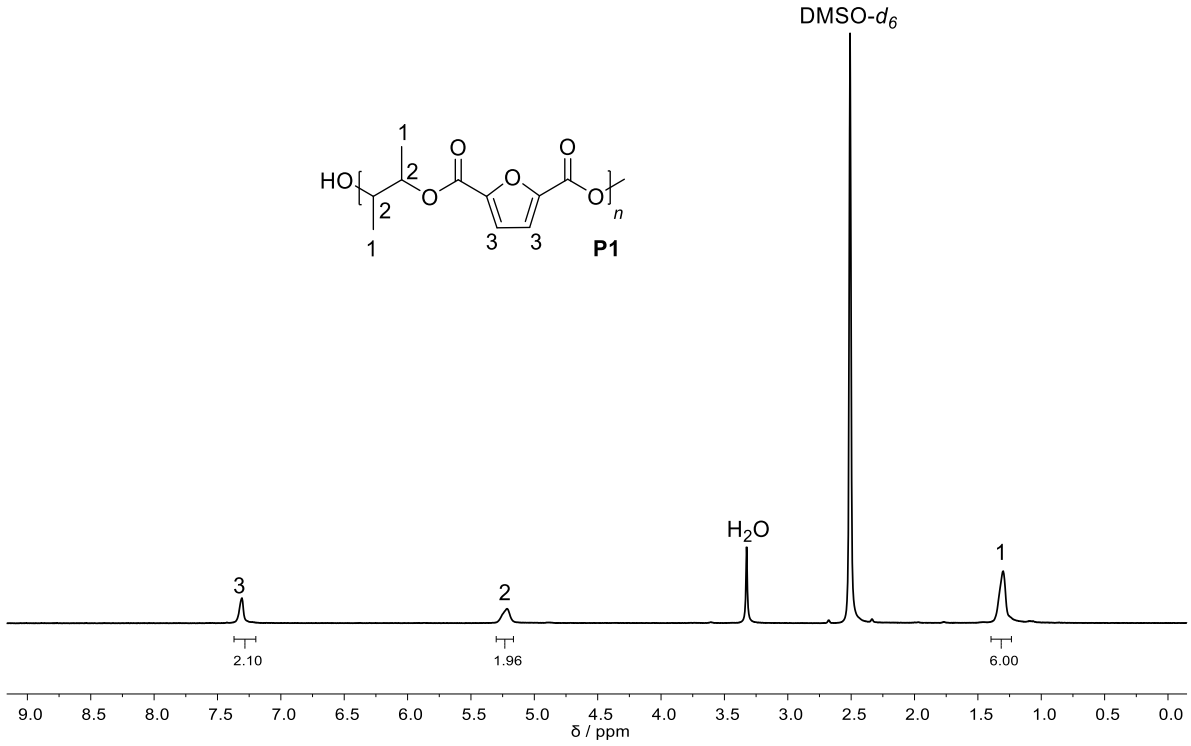

*Figure S 19. ^{1}H NMR spectrum of polyester **P1** in DMSO-d$_6$.*

For polyester **P1-F1**, **F1** (1.56 g) was used as second monomer with 2.70 g BDO. The product was isolated as brownish solid.

P1-F1:

^{1}H NMR (400 MHz, DMSO-d_6) δ / ppm = 7.41 – 7.25 (m, 2H, CH^3), 5.36 – 5.10 (m, 2H, CH^2), 1.39 – 1.24 (m, 6H, $CH_3{}^1$).

IR (ATR) $\tilde{\nu}$ / cm^{-1} = 1718, 1578, 1382, 1267, 1224, 1135, 1107, 1080, 1018, 996, 965, 825, 763, 617.

$T_{d,5\%}$ = 251 °C (TGA), $T_{d,15\%}$ = 343 °C (TGA), M_n = 6 kDa and Đ = 2.27 (SEC-THF), T_g = 95 °C (DSC).

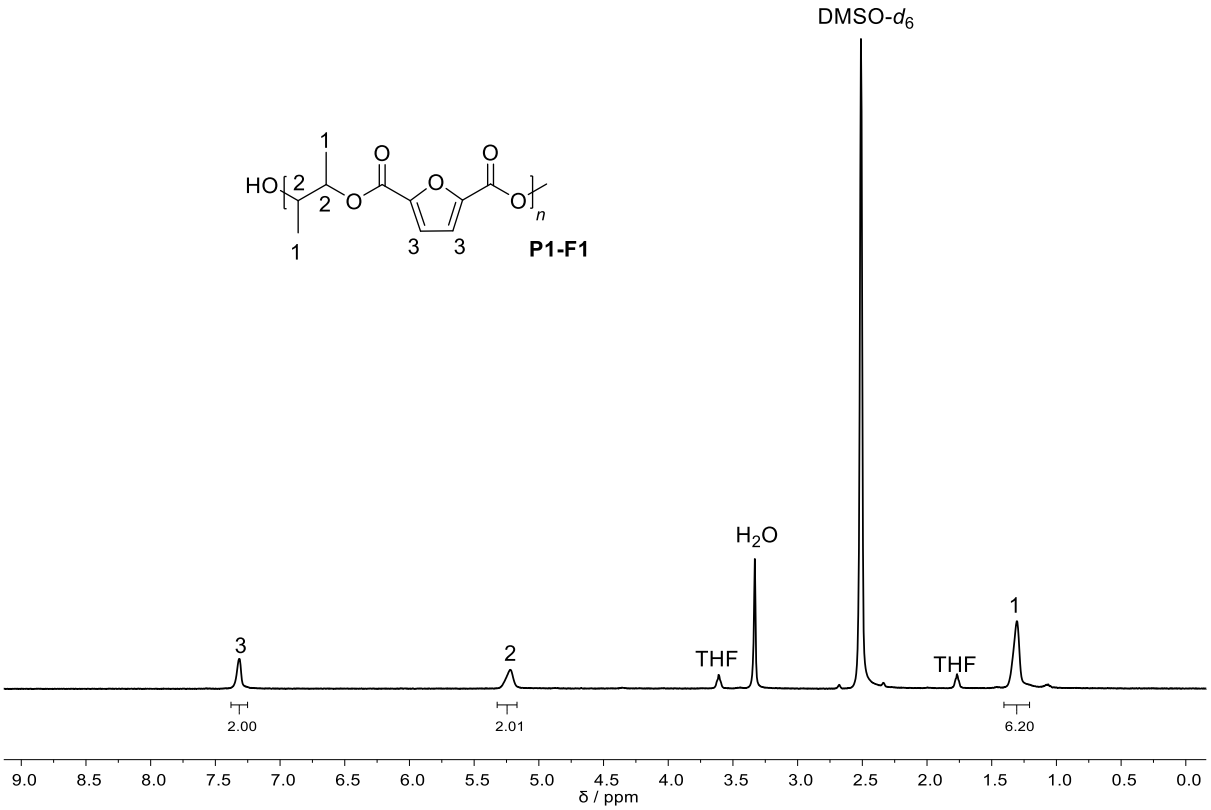

*Figure S 20. ^{1}H NMR spectrum of polyester **P1-F1** in DMSO-d_6.*

For polyester **P1-F2**, **F2** (1.84 g) was used as dicarboxylic acid with 2.70 g BDO. The product was isolated as brownish solid.

P1-F2:

^{1}H NMR (400 MHz, DMSO-d_6) δ / ppm = 8.12 – 7.96 (m, side-product), 7.48 – 7.17 (m, 2H, CH^3), 5.31 – 5.08 (m, 2H, CH_2^2), 1.40 – 1.12 (m, 6H, CH_3^1).

IR (ATR) $\tilde{\nu}$ / cm^{-1} = 2989, 1715, 1578, 1448, 1380, 1265, 1220, 1129, 1098, 1076, 1018, 998, 963, 905, 893, 868, 825, 761, 734, 685, 617.

$T_{d,5\%}$ = 172 °C (TGA), $T_{d,15\%}$ = 329 °C (TGA), M_n = 8 kDa and $Đ$ = 2.32 (SEC-THF), T_g = 90 °C (DSC).

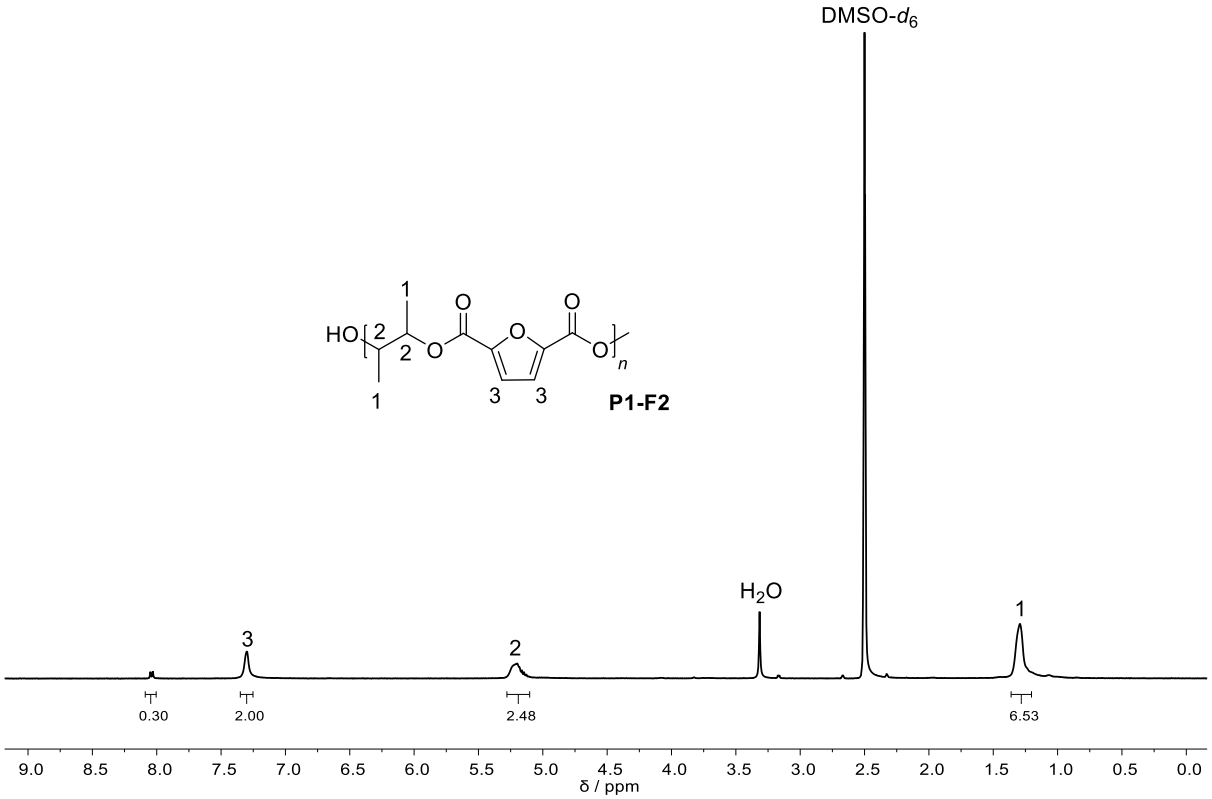

*Figure S 21. ^{1}H NMR spectrum of polyester **P1-F2** in DMSO-d_6.*

The proton signal at 8.12 – 7.96 ppm was presumed to be caused due to elimination of the BDO domain as side-reaction, but was not further analyzed.

For polyester **P2**, the dicarboxylic acid SA (1.18 g) was used with 2.70 g BDO. The product was isolated as brownish highly viscous liquid.

P2:

^{1}H NMR (400 MHz, $CDCl_3$) δ / ppm = 5.09 – 4.87 (m, 2H, CH^2), 2.71 – 2.49 (m, 4H, CH_2^3), 1.34 – 1.07 (m, 6H, CH_3^1).

IR (ATR) $\tilde{\nu}$ / cm^{-1} = 2987, 2941, 1726, 1537, 1446, 1413, 1376, 1349, 1316, 1261, 1240, 1209, 1152, 1100, 1082, 1035, 1020, 1000, 965, 921, 860, 802, 570.

$T_{d,\%}$ = 280 °C (TGA), $T_{d,15\%}$ = 336 °C (TGA), M_n = 5 kDa and $Đ$ = 1.47 (SEC-HFIP).

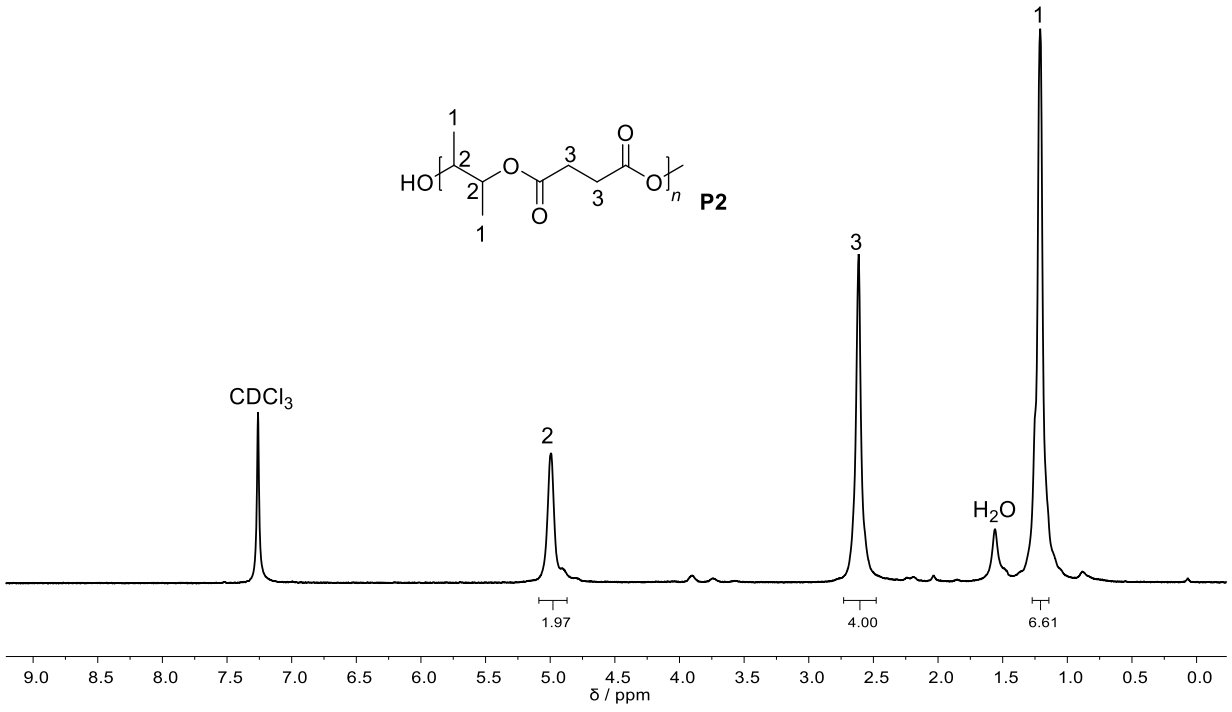

*Figure S 22. ^{1}H NMR spectrum of polyester **P2** in $CDCl_3$.*

For polyester **P3**, the dicarboxylic acid AA (1.46 g) was used with 2.70 g BDO. The product was isolated as brownish highly viscous liquid.

P3:

^{1}H NMR (400 MHz, DMSO-d_6) δ / ppm = 4.98 – 4.80 (m, 2H, CH^2), 4.33 (d, J = 5.3 Hz, 1H, OH^7), 3.44 (t, J = 6.6 Hz, 2H, CH^6), 2.36 – 2.19 (m, 4H, $CH_2{}^3$), 1.60 – 1.46 (m, 4H, $CH_2{}^4$), 1.18 – 1.07 (m, 6H, $CH_3{}^1$), 1.07 (s, 3H, $CH_3{}^5$).

IR (ATR) $\tilde{\nu}$ / cm^{-1} = 2985, 2941, 1728, 1528, 1448, 1419, 1378, 1312, 1286, 1240, 1216, 1166, 1137, 1100, 1080, 1043, 1022, 1002, 946.

$T_{d,5\%}$ = 326 °C (TGA), M_n = 8 kDa and $Đ$ = 1.44 (SEC-HFIP).

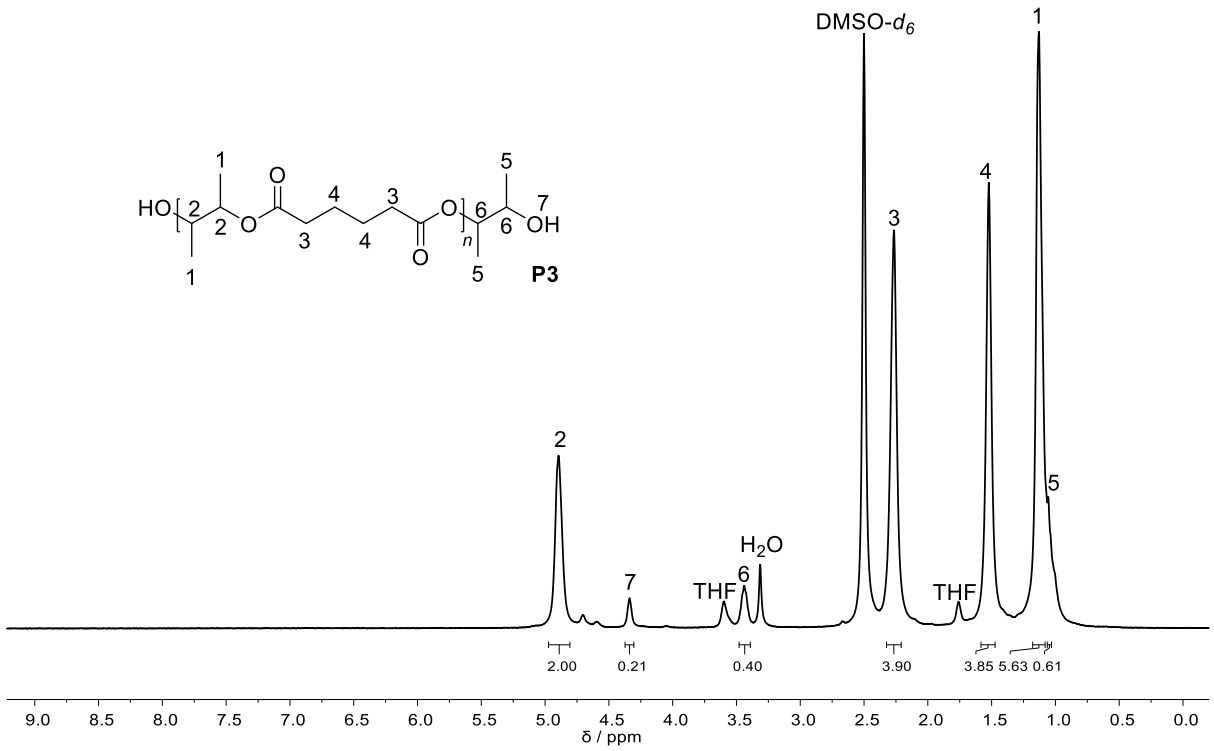

*Figure S 23. ^{1}H NMR spectrum of polyester **P3** in DMSO-d_6.*

For polyester **P4**, the dicarboxylic acid SBA (2.02 g) was used with 2.70 g BDO. The product was isolated as brownish highly viscous liquid.

P4:

^{1}H NMR (400 MHz, DMSO-d_6) δ / = 4.96 – 4.82 (m, 2H, CH^2), 2.28 – 2.17 (m, 4H, $CH_2{}^3$), 1.54 – 1.45 (m, 4H, $CH_2{}^4$), 1.28 – 1.20 (m, 8H, $CH_2{}^5$), 1.16 – 0.98 (m, 6H, $CH_3{}^1$).

IR (ATR) $\tilde{\nu}$ / cm^{-1} = 2983, 2931, 2855, 1732, 1450, 1419, 1378, 1349, 1316, 1300, 1242, 1166, 1131, 1100, 1082, 1035, 1004, 944, 868, 726.

$T_{d,5\%}$ = 358 °C (TGA), M_n = 10 kDa and $Đ$ = 1.47 (SEC-HFIP).

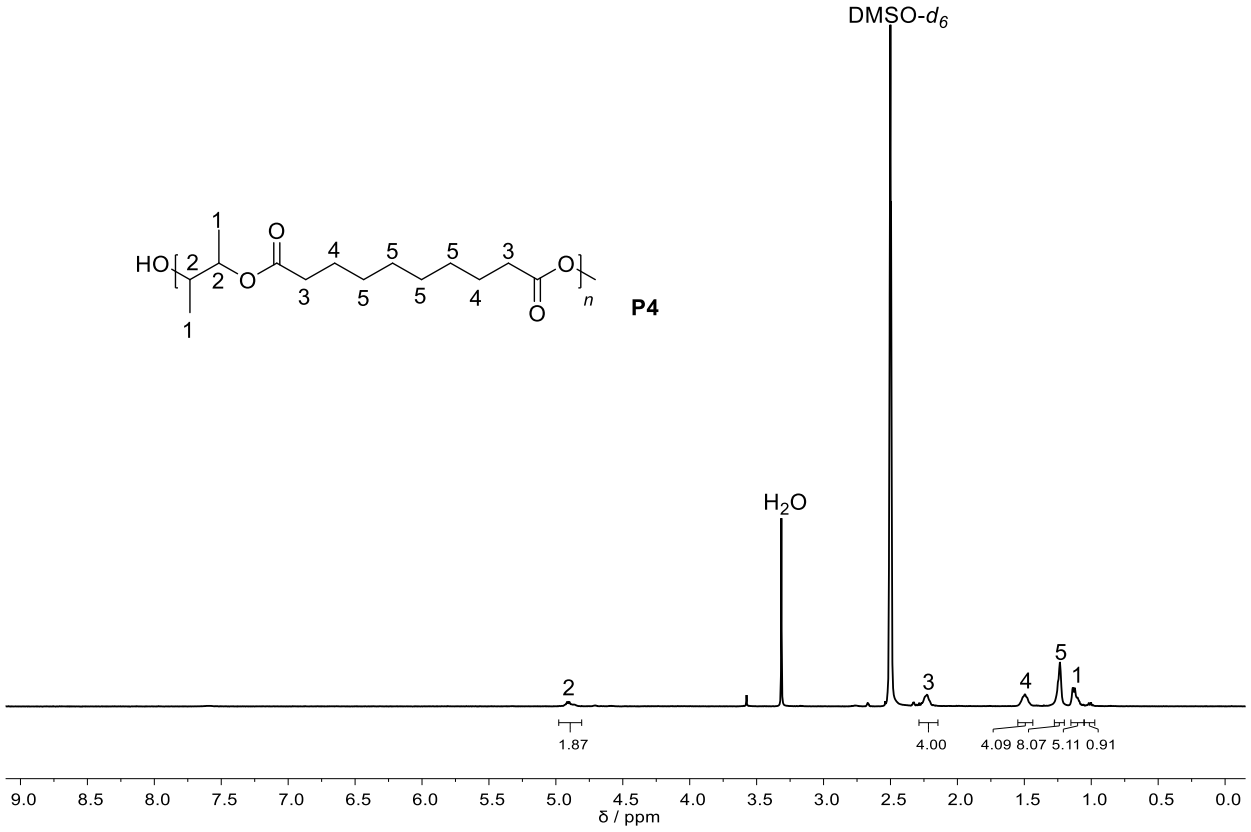

*Figure S 24. ^{1}H NMR spectrum of polyester **P4** in DMSO-d$_6$.*

General procedure of polycondensation reaction based on two dicarboxylic acids and BDO to copolyesters

2.70 g of BDO (3.00 equiv., 30.0 mmol, racemic mixture purchased from SIGMA-ALDRICH) were added to a flask containing 1 equiv. (1 mmol) of a mixture of two dicarboxylic acids (FDCA and either SA, SBA, or AA). $FeCl_3$ (1.25 mol%., 20.0 mg, 0.120 mmol) was added as catalyst. An oil bath was preheated to 160 °C in which the reaction mixture was stirred in a round-bottom flask for 17 hours. The temperature was increased to 215 °C and vacuum (<1 mbar) was applied to the system. After the polycondensation reaction was finished, the mixture was cooled to room temperature, dissolved in THF, and precipitated in a mixture of 1:1 (v/v) ice-cold water to ethanol. The isolated copolyester was dried under vacuum (<1mbar) at room temperature. However, some polymers still showed water traces in the NMR spectrum, which was also visible when measuring TGA. Thus, for TGA two degradation temperatures are listed, for a better comparison of all polymers.

The obtained copolyesters of this thesis are not specified and depicted accordingly with *co* = unspecified.[305] Therefore, a shifting of CH (BDO) and CH_2 signals (dicarboxylic acid domain) is visible in the respective ^{1}H NMR spectra. Furthermore, a racemic mixture of BDO obtained from SIGMA-ALDRICH was used, meaning meso-BDO in the polymer leads to an CH and CH_3 group shifting in the respective ^{1}H NMR spectra compared to RR/SS-BDO. No further assignment was possible.

SA6:

For copolyester **SA6**, a dicarboxylic acid mixture of 94% FDCA (9.40 mmol, 1.46 g) and 6% SA (0.60 mmol, 71.0 mg) was used. The product was isolated as brownish solid.

^{1}H NMR (400 MHz, $CDCl_3$) δ / ppm = 7.20 – 7.10 (m, 2H, CH^3), 5.35 – 5.24 (m, 2H, CH^4), 5.21 – 5.05 (m, 2H, CH^2), 2.69 – 2.55 (m, 4H, $CH_2{}^6$), 1.47 – 1.30 (m, 6H, $CH_3{}^5$), 1.28 – 1.23 (m, 6H, $CH_3{}^1$).

IR (ATR) $\tilde{\nu}$ / cm^{-1} = 2987, 1715, 1580, 1448, 1380, 1265, 1220, 1131, 1107, 1076, 1016, 996, 963, 907, 866, 823, 792, 761, 720, 617.

$T_{d,5\%}$ = 300 °C, $T_{d,15\%}$ = 329 °C (TGA), M_n = 13 kDa and $Đ$ = 1.71 (SEC-HFIP), T_g = 94 °C (DSC).

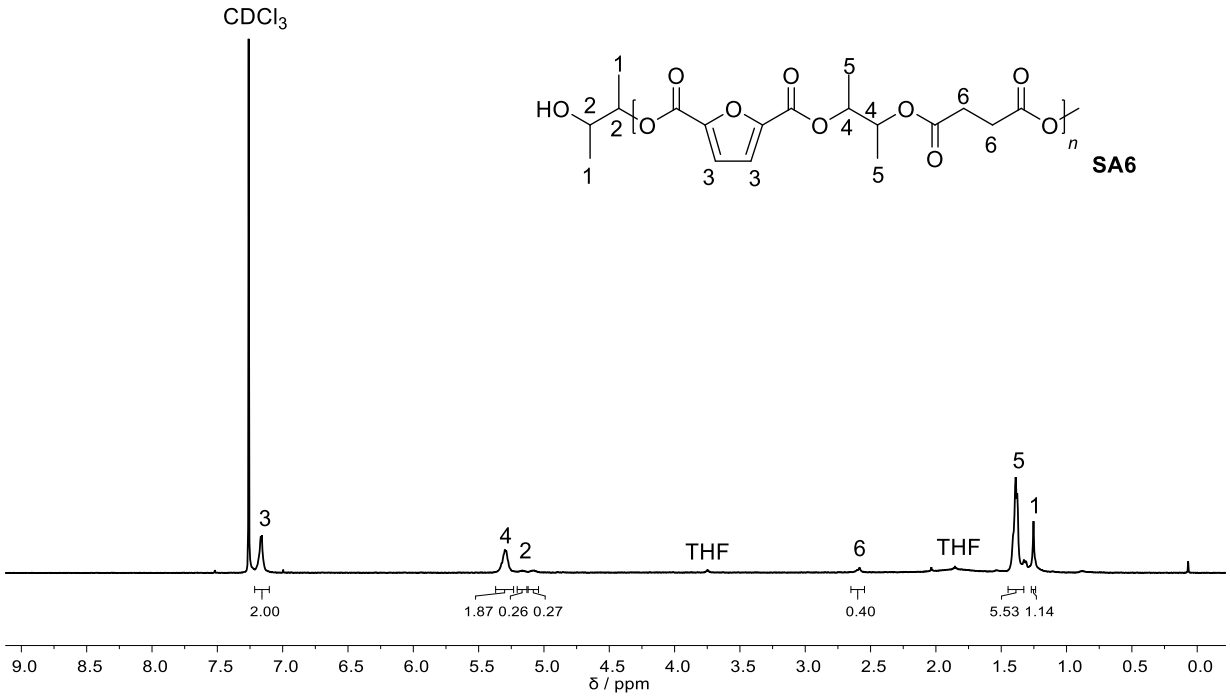

*Figure S 25. ^{1}H NMR spectrum of copolyester **SA6** in $CDCl_3$.*

For copolyester **SA12**, a dicarboxylic acid mixture of 88% FDCA (8.80 mmol, 1.37 g) and 12% SA (1.20 mmol, 142 mg) was used. The product was isolated as brownish solid.

SA12:

^{1}H NMR (400 MHz, $CDCl_3$) δ / ppm = 7.21 – 7.09 (m, 2H, CH^1), 5.40 – 5.00 (m, 4H, CH^2), 2.64 – 2.53 (m, 4H, CH_2^4), 1.45 – 1.19 (m, 12H, CH_3^3).

IR (ATR) $\tilde{\nu}$ / cm^{-1} = 2987, 1715, 1580, 1506, 1448, 1380, 1265, 1220, 1131, 1107, 1076, 1016, 996, 963, 907, 866, 823, 763, 619.

$T_{d,5\%}$ = 318 °C, $T_{d,15\%}$ = 343 °C (TGA), M_n = 12 kDa and $Đ$ = 1.64 (SEC-HFIP), T_g = 84 °C (DSC).

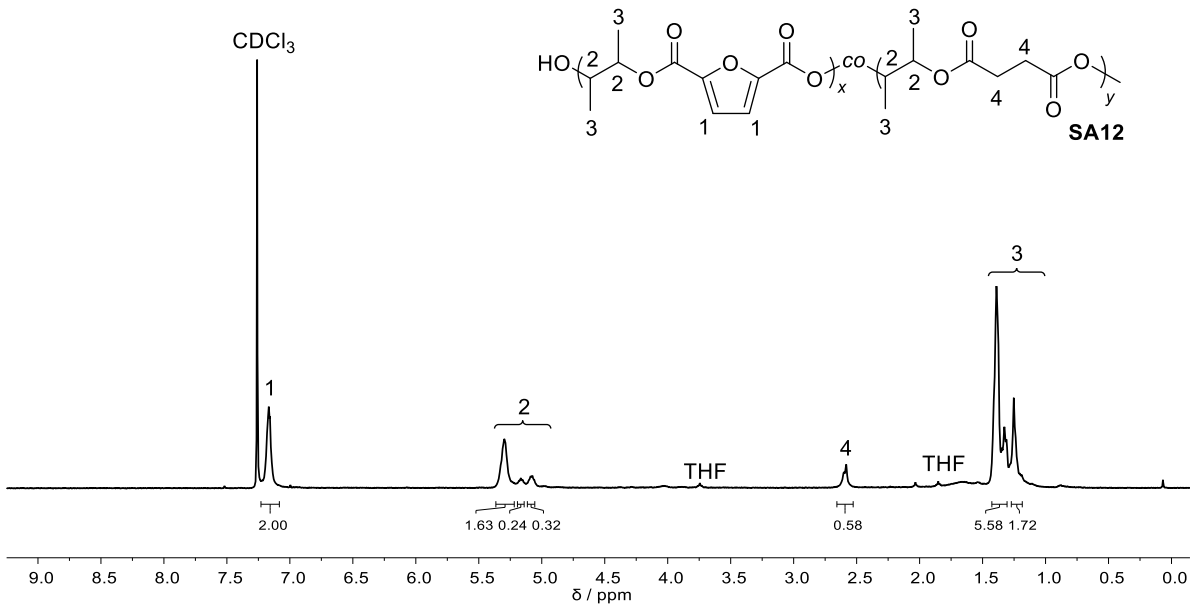

*Figure S 26. ^{1}H NMR spectrum of copolyester **SA12** in $CDCl_3$.*

For copolyester **SA18**, a dicarboxylic acid mixture of 82% FDCA (8.20 mmol, 1.28 g) and 18% SA (1.80 mmol, 213 mg) was used. The product was isolated as brownish solid.

SA18:

^{1}H NMR (400 MHz, $CDCl_3$) δ / ppm = 7.24 – 7.08 (m, 2H, CH^1), 5.40 – 4.96 (m, 4H, CH^2), 2.72 – 2.48 (m, 4H, $CH_2{}^4$), 1.50 – 1.13 (m, 12H, $CH_3{}^3$).

IR (ATR) $\tilde{\nu}$ / cm^{-1} = 2985, 2941, 1715, 1580, 1448, 1380, 1345, 1265, 1222, 1133, 1100, 1078, 1016, 1000, 963, 907, 866, 825, 763, 617.

$T_{d,5\%}$ = 145 °C (TGA), $T_{d,15\%}$ = 328 °C (TGA), M_n = 10 kDa and $Đ$ = 1.46 (SEC-HFIP), T_g = 71 °C (DSC).

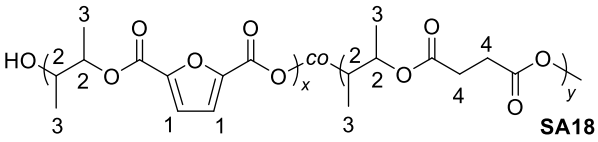

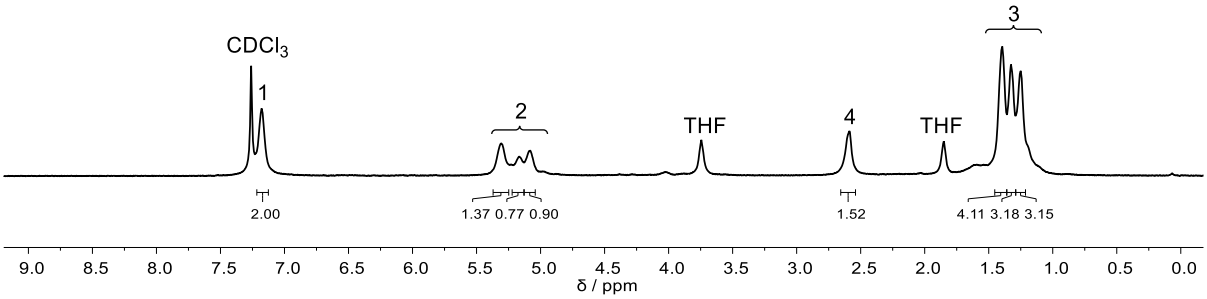

*Figure S 27. ^{1}H NMR spectrum of copolyester **SA18** in $CDCl_3$.*

For copolyester **SA24**, a dicarboxylic acid mixture of 76% FDCA (7.60 mmol, 1.18 g) and 24% SA (2.40 mmol, 283 mg) was used. The product was isolated as brownish solid.

SA24:

^{1}H NMR (400 MHz, $CDCl_3$) δ / ppm = 7.23 – 7.09 (m, 2H, CH^1), 5.39 – 4.93 (m, 4H, CH^2), 2.64 – 2.52 (m, 4H, CH_2^4), 1.44 – 1.15 (m, 12H, CH_3^3).

IR (ATR) $\tilde{\nu}$ / cm^{-1} = 2987, 2941, 1715, 1578, 1448, 1380, 1345, 1267, 1222, 1133, 1105, 1078, 1016, 998, 963, 907, 866, 825, 763, 617.

$T_{d,5\%}$ = 137 °C (TGA), $T_{d,15\%}$ = 329 °C (TGA), M_n = 14 kDa and $Đ$ = 1.70 (SEC-HFIP), T_g = 62 °C (DSC).

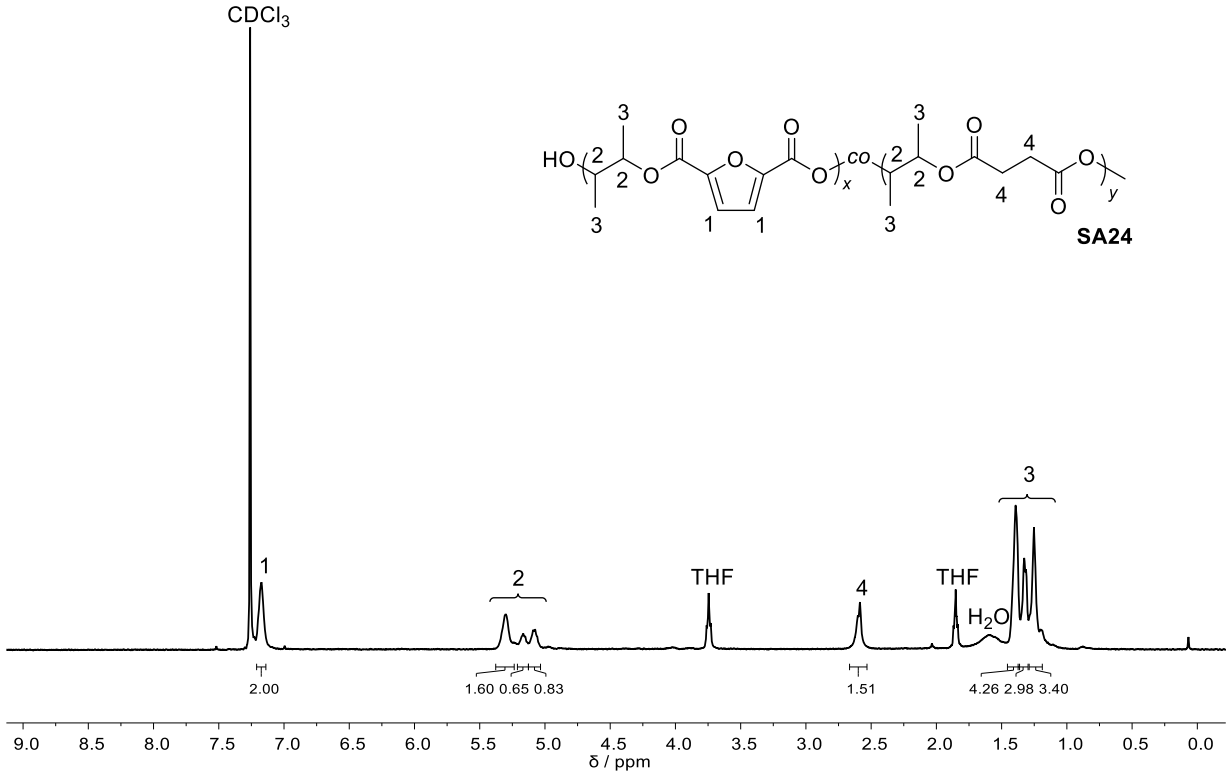

*Figure S 28. ^{1}H NMR spectrum of copolyester **SA24** in $CDCl_3$.*

For copolyester **SA30**, a dicarboxylic acid mixture of 70% FDCA (7.00 mmol, 1.09 g) and 30% SA (3.00 mmol, 354 mg) was used. The product was isolated as brownish solid.

SA30:

^{1}H NMR (400 MHz, $CDCl_3$) δ / ppm = 7.22 – 7.11 (m, 2H, CH^1), 5.36 – 4.99 (m, 4H, CH^2), 2.67 – 2.51 (m, 4H, $CH_2{}^4$), 1.47 – 1.08 (m, 12H, $CH_3{}^3$).

IR (ATR) $\tilde{\nu}$ / cm^{-1} = 2985, 2941, 1715, 1580, 1448, 1409, 1380, 1345, 1267, 1222, 1135, 1105, 1078, 1016, 963, 907, 864, 827, 763, 617.

$T_{d,5\%}$ = 141 °C (TGA), $T_{d,15\%}$ = 316 °C (TGA), M_n = 10 kDa and $Đ$ = 1.58 (SEC-HFIP), T_g = 51 °C (DSC).

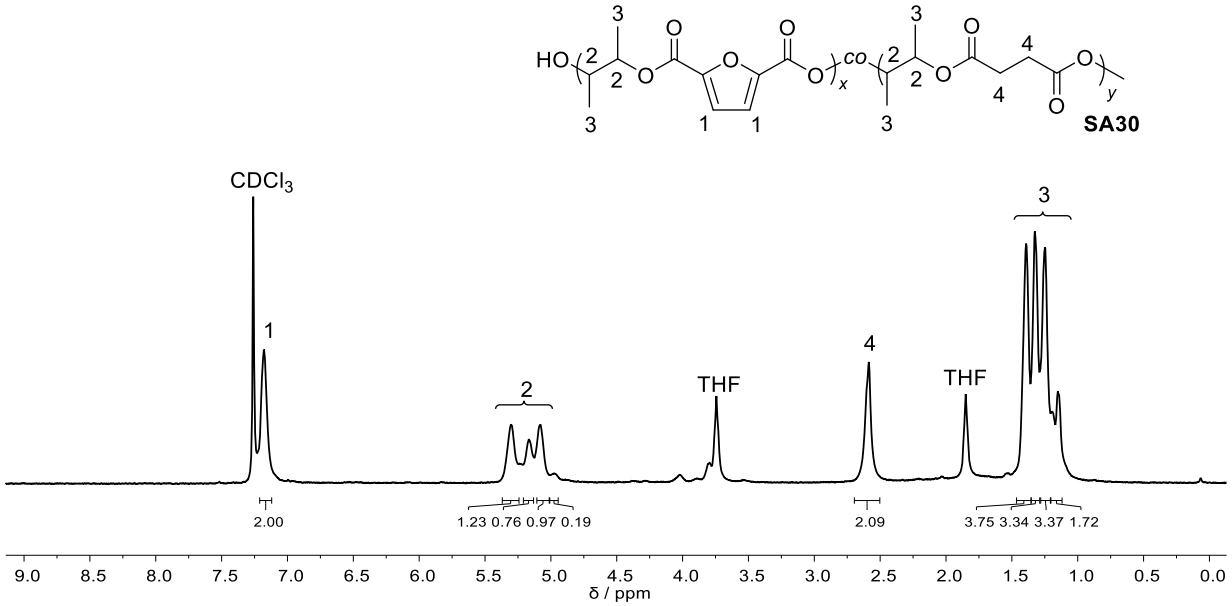

*Figure S 29. ^{1}H NMR spectrum of copolyester **SA30** in $CDCl_3$.*

For copolyester **SA40**, a dicarboxylic acid mixture of 60% FDCA (6.00 mmol, 937 mg) and 40% SA (4.00 mmol, 472 mg) was used. The product was isolated as brownish solid.

SA40:

^{1}H NMR (400 MHz, $CDCl_3$) δ / ppm = 7.22 – 7.13 (m, 2H, CH^1), 5.37 – 4.90 (m, 4H, CH^2), 2.71 – 2.47 (m, 4H, CH_2^4), 1.50 – 1.10 (m, 12H, CH_3^3).

IR (ATR) $\tilde{\nu}$ / cm^{-1} = 2987, 2941, 1715, 1580, 1448, 1411, 1380, 1345, 1269, 1222, 1137, 1103, 1078, 1018, 963, 924, 864, 827, 763, 617.

$T_{d,5\%}$ = 209 °C (TGA), $T_{d,15\%}$ = 328 °C (TGA), M_n = 8 kDa and $Đ$ = 1.50 (SEC-HFIP), T_g = 50 °C (DSC).

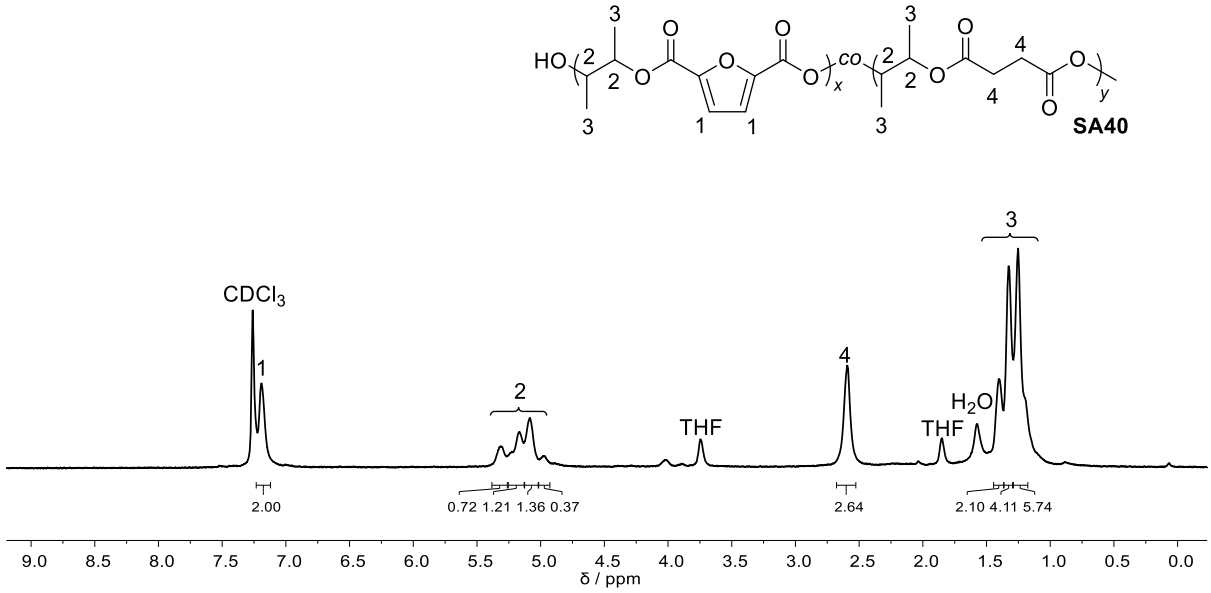

*Figure S 30. ^{1}H NMR spectrum of copolyester **SA40** in $CDCl_3$.*

For copolyester **SA60**, a dicarboxylic acid mixture of 40% FDCA (4.00 mmol, 624 mg) and 60% SA (6.00 mmol, 709 mg) was used. The product was isolated as brownish solid.

SA60:

^{1}H NMR (400 MHz, DMSO-d_6) δ / ppm = 7.45 – 7.29 (m, 2H, CH^1), 5.41 – 4.61 (m, 4H, CH^2), 1.38 – 0.90 (m, 12H, $CH_3{}^3$).

IR (ATR) $\tilde{\nu}$ / cm^{-1} = 2985, 2941, 1724, 1580, 1448, 1411, 1378, 1347, 1271, 1222, 1154, 1140, 1100, 1080, 1035, 1018, 1000, 963, 921, 901, 864, 829, 804, 765, 619.

$T_{d,5\%}$ = 269 °C (TGA), $T_{d,15\%}$ = 336 °C (TGA), M_n = 7 kDa and $Đ$ = 1.56 (SEC-HFIP), T_g = 26 °C (DSC).

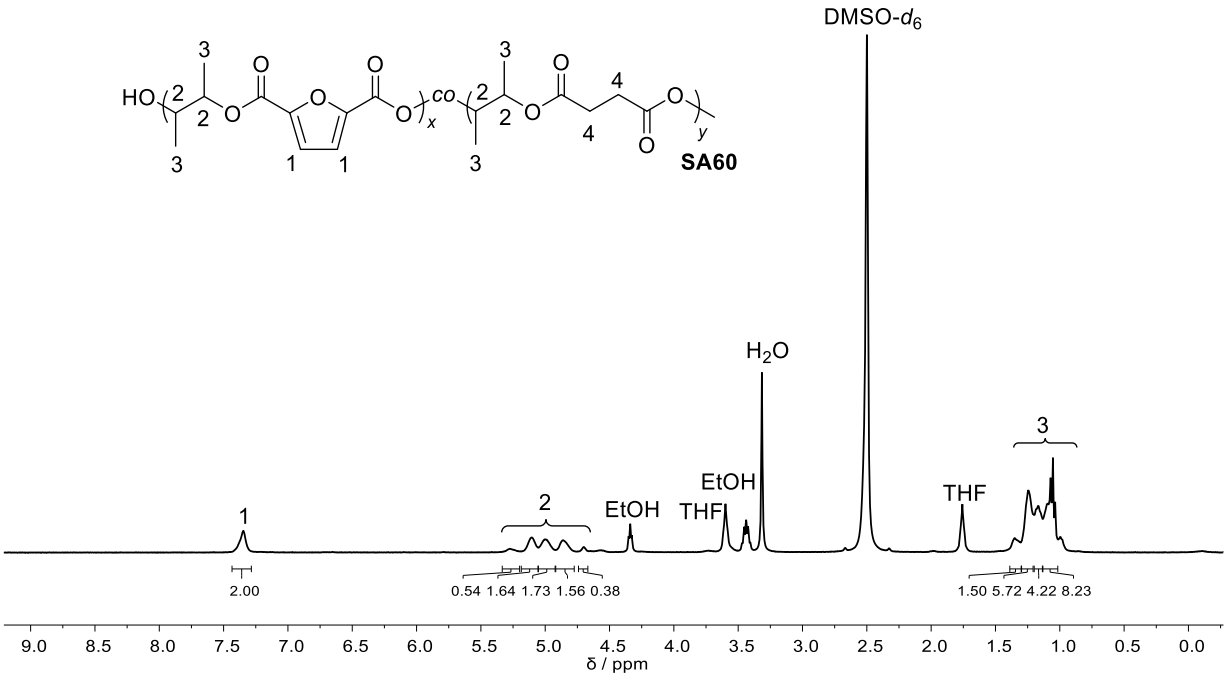

*Figure S 31. ^{1}H NMR spectrum of copolyester **SA60** in DMSO-d$_6$.*

For copolyester **AA6**, a dicarboxylic acid mixture of 94% FDCA (9.40 mmol, 1.46 g) and 6% AA (0.60 mmol, 88.0 mg) was used. The product was isolated as brownish solid.

AA6:

^{1}H NMR (400 MHz, DMSO-d_6) δ / ppm = 7.43 – 7.20 (m, 2H, CH^1), 5.30 – 4.89 (m, 4H, CH^2), 2.30 – 2.11 (m, 4H, CH$_2^4$), 1.48 – 1.36 (m, 4H, CH$_2^5$), 1.36 – 1.08 (m, 12H, CH$_3^3$).

IR (ATR) $\tilde{\nu}$ / cm^{-1} = 2987, 1715, 1578, 1506, 1448, 1380, 1265, 1220, 1131, 1107, 1078, 1016, 996, 963, 905, 866, 825, 784, 761, 720, 617.

$T_{d,5\%}$ = 310 °C (TGA), $T_{d,15\%}$ = 340 °C (TGA), M_n = 15 kDa and $Đ$ = 1.62 (SEC-HFIP), T_g = 84 °C (DSC).

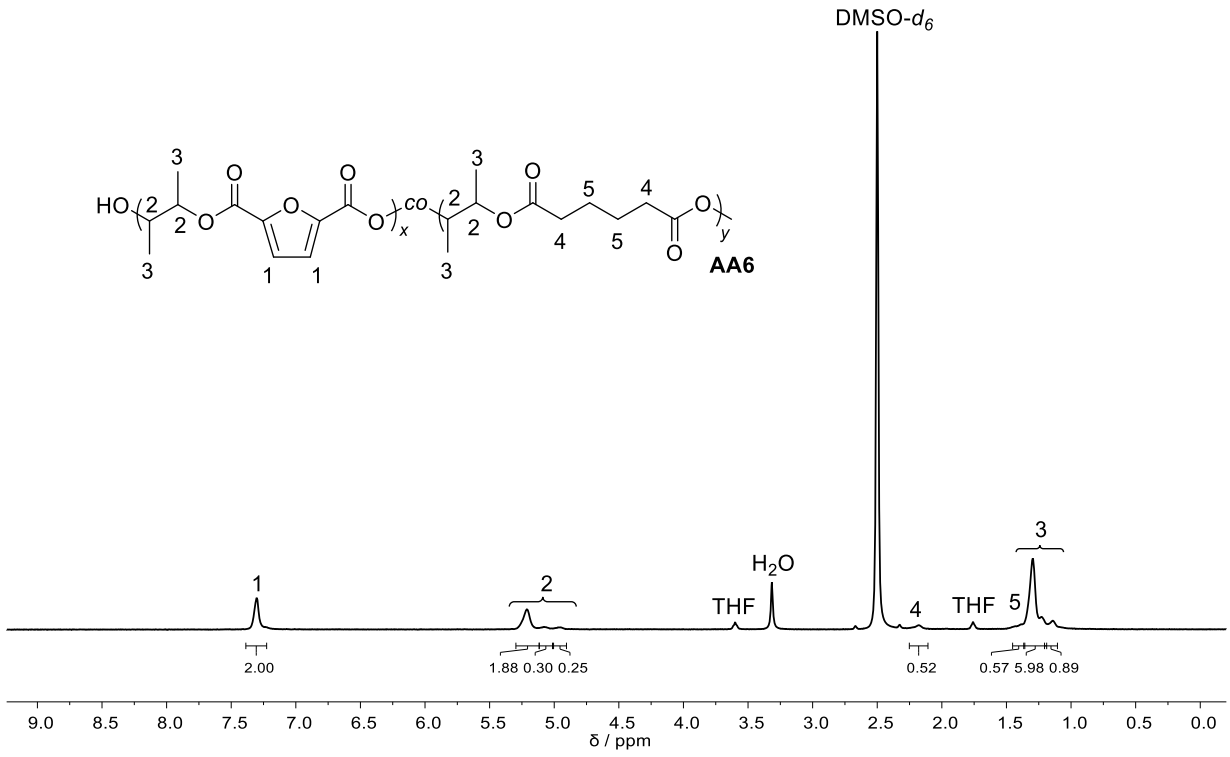

*Figure S 32. ^{1}H NMR spectrum of copolyester **AA6** in DMSO-d_6.*

For copolyester **AA12**, a dicarboxylic acid mixture of 88% FDCA (8.80 mmol, 1.37 g) and 12% AA (1.20 mmol, 175 mg) was used. The product was isolated as brownish solid.

AA12:

^{1}H NMR (400 MHz, DMSO-d_6) δ / ppm = 7.40 – 7.23 (m, 2H, CH^1), 5.34 – 4.90 (m, 4H, CH^2), 2.22 – 2.11 (m, 4H, CH_2^4), 1.50 – 1.36 (m, 4H, CH_2^5), 1.36 – 1.10 (m, 12H, CH_3^3).

IR (ATR) $\tilde{\nu}$ / cm^{-1} = 2989, 1715, 1580, 1448, 1380, 1265, 1220, 1131, 1107, 1078, 1016, 996, 963, 905, 866, 825, 763, 617.

$T_{d,5\%}$ = 324 °C (TGA), $T_{d,15\%}$ = 343 °C (TGA), M_n = 21 kDa and $Đ$ = 1.80 (SEC-HFIP), T_g = 81 °C (DSC).

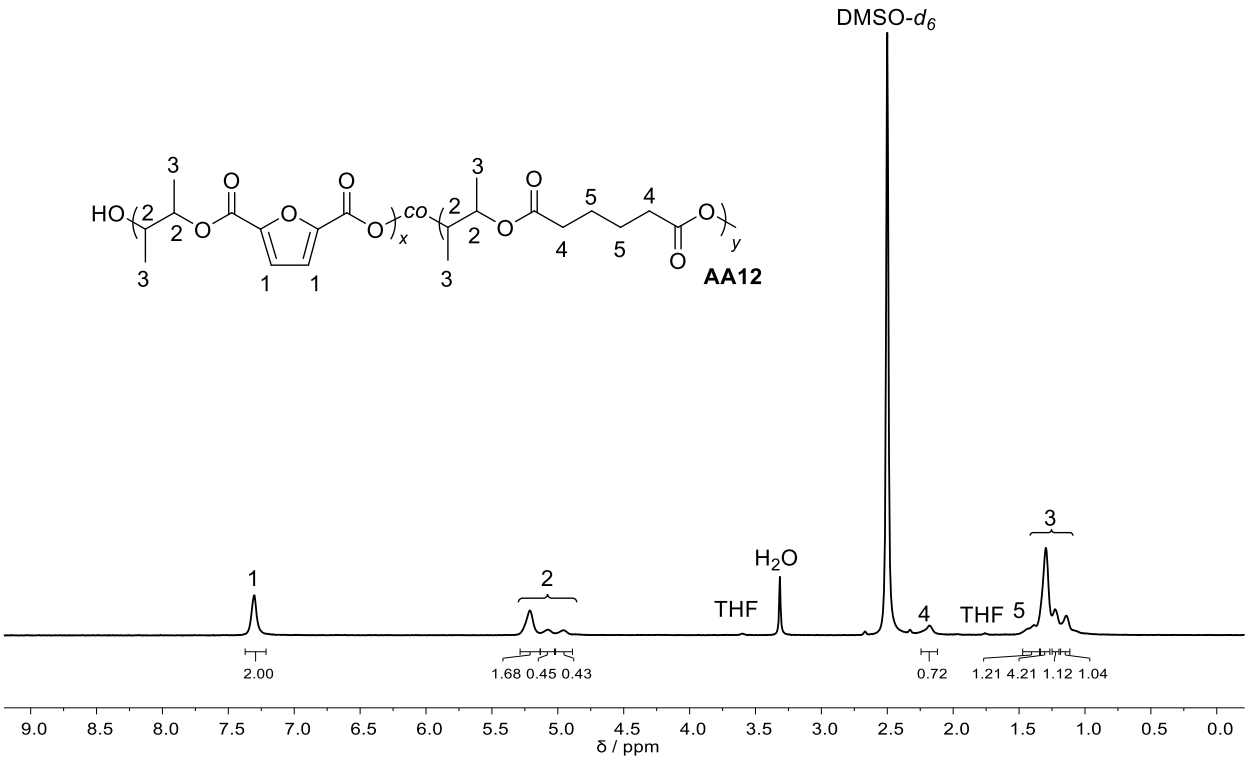

*Figure S 33. ^{1}H NMR spectrum of copolyester **AA12** in DMSO-d_6.*

For copolyester **AA18**, a dicarboxylic acid mixture of 82% FDCA (8.20 mmol, 1.28 g) and 18% AA (1.80 mmol, 263 mg) was used. The product was isolated as brownish solid.

AA18:

^{1}H NMR (400 MHz, DMSO-d_6) δ / ppm = 7.49 – 7.13 (m, 2H, CH^1), 5.37 – 4.89 (m, 4H, CH^2), 2.30 – 2.06 (m, 4H, $CH_2{}^4$), 1.47 – 1.38 (m, 4H, $CH_2{}^5$), 1.35 – 0.84 (m, 12H, $CH_3{}^3$).

IR (ATR) $\tilde{\nu}$ / cm^{-1} = 2987, 2934, 1715, 1578, 1448, 1380, 1347, 1335, 1265, 1220, 1131, 1107, 1078, 1016, 996, 963, 905, 866, 825, 792, 763, 617.

$T_{d,5\%}$ = 149 °C (TGA), $T_{d,15\%}$ = 337 °C (TGA), M_n = 16 kDa and $Đ$ = 1.84 (SEC-HFIP), T_g = 62 °C (DSC).

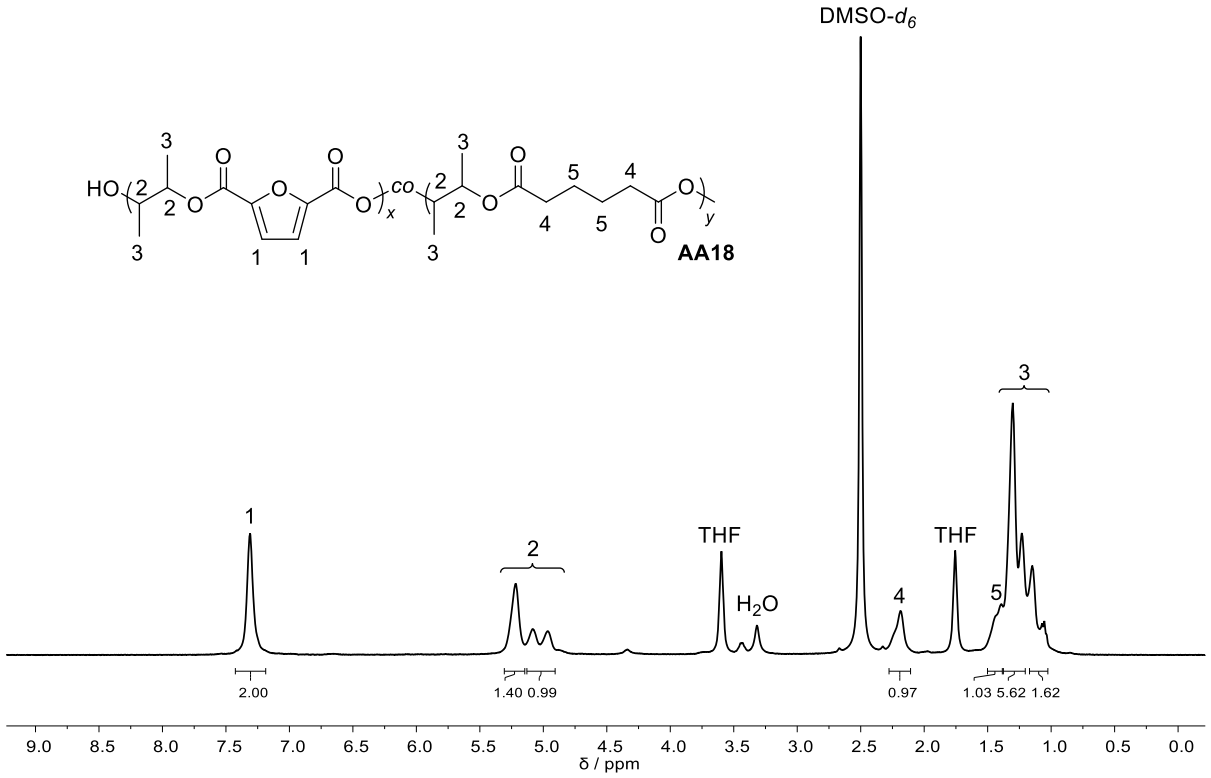

*Figure S 34. ^{1}H NMR spectrum of copolyester **AA18** in DMSO-d_6.*

For copolyester **AA24**, a dicarboxylic acid mixture of 76% FDCA (7.60 mmol, 1.18 g) and 24% AA (2.40 mmol, 351 mg) was used. The product was isolated as brownish solid.

AA24:

^{1}H NMR (400 MHz, DMSO-d_6) δ / ppm = 7.51 – 7.12 (m, 2H, CH^1), 5.42 – 4.78 (m, 4H, CH^2), 2.33 – 2.04 (m, 4H, CH$_2^4$), 1.55 – 1.34 (m, 4H, CH$_2^5$), 1.36 – 1.02 (m, 12H, CH$_3^3$).

IR (ATR) $\tilde{\nu}$ / cm^{-1} = 2985, 2941, 1715, 1580, 1448, 1380, 1339, 1267, 1222, 1133, 1107, 1078, 1016, 963, 905, 866, 827, 763, 617.

$T_{d,5\%}$ = 145 °C (TGA), $T_{d,15\%}$ = 338 °C (TGA), M_n = 14 kDa and $Đ$ = 1.68 (SEC-HFIP), T_g = 58 °C (DSC).

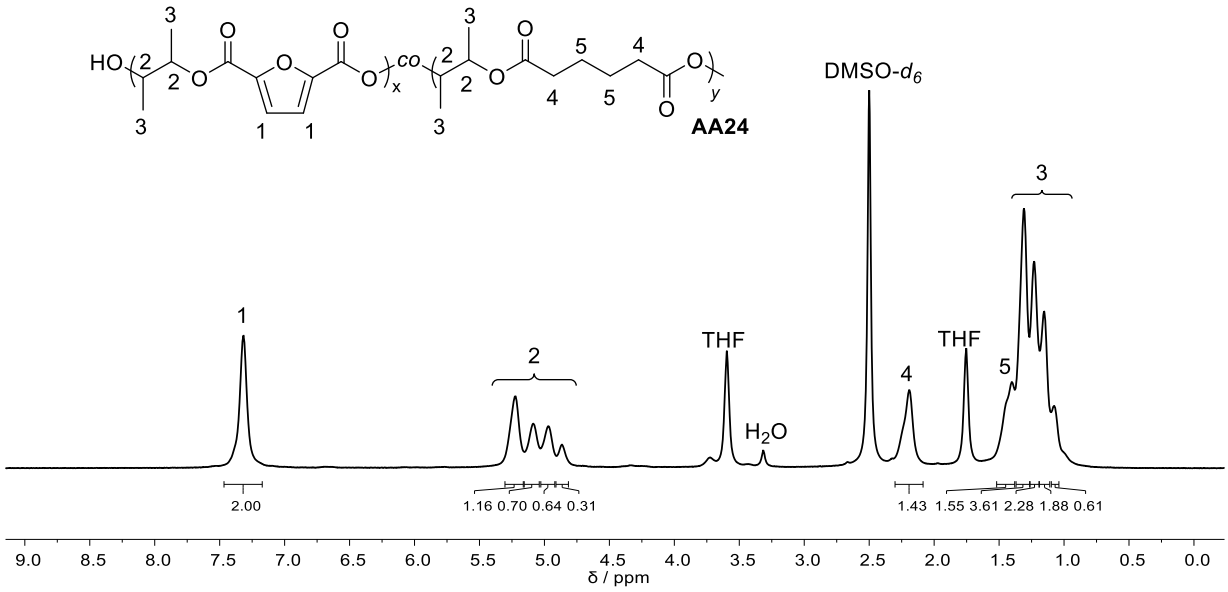

*Figure S 35. ^{1}H NMR spectrum of copolyester **AA24** in DMSO-d_6.*

For copolyester **AA30**, a dicarboxylic acid mixture of 70% FDCA (7.00 mmol, 1.09 g) and 30% AA (3.00 mmol, 483 mg) was used. The product was isolated as brownish solid.

AA30:

^{1}H NMR (400 MHz, DMSO-d_6) δ / ppm = 7.47 – 7.19 (m, 2H, CH^1), 5.34 – 4.78 (m, 4H, CH^2), 2.28 – 2.13 (m, 4H, $CH_2{}^4$), 1.54 – 1.36 (m, 4H, $CH_2{}^5$), 1.37 – 1.02 (m, 12H, $CH_3{}^3$).

IR (ATR) $\tilde{\nu}$ / cm^{-1} = 2985, 2941, 1715, 1580, 1448, 1380, 1341, 1267, 1222, 1160, 1133, 1105, 1078, 1037, 1016, 963, 903, 866, 827, 763, 617.

$T_{d,5\%}$ = 245 °C (TGA), $T_{d,15\%}$ = 338 °C (TGA), M_n = 10 kDa and $Đ$ = 1.73 (SEC-HFIP), T_g = 40 °C (DSC).

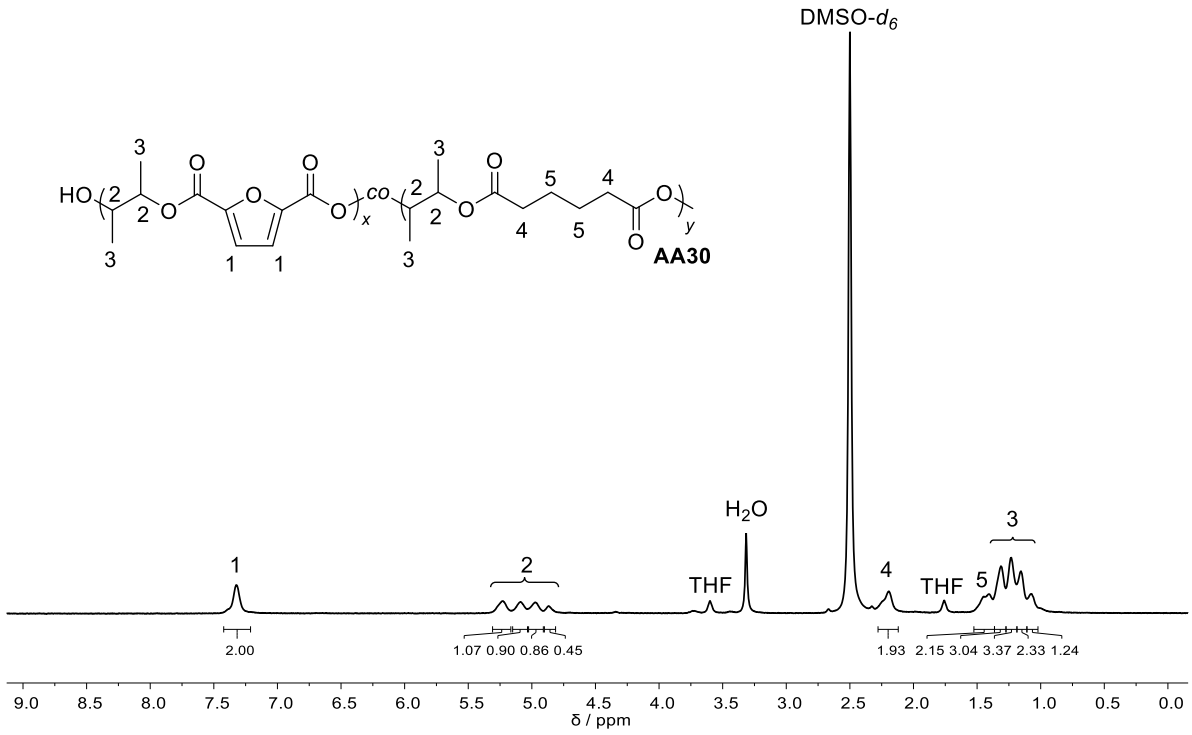

*Figure S 36. ^{1}H NMR spectrum of copolyester **AA30** in DMSO-d_6.*

For copolyester **AA40**, a dicarboxylic acid mixture of 60% FDCA (6.00 mmol, 937 mg) and 40% AA (4.00 mmol, 585 mg) was used. The product was isolated as brownish viscous liquid.

AA40:

^{1}H NMR (400 MHz, DMSO-d_6) δ / ppm = 7.43 – 7.23 (m, 2H, CH^1), 5.35 – 4.78 (m, 4H, CH^2), 2.31 – 2.10 (m, 4H, CH$_2^4$), 1.61 – 1.39 (m, 4H, CH$_2^5$), 1.36 – 1.01 (m, 12H, CH$_3^3$).

IR (ATR) $\tilde{\nu}$ / cm^{-1} = 2987, 2941, 1715, 1580, 1448, 1417, 1380, 1345, 1267, 1222, 1162, 1133, 1109, 1078, 1037, 1018, 899, 866, 827, 784, 763, 617.

$T_{d,5\%}$ = 243 °C (TGA), $T_{d,15\%}$ = 337 °C (TGA), M_n = 12 kDa and $Đ$ = 1.67 (SEC-HFIP).

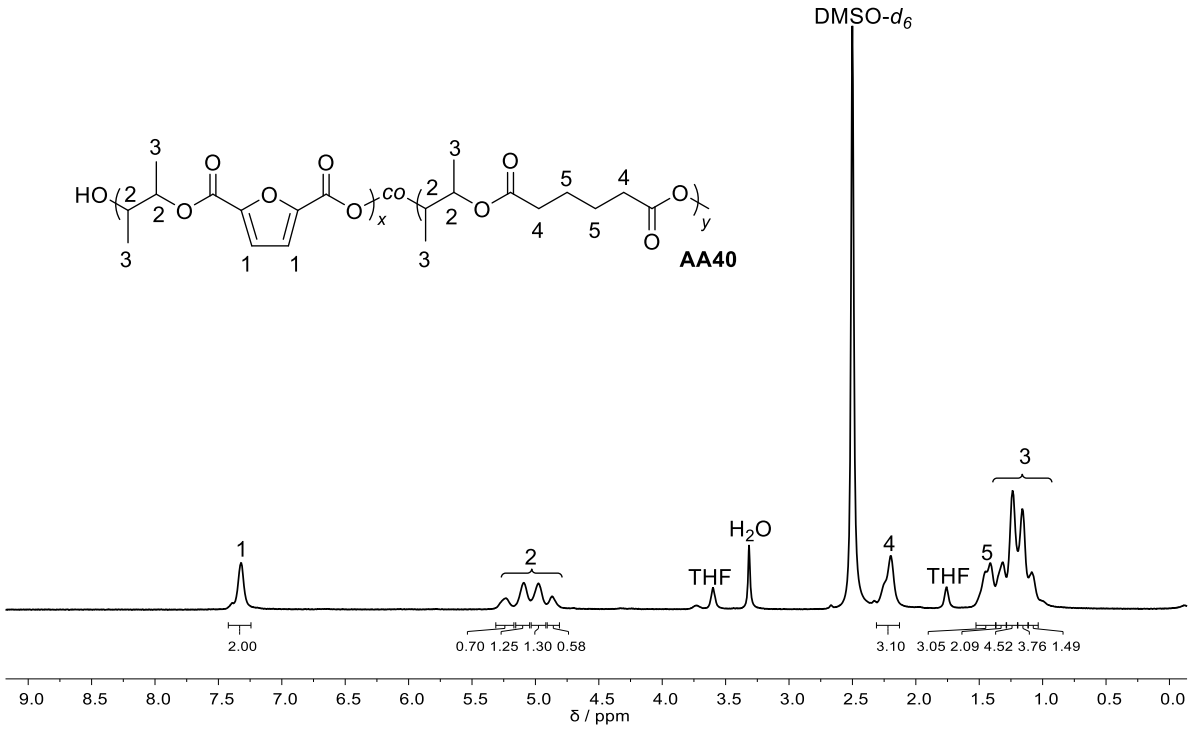

*Figure S 37. ^{1}H NMR spectrum of copolyester **AA40** in DMSO-d_6.*

For copolyester **AA60**, a dicarboxylic acid mixture of 40% FDCA (4.00 mmol, 624 mg) and 60% AA (6.00 mmol, 877 mg) was used. The product was isolated as brownish viscous liquid.

AA60:

^{1}H NMR (400 MHz, DMSO-d_6) δ / ppm = 7.40 – 7.27 (m, 2H, CH^1), 5.34 – 4.78 (m, 4H, CH^2), 2.35 – 2.10 (m, 4H, $CH_2{}^4$), 1.58 – 1.38 (m, 4H, $CH_2{}^5$), 1.33 – 0.49 (m, 12H, $CH_3{}^3$).

IR (ATR) $\tilde{\nu}$ / cm^{-1} = 2987, 2941, 1722, 1580, 1448, 1419, 1380, 1271, 1222, 1164, 1135, 1100, 1080, 1039, 1018, 1002, 965, 897, 866, 829, 765, 617.

$T_{d,5\%}$ = 274 °C (TGA), $T_{d,15\%}$ = 343 °C (TGA), M_n = 6 kDa and $Đ$ = 1.48 (SEC-HFIP).

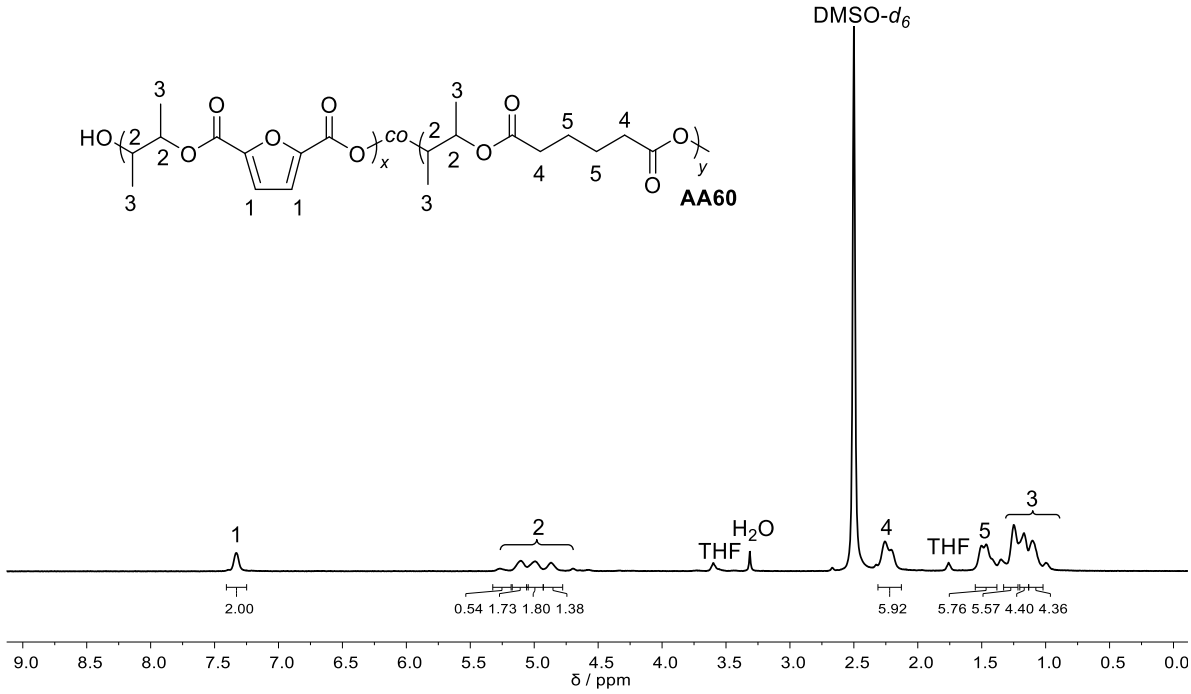

*Figure S 38. ^{1}H NMR spectrum of copolyester **AA60** in DMSO-d$_6$.*

For copolyester **SBA6**, a dicarboxylic acid mixture of 94% FDCA (9.40 mmol, 1.46 g) and 6% SBA (0.60 mmol, 121 mg) was used. The product was isolated as brownish solid.

SBA6:

^{1}H NMR (400 MHz, DMSO-d_6) δ / ppm = 7.37 – 7.24 (m, 2H, CH^{1}), 5.30 – 4.94 (m, 4H, CH^{2}), 2.22 – 2.13 (m, 4H, CH_2^{4}), 1.39 – 1.22 (m, 12H, CH_3^{3}), 1.18 – 0.97 (m, 12H, $CH_2^{5\text{-}6}$).

IR (ATR) $\tilde{\nu}$ / cm^{-1} = 2987, 2941, 1715, 1580, 1448, 1380, 1265, 1220, 1131, 1107, 1078, 1016, 998, 963, 905, 866, 825, 784, 763, 720, 617.

$T_{d,5\%}$ = 313 °C (TGA), $T_{d,15\%}$ = 340 °C (TGA), M_n = 11 kDa and $Đ$ = 1.59 (SEC-HFIP), T_g = 84 °C (DSC).

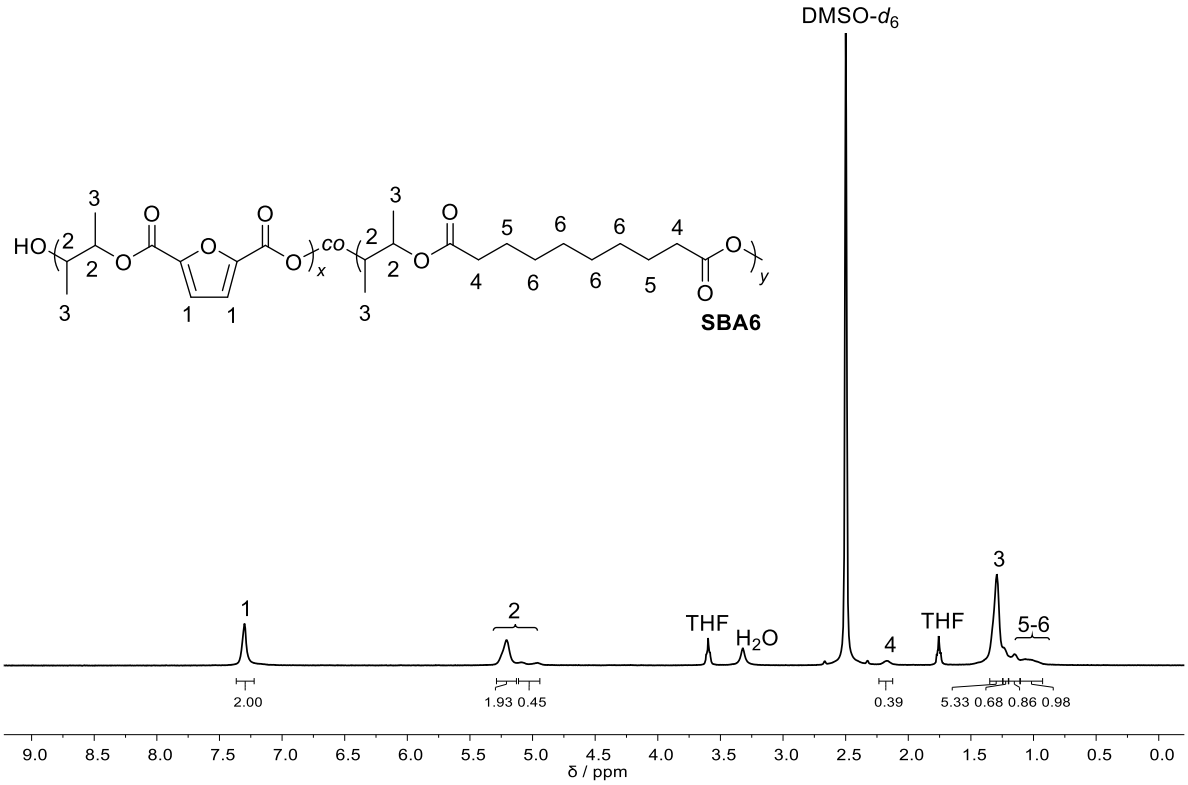

*Figure S 39. ^{1}H NMR spectrum of copolyester **SBA6** in DMSO-d_6.*

For copolyester **SBA12**, a dicarboxylic acid mixture of 88% FDCA (8.80 mmol, 1.37 g) and 12% SBA (1.20 mmol, 243 mg) was used. The product was isolated as brownish solid.

SBA12:

^{1}H NMR (400 MHz, DMSO-d_6) δ / ppm = 7.41 – 7.23 (m, 2H, CH^1), 5.29 – 4.94 (m, 4H, CH^2), 2.25 – 2.12 (m, 4H, CH$_2^4$), 1.42 – 1.20 (m, 12H, CH$_3^3$), 1.19 – 0.95 (m, 12H, CH$_2^{5,6}$).

IR (ATR) $\tilde{\nu}$ / cm^{-1} = 2987, 2939, 1715, 1580, 1448, 1380, 1265, 1220, 1131, 1105, 1078, 1016, 996, 963, 905, 866, 825, 786, 763, 724, 617.

$T_{d,5\%}$ = 328 °C (TGA), $T_{d,15\%}$ = 346 °C (TGA), M_n = 15 kDa and $Đ$ = 1.35 (SEC-HFIP), T_g = 67 °C (DSC).

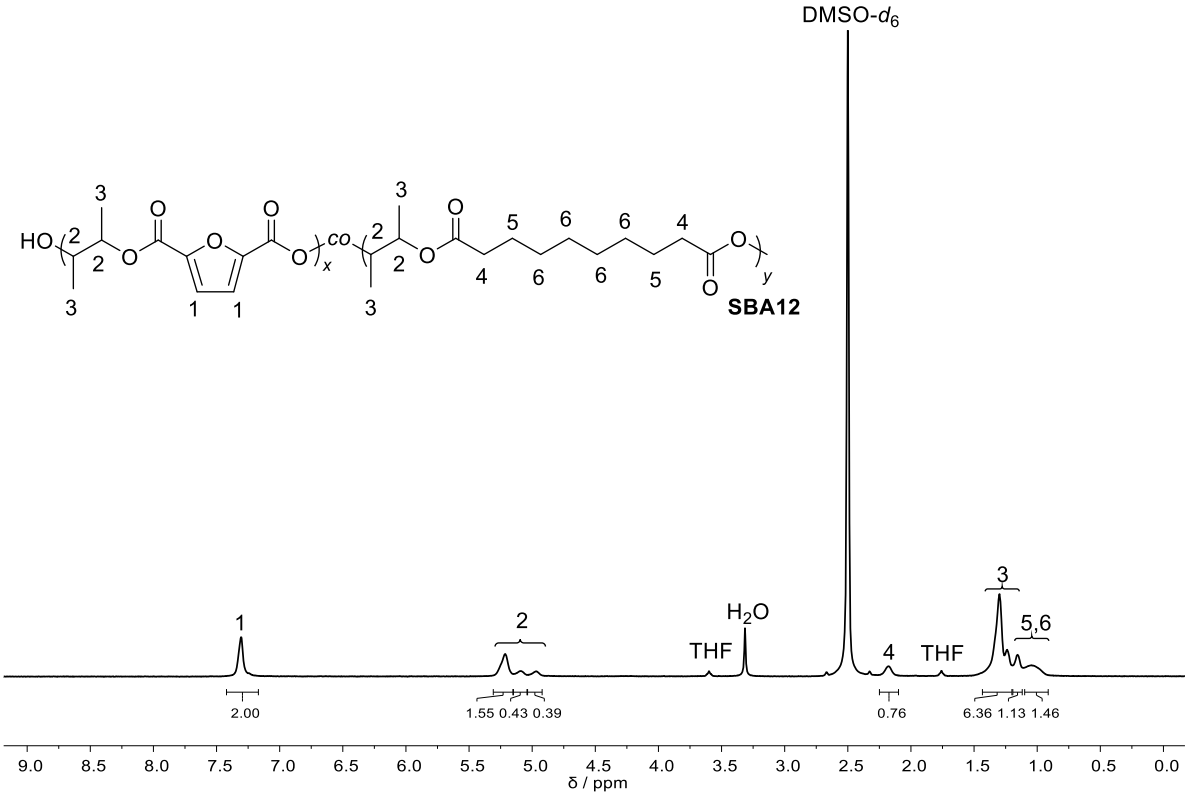

*Figure S 40. ^{1}H NMR spectrum of copolyester **SBA12** in DMSO-d$_6$.*

For copolyester **SBA18**, a dicarboxylic acid mixture of 82% FDCA (8.20 mmol, 1.28 g) and 18% SBA (1.80 mmol, 364 mg) was used. The product was isolated as brownish solid.

SBA18:

^{1}H NMR (400 MHz, DMSO-d_6) δ / ppm = 7.46 – 7.16 (m, 2H, CH^{1}), 5.37 – 4.79 (m, 4H, CH^{2}), 2.29 – 2.09 (m, 4H, CH_2^{4}), 1.51 – 0.93 (m, 24H, CH_3^{3} and $CH_2^{5,6}$).

IR (ATR) $\tilde{\nu}$ / cm^{-1} = 2987, 2937, 2859, 1715, 1580, 1506, 1448, 1380, 1265, 1220, 1133, 1103, 1078, 1016, 963, 905, 866, 825, 786, 763, 617.

$T_{d,5\%}$ = 165 °C (TGA), $T_{d,15\%}$ = 338 °C (TGA), M_n = 14 kDa and $Đ$ = 1.67 (SEC-HFIP), T_g = 53 °C (DSC).

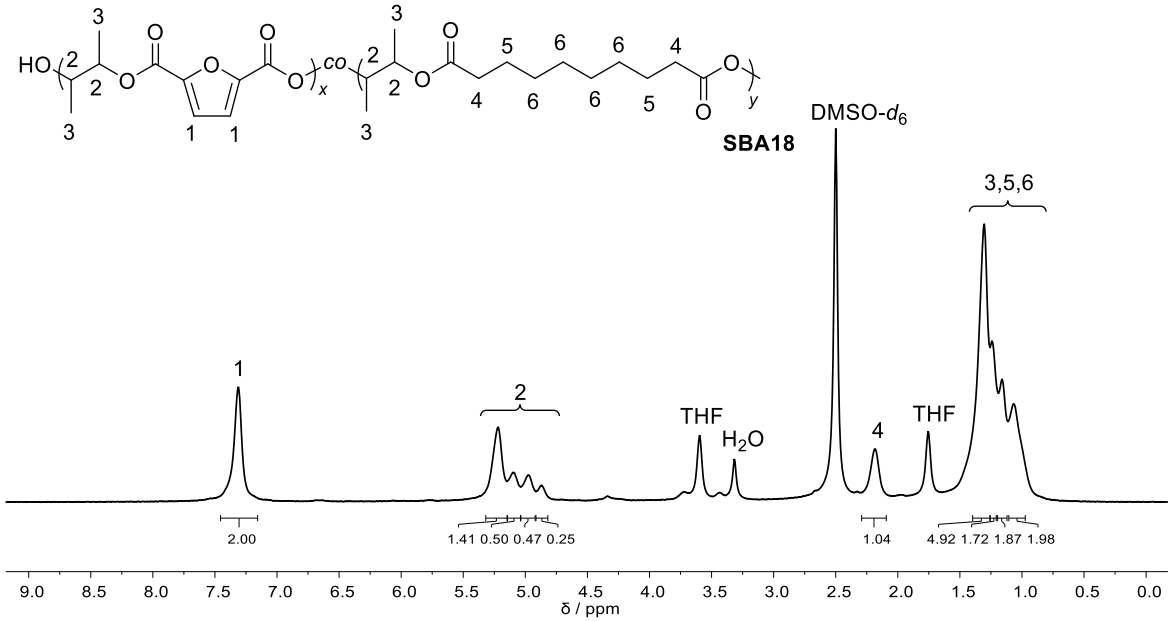

*Figure S 41. ^{1}H NMR spectrum of copolyester **SBA18** in DMSO-d_6.*

For copolyester **SBA24**, a dicarboxylic acid mixture of 76% FDCA (7.60 mmol, 1.18 g) and 24% SBA (2.40 mmol, 485 mg) was used. The product was isolated as brownish solid.

SBA24:

^{1}H NMR (400 MHz, DMSO-d_6) δ / ppm = 7.45 – 7.23 (m, 2H, CH^{1}), 5.34 – 4.80 (m, 4H, CH^{2}), 2.27 – 2.10 (m, 4H, CH_2^{4}), 1.48 – 0.89 (m, 24H, CH_3^{3} and $CH_2^{5,6}$).

IR (ATR) $\tilde{\nu}$ / cm^{-1} = 2985, 2937, 2857, 1715, 1580, 1506, 1448, 1380, 1267, 1222, 1133, 1100, 1078, 1037, 1016, 963, 905, 866, 827, 786, 763, 617.

$T_{d,5\%}$ = 214 °C (TGA), $T_{d,15\%}$ = 339 °C (TGA), M_n = 23 kDa and $Đ$ = 2.17 (SEC-HFIP), T_g = 41 °C (DSC).

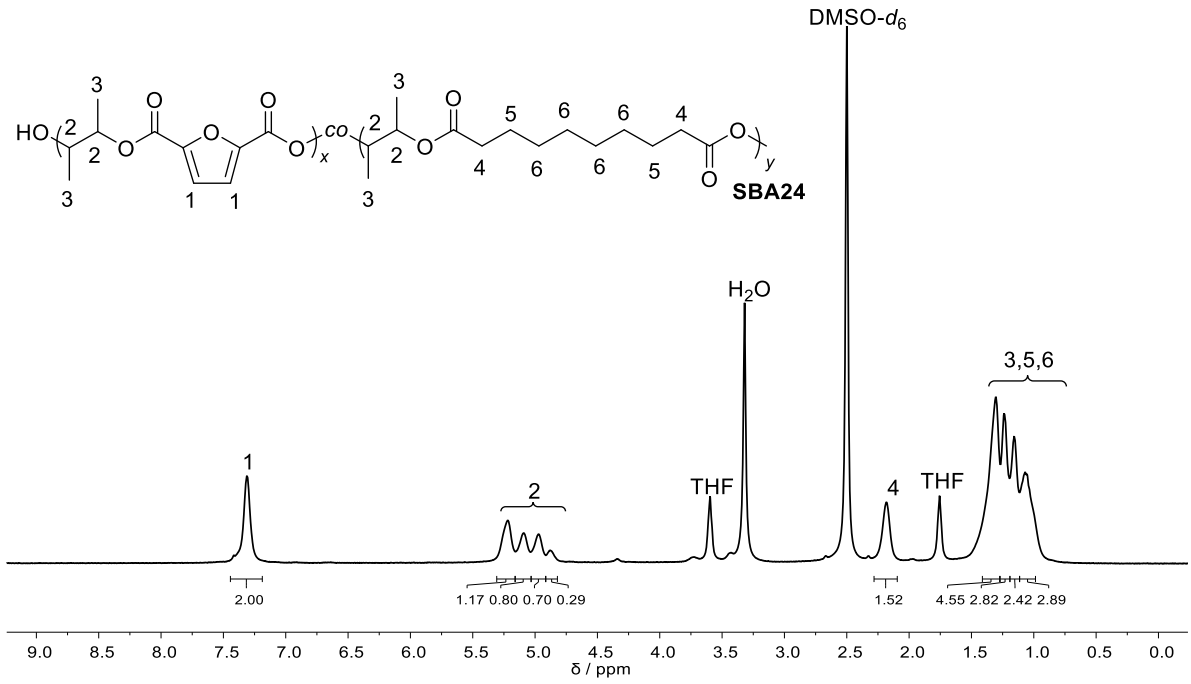

*Figure S 42. ^{1}H NMR spectrum of copolyester **SBA24** in DMSO-d_6.*

For copolyester **SBA30**, a dicarboxylic acid mixture of 70% FDCA (7.00 mmol, 1.09 g) and 30% SBA (3.00 mmol, 607 mg) was used. The product was isolated as brownish solid.

SBA30:

^{1}H NMR (400 MHz, DMSO-d_6) δ / ppm = 7.41 – 7.26 (m, 2H, CH^{1}), 5.31 – 4.83 (m, 4H, CH^{2}), 2.28 – 2.14 (m, 4H, CH_2^{4}), 1.48 – 1.09 (m, 24H, CH_3^{3} and $CH_2^{5,6}$).

IR (ATR) $\tilde{\nu}$ / cm^{-1} = 2987, 2935, 2857, 1718, 1580, 1448, 1415, 1380, 1343, 1269, 1222, 1160, 1133, 1100, 1080, 1039, 1018, 1016, 963, 899, 866, 827, 784, 765, 726, 619.

$T_{d,5\%}$ = 299 °C (TGA), $T_{d,15\%}$ = 348 °C (TGA), M_n = 17 kDa and $Đ$ = 1.82 (SEC-HFIP), T_g = 27 °C (DSC).

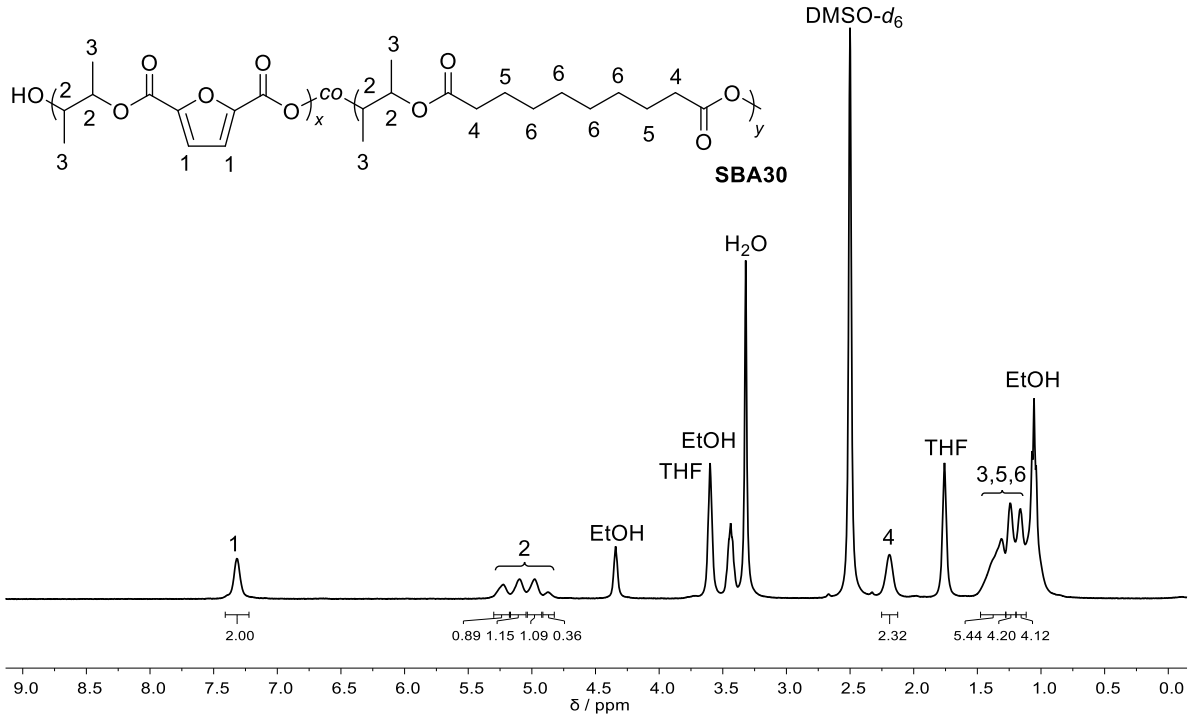

*Figure S 43. ^{1}H NMR spectrum of copolyester **SBA30** in DMSO-d_6.*

For copolyester **SBA40**, a dicarboxylic acid mixture of 60% FDCA (6.00 mmol, 937 mg) and 40% SBA (4.00 mmol, 809 mg) was used. The product was isolated as brownish viscous liquid.

SBA40:

^{1}H NMR (400 MHz, DMSO-d_6) δ / ppm = 7.43 – 7.25 (m, 2H, CH^2), 5.35 – 4.82 (m, 4H, CH^2), 2.29 – 2.12 (m, 4H, CH_2^4), 1.51 – 0.97 (m, 4H, CH_2^4), 1.30 – 1.10 (m, 8H, CH_2^6), 1.15 – 0.96 (m, 24H, CH_3^3 and $CH_2^{5,6}$).

IR (ATR) $\tilde{\nu}$ / cm^{-1} = 2985, 2933, 2857, 1718, 1580, 1448, 1417, 1380, 1341, 1269, 1222, 1162, 1135, 1100, 1080, 1039, 1018, 965, 921, 897, 866, 827, 765, 617.

$T_{d,5\%}$ = 333 °C (TGA), $T_{d,15\%}$ = 354 °C (TGA), M_n = 8 kDa and $Đ$ = 1.48 (SEC-HFIP).

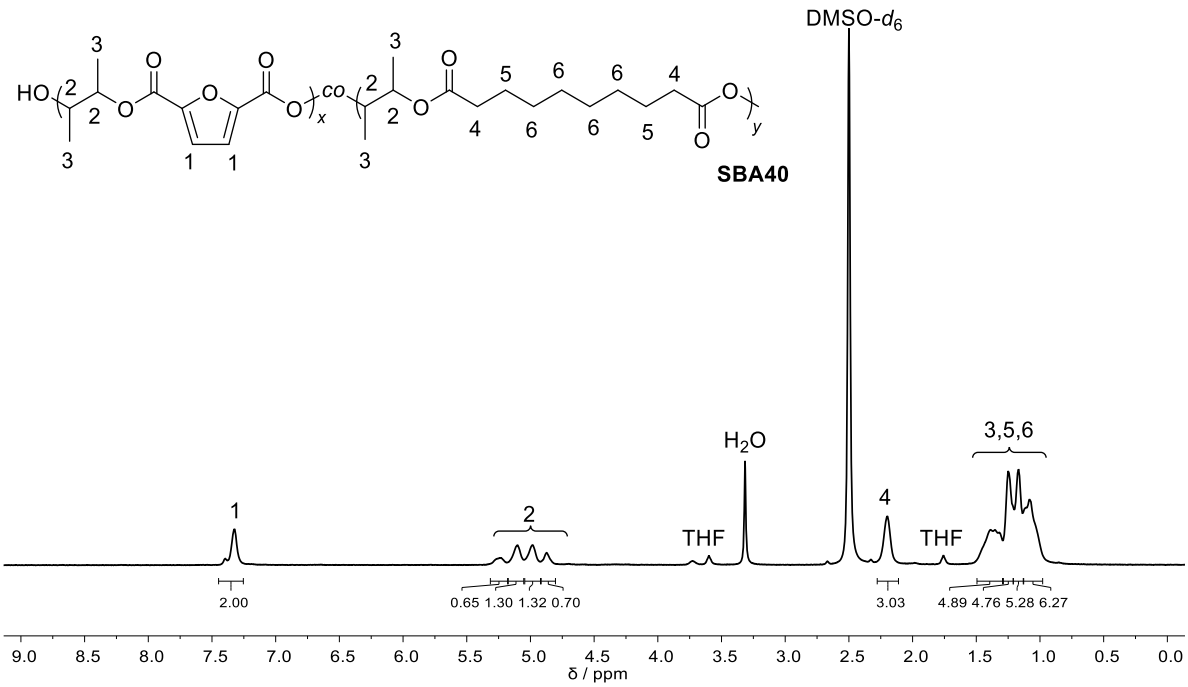

*Figure S 44. ^{1}H NMR spectrum of copolyester **SBA30** in DMSO-d_6.*

For copolyester **SBA60**, a dicarboxylic acid mixture of 40% FDCA (4.00 mmol, 624 mg) and 60% SBA (6.00 mmol, 1.21 g) was used. The product was isolated as brownish viscous liquid.

SBA60:

^{1}H NMR (400 MHz, DMSO-d_6) δ / ppm = 7.42 – 7.28 (m, 2H, CH^1), 5.33 – 4.80 (m, 4H, CH^2), 2.31 – 2.14 (m, 4H, CH_2^4), 1.59 – 1.03 (m, 24H, CH_3^3 and $CH_2^{5,6}$).

IR (ATR) $\tilde{\nu}$ / cm^{-1} = 2985, 2933, 2857, 1724, 1580, 1450, 1417, 1378, 1345, 1271, 1224, 1164, 1135, 1080, 1039, 1018, 1002, 965, 893, 866, 827, 765, 726, 617.

$T_{d,5\%}$ = 322 °C (TGA), $T_{d,15\%}$ = 357 °C (TGA), M_n = 5 kDa and $Đ$ = 1.30 (SEC-HFIP).

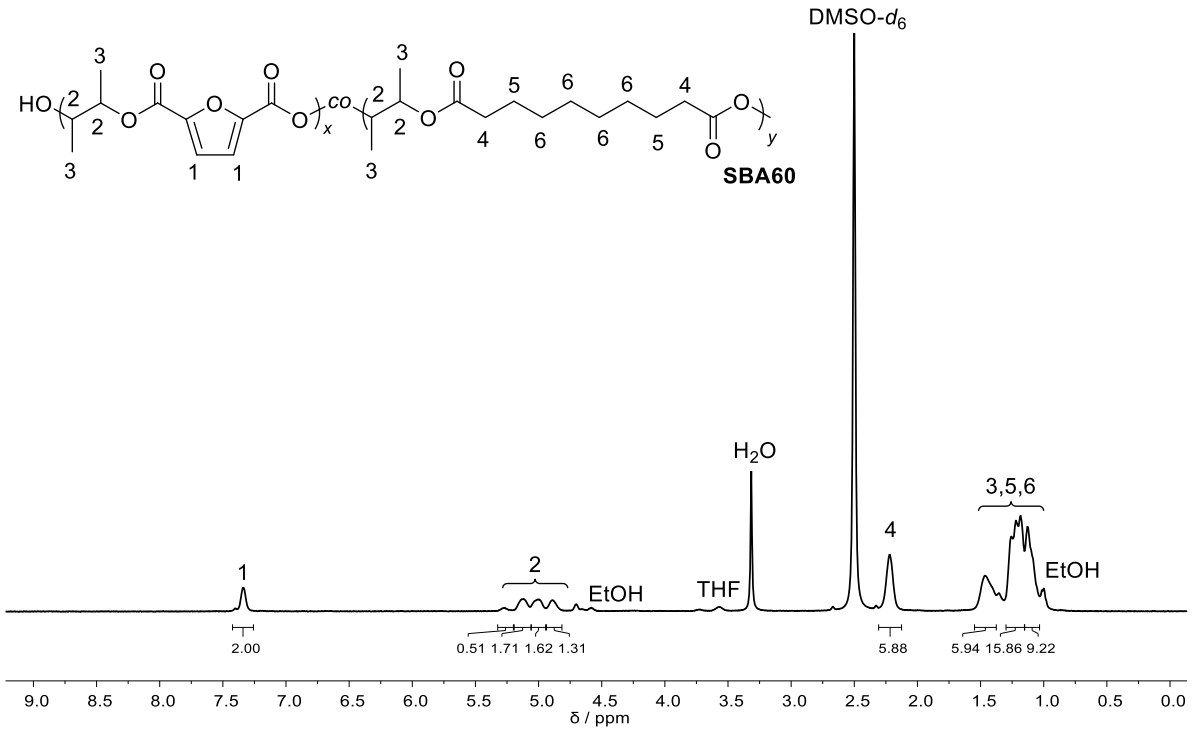

*Figure S 45. ^{1}H NMR spectrum of copolyester **SBA60** in DMSO-d_6.*

6.2.3 Experimental Procedures of 4.3 Polycondensation Reaction of Fermentation-generated 2,3-Butanediol towards a Renewable Polyester

The author of this thesis developed the synthetic procedure, planned, and evaluated the experiments, and wrote the manuscript.

Samples of 2,3-Butanediol from fermentation were provided by the working group of Prof. Dr. J. Gescher from Technical University Hamburg.

General procedure of purification strategies of BDO-F obtained from fermentation

Collaboration partners of the Technical University Hamburg were performing a fermentation cultivated in LB-Medium (Lennox) with production strain *Cupriavidus necator* H16. To extract BDO from the fermentation broth, isopropanol was used to perform a liquid-liquid extraction. Anvari and Khayati reported such an extraction.[106] Thus, a mixture of mainly isopropanol, with an unknown amount of BDO, acetoin and further protein residues was sent to our department. For the purification of this fermentation mixture, vacuum distillation was successfully performed. Such a vacuum distillation was reported by Song *et al.*[108] Herein, isopropanol was removed at reduced pressure using a rotary evaporator. Then, a distillation was carried out, using ball tubes, heating the remaining mixture to 130 °C under low pressure. At ~13 mbar and 130 °C, **BDO-F** was distilled.

BDO-F:

^{1}H NMR (400 MHz, DMSO-d_6) δ / ppm = 4.33 – 4.27 (m, 2H, O*H*), 3.42 – 3.34 (m, 2H, CH^2), 1.02 – 0.99 (m, 6H, $CH_3{}^3$), 0.91 – 0.94 (m, 6H, $CH_3{}^1$). The proton signal of CH^4 is overlapping with the water signal at 3.33 ppm.

IR (ATR) $\tilde{\nu}$ / cm^{-1} = 3359, 3351, 2974, 2931, 2882, 1450, 1397, 1374, 1323, 1269, 1162, 1115, 1084, 1053, 1010, 993, 965, 928, 887, 671, 644, 613, 597.

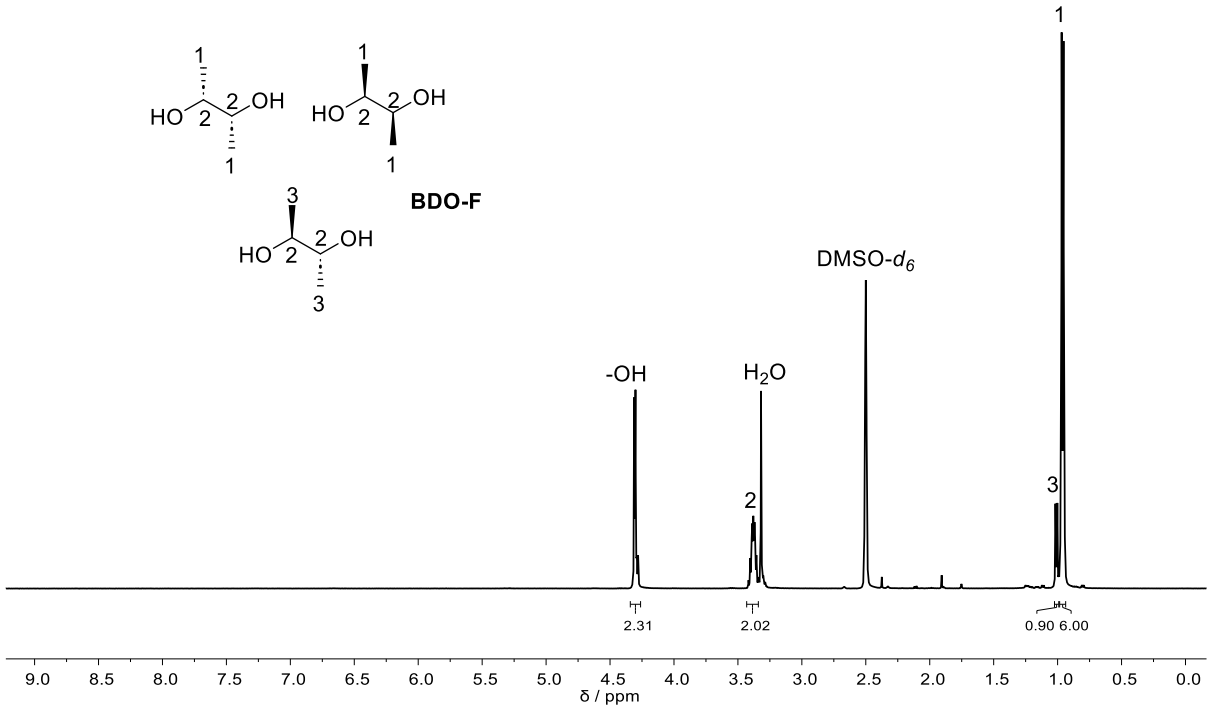

*Figure S 46. ^{1}H NMR spectrum of copolyester **BDO-F** in DMSO-d_6.*

General procedure of the polycondensation reaction of BDO isomers with FDCA

The synthetic procedure for the polycondensation of BDO and FDCA was carried out in a similar fashion described in **chapter 6.2.2 Experimental Procedures of 4.2 Polymerization of 2,3-Butanediol and Renewable Dicarboxylic Acids using Iron(III)chloride as Catalyst.** The difference in the current chapter is that different stereoisomers of BDO were employed. Polyester **P1-SS** was synthesized by using (2S, 3S)-butane-2,3-diol (BDO-SS) purchased from BLD PHARM. Polyester **P1-RR** was synthesized by using (2R, 3R)-(-)-2,3-butanediol (BDO-RR) purchased from SIGMA-ALDRICH. Polyester **P1-Meso** was synthesized by using meso-2,3-butanediol (BDO-Meso) purchased from SIGMA-ALDRICH. Furthermore, collaboration partners were synthesizing **BDO-F** during fermentation. Thus, **BDO-F** was polymerized accordingly to the desired polyester **P1-F**.

For the preparation of **P1-SS**, 3.00 equiv. of BDO-SS (1.35 g, 15.0 mmol) were used with 1.00 equiv. FDCA (0.780 g, 5.00 mmol) catalyzed by 1.25 mol% $FeCl_3$. **P1-SS** was precipitated as brownish solid.

P1-SS:

^{1}H NMR (400 MHz, DMSO-d_6) δ / ppm = 7.37 – 7.29 (m, 2H, CH^3), 5.35 – 5.17 (m, 2H, CH^2), 1.40 – 1.24 (m, 6H, $CH_3{}^1$).

IR (ATR) $\tilde{\nu}$ / cm^{-1} = 2987, 1715, 1578, 1506, 1380, 1265, 1222, 1131, 1098, 1078, 1020, 1000, 987, 963, 905, 868, 825, 763, 618.

$T_{d,5\%}$ = 267 °C (TGA), M_n = 3.6 kDa and $Đ$ = 2.18 (SEC-THF), T_g = 102 °C (DSC).

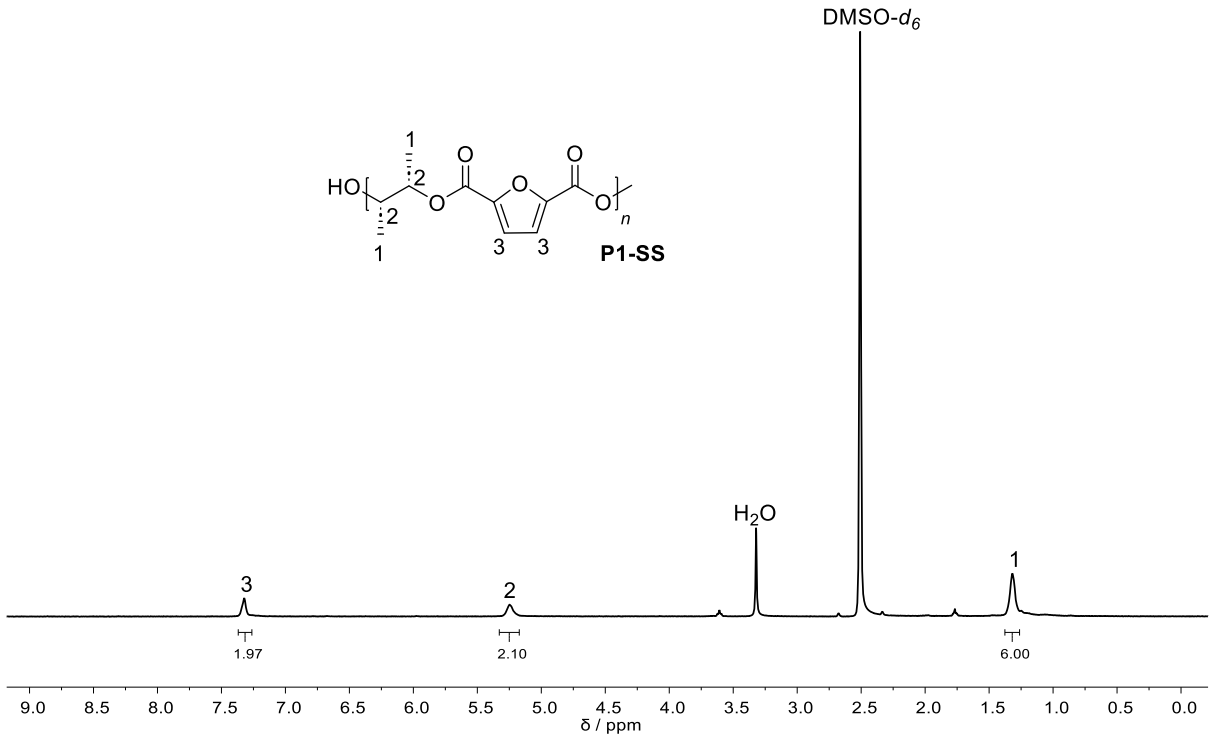

*Figure S 47. ^{1}H NMR spectrum of polyester **P1-SS** in DMSO-d$_6$.*

For the preparation of **P1-RR**, 3.00 equiv. of BDO-RR (1.35 g, 15.0 mmol) were used with 1.00 equiv. FDCA (0.780 g, 5.00 mmol) catalyzed by 1.25 mol% $FeCl_3$. **P1-RR** was precipitated as brownish solid.

P1-RR:

^{1}H NMR (400 MHz, DMSO-d_6) δ / ppm = 7.36 – 7.26 (m, 2H, CH^3), 5.33 – 5.19 (m, 2H, CH^2), 1.43 – 1.20 (m, 6H, $CH_3{}^1$).

IR (ATR) $\tilde{\nu}$ / cm^{-1} = 2985, 1715, 1578, 1448, 1382, 1265, 1222, 1131, 1098, 1078, 1018, 1000, 963, 905, 868, 825, 763, 617.

$T_{d,5\%}$ = 166 °C (TGA), M_n = 2.4 kDa and $Đ$ = 1.85 (SEC-THF), T_g = 88 °C (DSC).

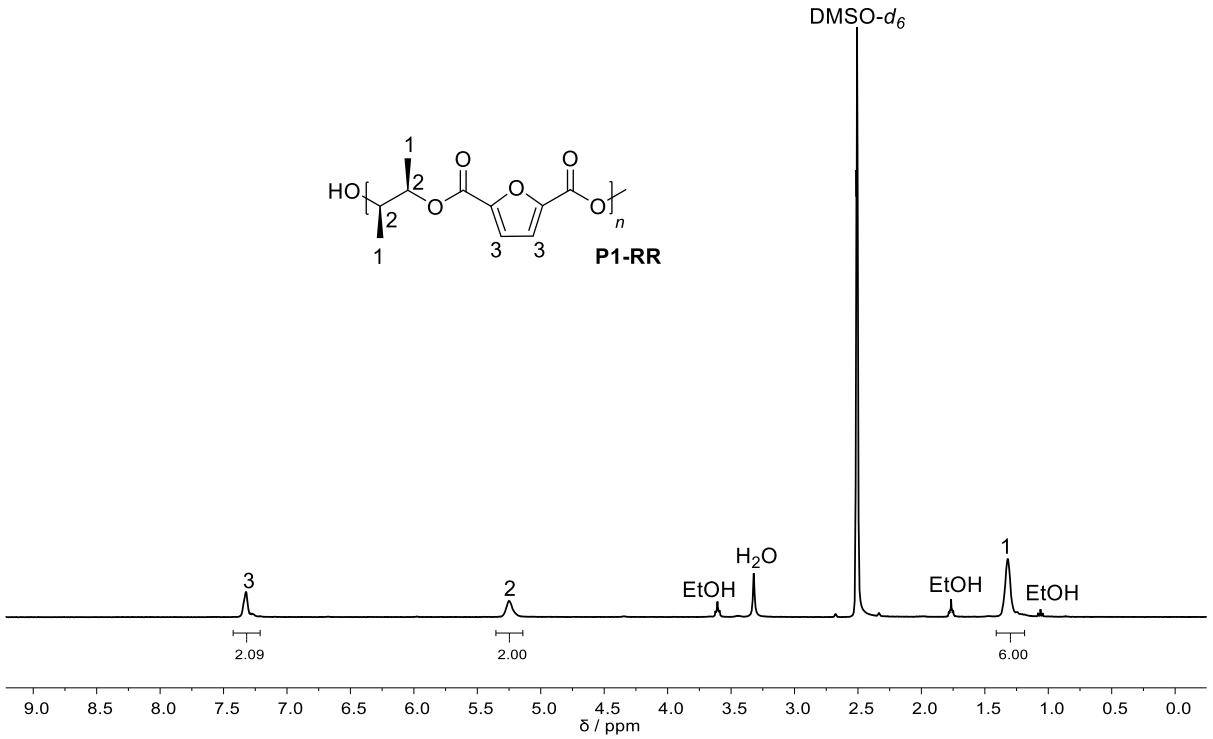

*Figure S 48. ^{1}H NMR spectrum of polyester **P1-RR** in DMSO-d_6.*

For the preparation of **P1-Meso**, 3.00 equiv. of BDO-Meso (1.35 g, 15.0 mmol) were used with 1.00 equiv. FDCA (0.780 g, 5.00 mmol) catalyzed by 1.25 mol% $FeCl_3$. **P1-Meso** was precipitated as brownish solid.

P1-Meso:

^{1}H NMR (400 MHz, DMSO-d_6) δ / ppm = 7.35 – 7.25 (m, 2H, CH^3), 5.30 – 5.17 (m, 2H, CH^2), 1.41 – 1.21 (m, 6H, $CH_3{}^1$).

IR (ATR) $\tilde{\nu}$ / cm^{-1} = 1718, 1580, 1448, 1380, 1267, 1222, 1135, 1107, 1080, 1018, 1000, 996, 963, 907, 866, 825, 763, 619.

$T_{d,5\%}$ = 280 °C (TGA), M_n = 5.0 kDa and $Đ$ = 1.68 (SEC-THF), T_g = 100 °C (DSC).

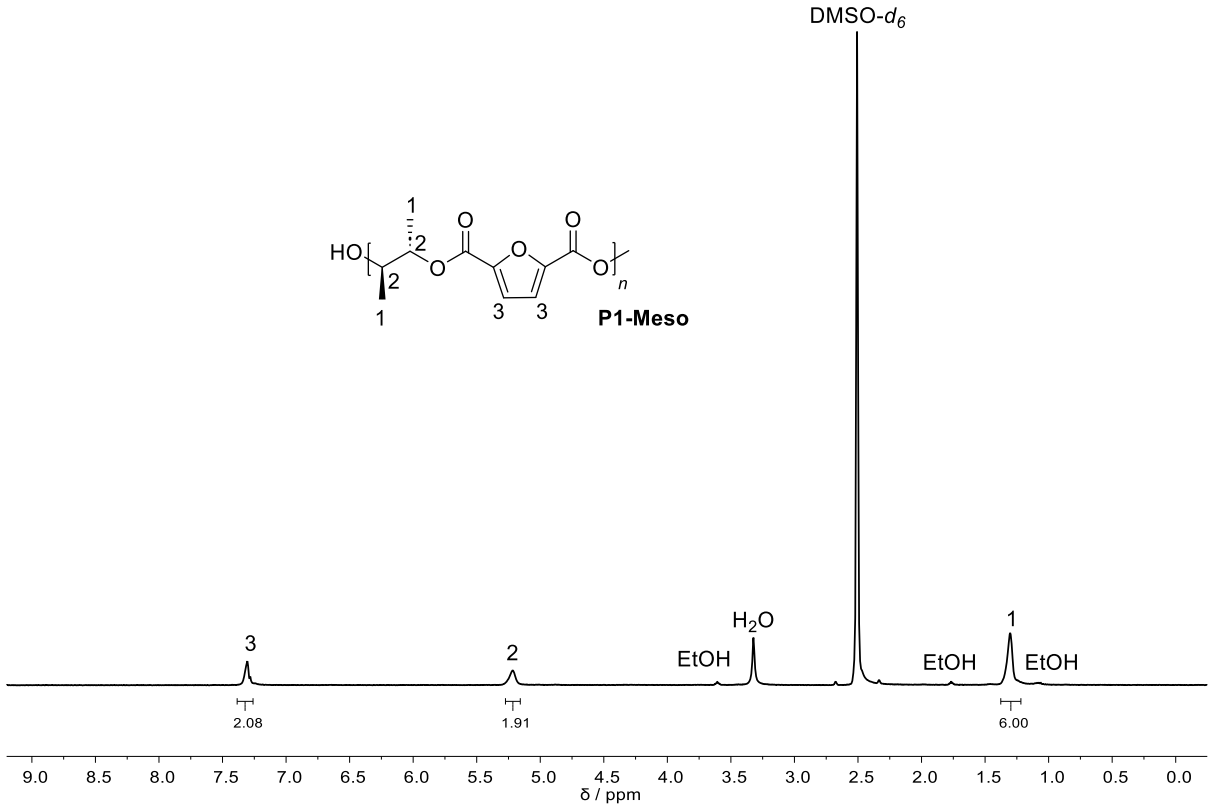

*Figure S 49. ^{1}H NMR spectrum of polyester **P1-Meso** in DMSO-d_6.*

For the preparation of **P1-F**, 3.00 equiv. of **BDO-F** (0.901 g, 10.0 mmol) were used with 1.00 equiv. FDCA (0.520 g, 3.33 mmol) catalyzed by 1.25 mol% $FeCl_3$. **P1-F** was precipitated as brownish solid.

P1-F:

^{1}H NMR (400 MHz, DMSO-d_6) δ / ppm = 7.39 – 7.29 (m, 2H, CH^3), 5.37 – 5.18 (m, 2H, CH^2), 1.42 – 1.17 (m, 6H, $CH_3{}^1$).

IR (ATR) $\tilde{\nu}$ / cm^{-1} = 1715, 1580, 1448, 1382, 1267, 1222, 1133, 1098, 1078, 1018, 1000, 993, 905, 868, 825, 763, 617.

$T_{d,5\%}$ = 264 °C (TGA), M_n = 3.0 kDa and $Đ$ = 2.35 (SEC-THF), T_g = 89 °C (DSC).

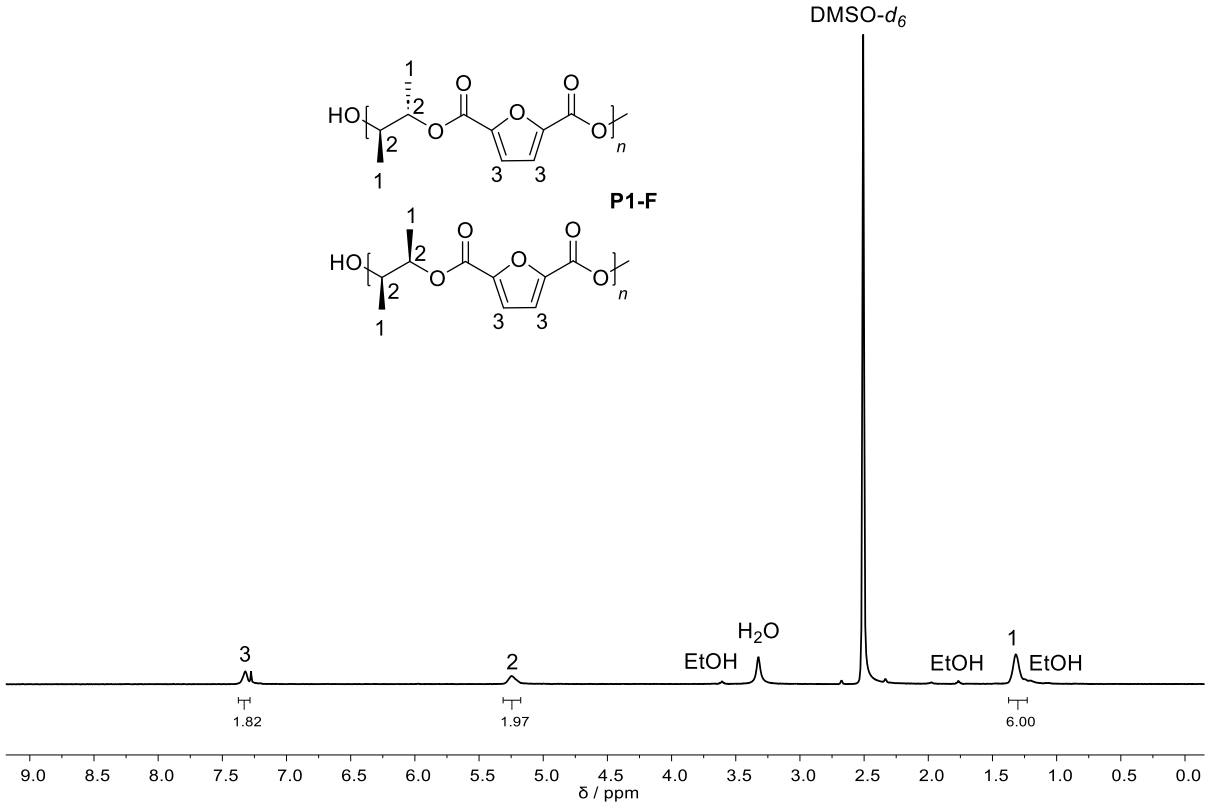

*Figure S 50. ^{1}H NMR spectrum of polyester **P1-F** in DMSO-d_6.*

7. Appendix

7.1 Abbreviations

µL	*Microliter*
µm	*Micrometer*
4-CBA	*4-Carboxybenzaldehyde*
Å	Ångström
AA	*Adipic acid*
AAE	*Actual atom economy*
AE	*Atom Economy*
BDO	*2,3-Butanediol*
BHET	*Bis-(2-hydroxyethyl) terephthalate*
BPEO	*Best practicable envionmental option*
cEF	*Complete E-factor*
cm	*Centimeter*
COSY	*Correlated Spectroscopy*
d	*Doublet*
Da	*Dalton*
DBN	*1,5-Diazabicyclo[4.3.0]non-5-ene*
DBU	*1,8-Diazabicyclo[5.4.0]undec-7-ene*
DFF	*2,5-Diformylfuran*
DMC	*Dimethyl carbonate*
DSC	*Differential scanning calorimetry*
e.g.	*Exempli gratia*
E-factor	*Environmental factor*
EG	*Ethylene glycol*
equiv.	*Equivalent*
ESI-MS	*Electrospray-ionization mass spectroscopy*
EVF	*Extensional viscosity fixture*
FAB	*Fast atom bombardment*
FDCA	*2,5-Furandicarboxylic acid*
FFCA	*5-Formyl-furan-2-carboxylic acid*
FID	*Flame ionization detection*
FLASC	*Fast life cycle assessment of synthetic chemistry*
g	*Gram*

GC	*Gas chromatography*
h	*Hour*
H12 MDI	*Hydrogenated MDI*
HDI	*Hexamethylene diisocyanate*
HMBC	*Heteronuclear multiple bond correlation*
HMF	*5-Hydroxymethylfurfural*
HMFCA	*5-Hydroxymethylfuran-2-carboxylic acid*
HPLC	*High pressure liquid chromatography*
HSQC	Heteronuclear single quantum coherence
Hz	*Hertz*
i.e.	*Id est*
ICP-OES	*Inductively coupled plasma optical emission spectroscopy*
IPDI	*Isophorone diisocyanate*
IR	*Infrared*
ISO	*Organization for Standardization*
J	*Coupling constants*
K	*Kelvin*
K. pneumoniae	*Klebsiella pneumoniae*
kDa	*Kilodalton*
kN	Kilonewton
kV	*Kilovolt*
LB	*Lysogeny broth*
LCA	*Life cycle assessment*
LD_{50}	Median lethal dose
LDPE	*Low density polyethylene*
LVE	*Linear viscoelastic*
m	*Multiplett*
M	*Molar mass*
m/z	*Mass to charge ratio*
mbar	*Millibar*
MDI	*Methylene diphenyl diisocyanate*
mg	*Milligram*
MI	*Mass intensity*
min	*Minutes*
mL	*Milliliter*
mm	*Millimeter*

mM	*Millimolar*
mmol	*Millimol*
M_n	*Number average molecular weight*
MO	*Multiobjective optimization*
MRFA	*Met-Arg-Phe-Ala (methionine, arginine, phenylalanine, alanine)*
M_w	*Weight average molecular weight*
N	*Newton*
NIPUs	*Non-isocyanate polyurethanes*
NMR	*Nuclear magnetic resonance*
P. polymyxa	*Peanibacillus polymyxa*
PBF	*Poly(1,4-butylene furan dicarboxylate)*
PBS	*Poly(butylene succinate)*
PBT	*Poly(butylene terephthalate)*
PE	*Polyethylene*
PEF	*Poly(ethylene furanoate)*
PET	*Poly(ethylene terephthalate)*
PG	*Propylene glycol*
PHB	*Poly(hydroxybutyrate)*
PHU	*Poly(hydroxy urethane)s*
PLA	*Poly(lactide acid)*
PP	*Polypropylene*
ppm	*Parts per million*
PUs	*Polyurethanes*
R_F	*Retention factor*
RME	*Reaction mass efficiency*
ROP	*Ring-opening polymerization*
s	*Singlet*
SA	*Succinic acid*
SBA	*Sebacic acid*
sec	*Second*
sEF	*Simple E-factor*
SEM	*Scanning electron microscopy*
t	*Triplett*
TBD	*1,4,7-Triazabicyclo[4.4.0]dec-5-ene*
T_c	*Crystallization temperature*
T_d	*Degradation temperature*

TDI	*Toluene diisocyanate*
T_g	*Glass transition temperature*
TGA	*Thermogravimetric analysis*
TLC	*Thin layer chromatography*
T_m	*Melting temperature*
TMG	*1,1,3,3-Tetramethylguanidine*
TPA	*Terephthalic acid*
TTIP	*Titanium(IV) isopropoxide*
$\tilde{\nu}$	*Wavenumber*
VER	*Volume expansion ratio*
wt%	*Weight percent*
γ	*Strain sweep*
ρ	*Density*
ω	*Angular frequency*

7.2 List of Figures

7.3 List of Schemes

7.4 List of Tables

7.5 List of Equations

8. List of Publications

The listed publications are related to this thesis:

A. Kirchberg, M. K. Esfahani, M. Röpert, M. Wilhelm, M. A. R. Meier*, Sustainable Synthesis of Non-Isocyanate Polyurethanes Based on Renewable 2,3-Butanediol, *Macromol. Chem. Phys.* **2022**, 2200010.

Further publications not related to this thesis:

A. Kirchberg, M. A. R. Meier*, Regeneration of Cellulose from a Switchable Ionic Liquid: Towards more Sustainable Cellulose Fibers*, Macromol. Chem. Phys*. **2021**, 2000433.

M. Schoppet, M. Peschke, **A. Kirchberg**, V. Wiebach, R. D. Süssmuth, E. Stegmann, M. J. Cryle*, The Biosynthetic Applications of Late-stage Condensation Domain Selectivity During Glycopeptide Antibiotic Biosynthesis, *Chem. Sci.* **2019**, 10, 118.

Acknowledged in helping with protein preparations for: M. Schoppet, J. Tailhades, K. Kulkarni, M. J. Cryle*, Precursor Manipulation in Glycopeptide Antibiotic Biosynthesis: Are β-Amino Acids Compatible with the Oxidative Cyclization Cascade?, *J. Org. Chem.* **2018**, 83 (13), 7214.

9. Bibliography

[1] J. Craig, F. Gerali, F. MacAulay, R. Sorkhabi, *SP* **2018**, *465*, 1.

[2] R. Mülhaupt, *Macromol. Chem. Phys.* **2013**, *214*, 159.

[3] R. Mülhaupt, *Angew. Chem.* **2004**, *43*, 1054.

[4] S. Fakirov, *Fundamentals of polymer science for engineers*, Wiley-VCH Verlag GmbH & Co. KGaA, Weinheim, **2017**.

[5] OECD, *Environment at a Glance 2020*, OECD Publishing, Paris, **2020**.

[6] Plastics Europe. Plastics The Facts 2022: An Analysis of European Plastics Production, Demand and Waste data, *Plastics Europe: Brussels, Belgium* **2022**.

[7] T. Zink, R. Geyer, R. Startz, *Law Sci. Adv.* **2018**, *22*, 314.

[8] M. I. Peñas, R. A. Pérez-Camargo, R. Hernández, A. J. Müller, *Polymers* **2022**, *14*, 1025.

[9] Plastics Europe, *European Bioplastics, Berlin* **2022**.

[10] H. J. Longwell, *World Energy* **2002**, 100.

[11] G. Gwehenberger, M. Narodoslawsky, *Process Saf. Environ. Prot.* **2008**, *86*, 321.

[12] I. T. Horváth, *Chem. Rev.* **2018**, *118*, 369.

[13] M. M. Kirchhoff, *Resour. Conserv. Recycl.* **2005**, *44*, 237.

[14] P. Anastas, N. Eghbali, *Chem. Soc. Rev.* **2010**, *39*, 301.

[15] C. Okkerse, H. van Bekkum, *Green Chem.* **1999**, 107.

[16] C. Blum, D. Bunke, M. Hungsberg, E. Roelofs, A. Joas, R. Joas, M. Blepp, H.-C. Stolzenberg, *Sustain. Chem. Pharm.* **2017**, *5*, 94.

[17] B. Purvis, Y. Mao, D. Robinson, *Sustain. Sci.* **2019**, *14*, 681.

[18] P. Gallezot, *Chem. Soc. Rev.* **2012**, *41*, 1538.

[19] Program. Ember, *L. Chem. Eng. News* **1991**, 7.

[20] P. T. Anastas, M. M. Kirchhoff, *Acc. Chem. Res.* **2002**, *35*, 686.

[21] J. G. Huddleston, H. D. Willauer, R. P. Swatloski, A. E. Visser, R. D. Rogers, *Chem. Commun.* **1998**, 1765.

[22] M. A. Dubé, S. Salehpour, *Macromol. React. Eng.* **2014**, *8*, 7.

[23] B. Brehmer, R. M. Boom, J. Sanders, *Chem. Eng. Res. Des.* **2009**, *87*, 1103.

[24] I. Pálinkó, *Green. Chem.* **2018**, 415.

[25] P. Anastas, J. C. Warner, *Oxford University Press* **1998**, *39*, 10.

[26] H. C. Erythropel, J. B. Zimmerman, T. M. de Winter, L. Petitjean, F. Melnikov, C. H. Lam, A. W. Lounsbury, K. E. Mellor, N. Z. Janković, Q. Tu et al., *Green Chem.* **2018**, *20*, 1929.

[27] S. Y. Tang, R. A. Bourne, R. L. Smith, M. Poliakoff, *Green Chem.* **2008**, *10*, 268.

[28] S. L. Y. Tang, R. L. Smith, M. Poliakoff, *Green Chem.* **2005**, *7*, 761.

[29] J. H. Clark, *Green Chem.* **2006**, *8*, 17.

[30] B. M. Trost, *Science* **1991**, 1471.
[31] G. Fiorentino, A. Zucaro, S. Ulgiati, *Energy* **2019**, *170*, 720.
[32] R. A. Sheldon, *Chem. Ind.* **1992**, *6*, 903.
[33] R. A. Sheldon, *Green Chem.* **2007**, *9*, 1261.
[34] F. Roschangar, R. A. Sheldon, C. H. Senanayake, *Green Chem.* **2015**, *17*, 752.
[35] R. A. Sheldon, *Green Chem.* **2017**, *19*, 18.
[36] K. M. Doxsee, J. E. Hutchison, *Brook/Cole Belmont* **2004**, 89.
[37] A. D. Curzons, D. N. Mortimer, D. J. C. Constable, V. L. Cunningham, *Green Chem.* **2001**, *3*, 1.
[38] D. J. C. Constable, A. D. Curzons, V. L. Cunningham, *Green Chem.* **2002**, *4*, 521.
[39] P. T. Anastas, R. L. Lankey, *Green Chem.* **2000**, *2*, 289.
[40] A. A. Burgess, D. J. Brennan, *Chem. Eng. Sci.* **2001**, 259.
[41] G. Finnveden, M. Z. Hauschild, T. Ekvall, J. Guinée, R. Heijungs, S. Hellweg, A. Koehler, D. Pennington, S. Suh, *J. Environ. Manage.* **2009**, *91*, 1.
[42] A. Azapagic, R. Clift, *Comput. Chem. Eng.* **1999**, 1509.
[43] D. Kralisch, D. Ott, D. Gericke, *Green Chem.* **2015**, *17*, 123.
[44] J. B. Guinée, R. Heijungs, G. Huppes, A. Zamagni, P. Masoni, R. Buonamici, T. Ekvall, T. Rydberg, *Environ. Sci. Technol.* **2011**, *45*, 90.
[45] P. Saling, A. Kicherer, B. Dittrich-Krämer, R. Wittlinger, W. Zombik, I. Schmidt, W. Schrott, S. Schmidt, *Int. J. Life Cycle Assess.* **2002**, 203.
[46] A. D. Curzons, C. Jiménez-González, A. L. Duncan, D. J. C. Constable, V. L. Cunningham, *Int. J. Life Cycle Assess.* **2007**, *12*, 272.
[47] T. O. Wiedmann, H. Schandl, M. Lenzen, D. Moran, S. Suh, J. West, K. Kanemoto, *Proc. Natl. Acad. Sci.* **2015**, *112*, 6271.
[48] C. A. Bakker, R. Wever, C. Teoh, S. de Clercq, *Int. J. Sustain. Eng.* **2010**, *3*, 2.
[49] F. G. Calvo-Flores, *ChemSusChem* **2009**, *2*, 905.
[50] B. O. Al-sasi, O. Taylan, A. Demirbas, *Energy Sources* **2017**, *12*, 847.
[51] UBA Resources Report, "Resource use in Germany", **2022**.
[52] V. Siracusa, I. Blanco, *Polymers* **2020**, *12*.
[53] V. B. Borugadda, V. V. Goud, *Renew. Sust. Energ. Rev.* **2012**, *16*, 4763.
[54] G. Centi, S. Perathoner, *Catalysis Today* **2020**, *342*, 4.
[55] P. Gallezot, *Green Chem.* **2007**, *9*, 295.
[56] M. Narodoslawsky, A. Niederl-Schmidinger, L. Halasz, *J. Cleaner Prod.* **2008**, *16*, 164.
[57] A.-C. Albertsson, S. Karlsson (Eds.) *Biodegradable Polymers*, Comprehensive Polymer Science and Supplements, **1989**.
[58] N. Karak (Ed.) *Vegetable Oil Based Polymers*, Woodhead, **2012**.

[59] J. M. Schakenraad, P. J. Dijkstra, *Clin. Mater.* **1991**, 253.
[60] C.-Y. Loo, W.-H. Lee, T. Tsuge, Y. Doi, K. Sudesh, *Biotechnol. Lett.* **2005**, *27*, 1405.
[61] J. O. Metzger, *Eur. J. Lipid Sci. Technol.* **2009**, *111*, 865.
[62] E. Castro-Aguirre, F. Iñiguez-Franco, H. Samsudin, X. Fang, R. Auras, *Adv. Drug Deliv. Rev.* **2016**, *107*, 333.
[63] K. Sudesh, T. Iwata, *Clean Soil Air Water* **2008**, *36*, 433.
[64] N. Lucas, C. Bienaime, C. Belloy, M. Queneudec, F. Silvestre, J.-E. Nava-Saucedo, *Chemosphere* **2008**, *73*, 429.
[65] H. Salehizadeh, M. C. M. van Loosdrecht, *Biotechnol. Adv.* **2004**, *22*, 261.
[66] H. T. H. Nguyen, P. Qi, M. Rostagno, A. Feteha, S. A. Miller, *J. Mater. Chem. A* **2018**, *6*, 9298.
[67] C. M. Mendieta, M. E. Vallejos, F. E. Felissia, G. Chinga-Carrasco, M. C. Area, *J. Polym. Environ.* **2020**, *28*, 1.
[68] J. A. Melero, J. Iglesias, A. Garcia, *Energy Environ. Sci.* **2012**, *5*, 7393.
[69] I. Delidovich, P. J. C. Hausoul, L. Deng, R. Pfützenreuter, M. Rose, R. Palkovits, *Chem. Rev.* **2016**, *116*, 1540.
[70] W. Deng, Y. Feng, J. Fu, H. Guo, Y. Guo, B. Han, Z. Jiang, L. Kong, C. Li, H. Liu et al., *Green Energy Environ.* **2023**, *8*, 10.
[71] Avinash P. Ingle, Anuj Kumar Chandel, and Silvio Silvério da Silva (Eds.) *Biopolymers from Lignocellulosic Biomass*, Lignocellulosic Biorefinig Technologies, **2020**.
[72] R. A. Sheldon, *Green Chem.* **2014**, *16*, 950.
[73] M. A. R. Meier, J. O. Metzger, U. S. Schubert, *Chem. Soc. Rev.* **2007**, *36*, 1788.
[74] B. Grignard, S. Gennen, C. Jérôme, A. W. Kleij, C. Detrembleur, *Chem. Soc. Rev.* **2019**, *48*, 4466.
[75] T. Sakakura, J.-C. Choi, H. Yasuda, *Chem. Rev.* **2007**, *107*, 2365.
[76] M. Aresta, A. Dibenedetto, A. Angelini, *Chem. Rev.* **2014**, *114*, 1709.
[77] I. Omae, *Coord. Chem. Rev.* **2012**, *256*, 1384.
[78] S. Dabral, T. Schaub, *Adv. Synth. Catal.* **2019**, *361*, 223.
[79] S. Octave, D. Thomas, *Biochimie* **2009**, *91*, 659.
[80] H. Ohara, *Appl. Microbiol. Biotechnol.* **2003**, *62*, 474.
[81] J. Xu, C. Li, L. Dai, C. Xu, Y. Zhong, F. Yu, C. Si, *ChemSusChem* **2020**, *13*, 4284.
[82] Y. Zhang, S. Ni, R. Wu, Y. Fu, M. Qin, S. Willför, C. Xu, *Ind. Crops. Prod.* **2022**, *177*, 114451.
[83] B. Kamm, M. Kamm, *Appl. Microbiol. Biotechnol.* **2004**, *64*, 137.
[84] P. Manzanares, M. J. Negro, R. Saez, C. Martin, *Bioresour. Technol.* **1993**, 95.
[85] J. D. McMillan, *Renewable Energy* **1997**, 295.

[86] N. Sarkar, S. K. Ghosh, S. Bannerjee, K. Aikat, *Renewable Energy* **2012**, *37*, 19.

[87] IEA, International Energy Agency, "Renewables 2021 - Analysis and forecast to 2026", **2021**.

[88] S. Mecking, *Angew. Chem.* **2004**, *116*, 1096.

[89] S. Kandasamy, S. P. Samudrala, S. Bhattacharya, *Catal. Sci. Technol.* **2019**, *9*, 567.

[90] P. Nachtergaele, S. de Meester, J. Dewulf, *J. Chem. Technol. Biotechnol.* **2019**, *94*, 1808.

[91] V. Samoilov, D. Ni, A. Goncharova, D. Zarezin, M. Kniazeva, A. Ladesov, D. Kosyakov, M. Bermeshev, A. Maximov, *Molecules* **2020**, *25*, 1723.

[92] M. J. Syu, *Appl. Microbiol.* **2001**, *55*, 10.

[93] E. Celińska, W. Grajek, *Biotechnol. Adv.* **2009**, *27*, 715.

[94] J. W. K. Oliver, I. M. P. Machado, H. Yoneda, S. Atsumi, *PNAS USA* **2013**, *110*, 1249.

[95] X.-J. Ji, H. Huang, P.-K. Ouyang, *Biotechnol. Adv.* **2011**, *29*, 351.

[96] B. G. Harvey, W. W. Merriman, R. L. Quintana, *ChemSusChem* **2016**, *9*, 1814.

[97] H. Arthur, S. W. George, *Lister Insitute* **1905**, 399.

[98] Ellis I. Fulmer, L. M. Christensen, A. R. Kendali, *Ind. Eng. Chem.* **1933**, *7*, 798.

[99] H.-P. Li, Y.-N. Gan, L.-J. Yue, Q.-Q. Han, J. Chen, Q.-M. Liu, Q. Zhao, J.-L. Zhang, *Front. Microbiol.* **2022**, *13*, 833313.

[100] A. K. Chandel, O. V. Singh, L. Venkateswar Rao (Eds.) *Biotechnological Applications of Hemicellulosic Derived Sugars: State-of-the-Art*, Springer Netherlands, **2010**.

[101] W. Sabra, H. Quitmann, A.-P. Zeng, J.-Y. Dai, Z.-L. Xiu in *Comprehensive Biotechnol. 2011*, p. 87.

[102] Y. Yan, C.-C. Lee, J. C. Liao, *Org. Biomol. Chem.* **2009**, *7*, 3914.

[103] O. Cofré, M. Ramírez, J. M. Gómez, D. Cantero, *Biomass Bioenergy* **2016**, *91*, 37.

[104] C. Windhorst, J. Gescher, *Biotechnol. Biofuels* **2019**, *12*, 163.

[105] D. Härrer, C. Windhorst, N. Böhner, J. Novion Ducassou, Y. Couté, J. Gescher, *Bioresour. Technol.* **2021**, *329*, 124866.

[106] M. Anvari, H. Pahlavanzadeh, E. Vasheghani-Farahani, G. Khayati, *J. Ind. Microbiol. Biotechnol.* **2009**, *36*, 313.

[107] D. Tinôco, S. Borschiver, P. L. Coutinho, D. M. G. Freire, *Bioprod. Bioref.* **2021**, *15*, 357.

[108] S. Jeon, D.-K. Kim, H. Song, H. J. Lee, S. Park, D. Seung, Y. K. Chang, *J. Biosci. Bioeng.* **2014**, *117*, 464.

[109] G. R. Harvianto, J. Haider, J. Hong, N. van Duc Long, J.-J. Shim, M. H. Cho, W. K. Kim, M. Lee, *Biotechnol. Biofuels* **2018**, *11*, 18.

[110] K. Petrov, P. Petrova, *Fermentation* **2021**, *7*, 307.

[111] A. Kirchberg, M. Khabazian Esfahani, M.-C. Röpert, M. Wilhelm, M. A. R. Meier, *Macromol. Chem. Phys.* **2022**, *223*, 2200010.

[112] X. Hu, X. Shen, M. Huang, C. Liu, Y. Geng, R. Wang, R. Xu, H. Qiao, L. Zhang, *Polymer* **2016**, *84*, 343.

[113] E. Gubbels, L. Jasinska-Walc, C. E. Koning, *J. Polym. Sci. A Polym. Chem.* **2013**, *51*, 890.

[114] B. Eling, Ž. Tomović, V. Schädler, *Macromol. Chem. Phys.* **2020**, *221*, 2000114.

[115] L. Maisonneuve, O. Lamarzelle, E. Rix, E. Grau, H. Cramail, *Chem. Rev.* **2015**, *115*, 12407.

[116] Statista Research Department, "Market volume of polyurethane worldwide from 2015 to 2022", can be found under https://www.statista.com/statistics/720341/global-polyurethane-market-size-forecast/, **2023**.

[117] A. Gomez-Lopez, F. Elizalde, I. Calvo, H. Sardon, *Chem. Commun.* **2021**.

[118] E. Delebecq, J.-P. Pascault, B. Boutevin, F. Ganachaud, *Chem. Rev.* **2013**, *113*, 80.

[119] A. A. Caraculacu, S. Coseri, *Prog. Polym. Sci.* **2001**, *26*, 799.

[120] B. Otto, *Angew. Chem.* **1947**, *59*, 257.

[121] E. Sharmin, F. Zafar (Eds.) *Polyurethane: An Introduction*, INTECH, **2012**.

[122] M. Ates, S. Karadag, A. A. Eker, B. Eker, *Polym. Int.* **2022**, *71*, 1157.

[123] M. A. Aristri, M. A. R. Lubis, S. M. Yadav, P. Antov, A. N. Papadopoulos, A. Pizzi, W. Fatriasari, M. Ismayati, A. H. Iswanto, *Appl. Sci.* **2021**, *11*, 4242.

[124] H.-W. Engels, H.-G. Pirkl, R. Albers, R. W. Albach, J. Krause, A. Hoffmann, H. Casselmann, J. Dormish, *Angew. Chem.* **2013**, *52*, 9422.

[125] O. Kreye, H. Mutlu, M. A. R. Meier, *Green Chem.* **2013**, *15*, 1431.

[126] P. Stachak, I. Łukaszewska, E. Hebda, K. Pielichowski, *Materials* **2021**, *14*, 1.

[127] United States Environmental Protection Agency, "hexamethylene-diisocyanate", can be found under www.epa.gov.

[128] H. J. Twitchett, J. Zhang, *Chem. Soc. Rev.* **1974**, 209.

[129] M. O. Ganiu, B. Nepal, J. P. van Houten, R. Kartika, *Tetrahedron* **2020**, *76*.

[130] BASF SE, "Isocyanates", can be found under www.chemicals.basf.com, **2023**.

[131] EMERGEN Research, "MDI Market", can be found under www.emergenresearch.com, **2022**.

[132] M. Ghasemlou, F. Daver, E. P. Ivanova, B. Adhikari, *Ind. Crop. Prod.* **2019**, *142*, 111841.

[133] Z. Petrovic, *Polymer Revs.* **2008**, *48*, 109.

[134] R. Gabriel, P. Anna, *Polymer* **2002**, *43*, 2927.

[135] N. V. Gama, A. Ferreira, A. Barros-Timmons, *Materials* **2018**, *11*, 1841.

[136] A. S. Dutta, *Recycling of polyurethane foams* **2018**, 17.

[137] M. Bourguignon, B. Grignard, C. Detrembleur, *Angew. Chem.* **2022**, 1-10.

[138] F. M. Casati, R. M. Herrington, R. Broos, and Y. Miyazaki, *J. Cell. Plast.* **1998**, 430.

[139] W. Stecen Edward, S. Theodore Michael, M. Donald C., C08J 9/30, **1996**.

[140] V. A. Yakushin, N. P. Zhmud, U. K. Stirna, *Mech. Compos. Meter.* **2002**.

[141] J. K. Limbasiya, D. M. Priyamkumar, K. A. Dharmik, K. S. Yash, S. K. Devganiya, "Environmental Protection Treatment and Pollution Prevention on Waste Refrigerators", **2009**.

[142] W. Yang, Q. Dong, S. Liu, H. Xie, L. Liu, J. Li, *Procedia Environ. Sci.* **2012**, *16*, 167.

[143] K. M. Zia, H. N. Bhatti, I. Ahmad Bhatti, *React. Funct. Polym.* **2007**, *67*, 675.

[144] A. Kemona, M. Piotrowska, *Polymers* **2020**, *12*, 1752.

[145] Puren GmbH, "Next Step PU", can be found under www.next-step-pu.com.

[146] D. E. Nestle, 5 292 462, **1994**.

[147] A. J. Hulme, T. C. Goodhead, *J. Mater. Process. Technol.* **2003**, *139*, 322.

[148] J. Becker, C. Wittmann, *Angew. Chem.* **2015**, *54*, 3328.

[149] A.-D. Dieu Vo, A. Elraghy, R. E. Spence, K. B. McAuley, *Macromol. React. Eng.* **2020**, *14*, 1900045.

[150] BASF, "BASF now offers bio-based PolyTHF", can be found under https://www.basf.com/global/en/media/news-releases, **2015**.

[151] K. Andreas, B. Eling, S. Markus, K. Sebastian, K. Christian, WO2013/127647 A1, **2013**.

[152] S. Hu, X. Luo, Y. Li, *J. Appl. Polym. Sci.* **2015**, *132*, 1-8.

[153] M. Rhein, A. Demharter, B. Felker, M. A. R. Meier, *ACS Appl. Polym. Mater.* **2022**.

[154] W. B. Hardy, R. P. Bennett, *Tetrahedron Lett.* **1967**, 961.

[155] A. M. Tafesh, J. Weiguny, *Chem. Rev.* **1996**, 2035.

[156] Y. Watanabe, Y. Tsuji, R. Takeuchi, *Bull. Chem. Sci. Jpm.* **1984**, 3011.

[157] T. Curtius, *Ber. Dtsch. Chem. Ges.* **1890**, 3023.

[158] A. W. Hofmann, *Ber. Dtsch. Chem. Ges.* **1881**, 2725.

[159] W. Lossen, *Justus Liebigs Ann. Chem.* **1872**, 347.

[160] H. V. Le, B. Ganem, *Org. Synth.* **2012**, *89*, 404.

[161] W. Qian, X. Tan, Q. Su, W. Cheng, F. Xu, L. Dong, S. Zhang, *ChemSusChem* **2019**, *12*, 1169.

[162] A. Cornille, R. Auvergne, O. Figovsky, B. Boutevin, S. Caillol, *Europ. Polym. J.* **2017**, *87*, 535.

[163] N. D. Ghatge, J. Y. Jadhav, *J. Polym. Sci. A Polym. Chem.* **1983**, 194.

[164] L. Filippi, M. A. R. Meier, *Macromol. Rapid Commun.* **2021**, *42*, 2000440.

[165] M. Unverferth, O. Kreye, A. Prohammer, M. A. R. Meier, *Macromol. Rapid Commun.* **2013**, *34*, 1569.

[166] O. Figovsky, L. Shapovalov, A. Leykin, O. Birukova, R. Potashnikova, *Chem. Chem. Technol.* **2013**, 79.

[167] C. Hahn, H. Keul, M. Möller, *Polym. Int.* **2012**, *61*, 1048.

[168] O. Figovsky, A. Cornille, R. Auvergne, B. Boutevin, S. Caillol, *NanoTech Industries* **2016**.

[169] H. K. Hall, A. K. Schneider, *J. Am. Chem. Soc.* **1958**, *80*, 6409.

[170] S. Neffgen, H. Keul, H. Höcker, *Macromol. Rapid Commun.* **1996**, *17*, 373.

[171] D. Zhang, Y. Zhang, Y. Fan, M.-N. Rager, V. Guérineau, L. Bouteiller, M.-H. Li, C. M. Thomas, *Macromolecules* **2019**, *52*, 2719.

[172] R. D. Lundberg, S. Albans, D. R. Montgomery, 3 523 924, **1970**.

[173] E. Rix, E. Grau, G. Chollet, H. Cramail, *Eur. Polym. J.* **2016**, *84*, 863.

[174] T. Lebarbé, L. Maisonneuve, T. H. Nga Nguyen, B. Gadenne, C. Alfos, H. Cramail, *Polym. Chem.* **2012**, *3*, 2842.

[175] D. V. Palaskar, A. Boyer, E. Cloutet, C. Alfos, H. Cramail, *Biomacromolecules* **2010**, *11*, 1202.

[176] E. Dyer, H. Scott, *J. Am. Chem. Soc.* **1957**, 672.

[177] A. Cornille, S. Dworakowska, D. Bogdal, B. Boutevin, S. Caillol, *Eur. Polym. J.* **2015**, *66*, 129.

[178] M. S. Kathalewar, P. B. Joshi, A. S. Sabnis, V. C. Malshe, *RSC Adv.* **2013**, *3*, 4110.

[179] P. Olsén, M. Oschmann, E. V. Johnston, B. Åkermark, *Green Chem.* **2018**, *20*, 469.

[180] C. Carré, Y. Ecochard, S. Caillol, L. Avérous, *ChemSusChem* **2019**, *12*, 3410.

[181] M. Alves, B. Grignard, R. Mereau, C. Jerome, T. Tassaing, C. Detrembleur, *Catal. Sci. Technol.* **2017**, *7*, 2651.

[182] A. J. Kamphuis, F. Picchioni, P. P. Pescarmona, *Green Chem.* **2019**, *21*, 406.

[183] S. Inoue, H. Koinuma, T. Tsuruta, *J. Polym. Sci. B Polym. Lett.* **1969**, *7*, 287.

[184] M. Taherimehr, P. P. Pescarmona, *J. Appl. Polym. Sci.* **2014**, *131*.

[185] P. P. Pescarmona, M. Taherimehr, *Catal. Sci. Technol.* **2012**, *2*, 2169.

[186] R. I. Khusnutdinov, N. A. Shchadneva, Y. Y. Mayakova, *Russ. J. Org. Chem.* **2014**, *50*, 948.

[187] S. Usachev, A. Gridnev, *Syn. Comm.* **2011**, *41*, 3683.

[188] H. Mutlu, J. Ruiz, S. C. Solleder, M. A. R. Meier, *Green Chem.* **2012**, *14*, 1728.

[189] I. R. Shaikh, *J. Catal.* **2014**, *2014*, 1.

[190] R. H. Lambeth, T. J. Henderson, *Polymer* **2013**, *54*, 5568.

[191] P. Nachtergaele, S. de Meester, J. Dewulf, *J. Chem. Technol. Biotechnol.* **2019**, *94*, 1808.

[192] T. M. McGuire, E. M. López-Vidal, G. L. Gregory, A. Buchard, *J. CO2 Util.* **2018**, *27*, 283.

[193] E. Fritz-Langhals, *Org. Process Res. Dev.* **2022**, *26*, 3015.

[194] T. Ishikawa, L. M. Harwood, *Synlett* **2013**, *24*, 2507.

[195] R. M. Garipov, V. A. Sysoev, V. V. Mikheev, A. I. Zagidullin, R. Ya. Deberdeev, V. I. Irzhak, Al. Al. Berlin, *Phys. Chem.* **2003**, *393*, 61.

[196] D. Tang, D.-J. Mulder, B. A. J. Noordover, C. E. Koning, *Macromol. Rapid Commun.* **2011**, *32*, 1379.

[197] C. Duval, N. Kébir, A. Charvet, A. Martin, F. Burel, *J. Polym. Sci. Part A: Polym. Chem.* **2015**, *53*, 1351.

[198] A. Llevot, M. Meier, *Polym. Int.* **2019**, *68*, 826.

[199] H. Blattmann, M. Lauth, R. Mülhaupt, *Macromol. Mater. Eng.* **2016**, *301*, 944.

[200] N. Fanjul-Mosteirín, R. Aguirresarobe, N. Sadaba, A. Larrañaga, E. Marin, J. Martin, N. Ramos-Gomez, M. C. Arno, H. Sardon, A. P. Dove, *Chem. Mater.* **2021**, *33*, 7194.

[201] H. Khatoon, S. Iqbal, M. Irfan, A. Darda, N. K. Rawat, *Progress in Organic Coatings* **2021**, *154*, 106124.

[202] U. Edlund, A.-C. Albertsson, *Adv. Drug Deliv. Rev.* **2003**, *55*, 585.

[203] W. H. Carothers, G. J. Berchet, *Du Pont de Nemours & Company* **1930**, 5289.

[204] J. R. Whinfield, J. T. Dickson, *UK 578079*, **1946**.

[205] K. Pang, R. Kotek, A. Tonelli, *Prog. Polym. Sci.* **2006**, *31*, 1009.

[206] Y. Tokiwa, B. P. Calabia, *J. Polym. Environ.* **2007**, *15*, 259.

[207] Q. Ding, M. Soccio, N. Lotti, D. Cavallo, R. Androsch, *Chin. J. Polym. Sci.* **2020**, *38*, 311.

[208] M. A. Hillmyer, W. B. Tolman, *Acc. Chem. Res.* **2014**, *47*, 2390.

[209] M. Vert, *Biomacromolecules* **2005**, *6*, 538.

[210] J. M. Longo, M. J. Sanford, G. W. Coates, *Chem. Rev.* **2016**, *116*, 15167.

[211] J. K. Stille, *J. Chem. Ed.* **1981**, *58*, 862.

[212] G. Odian, *Principles of Polymerization*, John Wiley & Sons, Inc. Publication, Hoboken NY, **2004**.

[213] Q. Peng, K. Mahmood, Y. Wu, L. Wang, Y. Liang, J. Shen, Z. Liu, *Green Chem.* **2013**, 1.

[214] X.-L. Qu, M. Jiang, B. Wang, J. Deng, R. Wang, Q. Zhang, G.-Y. Zhou, J. Tang, *ChemSusChem* **2019**, *12*, 4927.

[215] Y. Jinang, A. J. J. Woortman, Alberda van Ekenstein, Gert. O. R., K. Loos, *Biocatal. Polym. Chem.* **2010**, 83.

[216] M. Rabnawaz, I. Wyman, R. Auras, S. Cheng, *Green Chem.* **2017**, *19*, 4737.

[217] S. Paul, Y. Zhu, C. Romain, R. Brooks, P. K. Saini, C. K. Williams, *ChemComm* **2015**, *51*, 6459.

[218] K. Loos, R. Zhang, I. Pereira, B. Agostinho, H. Hu, D. Maniar, N. Sbirrazzuoli, A. J. D. Silvestre, N. Guigo, A. F. Sousa, *Front. Chem.* **2020**, *8*, 585.

[219] E. R. Witt, C. Christi, 3 654 351, **1972**.

[220] K. Ravindranath, R. A. Mashelkar, *Chem. Eng. Sci.* **1986**, 2969.

[221] A. S. Chegolya, V. V. Shevchenko, G. D. Mikhailov, *J. Polym. Sci. Polym. Chem. Ed.* **1979**, *17*, 889.

[222] G. Z. Papageorgiou, V. Tsanaktsis, D. N. Bikiaris, *Physical chemistry chemical physics : PCCP* **2014**, *16*, 7946.

[223] W. A. MacDonald, *Polym. Int.* **2002**, *51*, 923.

[224] K. Tomita, H. Ida, *Polymer*, *1973*, 55-60.

[225] T. H. Shah, J. I. Bhatty, G. A. Gamien, *Polymer* **1984**, 1333.

[226] A. Pellis, E. Herrero Acero, L. Gardossi, V. Ferrario, G. M. Guebitz, *Polym. Int.* **2016**, *65*, 861.

[227] J.-G. Rosenboom, D. K. Hohl, P. Fleckenstein, G. Storti, M. Morbidelli, *Nat. Commun.* **2018**, *9*, 2701.

[228] X. Fei, J. Wang, J. Zhu, X. Wang, X. Liu, *ACS Sustain. Chem. Eng.* **2020**, *8*, 8471.

[229] The Coca Cola Company, "The Coca-Cola Company Announces Partnerships to Develop Commercial Solutions for Plastic Bottles Made Entirely from Plants", can be found under www.thecoca-colacompany.com, **2011**.

[230] K.-R. Hwang, W. Jeon, S. Y. Lee, M.-S. Kim, Y.-K. Park, *Chem. Eng. J.* **2020**, *390*, 124636.

[231] J. J. Bozell, G. R. Petersen, *Green Chem.* **2010**, *12*, 539.

[232] T. Werpy, G. Petersen, *U.S. Department of Energy* **2004**, 1.

[233] W. Partenheimer, V. V. Grushin, *Adv. Synth. Catal.* **2001**, *343*, 102.

[234] B. Saha, S. Dutta, M. M. Abu-Omar, *Catal. Sci. Technol.* **2012**, *2*, 79.

[235] R. Sahu, P. L. Dhepe, *Reac. Kinet. Mech. Cat.* **2014**, *112*, 173.

[236] Avantium, "FDCA and plantMEG together make a 100% plant-based plastic PEF", can be found under https://www.avantium.com/lead-products/, **opened 2023**.

[237] A. J. J. E. Eerhart, A. P. C. Faaij, M. K. Patel, *Energy Environ. Sci.* **2012**, *5*, 6407.

[238] A. F. Sousa, C. Vilela, A. C. Fonseca, M. Matos, C. S. R. Freire, G.-J. M. Gruter, J. F. J. Coelho, A. J. D. Silvestre, *Polym. Chem.* **2015**, *6*, 5961.

[239] M. Jiang, Q. Liu, Q. Zhang, C. Ye, G. Zhou, *J. Polym. Sci. A Polym. Chem.* **2012**, *50*, 1026.

[240] V. Tsanaktsis, G. Z. Papageorgiou, D. N. Bikiaris, *J. Polym. Sci. A Polym. Chem.* **2015**, *53*, 2617.

[241] M. J. Soares, P.-K. Dannecker, C. Vilela, J. Bastos, M. A. Meier, A. F. Sousa, *Europ. Polym. J.* **2017**, *90*, 301.

[242] S. Thiyagarajan, W. Vogelzang, R. J. I. Knoop, A. E. Frissen, J. van Haveren, D. S. van Es, *Green Chem.* **2014**, *16*, 1957.

[243] G. Z. Papageorgiou, D. G. Papageorgiou, Z. Terzopoulou, D. N. Bikiaris, *Eur. Polym. J.* **2016**, *83*, 202.

[244] E. Gubbels, L. Jasinska-Walc, B. A. Noordover, C. E. Koning, *Eur. Polym. J.* **2013**, *49*, 3188.

[245] J. G. Zeikus, M. K. Jain, P. Elankovan, *Appl. Microbiol. Biotechnol.* **1999**, 545.

[246] M. Patel, M. Crank, V. Dornburg, B. Hermann, B. Hüsing, L. Overbeek, E. Terragni, E. Recchia, *European Commissions GROWTH Programme, Utrecht* **2006**.

[247] I. Bechthold, K. Bretz, S. Kabasci, R. Kopitzky, A. Springer, *Chem. Eng. Technol.* **2008**, *31*, 647.

[248] Succinity GmbH, *Biobased Polybutylene Succiniate (PBS) - An attractive polymer for biopolymer compounds*, **2016**.

[249] L. Aliotta, M. Seggiani, A. Lazzeri, V. Gigante, P. Cinelli, *Polymers* **2022**, *14*, 844.

[250] J. Xu, B.-H. Guo, *Biotechnol. J.* **2010**, *5*, 1149.

[251] S. A. Rafiqah, A. Khalina, A. S. Harmaen, I. A. Tawakkal, K. Zaman, M. Asim, M. N. Nurrazi, C. H. Lee, *Polymers* **2021**, *13*, 1436.

[252] BioPBS Marketing Group, *Mitsubishi chemical group*, *2017*.

[253] J. Han, J. Shi, Z. Xie, J. Xu, B. Guo, *Materials* **2019**, *12*, 1507.

[254] Y. Xu, J. Xu, D. Liu, B. Guo, X. Xie, *J. Appl. Polym. Sci.* **2008**, *109*, 1881.

[255] H. Hu, R. Zhang, J. Wang, W. Bin Ying, J. Zhu, *Eur. Polym. J.* **2018**, 101.

[256] M. Lang, H. Li, *ChemSusChem* **2022**, *15*, e202101531.

[257] D. R. Vardon, N. A. Rorrer, D. Salvachúa, A. E. Settle, C. W. Johnson, M. J. Menart, N. S. Cleveland, P. N. Ciesielski, K. X. Steirer, J. R. Dorgan et al., *Green Chem.* **2016**, *18*, 3397.

[258] W. Deng, Q. Zhang, Y. Wang, *J. Energy Chem.* **2015**, *24*, 595.

[259] T. Debuissy, E. Pollet, L. Avérous, *Polymer* **2016**, *99*, 204.

[260] U. Witt, R.-J. Müller, W.-D. Deckwer, *J. Environ. Polym. Degr.* **1995**, *3*, 215.

[261] E. Skoog, J. H. Shin, V. Saez-Jimenez, V. Mapelli, L. Olsson, *Biotechnol. Adv.* **2018**, *36*, 2248.

[262] A. Corona, M. J. Biddy, D. R. Vardon, M. Birkved, M. Z. Hauschild, G. T. Beckham, *Green Chem.* **2018**, *20*, 3857.

[263] B. Wu, Y. Xu, Z. Bu, L. Wu, B.-G. Li, P. Dubois, *Polymer* **2014**, *55*, 3648.

[264] J.-F. Stumbé, B. Bruchmann, *Macromol. Rapid Commun.* **2004**, *25*, 921.

[265] W.-Y. Jeon, M.-J. Jang, G.-Y. Park, H.-J. Lee, S.-H. Seo, H.-S. Lee, C. Han, H. Kwon, H.-C. Lee, J.-H. Lee et al., *Green Chem.* **2019**, *21*, 6491.

[266] M. Winnacker, B. Rieger, *Macromol. Rapid Commun.* **2016**, *37*, 1391.

[267] G. Wang, M. Jiang, Q. Zhang, R. Wang, G. Zhou, *RSC Adv.* **2017**, *7*, 13798.

[268] G. Wang, M. Jiang, Q. Zhang, R. Wang, X. Tong, S. Xue, G. Zhou, *Polym. Degrad. Stab.* **2017**, *143*, 1.

[269] G. Sailakshmi, T. Mitra, A. Gnanamani, *Progress in Biomaterials* **2013**, *2*, 1.

[270] A. K. Vasishtha, R. K. Trivedi, G. Das, *JAOCS* **1990**, *67*, 333.

[271] A. J. Hunt, A. S. Matharu, A. H. King, J. H. Clark, *Green Chem.* **2015**, *17*, 1949.

[272] J. R. Ludwig, C. S. Schindler, *Chem* **2017**, *2*, 313.

[273] X. Zhang, M. Fevre, G. O. Jones, R. M. Waymouth, *Chem. Rev.* **2018**, *118*, 839.

[274] J. Wisniak, *Educ. Quím.* **2010**, *21*, 60.

[275] Karl D. Collins, Tobias Gensch, Frank Glorius, *Nat. Chem.* **2014**, *6*, 859.

[276] G. N. Lewis, *University of Carlifornia, Barkeley* **1938**, 293.

[277] H. R. Kricheldorf, *Chem. Rev.* **2009**, *109*, 5579.

[278] A. Khrouf, M. Abid, S. Boufi, R. E. Gharbi, A. Gandini, *Macromol. Chem. Phys.* **1998**, *199*, 2755.

[279] Z. Terzopoulou, E. Karakatsianopoulou, N. Kasmi, V. Tsanaktsis, N. Nikolaidis, M. Kostoglou, G. Z. Papageorgiou, D. A. Lambropoulou, D. N. Bikiaris, *Polym. Chem.* **2017**, *8*, 6895.

[280] X. Qu, G. Zhou, R. Wang, H. Zhang, Z. Wang, M. Jiang, J. Tang, *J. Ind. Eng. Chem.* **2021**, *99*, 422.

[281] E. Wolf, E. Richmond, J. Moran, *Chem. Sci.* **2015**, *6*, 2501.

[282] P. S. Löser, P. Rauthe, M. A. R. Meier, A. Llevot, *Phil. Trans. R. Soc.* **2020**, *378*, 20190267.

[283] H. Mutlu, M. A. R. Meier, *Eur. J. Lipid Sci. Technol.* **2010**, *112*, 10.

[284] Elsevier (Ed.) *Introduction to Plastics Engineering*, Elsevier, **2018**.

[285] V. N. Novikov, E. A. Rössler, *Polymer* **2013**, *54*, 6987.

[286] G. Ungar, X. B. Zeng, *Chem. Rev.* **2001**, *101*, 4157.

[287] Z. S. Petrović, Z. Zavargo, J. H. Flyn, W. J. Macknight, *J. Appl. Polym. Sci.* **1994**, *51*, 1087.

[288] N. Ketata, C. Sanglar, H. Waton, S. Alamercery, F. Delolme, G. Raffin, and M.F. Grenier-Loustalot, *Polym. Compos.* **2005**, *13*, 1.

[289] A. Franck, "Viscoelasticity and dynamic mechanical testing", can be found under www.trinstruments.com.

[290] F. A. Mazzeo, "Importance of Oscillartory Time Sweeps in Rheology", can be found under www.tainstruments.com.

[291] J. M. Dealy, R. G. Larson, *Structure and rheology of molten polymers*. *From structure to flow behavior and back again*, Hanser, Munich, **2006**.

[292] M. Abbasi, L. Faust, K. Riazi, M. Wilhelm, *Macromolecules* **2017**, *50*, 5964.

[293] M. Mihai, M. A. Huneault, B. D. Favis, *Polym. Eng. Sci.* **2010**, *50*, 629.

[294] G. J. Nam, J. H. Yoo, J. W. Lee, *J. Appl. Polym. Sci.* **2005**, *96*, 1793.

[295] J. E. Martini, *Master thesis* **1981**, *Massachusetts Institute of Technology*.

[296] Vipin Kumar, Nam P. Suh, *Polym. Eng. Sci.* **1990**, *20*, 1323.

[297] M. Abbasi, L. Faust, M. Wilhelm, *Polymer* **2020**, *193*, 122354.

[298] R. L. Heck, *J. Vinyl Addit. Technol.* **1998**, *4*, 113.

[299] D. Diaz, P. Miranda, J. Padron, V. Martin, *COC* **2006**, *10*, 457.

[300] Elsevier (Ed.) *Theory and Practice of Histological Techniques*, Elsevier, **2008**.

[301] VALCO, "Manufacturing process of polyethylene terephthalate (PET)", can be found under www.valcogroup-valves.com, **2021**.

[302] S. Oelmann, M. A. R. Meier, *RSC Adv.* **2017**, *7*, 45195.

[303] M. Hong, L. Gao, G. Xiao, *J. Chem. Res.* **2014**, *38*, 679.

[304] S.-W. Liu, R.-F. Liao, X.-A. Lu, 10858332, **2020**.

[305] W. Ring, I. Mita, A. D. Jenkins, N. M. Bikales, *Pure & Appl. Chem.* **1985**, *57*, 1427.